University of Alberta

Probabilistic Modeling of Weed Distributions for Optimal Treatment

by

Tyrone Roger Faechner

A thesis submitted to the Faculty of Graduate Studies and Research in partial fulfillment of the requirements for the degree of **Doctor of Philosophy**.

in

Mining Engineering

Department of Civil and Environmental Engineering

Edmonton, Alberta
Spring 2003

National Library
of Canada

Acquisitions and
Bibliographic Services

395 Wellington Street
Ottawa ON K1A 0N4
Canada

Bibliothèque nationale
du Canada

Acquisisitons et
services bibliographiques

395, rue Wellington
Ottawa ON K1A 0N4
Canada

Your file Votre référence
ISBN: 0-612-82098-X
Our file Notre référence
ISBN: 0-612-82098-X

The author has granted a non-exclusive licence allowing the National Library of Canada to reproduce, loan, distribute or sell copies of this thesis in microform, paper or electronic formats.

The author retains ownership of the copyright in this thesis. Neither the thesis nor substantial extracts from it may be printed or otherwise reproduced without the author's permission.

L'auteur a accordé une licence non exclusive permettant à la Bibliothèque nationale du Canada de reproduire, prêter, distribuer ou vendre des copies de cette thèse sous la forme de microfiche/film, de reproduction sur papier ou sur format électronique.

L'auteur conserve la propriété du droit d'auteur qui protège cette thèse. Ni la thèse ni des extraits substantiels de celle-ci ne doivent être imprimés ou aturement reproduits sans son autorisation.

Canada

University of Alberta

Library Release Form

Name of Author: Tyrone Roger Faechner

Title of Thesis: Probabilistic Modeling of Weed Distributions for Optimal Treatment

Degree: Doctor of Philosophy

Year this Degree Granted: 2003

Permission is hereby granted to the University of Alberta Library to reproduce single copies of this thesis and to lend or sell such copies for private, scholarly or scientific research purposes only.

The author reserves all other publication and other rights in association with the copyright in the thesis, and except as herein before provided, neither the thesis nor any substantial portion thereof may be printed or otherwise reproduced in any material form whatever without the author's prior written permission.

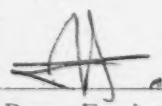

Tyrone Roger Faechner
300 Pilling Drive
Brandon, Manitoba
Canada, R7A 6T9

Date: Jan. 27/03

University of Alberta

Faculty of Graduate Studies and Research

The undersigned certify that they have read, and recommend to the Faculty of Graduate Studies and Research for acceptance, a thesis entitled **Probabilistic Modeling of Weed Distributions for Optimal Treatment** submitted by Tyrone Roger Faechner in partial fulfillment of the requirements for the degree of **Doctor of Philosophy** in *Mining Engineering*.

Dr. C. V. Deutsch (Supervisor)

Dr. R. Van Acker (External)

Dr. P. Crown

Dr. Y. Feng

Dr. T. Joseph

Date: Dec. 12/02

Abstract

Wild oat (*Avena fatua* L.) is an annual grass weed that is expensive to control in grain growing areas of western Canada and northern United States. Wild oat herbicides represent a significant cash cost of growing a cereal or oilseed crop. Crop yield loss due to wild oat interference is costly.

Optimizing herbicide rates based on the spatial distribution of weeds is possible because of global positioning technology. Exhaustive sampling would provide the exact locations of all wild oat for targeted herbicide application; however, the cost would be prohibitive. Instead, some reasonably spaced samples should be collected to identify weed locations and design an optimum herbicide treatment program. The optimum program will give the most profit, that includes revenue due to increased yield, herbicide cost, and sampling expenses. This research proposes a methodology to implement optimum herbicide rates with consideration of (1) wild oat in western Canadian crops, (2) locally varying herbicide treatments, (3) uncertainty in the predicted maps, and (4) economics in decision making.

Procedures for determining locally varying herbicide rates include kriging and simulation. The revenue from kriging and simulation plus two other weed prescription techniques is compared for different sampling designs. Of the sampling designs assessed, the simulated $Square_7$ with 98 sample locations in a square pattern for the Stony Plain field is the most profitable while at the Viking field, a simulated $Grid_{10}$ design with 100 sampling locations in a rectangular pattern generates the most profit. These designs have the smallest number of sampling locations and the lowest sampling expenses. Applying herbicide with the locally varying rates results in $3440 more revenue compared to a no herbicide option. Locally varying rates based on simulation or kriging average $570 field^{-1} more revenue than the conventional approach of a label rate.

Locally varying herbicide rates provide economic and environmental advantages for consideration. The profit of locally varying rates is based on weed sampling. Costs of weed sampling may decline with secondary data, historical records and satellite imagery. Locally varying rates reduce environmental loading of herbicides by up to 40% compared to the

conventional approach. Locally varying herbicide rates need to be integrated into weed control management programs.

Acknowledgements

I wish to express my gratitude to Professor C. V. Deutsch for his interest and support throughout this study. Thanks to my fellow grad students who provided a rich diversity of culture in which to learn. I would like to gratefully acknowledge Dr. Gordon Thomas with Agriculture and Agri-Food Canada, Saskatoon, Saskatchewan who provided weed data.

I thank staff at Alberta Agriculture, Food and Rural Development for financial support to undertake this research project. To Jack Moes and the staff at Assiniboine Community College for their patience while I completed my write up.

Finally, I would like to acknowledge my family's enduring commitment, support and love as I persisted in graduate studies and made a dream come true.

Table of Contents

1 Problem Setting/Literature Review 1

1.1 Problem Setting . . . 2

1.2 Precision Spraying . . . 3

1.3 Sampling Procedure . . . 4

1.4 Weed Density Mapping . . . 6

1.4.1 Weed Density . . . 6

1.4.2 Spatial Variability . . . 6

1.4.3 Geostatistical Analysis . . . 7

1.4.4 Interpretation . . . 8

1.5 Model for Optimal Herbicide Treatment . . . 10

1.5.1 Herbicide Efficacy . . . 10

1.5.2 Consequences of Under- and Over-Spraying Herbicides . . . 10

1.5.3 Optimal Herbicide Rate . . . 12

1.6 Accounting for Uncertainty . . . 12

1.7 Outline . . . 13

2 Methodology 14

2.1 Weed Density Mapping . . . 14

2.1.1 Random Function . . . 15

2.1.2 First and Second Order Moments . . . 15

2.1.3 Decisions of Stationarity . . . 16

2.1.4 Variography . . . 16

2.1.5 Kriging and Simulation . . . 17

2.2 Sampling . . . 19

2.3 Model of Optimal Treatment . . . 20

2.4 Uncertainty . . . 27

2.4.1 Accounting for Uncertainty . . . 29
2.4.2 Alternative Methods . . . 30

3 Sampling **32**
3.1 Synthetic Data . . . 32
3.2 Case Study . . . 38
3.2.1 Nested and Square Patterns . . . 38
3.2.2 Costs . . . 39
3.3 Discussion . . . 48

4 Examples of Weed Density Mapping **50**
4.1 Data Description . . . 50
4.2 Saskatoon Data . . . 51
4.2.1 Statistics . . . 54
4.2.2 Variography . . . 54
4.3 Viking and Stony Plain Data . . . 71
4.3.1 Statistics . . . 71
4.3.2 Variography . . . 71
4.3.3 Reference Map . . . 72

5 Application **80**
5.1 Model Application . . . 82

6 A Comparative Example **96**
6.1 Approach . . . 96
6.2 Comparative Example . . . 97
6.3 Optimal Sampling Design . . . 116
6.4 Summary of Results . . . 122

7 Future Work and Implementation **126**
7.1 Implementation . . . 129
7.2 Conclusion . . . 130

8 Bibliography **132**

9 Appendix **144**

List of Tables

2.1 Mean and standard deviation of price, weed-free crop yields, and crop density for barley and canola from the literature (Ali, 2001; Atkinson, 2001; Harker, 2001; O'Donovan, 1991; O'Donovan et al., 1999; O'Donovan et al., 1988) [1, 4, 62, 108, 113, 114]. 29

2.2 Means and standard deviations for dose-responses of wild oat to 6 herbicides that are applied in barley and canola (Lemerle & Verbeek, 1995; Madsen et al., 1999; Olofsdotter et al., 1994) [84, 87, 116]. 29

3.1 Sampling pattern and number of sampling locations for square and nested. The number in parenthesis for each pattern indicates the number of times a particular pattern is repeated at different locations in the field. $Nest_{10}$ represents a nested sampling pattern with five different levels and 85 sampling locations. 35

3.2 Mean and variance of wild oat m^{-2} for square and nested sampling patterns compared to the synthetic distribution. 35

3.3 Spatial parameters for isotropic variograms of various sampling patterns compared to the reference wild oat distribution for one realization. "Cont." refers to the variance contribution of each nested structure. The variograms are modeled with 1, 2, or 3 nested spherical structures. 40

3.4 Sampling inefficiency, in dollars $sample^{-1}$, for 4 different square and nested sampling patterns using SIE_{M_1} and SIE_{M_2}. 48

4.1 The Bayer code name, Latin name, and common name of weed species measured in 1995, 1996 and 1997 for a field near Saskatoon, Saskatchewan. Weed species found in this field are referred to by the Bayer code in Table 4.2. . . 52

4.2 A summary table of the mean and standard deviation, in plants m^{-2}, for all the weeds near Saskatoon. Occurrence represents the percentage of the total sampling locations for which a weed species appears. The 1996 small is the 100 point sampling grid. 53

4.3 A summary table of the mean, standard deviation, and maximum count, in plants m^{-2}, for each weed category in each year near Saskatoon. 54

4.4 Directional parameters for indicator grass weed density variograms models for 1995, 1996 and 1997 near Saskatoon. "Cont." refers to the variance contribution of each nested structure. The direction of maximal continuity is the E-W direction and variograms are modeled with 2 nested spherical, structures. 61

4.5 Directional parameters for continuous grass weed density variograms models for 1995, 1996 and 1997 near Saskatoon. "Cont." refers to the variance contribution of each nested structure. Two or 3 nested spherical, structures are used to model each variogram. 63

4.6 Directional parameters for continuous broad-leaved weed density variogram models for 1995, 1996 and 1997 near Saskatoon. "Cont." refers to the variance contribution of each nested structure. Two nested spherical, structures are used to model each variogram. 67

4.7 A comparison of the mean wild oat density and occupied 1 m^{-2} quadrats from 2 fields, the top table being for Viking, Alberta and the bottom table from Stony Plain, Alberta over 2 years. Sample scale refers to distance between sampling locations of 100, 20, 5, and 1 m for large, medium, fine and super fine grids. 72

4.8 Omnidirectional variogram model parameters using the nested pattern of sampling for the Viking and Stony Plain sites. "Cont." refers to the variance contribution of each nested structure. Two nested spherical, structures are used to model each variogram. 72

4.9 Correlation coefficients between the reference wild oat density map and the kriged or simulated wild oat density map for fields near Viking and Stony Plain, Alberta. 77

4.10 Omnidirectional variogram model parameters using the grid map derived from the Viking and Stony Plain reference maps of each field. "Cont." refers to the variance contribution of each nested structure. A spherical model is used for the 3 nested structures for the Viking grid map while a spherical model is used for the first structure and a Gaussian model for the second nested structure in the Stony Plain grid map. 78

4.11 Wild oat density parameters for the reference, grid, kriged and simulated map. The grid map is sampled every 42 m for a total of 361 sampling locations in each 64 ha field near Viking and Stony Plain, Alberta. 78

5.1 Economic parameters for barley and canola yield loss due to wild oat with different herbicides. 81

5.2 Six herbicides applied to different crops using the crop-weed-herbicide model at one location with 51 simulated wild oat density values. The correlation is between herbicide rate and simulated wild oat density. Average wild oat density is 45.6 plants m^{-2} with a minimum of 3 to a maximum of 232. . . . 83

5.3 Six herbicides applied to different crops using the crop-weed-herbicide model at 361 locations with 51 simulated wild oat density values. The correlation is between herbicide rate and simulated wild oat density. Average wild oat density is 94.5 plants m^{-2} with a minimum of 0 to a maximum of 885. . . . 83

5.4 Six herbicides applied to different crops using the crop-weed-herbicide model on a 64 ha field (640000 locations) with 51 simulated wild oat density values. The correlation is between herbicide rate and simulated wild oat density. Average wild oat density is 65.4 plants m^{-2} with a minimum of 0 to a maximum of 950. 84

5.5 Average revenue, in dollars ha^{-1}, and wild oat density, plants m^{-2}, after herbicides have been applied to different crops using the crop-weed-herbicide model on a 64 ha field. Revenue from a constant rate represents herbicide applied at a constant 100% of label rate. 84

6.1 Sampling designs with a varying number of sample locations applied to two 64 ha fields near Stony Plain and Viking, Alberta. 97

6.2 Wild oat density parameters for the reference, sample, kriged and simulated prescription maps for a field near Viking, Alberta. The grid is sampled every 42 m on a square pattern for a total of 361 sampling locations in a 64 ha field. Single, double and triple refer to single, double, and triple wild oat density. 99

6.3 Wild oat density parameters for the reference, sample, kriged and simulated prescription maps for a field near Stony Plain, Alberta. The grid is sampled every 42 m on a square pattern for a total of 361 sampling locations in a 64 ha field. Single, double and triple refer to single, double, and triple wild oat density. 100

6.4 Average (Ave.) herbicide rates, in % m^2, for wild oat distributions in fields near Viking and Stony Plain, Alberta. Area, in %, that herbicide rates exceed label rate for different wild oat distributions. 100

6.5 Total revenue, in dollars ha^{-1}, for a 64 ha field near Viking, Alberta for different mapping options. Weed density, in plants m^{-2}, represents the number of wild oat after herbicide treatment. Maximum total revenue with no wild oat interference is \$349 ha^{-1}. 101

6.6 Total revenue, in dollars ha^{-1}, for a 64 field near Stony Plain, Alberta for different mapping options. Final weed density, in plants m^{-2}, represents the number of wild oat after herbicide treatment. Maximum total revenue with no wild oat interference is \$349 ha^{-1}. 102

6.7 Total revenue, in dollars ha^{-1}, for a 64 ha field near Viking, Alberta using different mapping options. Herbicide and application costs are included in the total revenue while maximum total revenue with no wild oat interference is \$22340 $field^{-1}$. 103

6.8 Total revenue, in dollars ha^{-1}, for a 64 ha field near Stony Plain, Alberta using different mapping options. Herbicide and application costs are included in the total revenue while maximum total revenue with no wild oat interference is \$22340 $field^{-1}$. 104

6.9 Total revenue, in dollars ha^{-1}, for two 64 ha fields near Viking and Stony Plain, Alberta using different mapping options. This revenue represents the difference between no herbicide and a herbicide prescription. 105

6.10 Revenue, in dollars field^{-1}, for 3 sampling designs and 3 configurations from a 64 ha field of barley near Stony Plain, Alberta. Weed density, in plants m^{-2}, represents the number of wild oat after herbicide treatment and the field average is 65 plants m^{-2}. 116

6.11 Revenue and wild oat density differences, in dollars field^{-1}, when comparing 3 sampling designs and 3 configurations to a conventional approach from a 64 ha field of barley near Stony Plain, Alberta. The conventional approach is a 100% rate of herbicide. Weed density, in plants m^{-2}, represents the number of wild oat after herbicide treatment. 118

6.12 Profitability, in dollars field^{-1}, for 3 sampling designs and 3 configurations from a 64 ha field of barley near Stony Plain, Alberta. The *Gridnest* design used the variogram from a nested design while the other designs used the variogram from their design. Maximum attainable profit for this field given the reference weed distribution and corresponding herbicide rate is $19280. 119

6.13 Profitability, in dollars field^{-1}, for 3 sampling designs and 3 configurations from a 64 ha field of barley near Viking, Alberta. The *Gridnest* design used the variogram from a nested design while the other designs used the variogram from their design. Average wild oat density is 35 plants m^{-2} for this field. Maximum attainable profit for this field with the reference weed distribution and corresponding herbicide rate is $19400. 119

List of Figures

1.1 The economic threshold for controlling a weed is W_1. The cost of weed control is C. The dashed line is the value of increased yield (Auld et al., 1987) [6]. 11

2.1 A semivariogram function for a spherical isotropic model with a nugget variance (0.20). The dots represent calculated points of the experimental semivariogram while the solid line is the model semivariogram. 17

2.2 Exponential weight function, $wt(\mathbf{h}_s)$, for different distances. 20

2.3 Schematic illustration of fractional weed-free crop yield attained, $f(\mathbf{u})$, compared to increasing weed density, d, for a crop seeded at 100 plants m^{-2} using Equation 2.26. 22

2.4 Schematic illustration of fractional weed-free crop yield, $f(\mathbf{u})$, compared to t, the relative time of emergence in days of weeds compared to the crop. Zero on the x axis represents crop and weed plants emerging at the same time while a negative value represents weeds emerging earlier than the crop and a positive value is crop emerging before weeds. 22

2.5 Schematic illustration of fractional weed-free crop yield, $f(\mathbf{u})$, compared to increasing crop density, c, for a crop infested with 100 weeds m^{-2} using Equation 2.26. 23

2.6 Schematic displaying a relationship between herbicide application rate, g ai ha^{-1}, and fractional weed control, $H(a)$, indicating that as herbicide rate increases, a higher proportion of weeds are controlled. 24

2.7 Schematic rate-response curve, where ED_{50} represents a herbicide rate, 1X, that causes 50% injury as measured by a decrease in the fractional control of a weed. The parameter, m, describes the slope of the curve that occurs where the ED_{50} value is indicated. The upper limit near 1, A, is fractional weed control at a zero herbicide rate and the lower limit near 0, B, is fractional weed control for a high rate of herbicide (Streibig, 1988) [141]. 25

2.8 Increasing application rate, a, results in increased herbicide application costs but decreased crop yield loss costs. The herbicide cost $hc(\mathbf{u})$ (short dash) and cost due to crop loss from weeds $r(\mathbf{u})$ (solid line) are summed to obtain herbicide cost + crop loss cost $pc(\mathbf{u})$ (long dash). The optimal herbicide rate, $a_{opt}(\mathbf{u})$, is indicated by the black arrow. 26

2.9 An example of the models that form part of the methodology to determine optimal herbicide treatment for a weed infestation in a crop. Optimal rate is 80% of the recommended rate in this example. 28

2.10 Probability distribution of optimal herbicide rates (bottom figure) from 51 realizations of weed density at a single location based on the crop-weed-herbicide model. The arrow points to the expected value that is optimal for this model from the probability distribution. 31

2.11 Four probability distributions of cost from 51 realizations of weed density at a single location based on the crop-weed-herbicide model. The arrow points to the minimum expected cost that is optimal for this model. The black, curved line represents expected cost that is an average of the 51 realizations. 31

3.1 Histogram and location map of wild oat density from a field near Stony Plain, Alberta. This is used for generating unconditional simulated wild oat densities for evaluating different sampling schemes. Wild oat, in plants m^{-2}, are identified at each location. Increasing greyscale indicates increasing wild oat density so white is no wild oat while black represents over 200 wild oat m^{-2}. 33

3.2 Original variogram of wild oat density in a 64 ha field near Stony Plain, Alberta (solid line is model and dashed line is experimental). 34

3.3 Histogram and map of synthetic reference wild oat densities from a field near Stony Plain, Alberta that is used for assessment of sampling patterns. . . . 34

3.4 Wild oat sampling locations for 10 x 10, 13 x 13, 19 x 19, and 38 x 38 nodes for the square patterns. 36

3.5 Wild oat sampling locations at 102, 171, 355 and 1422 nodes for the nested patterns, that is $Nest_{10}$, $Nest_{13}$, $Nest_{19}$, and $Nest_{38}$. 37

3.6 M_1 and M_2 for square and nested sampling designs at different sampling numbers. M_2 represented by the dots is an average of the variogram values from 11 synthetic references. The solid line represents the square while the dashed line is the nested pattern. 38

3.7 M_1 and M_2 for square and nested sampling designs at different sample spacing. M_2 represented by the large dots is an average of the variogram values from 11 synthetic references. The solid line represents the square while the dashed line is the nested pattern. 39

3.8 Kriged wild oat distributions using the 4 different square sampling patterns. These kriged maps are generated for M_1 calculation. 40

3.9 Model variograms fitted from the experimental variogram using the 4 different square sampling patterns. The dashed line is the reference variogram while the solid line is the model. These variograms are generated for M_2 calculation. 41

3.10 Model and experimental variograms are shown on logarithm scale using the square patterns. The dashed line is the reference variogram while the solid line is the model. These variograms are generated for M_2 calculation. . . . 42

3.11 Kriged wild oat distributions using the 4 different nested sampling patterns. These kriged maps are generated for M_1 calculation. 43

3.12 Model variograms fitted from the experimental variogram using the 4 nested patterns. The dashed line is the reference variogram while the solid line is the model. 44

3.13 Model and experimental variograms are shown on logarithm scale using the nested patterns. The dashed line is the reference variogram while the solid line is the model. 45

3.14 Scatterplots of reference and estimated values for square patterns. 46

3.15 Scatterplots of reference and estimated values for nested patterns. 47

4.1 A map of weed density sampling locations for 1995, 1996 and 1997 from left to right near Saskatoon. Weed species and counts, in plants m^{-2}, are identified at each location. Increasing greyscale indicates increasing weed density so white is no weeds while black represents over 200 broad-leaved weeds m^{-2}. 51

4.2 A map of weed density sampling locations of two small grids taken in 1996 near Saskatoon. The grid in the north-east corner of the field is used for variography. The small dots represent sampling locations of weed density in 1996 and 1997. Weed species and counts, in plants m^{-2}, are identified at each location. 52

4.3 Histograms of the weed data near Saskatoon for each year. The histograms on the left are for grass weeds and the histograms on the right are for broad-leaved weeds. The top two histograms are 1995 data, the middle two histograms 1996 data, and the bottom two histograms 1997 data. 55

4.4 Histograms of grass and broad-leaved weed data for all years, 1995 to 1997, near Saskatoon. The histogram on the left is for grass weeds and the histogram on the right is for broad-leaved weeds. 56

4.5 Scatter plots of grass weed density compared to broad-leaved weed density for 1995, 1996, and 1997 near Saskatoon indicating that there is no correlation between grass and broad-leaved weed data. 56

4.6 Omnidirectional, experimental variograms of the continuous broad-leaved data near Saskatoon. The variogram on the top left is from 1995, top right is from 1996, bottom left is from 1997, and the bottom right is from the small grid in 1996. 57

4.7 Omnidirectional, experimental variograms of the continuous grass data near Saskatoon. The variogram on the top left is from 1995, top right is from 1996, bottom left is from 1997, and the bottom right is from the small grid in 1996. 58

4.8 Directional, experimental variograms of the continuous grass data near Saskatoon. The variogram on the top left is from 1995, top right is from 1996, bottom left is from 1997, and the bottom right is from the small grid in 1996. The dark, solid line is the experimental variogram in the direction of maximal continuity ($N90^oE$), and the fine, dashed line represents the experimental variogram for the direction of least continuity ($N0^oE$). 59

4.9 Directional, experimental variograms of the continuous broad-leaved data near Saskatoon. The variogram on the top left is from 1995, top right is from 1996, bottom left is from 1997, and the bottom right is from the small grid in 1996. The dark, solid line is the experimental variogram in the direction of maximal continuity ($N90^oE$), and the fine, dashed line represents the experimental variogram for the direction of least continuity ($N0^oE$). 60

4.10 The 1995 directional, indicator, variograms of continuous grass data near Saskatoon. The gray dashed and solid lines represent variograms in the direction of maximal continuity, and the dark dashed and solid lines are variograms in the direction of least continuity. The gray and dark solid lines are model variograms while the gray and dark dashed lines represent experimental variograms. 62

4.11 The 1996 directional, indicator, variograms of continuous grass data near Saskatoon. The gray dashed and solid lines represent variograms in the direction of maximal continuity, and the dark dashed and solid lines are variograms in the direction of least continuity. The gray and dark solid lines are model variograms while the gray and dark dashed lines represent experimental variograms. 62

4.12 The 1997 directional, indicator, variograms of continuous grass data near Saskatoon. The gray dashed and solid lines represent variograms in the direction of maximal continuity, and the dark dashed and solid lines are variograms in the direction of least continuity. The gray and dark solid lines are model variograms while the gray and dark dashed lines represent experimental variograms 63

4.13 Two realizations from sequential indicator simulation of weed density for grass data for 1995, 1996 and 1997 near Saskatoon. The top figures are 1995, the middle are 1996, and the bottom are 1997 where black represents presence of grass weeds. 64

4.14 The 1995 directional variograms of continuous grass data near Saskatoon. The gray dashed and solid lines represent variograms in the direction of maximal continuity, and the dark dashed and solid lines are variograms in the direction of least continuity. The gray and dark solid lines are model variograms while the gray and dark dashed lines represent experimental variograms. 65

4.15 The 1996 directional variograms of continuous grass data near Saskatoon. The gray dashed and solid lines represent variograms in the direction of maximal continuity, and the dark dashed and solid lines are variograms in the direction of least continuity. The gray and dark solid lines are model variograms while the gray and dark dashed lines represent experimental variograms. 65

4.16 The 1997 directional variograms of continuous grass data near Saskatoon. The gray dashed and solid lines represent variograms in the direction of maximal continuity, and the dark dashed and solid lines are variograms in the direction of least continuity. The gray and dark solid lines are model variograms while the gray and dark dashed lines represent experimental variograms. 66

4.17 The 1995, 1996 and 1997 directional variograms of continuous broad-leaved data near Saskatoon. The gray dashed and solid lines represent variograms in the direction of maximal continuity, and the dark dashed and solid lines are variogram in the direction of least continuity. The gray and dark solid lines are model variograms while the gray and dark dashed lines represent experimental variograms. 67

4.18 The 1995 simulated, variograms of continuous broad-leaved data near Saskatoon. The solid line represent the variogram model while the dashed lines are the variogram models for each of the 11 realizations for the E-W direction. 68

4.19 The 1996 simulated, variograms of continuous broad-leaved data near Saskatoon. The solid line represent the variogram model while the dashed lines are the variogram models for each of the 11 realizations for the E-W direction. 68

4.20 The 1997 simulated, variograms of continuous broad-leaved data near Saskatoon. The solid line represent the variogram model while the dashed lines are the variogram models for each of the 11 realizations for the E-W direction. 69

4.21 Simulation of broad-leaved weed density data illustrating a realization and histogram of the 1995 (left) and 1996 (right) weed distributions for the Saskatoon site. The last interval of weed density for the 1995 histogram represents number of weeds greater than 125 plants m^{-2}. 69

4.22 Simulation of 1997 broad-leaved weed density data illustrating a realization with a histogram of the weed distribution for that realization for the Saskatoon site. 70

4.23 A histogram and map of wild oat density sampling locations from a field near Viking, Alberta in 2000 that is used for generating a synthetic, reference wild oat distribution. Wild oat, in plants m^{-2}, is identified at each location. Increasing greyscale indicates increasing wild oat density so white is no wild oat present while black represents over 200 wild oat m^{-2}. 71

4.24 Omnidirectional variogram models from the nested sampling pattern of wild oat density for each 64 ha field near Stony Plain, Alberta (left) and Viking, Alberta (right). The solid lines are model variograms while the dashed lines represent experimental variograms. 73

4.25 Directional variograms of continuous wild oat data from a nested sampling pattern for each 64 ha field near Stony Plain, Alberta (left) and Viking, Alberta (right). The dashed lines are model variograms while the solid lines represent experimental variograms. The gray solid and short dashed lines represent variograms in the direction of least continuity, and the dark dashed and solid lines are variograms in the direction of maximal continuity. 73

4.26 Kriged maps and histograms of wild oat density from fields near Viking, Alberta (left) and Stony Plain, Alberta (right). 74

4.27 Simulated maps and histograms of wild oat density from fields near Viking, Alberta (left) and Stony Plain, Alberta (right). Each simulated map is one realization. The last interval of wild oat density for the Stony Plain histogram represents number of weeds greater than 200 plants m^{-2}. 75

4.28 Reference map (left) of wild oat density for a 64 ha field near Viking, Alberta and location map (right) of wild oat density for grid map from this same field. 76

4.29 Reference map (left) of wild oat density for a 64 ha field near Stony Plain, Alberta and location map (right) of wild oat density for grid map from this same field. 76

4.30 Omnidirectional variogram models for the grid maps of wild oat density for a 64 ha field near Viking, Alberta (left) and Stony Plain, Alberta (right). The solid lines are model variograms while the dashed lines represent experimental variograms. 77

4.31 A kriged and simulated weed density map, in wild oat plants m^{-2}, from a 64 ha field near Viking, Alberta. The simulated wild oat density map represents one realization. 78

4.32 A kriged and simulated weed density map, in wild oat plants m^{-2}, from a 64 ha field near Stony Plain, Alberta. The simulated wild oat density map represents one realization. 79

5.1 Comparison of dose-response curves for diclofop-methyl, fenoxaprop, and tralkoxydim where different herbicide rates result in different levels of wild oat injury as measured by a per cent decrease in weed biomass. 81

5.2 A histogram of wild oat density, in plants m^{-2}, for simulation at one location and the kriged weed density value for that location indicated by the dashed line (top, left figure). A comparison of the kriged, tralkoxydim cost curve (solid curve) and the average of 51 realizations from simulation (dashed curve) at the same location (top, right figure). A histogram of expected loss revenue, in dollars ha^{-1}, for simulation at one location and the kriged revenue value for that location indicated by the dashed line (bottom, left figure). The average of 51 realizations (black curve) and the 51 realizations (gray curves) from simulation at the same location (bottom, right) with the solid line indicating optimal herbicide rate. 86

5.3 Optimal diclofop-methyl (left) and fenoxaprop (right) cost curves in barley, in % m^{-2}, at one location from kriging (top figures). A comparison of the kriged, diclofop-methyl (left) and fenoxaprop (right) cost curves (solid curve) and the average of 51 realizations from simulation (dashed curve) at the same location (middle figures). The average of 51 realizations (black curve) and the 51 realizations (gray curves) from simulation at the same location for diclofop-methyl (left) and fenoxaprop (right), respectively (bottom figures) with the solid line indicating optimal herbicide rate. 87

5.4 A histogram of wild oat density, in plants m^{-2}, for simulation at one location and the kriged weed density value for that location indicated by dashed line (top, left figure). A comparison of the kriged, imazethapyr cost curve (solid curve) and the average of 51 realizations from simulation (dashed curve) at the same location (top, right figure). A histogram of expected loss revenue, in dollars ha^{-1}, for simulation at one location and the kriged revenue value for that location indicated by the dashed line (bottom, left figure). The average of 51 realizations (black curve) and the 51 realizations (gray curves) from simulation at the same location (bottom, right) for imazethapyr with the solid line indicating optimal herbicide rate. 88

5.5 Optimal glufosinate (left) and glyphosate (right) cost curves in canola, in % m^{-2}, at one location from kriging (top figures). A comparison of the kriged, glufosinate (left) and glyphosate (right) cost curves (solid curve) and the average of 51 realizations from simulation (dashed curve) at the same location (middle figures). The average of 51 realizations (black curve) and the 51 realizations (gray curves) from simulation at the same location for glufosinate (left) and glyphosate (right), respectively (bottom figures) with the solid line indicating optimal herbicide rate. 89

5.6 Wild oat density, in plants m^{-2}, for a 64 ha field near Stony Plain, Alberta prior to herbicide treatment (top left). The other maps are optimal herbicide rates, in % m^{-2}, for tralkoxydim (top right), fenoxaprop (bottom left), and glyphosate (bottom right). 90

5.7 Wild oat density, in plants m^{-2}, after treatment with tralkoxydim (top right), fenoxaprop (bottom left), and glyphosate (bottom right) compared to the same 64 ha field near Stony Plain with no herbicide treatment (top left). . . 91

5.8 Average expected revenue loss, in dollars ha^{-1}, for a barley and canola crop after herbicide has been applied to wild oat using the crop-weed-herbicide model in a 64 ha field near Stony Plain, Alberta as wild oat density, in plants m^{-2}, varies. Each average expected revenue value represents wild oat density values from 640000 locations. 92

5.9 Average expected revenue, in dollars ha^{-1}, for a barley and canola crop after herbicide has been applied to wild oat using the crop-weed-herbicide model in a 64 ha field near Stony Plain, Alberta as crop density, in plants m^{-2}, varies. Each average expected revenue value represents crop density values from 640000 locations. 93

5.10 Average expected revenue, in dollars ha^{-1}, for a barley and canola crop after herbicide has been applied to wild oat using the crop-weed-herbicide model in a 64 ha field near Stony Plain, Alberta as time of weed emergence, in days, varies. The dashed line represents when crop and wild oat emerge at the same time. Each average expected revenue value represents time of wild oat emergence values from 640000 locations. 93

5.11 Increasing herbicide application rate, in % m^{-2}, of diclofop-methyl, fenoxaprop and tralkoxydim on the left and imazethapyr, glufosinate and glyphosate on the right for treatment of wild oat in barley and canola in a 64 ha field near Stony Plain, Alberta. The herbicide cost $hc(\mathbf{u})$(long dash) and cost due to crop loss from wild oat $r(\mathbf{u})$(short dash) are summed to obtain herbicide cost + crop loss cost $pc(\mathbf{u})$(solid). The optimal herbicide rate, $a_{opt}(\mathbf{u})$, is indicated by the medium dashed vertical line. Each average expected revenue value, in dollars ha^{-1}, represents 640000 locations. 94

5.12 Average wild oat density, in plants m^{-2}, after herbicide treatment using the crop-weed-herbicide model in a 64 ha field near Stony Plain, Alberta as herbicide rate, in % m^{-2}, varies. Each average wild oat density represents 640000 locations. Rates of tralkoxydim (long dash), fenoxaprop (short dash), and diclofop-methyl (solid) in a barley field (right figure) and rates of glyphosate (long dash), glufosinate (short dash), and imazethapyr (solid) in a canola field (left figure). Average wild oat density is 65.4 plants m^{-2} with no herbicide. 95

6.1 Wild oat density, in number m^{-2}, from kriging (left) and simulation (right) from a 64 ha field near Viking, Alberta. The simulation represents one realization. 98

6.2 Wild oat density, in number m^{-2}, from kriging (left) and simulation (right) from a 64 ha field near Stony Plain, Alberta. The simulation represents one realization. 98

6.3 Total revenue, in dollars m^{-2}, for no herbicide, a 100% herbicide rate, a kriged map and simulated map of herbicide rates for a single wild oat density at Viking, Alberta. 105

6.4 Total revenue, in dollars m^{-2}, for no herbicide, a 100% herbicide rate, a kriged map and simulated map of herbicide rates for a single wild oat density at Stony Plain, Alberta. 106

6.5 The top kriged (right) and simulated (left) maps of herbicide rates, in % m^{-2}, for a single wild oat density from a field near Viking, Alberta. The bottom histograms are the kriged (left) and simulated maps (right) of herbicide rates. 107

6.6 The top kriged (right) and simulated (left) maps of herbicide rates, in % m^{-2}, for a double wild oat density from a field near Viking, Alberta. The bottom histograms are the kriged (left) and simulated maps (right) of herbicide rates. 108

6.7 The top kriged (right) and simulated (left) maps of herbicide rates, in % m^{-2}, for a triple wild oat density from a field near Viking, Alberta. The bottom histograms are the kriged (left) and simulated maps (right) of herbicide rates. 109

6.8 Histograms of a single wild oat density, in plants m^{-2}, for kriged (top) and simulated (bottom) maps for the Viking (left) and Stony Plain (right) fields. The last interval of weed density for each histogram represents number of weeds greater than 100 or 250 plants m^{-2}. 110

6.9 Histograms of revenue, in dollars ha^{-1}, for a single, simulated wild oat density at the Viking (left) and Stony Plain (right) sites. The histograms characterize uncertainty in revenue from the simulated maps. 111

6.10 The top kriged (left) and simulated (right) maps of herbicide rates, in % m^{-2}, for a single wild oat density from a field near Stony Plain, Alberta. The bottom histograms are the kriged (left) and simulated maps (right) of herbicide rates. 112

6.11 The top kriged (left) and simulated (right) maps of herbicide rates, in % m^{-2}, for a double wild oat density from a field near Stony Plain, Alberta. The bottom histograms are the kriged (left) and simulated maps (right) of herbicide rates. 113

6.12 The top kriged (left) and simulated (right) maps of herbicide rates, in % m^{-2}, for a triple wild oat density from a field near Stony Plain, Alberta. The bottom histograms are the kriged (left) and simulated maps (right) of herbicide rates. 114

6.13 Kriged and simulated herbicide rates, in % m^{-2}, for a single wild oat density from the Viking (top) and Stony Plain (bottom) fields. 115

6.14 Wild oat densities, in plants m^{-2}, for reference, kriged $Grid_{10}$, simulated $Grid_{10}$ and simulated $Square_7$ designs, clockwise respectively, for a field near Stony Plain, Alberta in 2000. For the simulated $Grid_{10}$ and $Square_7$ designs, this is one realization of 101. 120

6.15 Herbicide rates, in % m^{-2}, for reference, kriged $Grid_{10}$, simulated $Grid_{10}$ and simulated $Square_7$ designs, clockwise respectively, for a wild oat infested field near Stony Plain, Alberta in 2000. 121

6.16 Wild oat densities, in plants m^{-2}, for reference, kriged $Grid_{10}$, simulated $Grid_{10}$ and simulated $Gridnest_{10}$ designs, clockwise respectively, for a field near Viking, Alberta in 2000. For the simulated $Nest_{10}$ and $Gridnest_{10}$ designs, this is one realization of 101. 123

6.17 Herbicide rates, in % m^{-2}, for reference, kriged $Grid_{10}$, simulated $Grid_{10}$ and simulated $Gridnest_{10}$ designs, clockwise respectively, for a wild oat infested field near Viking, Alberta in 2000. 124

Chapter 1

Problem Setting/Literature Review

Wild oat is an expensive weed to control in annual cropped areas of western Canada and northern United States. Wild oat herbicides represent one third of the total cash cost of growing a cereal or oilseed crop. Yield loss due to wild oat is also costly. In barley (*Hordeum vulgare*), the most competitive of spring seeded cereal and oilseed crops, yield may be reduced 12% to 26% depending on when wild oat seedlings emerge (O'Donovan et al., 1985) [111]. Because wild oat herbicides are applied to more than 60% of the cropped acres in western Canada, there is an environmental cost as well (Anonymous, 2001) [3]. Some wild oat herbicides have been found in ground water. Optimizing herbicide application rates would reduce environmental impact.

Most of the agricultural landbase seeded to annual crops in Alberta is sprayed by private herbicide applicators. Herbicide application involves scouting fields to determine the weed species and their density. Scouting and other weed density measurements can provide accurate maps of weed distributions for herbicide application.

Wild oat spatial distributions have been characterized as patchy (Colliver et al., 1996) [25]. "Patchy" refers to clearly defined areas that contain weeds in a background of low weed densities. Wild oat spatial characteristics have not been documented in western Canada by weed scientists. However, it is expected that their spatial correlation is similar to other international studies (Hanson et al., 1995; Lamb et al., 1999; Thorton et al., 1990) [61, 83, 150].

Western Canadian farm managers could realize substantial economic benefit since cereal crops are grown on a majority of the Prairies. Locally varying herbicide rates may result in a 27-95% decrease in herbicide per hectare, compared to a constant rate, with no effect on crop yield (Johnson et al., 1995a; Rew et al., 1996) [75, 127]. Moreover, increased herbicide application would be restricted to high weed density areas.

This research will focus on weed density data to gain insight into (1) optimal sampling methodology for characterizing wild oat distributions, (2) appropriate procedures for weed density mapping, and (3) procedures for determining optimal application rate, accounting for uncertainty. Optimal herbicide rate refers to a rate that maximizes profit per hectare.

1.1 Problem Setting

Wild oat is one of the most prolific weeds in western Canada and is expensive to control (Thomas et al., 1998) [147]. Wild oat appears to be a suitable target for site specific spraying with optimal herbicide rate determination because of its control costs and spatial distribution.

Traditionally, the decision to control wild oat distributions has been to apply a uniform rate of herbicide at the manufacturer's recommended rate (Anonymous, 1998; Dieleman & Mortensen 1998) [2, 40]. More recently, site specific herbicide application is being implemented to control weed populations (Dieleman & Mortensen 1998; Nordho & Christensen 1995) [40, 106]. This type of application can take two forms: (1) the sprayer is turned on where weeds are present, or (2) continuous herbicide application with varying rate that depends on weed density.

Site specific weed management involves characterizing the local weed density and the effect on the crop yield. Optimal herbicide rates are those that (1) maximize total crop revenue, (2) minimize the adverse economic consequences of over- or under-spraying, and (3) account for uncertainty.

Quantifying the spatial distribution of weeds using risk and uncertainty has not been considered by the agriculture industry (Cardina et al., 1997) [16]. Mapping techniques such as kriging create smooth maps and do not provide a quantitative measure of uncertainty (Gerhards et al., 1997; Goovaerts, 1999) [50, 54]. Multiple geostatistical realizations provide a model of spatial uncertainty, for example, high weed densities are certain if they are seen on most of the simulated weed density maps. Determining the spatial relationships of weeds may allow locally variable herbicide application.

Locally variable rates of herbicides depend on several factors including (1) precision spraying, (2) spatial distribution of weeds, (3) efficacy of herbicide at different rates, (4) the economic and environmental consequences of under- or over- spraying, and (5) uncertainty in our knowledge of the true distribution of weeds.

Precision spraying equipment may be modified to apply locally variable rates of herbicide. Applications reported in the literature have been for areas smaller than 4 ha with prototype machines (Goudy, 2000) [55]. On/off herbicide application to a 28 ha field was reported in one study (Faechner & Hall, 1999) [46]. Locally varying rates of herbicide have not been reported in the literature. However, anecdotal evidence suggests that some farm managers are varying herbicide rates (Dieleman, 1998) [39]. Spray equipment in western Canada typically has a boom length of 20 to 40 m, that can be altered to apply different rates for each half. Larger scales of application are technically possible but not commercially available at this time.

A crop's competitive position relative to the weeds is enhanced by herbicide treatment. Crop yield response will determine the herbicide rate that is economically beneficial to apply and in areas of low weed density, low rates of herbicide will ensure that the crop is competitive and has the potential to yield (Faechner et al., 2002) [48]. No consideration has been given to the spatial nature of weed infestations in determining economic thresholds for label rates of herbicide (Cousens, 1985; Cousens & Mortimer, 1995) [27, 30].

Predicted crop yield loss may be overestimated with a random distribution compared to a patchy distribution (Brain & Cousens, 1990) [12]. This could result in lower than necessary thresholds for weed control and over-application of herbicide.

Herbicide efficacy is a measure of a herbicide's performance based on reduction in the

weed biomass (Dieleman, 1998) [39]. This estimate is used to determine an appropriate label rate that effectively controls a weed without damaging the crop under a range of environmental conditions. In Canada, the label rate is legally required to reduce the weed biomass by at least 80% (Anonymous, 1998) [2]. Rates below the label rates are not supported by the manufacturer and risk of non-performance is assumed by the producer or applicator. Regardless of herbicide application rate there will be weed escapes and additions to the weed seed bank. Moreover, there may be weeds that germinate after spraying or weed seeds that lay dormant for one or more years. For these reasons, weed control is an ongoing requirement; it is impractical to eradicate a weed species with spraying.

Herbicide efficacy is influenced by the crop and weed stage and other environmental conditions (Dieleman & Mortensen, 1998) [40]. Weeds are controlled at an earlier stage of development more easily than at a later stage of growth. This affects the rate of herbicide chosen to achieve the desired level of control. Timing the herbicide application in response to the weed and crop stage attempts to maximize the herbicide's effect by spraying weeds at their most susceptible stage while minimizing crop damage (Dieleman & Mortensen, 1998) [40]. Environmental conditions such as temperature, humidity, sunlight, and rainfall will affect the rate and uptake of herbicide (Cousens & Mortimer, 1995; Devine, 1989; Devine et al., 1993) [30, 37, 38].

Spraying a herbicide below recommended label rate may result in weed escapes or partial treatment so seed is added to the seed bank in the soil. This may result in lower crop yield or higher herbicide requirements in subsequent years. In contrast, over-spraying is expensive in terms of extra herbicide and it may lead to environmental loading of herbicides on non-target organisms.

This research will characterize the spatial variability of wild oat with a view to designing optimal herbicide application strategies.

1.2 Precision Spraying

Two methods have been adopted to utilize precision spraying technologies (Johnson et al., 1997) [73]. In the first approach, weed monitoring and spraying are carried out simultaneously (real-time concept). Currently, real time precision application is limited to non-cropped areas because of poor discrimination of weeds from crops (Blackshaw et al., 1998; Gerhards et al., 1997; Thompson et al., 1991) [9, 50, 149]. In the second approach, weeds are mapped prior to spraying, a prescription map is developed, and locally variable application is made on the basis of that map (Faechner et al., 2002; Lutman & Perry, 1999; Miller et al., 1995) [48, 86, 95].

Patch spraying was simulated to determine the reduction in herbicide for the spatial resolution of the sprayer and weed. The reduction in herbicide comparing a whole field application to patch spraying was 41% for a sprayer with a resolution of 1 x 1 m (Wallinga et al., 1998) [153]. In another study, the predicted savings accrued over a 10 year period by on/off spraying with a sprayer resolution of 4 x 4 m compared to a constant herbicide rate varied from 1% to 21% annually depending on the weed distribution (Rew et al., 1997) [128]. Patch spraying at a resolution less than 6 x 6 m would provide an economic advantage over blanket spraying especially when weed density is low and dispersal distance is short (Paice et al., 1998) [117].

Research that compares precision spraying application to conventional broadcast spraying on a 64 ha field is limited. Site specific was compared to broadcast herbicide application

over 2 years for broad-leaved and grass weeds in a 4 ha field (Goudy, 2000) [55]. The average area sprayed in site specific treatments was reduced by 26% and crop yields from these treatments were not significantly different from the broadcast application. Prescription maps have been derived for small fields (3.8 and 2.5 ha) of winter wheat and it was found that 21% less herbicide was applied (Gerhards et al., 1997) [50].

1.3 Sampling Procedure

Field sampling or ground based scouting for herbicide application relies on assessing the weed species and density by field counts, converting these data to a map that controls the field sprayer equipment (Nordho et al., 1994) [105]. Weed assessment for effective herbicide rate maps will depend on verifying weed densities (Faechner & Hall, 1999; Lutman & Perry, 1999) [46, 86]. Variations of these weed monitoring techniques have been summarized from studies in Europe (Christensen et al., 1998) [21].

Spatial variability was detected for pigweed (*Amaranthus spp.*) and nightshade (*Solanum spp.*) in a center pivot irrigated field of corn using regular grid and a random-directed grid sampling (Wyse-Pester et al., 1999) [165]. Unexplained variation accounted for 78% of the variance for pigweed compared to 13% for nightshade over a range of 80 m.

Sampling design has been investigated by simulation to provide insight into how sampling plans for weeds can be evaluated (Wiles et al., 1992) [158]. Weed density data, gathered from 14 North Carolina soybean fields, was simulated by bootstrapping that is a statistical resampling technique for quantification of uncertainty. This simulation procedure assumes the weed density data are independent and uncorrelated with each other.

For an understanding of weed dynamics and biology, sampling pattern can vary in spacing and quadrat size. A recent survey of published studies for weed sampling indicated that grid spacing varied from 1.8 m to 40 m while weed sample size varied from 0.0025 to 1.46 m^{-2} (Rew & Cousens, 2001) [125]. Only one scale was chosen for discrete sampling in each study. One of the limitations from a weed ecology perspective is that none of these studies incorporated any analysis of scale.

Knowing the variogram for an attribute of interest allows kriging estimates to be made. A square grid was used at different intervals for sampling 3 soil properties at 3 different farms (McBratney & Webster, 1983) [93]. Estimation variance for loam thickness was 0.51 for kriging compared to 1.74 for the classical method of estimating sample size with probability levels and a Student t test (McBratney & Webster, 1983) [93]. Sampling methods can be evaluated by determining the estimation variance from the predictions provided by kriging (Burgess et al., 1981; Corsten & Stein, 1994; McBratney & Webster, 1983; Olea, 1984; Yeakel et al., 1992) [15, 26, 93, 115, 166].

Sampling patterns have been investigated for different natural resource phenomena such as soil (Burgess et al., 1981; Russo, 1984) [15, 131], geology (Yeakel et al., 1992) [166], shrimp (Simard et al., 1992) [136], forestry (Matern, 1960) [89], weeds (Nordho & Christensen, 1995; Nordho & Christensen, 1995; Rew et al., 2001; Wyse-Pester et al., 1999) [106, 107, 129, 165] and insects (Weisz et al., 1995) [156]. A triangular, square and equilateral grid were compared for soil properties with different spatial structures (McBratney & Webster, 1981) [92]. Equilateral, triangle grids at 45 m were found to be equivalent in estimation variance to square grids with sampling spacing of 41.8 m in one example (McBratney & Webster, 1981) [92]. In a second study, sampling patterns were compared using average standard error and maximum standard error of estimation from universal kriging of water wells (Olea, 1984)

[115].

A nested grid is a form of multistage sampling because higher staged units are nested within lower staged units (Pettitt & McBratney, 1981) [122]. A nested grid approach for outcrop sampling was described to minimize sample density while maximizing spatial information (Webster, 1985; Wollenhaupt et al., 1997; Yeakel et al., 1992) [155, 164, 166]. The disadvantage of this technique is uneven coverage. The lack of comparisons between nested sampling and other designs for weeds has been reported (Rew & Cousens, 2001; Wollenhaupt et al., 1997) [125, 164].

Weeds have been traditionally sampled at a single scale with a W pattern (Cardina et al., 1997; Gerhards et al., 1997) [16, 50]. Grid, random and a W sampling pattern were evaluated on two 65 ha fields in South Dakota. Grid sampling at 15 x 30 m or 30 x 30 m (676 and 1352 sampling locations) was found to require significant time and labour while random sampling a W pattern missed patch locations (Clay et al., 1999) [23].

A sampling interval of 10 x 10 m gave good visual agreement between actual weed counts and those derived from kriging (Heisel et al., 1996) [65]. When the sampling interval was reduced to 20 x 30 m, there was poor agreement between the actual observations and the kriged estimates. These conclusions are based on five weed species sampled twice from one field.

Scouting a soybean field to incorporate uncertainty about weed density estimates for optimal post-emergence herbicide application was described (Wiles et al., 1993) [157]. Scouting involved taking a sample every 0.4 ha. Decision making was improved for herbicide rate using the decision model $HERB_k$, a computer program that evaluates soybean yield loss due to patchy weeds compared to HERB, that evaluates soybean yield loss due to a uniform weed distribution.

Parametric sequential sampling was evaluated for highly skewed weed seedling distributions and found to be prohibitive due to the number of samples required to accurately estimate the variability (Johnson et al., 1996) [77]. This is a procedure for estimating weed densities where the sample size depends on a stopping criteria. Weed density data are assumed to be parametric and follow a known distribution model such as a negative binomial.

Binomial and presence/absence sampling protocols were evaluated by simulation and found to require less effort per quadrat but more quadrats when weeds are patchy (Gold et al., 1996) [52]. Taking 10 to 12 full-count quadrats per field, binomial sampling is comparable to or better than full-count random sampling in fields smaller than 10 ha (Krueger et al., 2000) [81]. Fields in western Canada are usually 64 ha and it is unknown whether this technique will be an economically viable sampling protocol.

Continuous mapping techniques using all terrain vehicles, combines or tractors have been reported for describing spatial variability of weeds (Hall & Faechner, 1999; Rew & Cousens, 1998) [59, 124]. There is a risk of missing patch locations due to a limited range of vision.

A contiguous grid was used to measure velvetleaf (*Abutilon theophrasti*) density in 1.75 m^{-2} quadrats (Dieleman, 1998) [39]. A patch that was 96 m^{-2} at Alda-east was found to have no spatial autocorrelation that was suggested to be due to low weed densities (mean of 0.16 to 1.74 weeds m^{-2}) and no weeds in a number of quadrats. Other researchers have used indicator kriging to elucidate spatial dependence with similar data (Mortensen et al., 1995) [101].

Short range information about weeds may be unknown and yet important in estimation

(Pettitt & McBratney, 1984) [122]. Longer range information is also necessary since herbicide application equipment is typically 30 to 40 m in length and up to 40 m in the direction of spraying given the time required for herbicide rate changes.

1.4 Weed Density Mapping

1.4.1 Weed Density

Yield loss equations describe the effect of increasing weed density on the crop and have been expressed as (Cousens, 1985) [27]:

$$Y = Y_{wf}\left\{1 - \frac{ID}{100(1 + ID/A)}\right\}$$

where Y is the estimated crop yield, Y_{wf} is the estimated weed-free yield, I is the initial slope, D is the weed density, and A is the asymptote. These parameters were derived using mean weed densities. At low weed densities, the yield loss approximates a linear response and as density increases, weeds begin to compete intraspecifically and yield loss approaches an asymptote (Cousens, 1985) [27]. Weed-free areas in a field can provide an estimate for determining weed-free yield while yield data collected with a yield monitor can validate the effects of weed interference on crop yield loss.

Time of emergence for wild oat was incorporated into a crop yield loss and weed density equation for western Canadian data on barley and wheat (Cousens et al., 1987) [28]. Barley was found to be more competitive to earlier timings of wild oat emergence compared to wheat. As well, there were significant differences in the parameters from year to year, implying that a crop yield loss equation has to be adjusted according to crop, weed and environmental factors each year.

Wild oat emergence influences crop yield loss, especially when wild oat emerges earlier or at the same time as the crop. In the absence of herbicide, and with wild oat densities of 54 and 46 plants m^{-2}, the yield loss in barley was 16% with the early emerging wild oat (0 - $\frac{1}{2}$ leaf stage) compared to 2% at the later stage ($\frac{1}{2}$ - $2\frac{1}{2}$ leaf stage) (Peters, 1984) [120].

Weed seed production per plant is the least near a high density patch center compared to a patch edge where weeds are at low densities (Rew & Cussans, 1995) [126]. As weed density increases, interference becomes severe, plants die, and weed seeds are fewer. Thus, an established patch is expected to expand from its edge, that results in the development of new patches (Rew & Cussans, 1995) [126].

1.4.2 Spatial Variability

The mean and variance are used to describe and compare weed populations in classical statistical analysis. Spatial variation in weed density is accounted for in crop yield losses (Cousens et al. 1985; Lindquist et al., 1998) [31, 85]. Crop yield loss was predicted for a homogeneous weed distribution using mean weed density estimates and compared to patchy weed densities that were spatially mapped. Yield loss was consistently higher for weeds assumed to be homogeneously distributed across the field.

Mean weed density may be meaningless for decision-making at a field scale given that weed densities vary spatially (Groenendael, 1988; Johnson et al., 1995a; Navas, 1991; Thorton et al., 1990; Wiles et al., 1991) [57, 75, 103, 150, 158]. Current decision-making uses mean weed density (Cousens et al., 1987; Maxwell, 1992) [28, 90]. Herbicide manufacturers

use mean weed densities to guide users in their choice of rates for weed control. Using mean weed densities when weeds are not uniformly distributed results in incorrect prediction of yield loss and herbicide application (Brain & Cousens, 1990; Lindquist et al., 1998) [12, 85].

1.4.3 Geostatistical Analysis

Geostatistics is a set of tools where the assumptions of sample independence and homogeneity are removed (Hamlett et al., 1986; Upchurch et al., 1991) [60, 152]. These tools measure the degree of dependence of samples. They have been applied extensively in mining and petroleum exploration but on a limited basis in the field of weed science (Bourgault et al., 1997; Deutsch & Journel, 1998; Goovaerts, 1997; Goovaerts, 1999; Isaaks & Srivastava, 1989; Journel & Huijbregts, 1978) [11, 36, 53, 54, 71, 79].

A geostatistical analysis of wild oat data could consist of, (1) exploratory data analysis using descriptive statistics, (2) spatial continuity of wild oat density, (3) map building based on kriging and simulation, and (4) decision making in the presence of spatial uncertainty (Deutsch & Journel, 1998; Goovaerts, 1997; Isaaks & Srivastava, 1989) [36, 53, 71].

Spatial continuity of variables has led to the theory of regionalized variables. A random function (RF) is a set of random variables (RV) $Z(\mathbf{u})$ defined over multiple locations $\mathbf{u}$. The mathematical representation of this spatial variability may be provided by a random function concept (Isaaks & Srivastava, 1989; Journel, 1989; Journel & Huijbregts, 1978) [71, 78, 79].

Spatial modeling begins with determining the variogram parameters for a particular model (Johnson et al., 1996) [74]. Variogram analysis can be used to compare observations at different distances and directions. Weeds have significant large scale variability (Cardina et al., 1995; Cardina et al., 1996; Donald, 1994; Johnson et al., 1995) [17, 18, 44, 76]. Researchers found this distance to vary from 3.5 to 63 m for common lambsquarters, 25 to 113 m for total weed plants and *Veronica* sp. and 20 m for Canada thistle shoots, respectively (Cardina et al., 1996; Donald, 1994; Heisel et al., 1996) [17, 44, 65]. Elliptical weed patches were longest in the direction of the crop row that suggested a directional influence of agricultural machinery (Colbach et al., 2000) [24].

Variogram models can be fit for mapping. Nested spherical models were fit to empirical variograms for seven weed species over 5 years (Colbach et al., 2000) [24]. In a second study, exponential models were fit to data from three weed species over 2 years (Clay et al., 1999) [23].

Kriging is an interpolation procedure to predict weed density at unsampled locations in the field (Trangmar et al., 1985) [151]. Maps using sparse data at 18 observations per hectare were smooth (Heisel et al., 1999) [66]. Co-kriging with silt content improved the result by 15%. The prediction variance was calculated by cross-validation where the actual weed densities are deleted one at a time and re-estimated from the remaining neighboring weed densities.

Empirical observations suggest that large weed-free areas can occur in a field that can be accommodated in geostatistics using indicator kriging (Clay et al., 1999; Mortensen et al., 1995; Wiles et al., 1992; Wilson & Brain, 1991) [23, 101, 158, 163]. Indicator kriging is an interpolation technique that utilizes weed data coded as probability values (Deutsch, 2002) [35]. Blackgrass was not present in at least 60% of the locations surveyed (Wilson & Brain, 1991) [163]. For other weed species, similar frequency distributions have been recorded in which the mean density was low and 60 to 80% of the sampling points had no weeds present:

reliable spatial models may be difficult to derive (Clay et al., 1999; Mortensen et al., 1995; Wiles et al., 1992) [23, 101, 158].

Simulation or sequential Gaussian simulation has been applied to electromagnetic data from soils (Bourgault et al., 1997) [11] and to quantify uncertainty in weed density data (Faechner et al., 2002) [48]. Simulation generates realizations and differences between realizations can be used to provide a numerical measure of uncertainty that is applied to a crop-weed-herbicide model for herbicide rates (Faechner et al., 2002) [48]. Thus, simulation provides a more complete measure of local and global accuracy compared to kriging (Deutsch & Journel, 1998) [36].

1.4.4 Interpretation

Spatial and Temporal Factors

Weed researchers have assumed weeds occur uniformly throughout the field (Navas et al., 1984) [104]. Evidence has indicated that weeds are in patches or clumps (Groenendael, 1988; Johnson et al., 1996; Mortensen et al., 1993; Thorton et al., 1990) [57, 77, 96, 150]. Patches or clumps have been referred to as aggregated patterns. A patch has been defined as an area with contiguous weed infestations while a weed population has been defined as one species within a field (Gerhards et al., 1997) [51]. The definition of population is dependent on scale that is a field in this case. On a regional scale, a weed population can consist of a set of subpopulations where the same species lives in different fields. This is referred to as metapopulations (Kareiva, 1990) [80]. Metapopulations have no spatial structure.

Patch persistence has been validated by several researchers (Gerhards et al., 1997; Johnson et al., 1996; Mortensen et al., 1997) [51, 77, 97]. Patch size varied from 3000 to 35300 m^2 in these studies. Variation in weed densities has been shown for velvetleaf patches where edges are low density while centers are higher density (Dieleman, 1998) [39]. Producers may have to implement weed management systems that rely on density-dependent application to control high density patch centers compared to other areas of the field, if they desire to control the weed (Dieleman & Mortensen, 1999; Dieleman et al., 1999; Gerhards et al., 1997) [41, 43, 51].

Annual summer weeds that are long-lived in the seedbank (greater than 5 years) appear more temporally stable compared to short-lived species (Gerhards et al., 1997; Mortensen et al., 1998) [51, 99]. Wild oat species in wheat appear to have stability from year to year (Miller et al., 1995) [95]. Distribution of wild oat seed and panicles after 2 years of field operations such as tillage and harvesting was found to be 1-2 m from the initial, 3 x 3 m patch location (Perry & Lutman, 2001) [119].

Stability of a weed patch is defined as consistency in location and density over time (Rew & Cussans, 1995) [126]. Patches appeared stable with respect to location suggesting that historical records could be used to determine future areas of herbicide treatment (Dieleman, 1998; Heisel et al., 1996; Mortensen et al., 1998; Zhang et al., 1998) [39, 65, 98, 168]. Blackgrass was stable over 10 years under different management practices (Wilson & Brain, 1991) [163]. Common sunflower, velvetleaf and hemp dogbane patches were consistent over 4 years (Gerhards et al., 1997) [51]. This temporal stability, in the case of velvetleaf, may have been due to localized dispersal, a persistent seedbank and effective weed management (Dieleman, 1998) [39]. Temporal stability of weed patches may need to be investigated for other weeds to determine what factors are responsible for their stability. Locally varying herbicide rates are expected to restrict the spread of weed patches. Weed mapping becomes

easier since patch location is known. However, not all weeds exhibit the same level of stability and historical records are of limited value.

Management Factors

Herbicide choice, timing, and rate can have a significant effect on weed populations. Wild oat was best controlled from 31 to 40 days after seeding for a range of herbicide application times (Cousens & Mortimer, 1995) [30]. Herbicide performance was a function of the age of the group at the time of spraying.

Four different graminicides were applied from the 2 to 6 leaf stage of wild oat in wheat at 2 locations in central Saskatchewan, Canada (Holm et al., 2000) [69]. For low wild oat locations, a $\frac{1}{3}$ label rate for the different graminicides was effective at the dry site while a $\frac{2}{3}$ label rate was required at the wet site. Optimal timing and rates may be influenced by the graminicide, wild oat density and variable environmental conditions.

Concern about return of wild oat to the seedbank with lower herbicide rates prompted a study into applying imazamethabenz at 4 rates to a barley crop seeded with wild oat at 4 densities (Wille et al., 1998) [160]. Imazamethabenz at less than 75% of label rate resulted in wild oat seed production that was greater than the initial density for high weed density areas. Reduced herbicide rates may not lower the size of the seedbank.

Wild oat has a large seed and matures at a similar time as a cereal or oilseed crop and up to 75% of its seeds may be spread by the combine harvester (Cousens & Mortimer, 1995) [30]. Recent research suggests that wild oat spread only 0.5 m from year to year in crop-weed interference studies. Natural seed shed from mature wild oat resulted in 85% of the seeds falling within a 0.9 m radius of the mother plant (Shirtliffe, 1999) [135]. A chaff collector is a piece of equipment that attaches to the combine harvester. It is an important tool for controlling weed patches since the weed seeds are collected and removed from the field.

Environmental Factors

Spatial patterns of variability of soil phosphorus and wheat yield were correlated with soil organic matter content (Mulla, 1997) [102]. This co-dependence was believed to be a result of erosion on the steep hills that exposed subsoil and reduced topsoil. Higher organic matter soil is expected in the valleys but these areas were not assessed since soil phosphorous is usually sufficient. Targeted soil sampling combined with aerial imagery may be used to determine the phosphorus content of the soils for predicting wheat yield.

The spatial pattern of weeds may be correlated with other secondary factors such as water movement (Firbank et al., 1990) [49]. Dieleman et al., 1995 [42] and Mortensen et al., 1997 [97] indicated that common sunflowers were associated with high organic matter soils. Soil variables such as pH, phosphorus, potassium or the previous year's weed density may provide better estimates of weed density and patch establishment (Walter et al., 1997) [154]; however, correlations between weed densities and landscape factors such as slope and water movement ranged from 0.01 to 0.09 (Krusemark, 1998) [82]. Sampling technique and a flat slope over the field are believed to be responsible for these poor correlations. These soil properties lead to patch establishment since they affect the available habitat for an invading weed species.

1.5 Model for Optimal Herbicide Treatment

1.5.1 Herbicide Efficacy

Bioassay information from dose response curves can be used to quantify residual herbicides, test selectivity, and the joint action of mixtures, formulations and adjuvants (Seefeldt et al., 1995; Streibig et al., 1993) [134, 143]. Herbicide dose responses have been evaluated and found to follow a log-logistic function for velvetleaf (Schabenberger et al., 1999) [133].

To validate dose response curves, field data need to be collected. Soil applied isoxaflutole was assessed for control of *Abutilon theophrasti* Medic. in *Zea mays*(L.) and *Sorghum bicolor*(L.) (Williams II & Mortensen, 2000) [162]. Dose response curves were generated for this herbicide based on the premise that these curves can be used to infer crop and weed response. Environmental conditions such as temperature, wind, soil conditions, and watering affect dose response curves resulting in uncertainties in parameter values (Streibig & Kudsk, 1993) [144].

Two wild oat herbicides were applied on barley at 2 locations and 3 planting dates at 0, 25%, 50%, and 100% of label rate (Harker & Blackshaw, 1999) [63]. Control of wild oat at 25% of label rate was 28% to 76% and 5% to 95% for tralkoxydim and imazamethabenz, respectively. Relative humidity was strongly correlated with effectiveness of low herbicide application rates. Success of reduced herbicide rates depends on environmental conditions at the time of application.

As weeds increase in size, they generally become less susceptible to herbicide control. Spraying wild oat at the 4 leaf stage compared to the 2 leaf stage has resulted in poorer weed control (Harker & O'Sullivan, 1991) [64]. Later germinating wild oat is less deleterious to crop yield than early germinating wild oat; therefore, early herbicide applications while missing some wild oat seedlings, generally result in higher barley yield (O'Donovan et al., 1985; Stougaard et al., 1997) [111, 140].

Of special consideration in weed control is patch dynamics. Observations suggest that non-uniform herbicide rates may provide more effective long term control of patches. High density patches require a higher rate of herbicide to reduce patch persistence; otherwise, weeds may survive the herbicide and contribute to patch persistence (Mortensen & Dieleman, 1997) [97]. This may be due to a weed density effect where herbicide efficacy is proportional and a higher number of plants survive in patch centers.

Herbicide rates were varied according to weed density for winter barley and wheat (Christensen et al., 1997) [19]. Herbicide rates ranged from 80% to 120% of the labeled rate. The herbicide rate maps were created by kriging 12 x 12 m blocks. Herbicide dose could be adjusted to weed density using a simple decision algorithm on field scale basis.

A comparison of post-emergence herbicide application in corn for bluegrass (*Poa annua*), lambsquarters (*Chenopodium album*) and field violet resulted in a herbicide reduction of 10-50% (Williams II et al., 1998) [161]. Weed densities were sampled on a 15 x 15 m grid in this 2.5 ha field and interpolated by linear triangulation. Weed seedlings were controlled site-specifically with lower herbicide rates.

1.5.2 Consequences of Under- and Over-Spraying Herbicides

Economic thresholds for weeds have not been accepted by farm managers for decision-making. These thresholds rely on both the expected yield improvement or shape of the dashed line and the cost of weed control, C, in Figure 1.1. The rejection of economic

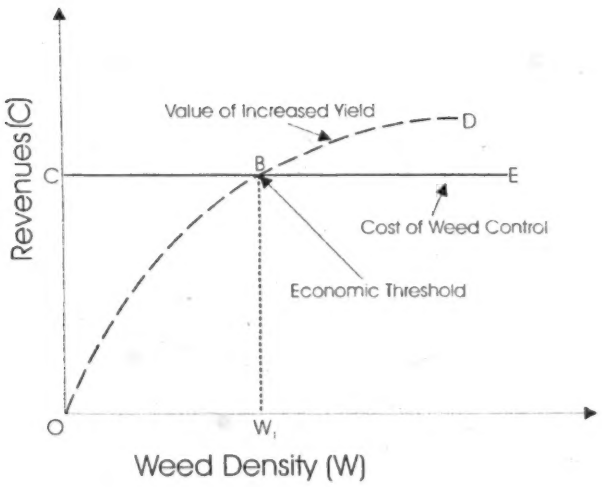

Figure 1.1: The economic threshold for controlling a weed is W_1. The cost of weed control is C. The dashed line is the value of increased yield (Auld et al., 1987) [6].

thresholds is due to risk and variability (Gunsolos & Buhler, 1999; Swanton et al., 1999) [58, 145].

Evaluation of optimal herbicide rates begins with an economic study of their cost effectiveness. Weed control in a corn-soybean rotation was evaluated for site specific compared to broadcast herbicide application in a 4 ha field (Goudy et al., 1999) [56]. The percent of area sprayed in the site specific treatment was 26% less than the broadcast treatment in 1998. No economic evaluation of the reduced amount of herbicide was provided. A 1999 summary of herbicide applications indicated a 9% to 94% savings in herbicide for site specific application (Christensen et al., 1999) [22].

The stochastic nature of crop price, yield, and weed density for cocklebur in soybeans was investigated and a model was developed to determine weed densities that support an optimal herbicide rate (Deen et al., 1993) [33]. A 53% cost savings in herbicide could be realized by patch spraying a 5.33 ha field using reduced doses of herbicide (Christensen et al., 1996) [20]. Profitability of patch spraying is greatest if there are many weed-free areas or areas of low weed density (Audsley, 1993; Zhang et al., 2000) [5, 169].

Reduced herbicide rates for wild oat control in wheat resulted in a $5 ha lower net return at one-third of the label rate compared to other rates (Holm et al., 2000) [69]. Herbicide efficacy, wild oat density, crop price, and herbicide cost were implicated in affecting these lower net returns. Wild oat control in wheat and barley with half rates of 5 different herbicides was lower while net economic return was greater than the non-treated control (Spandl et al., 1997) [138].

Variable rate herbicide application was evaluated over 8 years on 10 fields for spring cereal crops (Bostrom & Fogelfors, 2002) [10]. These rates varied from 20% to 70% of a label rate. At only 1 site did the weed density of difficult to control weeds increase for the variable rate treatment. No significant differences in crop yield were found at 3 sites while for 7 sites, crop yield was higher for the variable rate treatment. Variable rates were concluded to be an effective method for reducing herbicide use.

Simulation results for wild oat indicated that at low density thresholds (2-8 plants m^{-2}), economic returns were higher using site specific herbicide application compared to whole field thresholds (Maxwell & Colliver, 1995) [91]. Similarly, a decision aid model was recommended as a tool for managing low densities of broad-leaved weeds compared to high densities in soybean (Buhler et al., 1997) [14]. The model was not expected to consistently reduce herbicide use or increase returns when densities were high.

A full model incorporating crop-weed interaction with herbicide response was developed to enable crop yield to be predicted with different herbicide doses and weed densities (Brain et al., 1999) [13]. Seedbank wild oat is a concern when reduced rates of imazamethabenz are used: a 50% herbicide rate only controlled 57% of the seed production (Wille et al., 1998) [160]. This could result in a substantial contribution to the soil seedbank that allows wild oat to persist from year to year.

Environmental loading of herbicides needs to be measured when evaluating the consequent of over-application (Hill et al., 2001; Hill et al., 2002) [67, 68]. Bioassays of cereal and oilseed crops applied with sub-lethal doses of herbicide could provide an economic cost of over-application. A rating similar to the leaching potential ranking could serve as a relative index for a herbicide's potential to cause damage to sensitive plants.

1.5.3 Optimal Herbicide Rate

A low herbicide rate can result in a higher seedbank, that supports patch persistence. Alternatively, over-application of the herbicide rate increases environmental loading and expense to the grower. Optimizing herbicide rate requires an estimate of the impact of the crop yield loss for any rate. The optimal rate maximizes revenue or minimizes loss. Environmental loading of herbicide rates is not considered in the optimal estimate.

Optimal herbicide treatment involves varying application rates for maximum revenue. An economic threshold for including 2,4-D with clopyralid was 10 shoots m^{-2} so that densities of *C. juncea* (skeleton weed) above this density would require 2,4-D. Using a weed-free crop yield model and skeleton weed density data, profit of weed affected crop yield was optimized. For skeleton weed, the optimum profit was about \$38 ha^{-1} at a weed density of 90 plants m^{-2} (Streibig, 1989) [142].

1.6 Accounting for Uncertainty

Uncertainty has been modelled for crop price (Deen et al., 1993; Taylor & Burt, 1984) [33, 146], herbicide rates and weed density (Deen et al., 1993) [33], soil moisture and cropping history (Taylor & Burt, 1984) [146], and weather (McDonald & Riha, 1999) [94]. Uncertainty in our knowledge of the spatial distribution of weeds has not been considered (Cousens et al., 1985) [31]. Spatial models aid our understanding of weed distributions but they need to be validated in the field (Dieleman, 1998) [39].

Economic optimum thresholds for wild oat in winter wheat on an annual basis were found to be 8 to 10 seedlings m^{-2} (Cousens et al., 1986) [29]. This simulation model included initial seed bank size and seed return in subsequent years plus 20 other parameters (Cousens et al., 1986) [29]. Control of wild oat in spring wheat for north central Montana was modeled stochastically using wild oat density in the plow layer, cropping history, soil moisture and wheat price (Taylor & Burt, 1984) [146]. No allowance was made for spatial variability of wild oat.

Simulations using whole field and patch threshold decision rules were compared starting with a high initial wild oat infestation level (Maxwell et al., 1995) [91]. The annualized net return was double for the patch threshold decision rule, that is, applying more herbicide based on patches.

Sequential stochastic simulation was used to model seed dispersal and patch spraying (Paice et al., 1998) [117]. An annual grass weed, *Alopecurus myosuroides* Huds., was simulated in the frequency domain where the spectral density function expresses the variability at different frequencies. Data for this technique needs to have periodicity and be continuous to perform well (Webster, 1985) [155].

Weed distributions are affected by a large number of variables such as the soil properties, moisture, light, crop and herbicide. It is impossible to deterministically deduce the result of these interactions. Simulation provides a model of uncertainty in the weed response to herbicide rates (Faechner et al., 2002) [48]. Alternatively, indicator kriging and Latin hypercube sampling have been applied to account for uncertainty in wheat yield, soil pH and lime (Rossel et al., 2001) [130].

1.7 Outline

It is clear that many researchers have addressed varied topics in the general area of weed control. Nevertheless, no consistent approach has been developed for sampling, mapping and optimal herbicide rate determination at a field scale. This subject is addressed in the next 5 chapters.

Chapter 2 presents a unified methodology for the application of regionalized variable theory to weeds for herbicide treatment. This chapter presents the notation, definitions and methodology for determining an optimal herbicide treatment.

Chapter 3 discusses sampling for wild oat density. Different sampling patterns are compared for their ability to infer the variogram and minimize error variance estimates.

Chapter 4 examines the spatial variability of wild oat and how that data are considered for weed density mapping. The analysis of the spatial and temporal variability of weed data requires: (1) data description, (2) variography, and (3) weed density mapping. These geostatistical models are used to determine optimal herbicide rates for decision making in the presence of uncertainty.

Chapter 5 presents a crop-weed-herbicide model for optimal herbicide rate treatment. A stochastic model to quantify the uncertainty of various parameters for determining optimal herbicide rate has been derived. The final outcome is a herbicide rate map in % m^{-2}.

Chapter 6 discusses the application of the crop-weed-herbicide model with grid, gridnest and square sampling designs. The proposed methodology is compared to other alternatives. The optimal design for collecting weed data is provided.

Chapter 7 concludes with a discussion on ideas for future work and implementation of the crop-weed-herbicide model.

Chapter 2

Methodology

This chapter presents the notation, definitions and methodology for determining an optimal herbicide treatment. The general steps in the proposed methodology are (1) sampling weed density for mapping, (2) geostatistical prediction of weed density with an associated measure of uncertainty, (3) formulating a crop-weed-herbicide interaction model, and (4) calculation of optimal locally varying herbicide application rates.

A first step in developing locally varying herbicide rates is to establish a sampling protocol for obtaining weed density. Sampling must consider the available resources to collect the data and the relevance of the information to reduce uncertainty in weed density.

Geostatistics provides a set of quantitative tools for mapping weed density and decision making. The first step is an exploratory analysis of the weed density data. Problem data such as outliers are identified prior to weed density mapping. Defining the weed density data to be pooled together for spatial modeling requires a decision of stationarity. Quantifying spatial correlation of weed density is important for subsequent estimation and simulation. The variogram is used to measure spatial correlation. Weed densities can be estimated with kriging at unsampled locations. Kriging is appropriate for visualizing trends. It is also used to build conditional distributions for stochastic simulation. Simulation is suitable for building numerical models with the correct spatial statistics. Multiple realizations are generated for decision-making and risk assessment.

Crop yield is influenced by weed density, crop density, relative emergence time of the weed, herbicide efficacy, herbicide rate, and timing. These factors are incorporated into a crop-weed-herbicide model that is used to create an optimal herbicide rate map.

There is uncertainty in weed and crop densities, the effects of a herbicide on the weed, crop yield, and price. Traditionally, herbicide treatment does not incorporate these aspects of uncertainty and a label rate is applied for weed control. GPS and other instrumentation technologies have made varying rates of herbicide possible.

2.1 Weed Density Mapping

Geostatistics is a set of statistical tools where the assumption of sample independence is removed (Hamlett et al., 1986; Upchurch et al., 1991) [60, 152]. These tools measure the degree of dependence of samples for estimating the population parameters and making local predictions. When a variable is measured at a location in space, it is common for nearby values to have similar values; weed density can assume a continuum of values and be referred to as a continuous variable (Deutsch, 2002) [35]. Geostatistical tools have been

applied extensively in mining and petroleum, but are relatively new to the field of agriculture (Bourgault et al., 1997; Deutsch & Journel, 1998; Goovaerts, 1997; Goovaerts, 1999; Isaaks & Srivastava, 1989; Journel & Huijbregts, 1978) [11, 36, 53, 54, 71, 79].

2.1.1 Random Function

One mathematical representation of spatially distributed variables is the "random function" concept (Isaaks & Srivastava, 1989; Journel, 1989; Journel & Huijbregts, 1978) [71, 78, 79]. Uncertainty in the wild oat density, $z(\mathbf{u})$, at location $\mathbf{u}$ is modeled with a random variable (RV) $Z(\mathbf{u})$. The random variable, $Z(\mathbf{u})$, is location dependent. A set of RVs is called a random function (RF) denoted $\{Z(\mathbf{u}),\ \mathbf{u} \in \text{study area } A\}$.

For N locations $\mathbf{u}_i, i = 1, ..., N$, there corresponds a vector of N random variables $(Z(\mathbf{u}_1), ..., Z(\mathbf{u}_N))$ that is characterized by an N-variate or N-point cumulative distribution function (cdf):

$$F(\mathbf{u}_1, ..., \mathbf{u}_N; z_1, ...z_N) = Prob\{Z(\mathbf{u}_1) \leq z_1, ..., Z(\mathbf{u}_N) \leq z_N\} \tag{2.1}$$

This describes the joint probability distribution of the N values $(z(\mathbf{u}_1), ..., z(\mathbf{u}_N))$. The concept of a random function allows modeling the degree of correlation between any number of RVs and updating of prior cdfs.

2.1.2 First and Second Order Moments

A one-point cdf $F(\mathbf{u}; z) = Prob\{Z(\mathbf{u}) \leq z\} \in [0, 1]$ has a first order moment that is also known as the expectation or mean of the random variable, $Z(\mathbf{u})$, defined as:

$$E\{Z(\mathbf{u})\} = m(\mathbf{u}) = \int_{-\infty}^{+\infty} z dF(\mathbf{u}; z) \tag{2.2}$$

The expected value operator can be thought of as a probability weighted average. In practice, a continuous integral may be solved by creating a large number, L, of equal probability values.

The variance of $Z(\mathbf{u})$ is a second order moment about the expectation $m(\mathbf{u})$:

$$Var\{Z(\mathbf{u})\} = \sigma^2(\mathbf{u}) = E\{[Z(\mathbf{u}) - m(\mathbf{u})]^2\} \tag{2.3}$$

The covariance for two locations $\mathbf{u}_1$ and $\mathbf{u}_2$ is defined as:

$$C(\mathbf{u}_1, \mathbf{u}_2) = E\{[Z(\mathbf{u}_1) - m(\mathbf{u}_1)]\}E\{[Z(\mathbf{u}_2) - m(\mathbf{u}_2)]\} \tag{2.4}$$

The variogram for two locations $\mathbf{u}_1$ and $\mathbf{u}_2$ is defined as:

$$2\gamma(\mathbf{h}) = E\{[Z(\mathbf{u}_1) - Z(\mathbf{u}_2 + \mathbf{h})]^2\} \tag{2.5}$$

where $2\gamma(\mathbf{h})$ is the variogram, separated by vector $\mathbf{h}$ and a semi-variogram is one half a variogram, $\gamma(\mathbf{h})$.

The mean $m(\mathbf{u})$ is a measure of central tendency and the variance $\sigma^2(\mathbf{u})$ is a measure of spread. The covariance measures correlation or similarity of two RVs whereas the variogram measures variability or dissimilarity of two RVs.

2.1.3 Decisions of Stationarity

The first and second order moments described above depend on location $\mathbf{u}$. Statistical inference may require many repetitive realizations to calculate distributions and expected values. Such replication is unavailable and we must pool data from different locations. Then the $RF\{Z(\mathbf{u}),\ \mathbf{u} \in \text{study area } A\}$ is said to display first order stationarity since its univariate cdf and first order moment, the mean, are invariant. A decision of stationarity allows inference (Journel & Huijbregts, 1978) [79]. We further assume that pairs of data approximately a distance $\mathbf{h}$ apart within the study area, A, are repetitions of the pair $[Z(\mathbf{u}_1), Z(\mathbf{u}_2)]$ where $\mathbf{u}_1 - \mathbf{u}_2 \simeq \mathbf{h}$. This means that the statistical relationship between two data values does not depend on their positions within A, but only on their separation distance. This is a decision of second order stationarity. The concept of "stationarity" is the assumption of "spatial homogeneity" over a study area. More precisely, a RF is stationary if the two RVs $\{Z(\mathbf{u}_1), ..., Z(\mathbf{u}_N)\}$ and $\{Z(\mathbf{u}_1 + \mathbf{h}), ..., Z(\mathbf{u}_N + \mathbf{h})\}$ have the same N-variate distributions whatever the distance, $\mathbf{h}$. According to this definition, the stationary expected values are written:

$$E\{Z(\mathbf{u})\} = m, \quad \forall \mathbf{u} \in A \tag{2.6}$$

$$Var\{Z(\mathbf{u})\} = \sigma^2 = E\{[Z(\mathbf{u}) - m]^2\}, \quad \forall \mathbf{u} \in A \tag{2.7}$$

$$C(\mathbf{h}) = E\{Z(\mathbf{u} + \mathbf{h}) \cdot Z(\mathbf{u})\} - m^2 \quad \forall \mathbf{u} \in A \tag{2.8}$$

$$2\gamma(\mathbf{h}) = E\{[Z(\mathbf{u} + \mathbf{h}) - Z(\mathbf{u})]^2\}, \quad \forall \mathbf{u} \in A \tag{2.9}$$

The decision of stationarity for developing reliable inferences lies with the practitioner. If more data becomes available or the scale of the study changes, the decision of stationarity may change.

2.1.4 Variography

When weed density data are correlated in space they will have a lower semivariance or γ at smaller separation distances than at larger separation distances (Figure 2.1). The nugget represents unexplained variation due to measurement error and/or sources of spatial variation at very small distances. As separation distance increases beyond some distance called the range, the semivariance values often stay constant at a value known as the sill (Deutsch & Journel, 1998) [36].

A variogram model can be constructed as a sum of variogram functions:

$$\gamma(\mathbf{h}) = \sum_{i=1}^{nst} C_i \Gamma_i(\mathbf{h}) \tag{2.10}$$

where $\gamma(\mathbf{h})$ is a variogram model for direction and distance vector $\mathbf{h}$, nst is the number of variogram functions or "nested structures," $C_i, i = 1, ..., nst$ are the variance contributions for each nested structure, and $\Gamma_i, i = 1, ..., nst$ are the variogram functions. The variance contributions of each nested structure sum to one that is the sill. Each nested structure could have different range parameters in different directions.

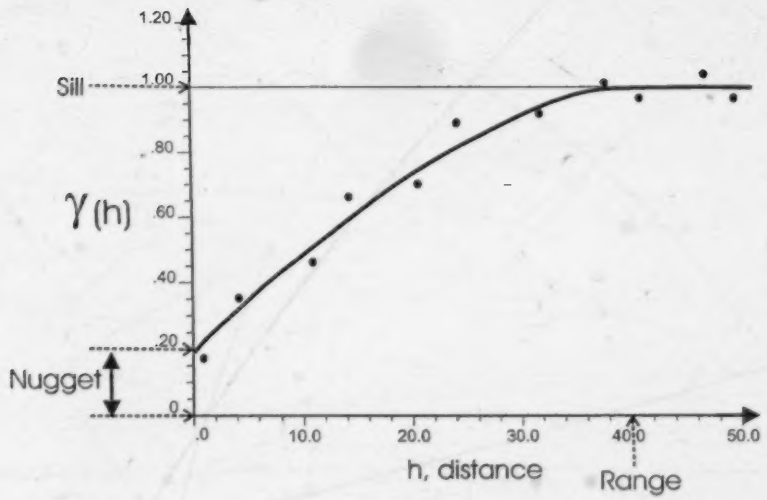

Figure 2.1: A semivariogram function for a spherical isotropic model with a nugget variance (0.20). The dots represent calculated points of the experimental semivariogram while the solid line is the model semivariogram.

Variogram models are often fit to experimentally calculated points. Each variogram model has a lag distance h as a parameter. This distance is calculated by breaking down the distance vector $\mathbf{h}$, into its 3 principal directions, vertical (h_{vert}), major horizontal ($h_{h-major}$) and minor horizontal ($h_{h-minor}$):

$$h = \sqrt{(\frac{h_{vert}}{a_{vert}})^2 + (\frac{h_{h-major}}{a_{h-major}})^2 + (\frac{h_{h-minor}}{a_{h-minor}})^2} \tag{2.11}$$

The distance range parameters, a, in a_{vert}, $a_{h\,major}$ and $a_{h\,minor}$ correspond to each direction for the nested variogram structure.

Geometric anisotropy results from variograms that have the same sill but different ranges whereas zonal anisotropy occurs when the sill changes with direction. Each structure may have its own anisotropy (Deutsch & Journel, 1998) [36].

Typical variogram models include linear, spherical, exponential, Gaussian, and Power law. A model for an empirical weed density variogram is the spherical model given by (Cardina et al., 1997) [16]:

$$\gamma(h) = C \cdot Sph(h) = \begin{cases} C \cdot [1.5(h) - 0.5(h)^3], & \text{if } h \leq 1 \\ C & \text{if } h \geq 1 \end{cases} \tag{2.12}$$

where C is the variance contribution for each nested structure. The range is 1 if h is normalized as above. Directional trends or anisotropy in weed data are common (Deutsch & Journel, 1998) [36].

2.1.5 Kriging and Simulation

Interpolation techniques include inverse distance, triangulation and kriging. Kriging measures variability with variograms to provide parameters for interpolating between unsampled

locations in a field (Deutsch & Journel, 1998) [36]. Inverse distance and triangulation do not consider the variogram. Kriging is an interpolation procedure that minimizes the error variance and accounts for redundant data more easily than inverse distance. Consider residual weed density values:

$$Y(\mathbf{u}_i) = Z(\mathbf{u}_i) - m(\mathbf{u}_i), \quad i = 1, ..., n \tag{2.13}$$

where $m(\mathbf{u}_i)$ is the location-dependent expected value of RV $Z(\mathbf{u})$, $Y(\mathbf{u}_i)$ is the residual value and $Z(\mathbf{u}_i)$ is the RV model for weed density at all data locations $\mathbf{u}$.

The variogram of stationary residuals can be inferred:

$$2\gamma(\mathbf{h}) = E\{[Y(\mathbf{u}) - Y(\mathbf{u}+\mathbf{h})]^2\} \tag{2.14}$$

The residual variable Y and the variogram are considered to be stationary.

A linear estimator at location $\mathbf{u}$ is defined as:

$$Y^*(\mathbf{u}) = \sum_{i=1}^{n} \lambda_i \cdot Y(\mathbf{u}_i) \tag{2.15}$$

where $Y^*(\mathbf{u})$ is an estimated value and λ_i $i = 1, ..., n$ are weights applied to the n nearby weed density data values $Y(\mathbf{u}_i)$. The error variance is defined as:

$$\sigma_E^2(\mathbf{u}) = E\{[Y^*(\mathbf{u}) - Y(\mathbf{u})]^2\} \tag{2.16}$$

where $Y^*(\mathbf{u})$ and $Y(\mathbf{u})$ are the estimated and true values. Simple kriging (SK) solves for weights that minimize this error variance. The minimized error variance or kriging variance can be calculated from the weights and variogram:

$$\sigma_{SK}^2(\mathbf{u}) = \sigma^2 - \sum_{i=1}^{n} \lambda_i \cdot [\sigma^2 - \gamma(\mathbf{u} - \mathbf{u}_i)] \tag{2.17}$$

where σ^2 is the stationary variance, $\gamma(\mathbf{u} - \mathbf{u}_i)$ $i = 1, ..., n$ are the variogram values between the location being estimated, $(\mathbf{u})$, and each of the weed density data locations, $\mathbf{u}_i$, $i = 1, ..., n$, and λ_i, $i = 1, ..., n$ are weights applied to the n data values. The greater these distances from a data location, the larger the kriging variance. Thus, the kriging variance measures the efficiency of different sampling patterns.

Although the covariance between a kriged estimate and the measured data are correct, the variance of the kriged estimate is too small:

$$Var\{Y^*(\mathbf{u})\} = \sigma^2 - \sigma_{SK}^2(\mathbf{u}) \tag{2.18}$$

where $\sigma_{SK}^2(\mathbf{u})$ is the kriging variance and σ^2 is the stationary variance. Sequential Gaussian simulation (SGS) provides the correct variogram and a distribution of possible densities for every point being estimated (Deutsch & Journel, 1998) [36]. This is done by drawing a random residual R($\mathbf{u}$) with Monte Carlo simulation that follows a normal distribution with a mean of 0 and error variance of $\sigma_{SK}^2(\mathbf{u})$. Then the kriged estimate and the residual are added to get a simulated value, $y_s(\mathbf{u})$:

$$Y_s(\mathbf{u}) = Y^*(\mathbf{u}) + R(\mathbf{u}) \tag{2.19}$$

Next $Y_s(\mathbf{u})$ is added to the set of data to ensure that the covariance with this data value and future predictions are correct. All nodes of the grid are visited randomly. At each node $\mathbf{u}$, a number of data are retained for estimation including the original data and some surrounding simulated grid node values. All data values and simulated values are back-transformed when the model is populated. If multiple realizations or images $\{z^{(l)}(\mathbf{u}),\ \mathbf{u} \in A\}, l = 1, \ldots, L$ are needed, then the above process is repeated L times with a different random seed number. A realization reflects properties that are inferred from the sample data and incorporated into the RF model $Z(\mathbf{u})$. Simulation provides the numerical measure of uncertainty at a given location $\mathbf{u}$ due to the differences between these realizations.

When applying SGS, the data need to be transformed to a standard normal distribution prior to simulation. All work in terms of simulation is performed in Gaussian space since the use of a Gaussian distribution will ensure the correct distribution of simulated values. When all grid nodes have been simulated, the normal score data are back transformed to 'real' space or the original data. This gives us one realization. The process is repeated using a different random number sequence to generate multiple realizations of the original map.

2.2 Sampling

Extensive sampling would be required to characterize the exact location of all wild oat in a field. This would be extremely laborious and expensive. The alternative is to perform limited sampling and then construct numerical models of the weed density at unsampled locations. The objective is to collect as few samples as possible and yet provide a numerical model that allows reliable site-specific herbicide application.

The "correct" or "optimal" number and location of samples is a difficult question. A numerical exercise will be constructed later in this thesis to assess different sample spacings and patterns. A reference distribution of weed density data is generated to provide data at all locations and to judge the efficacy of different sampling schemes. Variograms are also calculated for each candidate sampling pattern. Sampling efficiency is determined with the difference between the estimated weed density $z^{\star}(\mathbf{u}_i)$ and the reference value, $z(\mathbf{u}_i)$:

$$M_1 = \frac{1}{n}\sum_{i=1}^{n}[z^{\star}(\mathbf{u}_i) - z(\mathbf{u}_i)]^2 \tag{2.20}$$

where the differences are averaged over all estimated locations, $\mathbf{u}_i, i = 1, ..., n$, for an entire area of interest $n \in A$. M_1 is a mean squared error that provides a measure of sampling efficiency.

Another measure of sampling pattern efficiency is closeness of the experimental to the reference variogram. Reliable estimates at unsampled locations could only be made with an experimental variogram that closely approximates the underlying reference variogram. The experimental variogram values from different scales are combined. Two to three lags at each order of magnitude are chosen to define the variogram.

A measure of mismatch is calculated between a fitted model variogram, $\hat{\gamma}(\mathbf{h}_s)$ and the reference variogram:

$$M_2 = \frac{1}{C}\sum_{s=1}^{ns} wt(\mathbf{h}_s)[\hat{\gamma}(\mathbf{h}_s) - \gamma(\mathbf{h}_s)]^2 \tag{2.21}$$

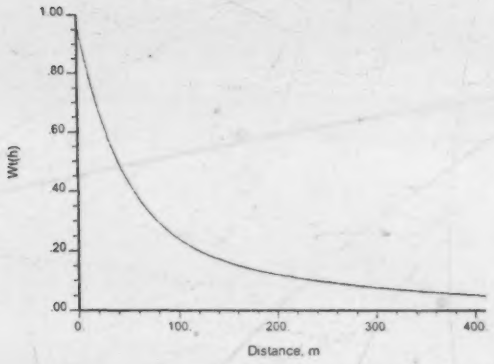

Figure 2.2: Exponential weight function, $wt(\mathbf{h}_s)$, for different distances.

where $\gamma(\mathbf{h}_s)$ is the reference variogram. C is a constant to standardize the weighting function $wt(\mathbf{h}_s)$, see Figure 2.2. The weighting function emphasizes large scale distances that are particularly important in estimation. All lags are included when determining M_2. A "good" model has a low value of M_2. This procedure assumes stationarity of the variogram.

The measures M_1 and M_2 are used to evaluate sampling efficiency. M_1 is the difference between kriging estimates and the reference values. M_2 measures the mismatch from a fitted model variogram and the reference variogram. Thus, different sampling patterns are evaluated with M_1 and M_2. Ultimately, however, the pattern with the best overall economics is deemed optimal.

2.3 Model of Optimal Treatment

The rate of herbicide measured in grams active ingredient (a.i.) ha^{-1} at location $\mathbf{u}$ is denoted $a(\mathbf{u})$, while the optimal rate is denoted as $a_{opt}(\mathbf{u})$. Note that $a(\mathbf{u})$ is not to be confused with the range a used in variogram calculations. Crop density, $c(\mathbf{u})$, is defined as the number of crop plants m^{-2} at location $\mathbf{u}$ while weed density $d(\mathbf{u})$ is the number of weeds m^{-2} at location $\mathbf{u}$. These variables are nominally categorical taking values from 0 to a maximum number of plants that could simultaneously grow in a square meter. In general, there are numerous weed species present in a field, but we only consider those weeds being sprayed for, such as wild oat. Different crops such as barley and canola can be considered.

A farm manager is unable to spray a different rate on each square meter of the field. Consider a selective spraying area (SSA) denoted v. This area is probably 20-35 m wide (depending on spray boom length and electronic controls built into the sprayer) and 1-2 m deep because of the possibility of spray drift. A SSA is defined for site specific conditions. Weed and crop densities must be volume averaged to a SSA, for example, for weed density:

$$d_v(\mathbf{u}) = \frac{1}{v}\int_v d(\mathbf{u}')\mathrm{d}\mathbf{u}' \tag{2.22}$$

Weed density is informed by either (1) weed density samples, (2) scouting, or (3) remotely sensed data, likely at a smaller scale. Maps of weed density, herbicide rate, expected revenue and expected profit that are illustrated in this thesis are at a 1 m^{-2} scale. These large scale

maps with lots of detail could be averaged up to a SSA that has less detail at a smaller scale.

Maximum attainable weed-free yield, $Y_{wf}(\mathbf{u})$, is another required input parameter that is weed-free crop yield in tonnes ha^{-1} at location $\mathbf{u}$ in a field. Historical information and recent environmental and weather conditions can provide an approximation of $Y_{wf}(\mathbf{u})$ annually over the entire field, A. Uncertainty in weed-free yield is included in the model.

Crop yield is a result of several factors including weed and crop density, time of emergence and environment. This is formulated as:

$$f(\mathbf{u}) = \varphi(d(\mathbf{u}), c(\mathbf{u}), t(\mathbf{u}), a(\mathbf{u})) \tag{2.23}$$

where $f(\mathbf{u})$ is fractional crop yield loss at location $\mathbf{u}$, $d(\mathbf{u})$ is weed density, $c(\mathbf{u})$ is crop density, $t(\mathbf{u})$ is time of emergence of weeds relative to the crop in days and $a(\mathbf{u})$ is herbicide rate in grams a.i. ha^{-1}. The effect of weed density, crop density and relative time of emergence are displayed schematically in Figure 2.3, 2.4, and 2.5.

When environmental factors such as growing degree days (GDD), temperature, and precipitation are incorporated into crop yield loss models, the models are expected to provide a more accurate description of crop loss (Hume, 1989; Peterson & Nalewaja, 1992) [70, 121]. For example, soil temperature and moisture influence germination since they can delay weed seedlings when moisture level is low or temperature is cool (Hume, 1989) [70]. In addition, crop seedlings can germinate more readily in these conditions compared to weeds. However, the effects from these factors are highly variable and few attempts have been made to include them in crop loss models for improved precision (O'Donovan, 1996) [110]. The effects from these environmental factors are considered in the function φ and reflected in weed-free yield $Y_{wf}(\mathbf{u})$ and crop yield $Y(\mathbf{u})$.

The fractional yield loss allows calculation of the crop yield, $Y(\mathbf{u})$:

$$Y(\mathbf{u}) = f(\mathbf{u}) \cdot Y_{wf}(\mathbf{u}) \tag{2.24}$$

Yield, $Y(\mathbf{u})$, is in units of tonnes ha^{-1}.

Weeds cause high crop yield loss at high densities, see Figure 2.3. In Figure 2.3, 300 weeds m^{-2} results in a 70% yield loss at a crop density of 100 m^{-2} compared to a 35% yield loss at 50 weeds m^{-2}. Fractional weed-free yield starts at 1 and decreases to some minimum value as weed density increases.

When weeds emerge prior to a crop, there is only intraspecific competition in heavy patches of weeds and consequently yield loss is near 100%, see Figure 2.4. When the weed emerges later interspecific competition between the crop and weed results in less crop yield loss and the fraction of weed-free yield attained is much higher.

Higher crop densities result in less crop yield loss due to competition from the additional crop plants, see Figure 2.5. In Figure 2.5, fractional weed-free yield went from 0 with complete crop yield loss to 0.75 at 300 crop plants m^{-2} at an infestation of 100 weeds m^{-2}.

A fitted model for the fractional weed-free yield of canola that is attained with wild oat infestation (O'Donovan, 1991; O'Donovan et al., 1988) [108, 114]:

$$f(\mathbf{u}) = \frac{1.7d(\mathbf{u})}{(e^{0.13t(\mathbf{u})} + 0.017d(\mathbf{u}) + 0.0097c(\mathbf{u}))} \tag{2.25}$$

where $f(\mathbf{u})$ is fractional weed-free canola yield attained, e is the base of natural logarithms, $d(\mathbf{u})$ is weed density m^{-2} as a result of herbicide treatment, $c(\mathbf{u})$ is crop density m^{-2} and

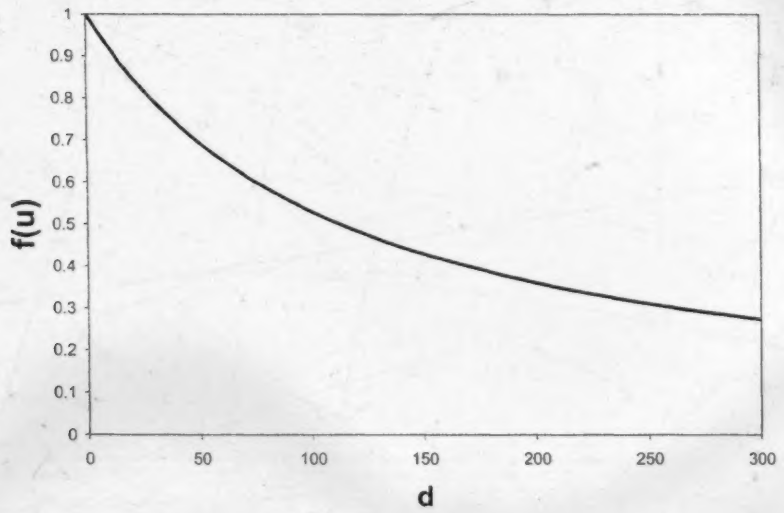

Figure 2.3: Schematic illustration of fractional weed-free crop yield attained, $f(\mathbf{u})$, compared to increasing weed density, d, for a crop seeded at 100 plants m^{-2} using Equation 2.26.

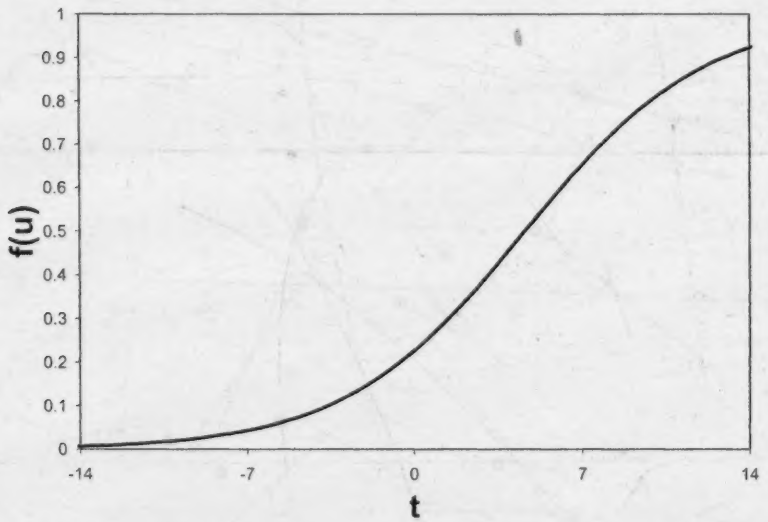

Figure 2.4: Schematic illustration of fractional weed-free crop yield, $f(\mathbf{u})$, compared to t, the relative time of emergence in days of weeds compared to the crop. Zero on the x axis represents crop and weed plants emerging at the same time while a negative value represents weeds emerging earlier than the crop and a positive value is crop emerging before weeds.

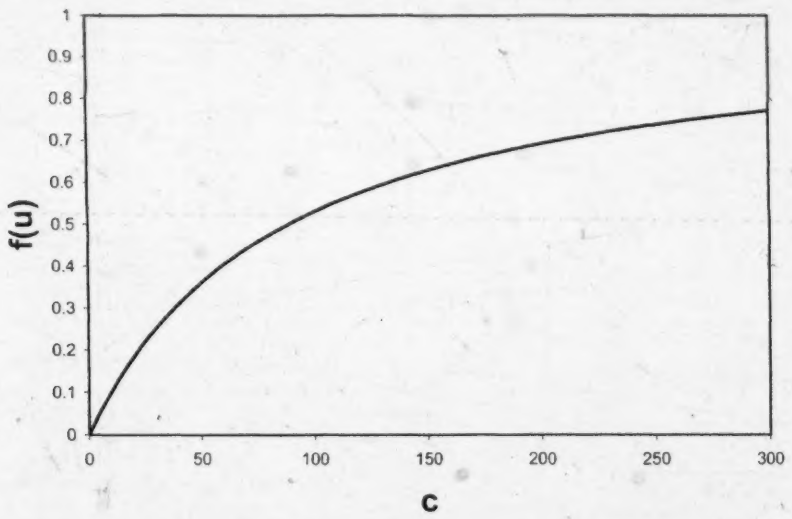

Figure 2.5: Schematic illustration of fractional weed-free crop yield, $f(\mathbf{u})$, compared to increasing crop density, c, for a crop infested with 100 weeds m^{-2} using Equation 2.26.

$t(\mathbf{u})$ is relative time of crop and weed emergence in days. A similar fractional weed-free crop yield model developed for barley (O'Donovan et al., 2001) [112] is:

$$f(\mathbf{u}) = \frac{1.6d(\mathbf{u})}{(e^{0.266t(\mathbf{u})} + 0.016d(\mathbf{u}) + 0.018c(\mathbf{u}))} \tag{2.26}$$

These models account for some biological occurrences:

1. 0% yield loss when no weeds are present,
2. Linear yield loss at low weed density since there is no intraspecific weed competition,
3. Maximum yield loss of 100% when weed density becomes large.

These fitted models have variation in the parameters; however, their simplicity is appealing for implementation by farm managers and agronomists on a field scale.

Environmental factors influence f and attempts have been made to recognize these factors in a crop-weed-herbicide model. Inclusion of new variables will entail field studies over multiple locations and years to develop complete crop-weed-herbicide models. The coefficients in these equations could be tailored to the specific conditions prevailing in a given field.

A critical piece of information is weed control as a function of the herbicide application rate, or $H(a)$, where a is the herbicide application rate in grams a.i. ha^{-1}. Herbicide manufacturers likely have very good data on this function; however, that data are not publicly available from the manufacturers or the federal government. Model parameters and bounds of this function are based on values from the literature: (1) it is bounded between 0 and 100%, (2) there is zero weed control at zero application rate, (3) there will be 80% or more control at the label application rate, and (4) full control, $H(a) = 1$, will

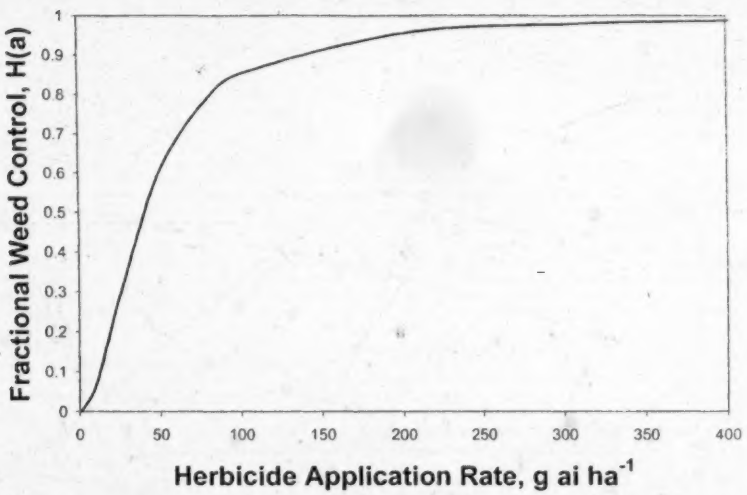

Figure 2.6: Schematic displaying a relationship between herbicide application rate, g ai ha^{-1}, and fractional weed control, $H(a)$, indicating that as herbicide rate increases, a higher proportion of weeds are controlled.

be reached asymptotically as $H(a)$ increases, see Figure 2.6. Experimental data or a fitted hyperbolic or exponential type function could be used to model $H(a)$. There are different $H(a)$ curves for herbicides with different formulations (Jensen & Kudsk, 1988) [72].

Some experimental herbicide rate-response curves are expressed in the following format (Seefeldt et al., 1995; Streibig, 1988) [134, 141]:

$$H(a) = \frac{B}{100} + \frac{\frac{A-B}{100}}{1 + e[m(log(a) - log(ED_{50}))]} \tag{2.27}$$

where $H(a)$ is fractional control of a weed and e is the base of natural logarithms. The lower limit of the curve in Figure 2.7, B, is fractional survival of the weed at high herbicide rates while the upper limit A is fractional survival of a weed at low herbicide rates. The ED_{50} is the effective dose of a herbicide giving a 50% injury response; m is the slope of the curve; and a is herbicide rate in g ai ha^{-1} (Seefeldt et al., 1995) [134]. Uniformity, size and number of weeds per unit area affects the outcome of Equation 2.23 [144]. Parameter values from the literature could be used (Lemerle & Verbeek, 1995; Madsen et al., 1999; Madsen et al., 1999; Seefeldt et al., 1995) [84, 87, 88, 134].

The fractional control of a weed, $H(a)$, is used to estimate the impact of a herbicide rate on weed density. The parameter, di, is the initial number of weeds m^{-2} at location $\mathbf{u}$, with no herbicide:

$$d(\mathbf{u}) = (1 - H(a)) \cdot di(\mathbf{u}) \tag{2.28}$$

while $d(\mathbf{u})$ is the number of weeds m^{-2} surviving the herbicide treatment "a" at location $\mathbf{u}$.

Other price and cost inputs are required. The net price of the crop, np, in the units of dollars $tonne^{-1}$ must be known. The cost of the herbicide, hd, in dollars $liter^{-1}$ must also be known.

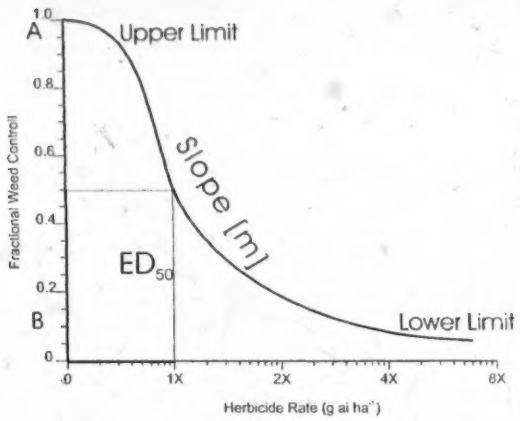

Figure 2.7: Schematic rate-response curve, where ED_{50} represents a herbicide rate, 1X, that causes 50% injury as measured by a decrease in the fractional control of a weed. The parameter, m, describes the slope of the curve that occurs where the ED_{50} value is indicated. The upper limit near 1, A, is fractional weed control at a zero herbicide rate and the lower limit near 0, B, is fractional weed control for a high rate of herbicide (Streibig, 1988) [141].

Using the input variables described above, it is possible to calculate a revenue for a specific application rate, a:

$$r(a;\mathbf{u}) = [f(d(\mathbf{u}), c(\mathbf{u}), t(\mathbf{u}), a(\mathbf{u})) - f(d(\mathbf{u}) \cdot H(a), c(\mathbf{u}), t(\mathbf{u}), a(\mathbf{u}))] \cdot Y_{wf}(\mathbf{u}) \cdot np \quad (2.29)$$

where the units of r are dollars ha^{-1}. The cost of applying herbicide must also be considered.

Yield loss and herbicide application both have associated costs. Increasing herbicide application rate costs more money due to increased product application. Decreasing herbicide rates reduce this application cost but increase yield loss. This is shown in Figure 2.8 where the long dashed line represents the sum of the cost of applying herbicide and the cost of crop yield loss. This figure shows "profit", however, most figures later in this thesis show cost. Minimum cost is then preferred. Herbicide application rate that is determined as % m^{-2} may be multiplied by the label rate, in g ai m^{-2}, to give an actual herbicide rate.

There are fixed costs for equipment ownership, depreciation, interest, insurance and so on. These fixed costs are not considered in the equation below since it is assumed that it is always worthwhile to spray; the goal is to determine the optimal application rate. Clearly, there are cases where the fixed costs exceed the total revenues and the correct decision is not to spray. Given that spraying will occur, the cost of applying herbicide rate, a, at location $\mathbf{u}$ is given by:

$$hc(a;\mathbf{u}) = \frac{-hd \cdot a(\mathbf{u})}{1000} \quad (2.30)$$

where the units of $hc(a)$ are in dollars ha^{-1}. The total profit or loss of spraying at rate a is the sum of $r(a)$ and $hc(a)$:

$$pc(a;\mathbf{u}) = r(a;\mathbf{u}) + hc(a;\mathbf{u}) \quad (2.31)$$

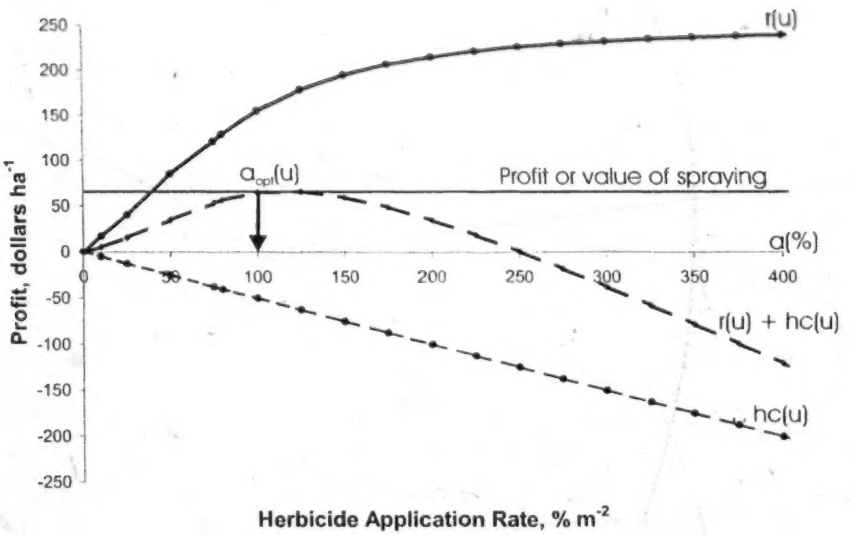

Figure 2.8: Increasing application rate, a, results in increased herbicide application costs but decreased crop yield loss costs. The herbicide cost $hc(\mathbf{u})$ (short dash) and cost due to crop loss from weeds $r(\mathbf{u})$ (solid line) are summed to obtain herbicide cost + crop loss cost $pc(\mathbf{u})$ (long dash). The optimal herbicide rate, $a_{opt}(\mathbf{u})$, is indicated by the black arrow.

The optimal rate, $a_{opt}(\mathbf{u})$, represents the value that maximizes profit or minimizes cost.

The optimal application rate and profit will be affected by several factors. Areas having a low weed density will likely have a low optimal application rate while areas having a high weed density will likely have high application rates. Thus, fields with a patchy weed distribution will be the most amenable to locally varying weed application rates. Two additional comments:

1. The revenue $r(a;\mathbf{u})$ curve flattens as a increases since the weed control, $H(a)$, and fractional yield loss response, $f(d(\mathbf{u}), c(\mathbf{u}), t(\mathbf{u}), a(\mathbf{u}))$, curves flatten off. The cost of herbicide, $hc(\mathbf{u})$, on the other hand, continues to decrease linearly since a constant per-liter cost is used. Thus, the optimal application rate $a_{opt}(\mathbf{u})$ is always finite.

2. The optimal rate will be zero if the herbicide is very expensive ($hc(\mathbf{u})$ large), there are few weeds ($d_v(\mathbf{u})$ low), and there is moderate response to the herbicide ($H(a)$ rises slowly).

The function $pc(a;\mathbf{u})$ may be maximized by any classical technique. The $pc(a;\mathbf{u})$ function is well behaved and evaluation of $pc(a;\mathbf{u})$ is extremely fast; therefore, almost any optimization technique can be considered.

There are four parameters that depend on location: weed density $d_v(\mathbf{u})$, crop density $c_v(\mathbf{u})$, maximum attainable weed-free yield $Y_{wf}(\mathbf{u})$, and relative time of weed emergence $t_v(\mathbf{u})$. Knowledge of these four parameters and parameters that give the response to herbicide $H(a)$ and fractional response $f(a)$ permits calculation of the optimal rate, see Figure 2.9

for an example calculation. For the location described in this example, the optimal rate is 80% of the recommended rate.

An important feature of field-scale weed treatment is that the weed density is not precisely known at each location. There is uncertainty in weed density for each SSA; the optimal herbicide application rate must account for this uncertainty.

2.4 Uncertainty

Uncertainty exists because of incomplete data and our incomplete understanding of the environmental and biological processes that control weed and crop growth. Uncertainty cannot be avoided, but can be managed. Steps to manage this uncertainty include conceptualizing an economic model for optimal application, quantifying the uncertainty in each of the inputs such as weed density, crop density and weed response to herbicide rates; transferring that uncertainty through to the output uncertainty and making optimal decisions in the presence of this uncertainty.

To incorporate uncertainty into an economic model of optimal herbicide treatment, a cdf must be generated for each of the following parameters; (1) crop density, c, (2) weed-free crop yield, Y_{wf}, (3) crop price, np, and (4) herbicide parameters such as ED_{50}.

Weed density is not precisely known at each location and there is uncertainty in weed density for each SSA. The optimal herbicide application rate must account for this uncertainty. Uncertainty exists in crop density due to crop germination, emergence, and micro-environmental influences. Furthermore crop competition has a major effect in controlling weeds once weeds have emerged. Mean canola plant density has been quantified in Table 2.1 at 102 plants m^{-2} from a seeding rate of 6.7 kg ha^{-1}. This crop density is an average over 3 sites and 4 years. If a 50% survival rate is assumed for this seeding rate, the resulting density for a 9.9 kg ha^{-1} seeding rate is 150 plants m^{-2}. Barley crop density utilizes data from the literature and is an average across years (O'Donovan et al., 1988) [114]. For example, a 100 kg ha^{-1} seeding rate is expected to result in 147 plants m^{-2} that emerge and survive. Crop density can be obtained by doing field counts prior to herbicide application.

Weed-free yields vary temporally and spatially due to weather, soil nutrients, moisture, crop cultivar, and seeding rate. Weed-free yield averaged 4.73 t ha^{-1} for barley over 7 years and sites (Harker, 2001; O'Donovan et al., 1999) [62, 113]. Weed-free canola yield had a mean of 1.89 t ha^{-1} over a number of sites and locations (Harker, 2001; O'Donovan, 1991; O'Donovan et al., 1988) [62, 108, 114]. Weed-free crop yield can be estimated and averaged from historical records of areas with no weeds. Similarly, crop prices and herbicide costs vary with supply and demand. The selling price of barley and canola in Canadian dollars t^{-1} indexed to 1992 dollars is averaged over the years 1971 to 2001 and that average is presented in Table 2.1 (Atkinson, 2001) [4]. These statistics are available from different government agencies. The standard deviations in Table 2.1 represent a large amount of variation that indicate the mean is less representative of each distribution compared to crop parameters with a standard deviation half as large.

Rate response curves that predict the weed response to different doses of herbicide are characterized by the ED_{50} and slope of the sigmoid rate response curve. Means and standard deviations are listed in Table 2.2 for wild oat herbicides applied in barley and canola (Lemerle & Verbeek, 1995; Madsen et al., 1999; Olofsdotter et al., 1994) [84, 87, 116]. Rate response parameters that are required may be available from government and

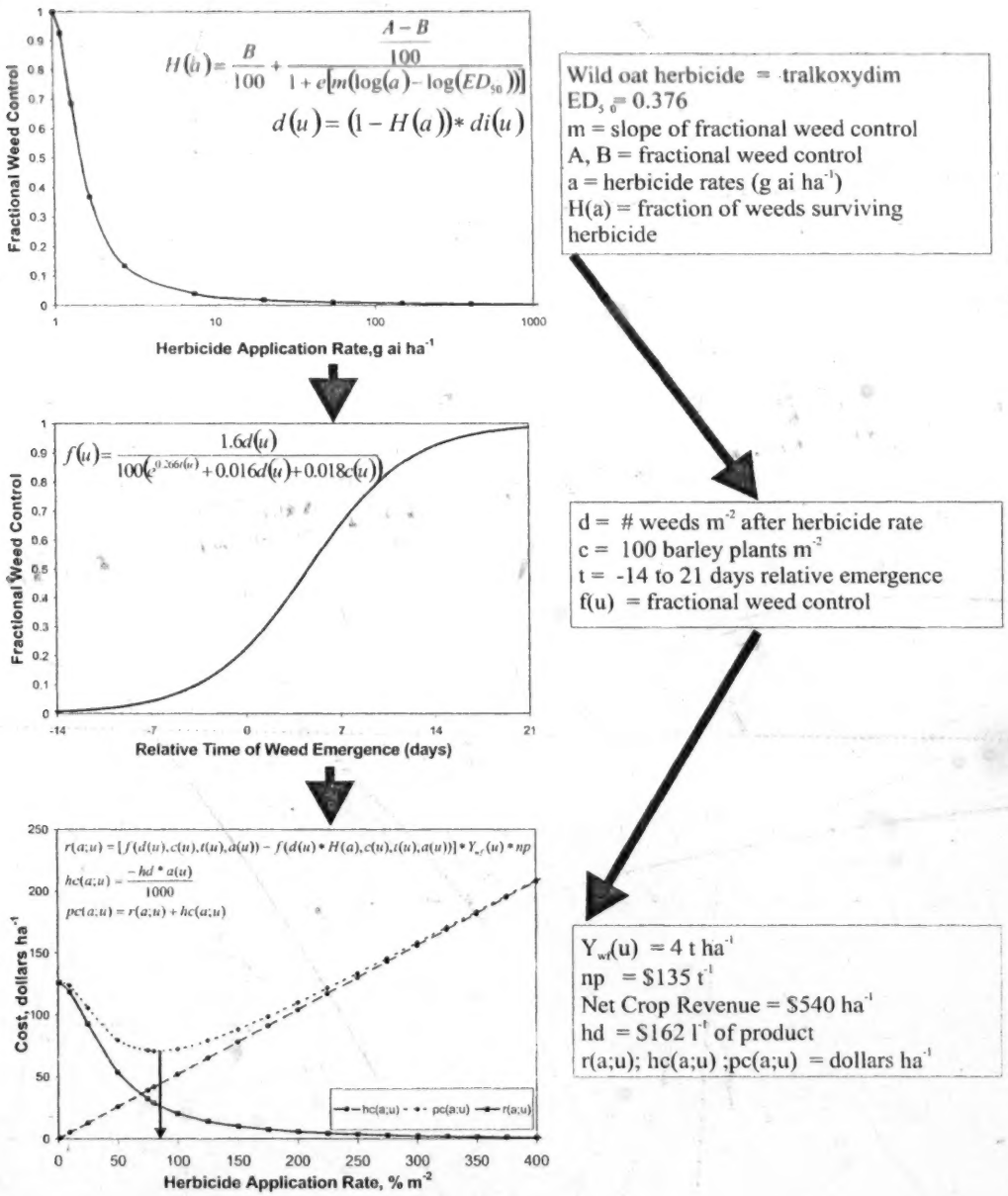
$H(a) = \frac{B}{100} + \frac{\frac{A-B}{100}}{1 + e^{[m(\log(a) - \log(ED_{50}))]}}$
$d(u) = (1 - H(a)) * di(u)$
Fractional Weed Control
Herbicide Application Rate,g ai ha-1
Wild oat herbicide = tralkoxydim
ED50 = 0.376
m = slope of fractional weed control
A, B = fractional weed control
a = herbicide rates (g ai ha-1)
H(a) = fraction of weeds surviving herbicide
$f(u) = \frac{1.6d(u)}{100(e^{0.266t(u)} + 0.016d(u) + 0.018c(u))}$
Fractional Weed Control
Relative Time of Weed Emergence (days)
d = # weeds m-2 after herbicide rate
c = 100 barley plants m-2
t = -14 to 21 days relative emergence
f(u) = fractional weed control
$r(a;u) = [f(d(u),c(u),t(u),a(u)) - f(d(u)*H(a),c(u),t(u),a(u))] * Y_{wt}(u) * np$
$hc(a;u) = \frac{-hd * a(u)}{1000}$
$pc(a;u) = r(a;u) + hc(a;u)$
Cost, dollars ha-1
hc(a;u)
pc(a;u)
r(a;u)
Herbicide Application Rate, % m-2
Ywt(u) = 4 t ha-1
np = $135 t-1
Net Crop Revenue = $540 ha-1
hd = $162 l-1 of product
r(a;u); hc(a;u) ;pc(a;u) = dollars ha-1

Figure 2.9: An example of the models that form part of the methodology to determine optimal herbicide treatment for a weed infestation in a crop. Optimal rate is 80% of the recommended rate in this example.

Crop Parameter	Mean	Standard Deviation
Barley Price, dollars t^{-1}	73.78	38.57
Barley Weed-Free Yield, t ha^{-1}	4.73	1.88
Barley Density, plants m^{-2}	147.8	32.7
Canola Price, dollars t^{-1}	213.43	107.12
Canola Weed-Free Yield, t ha^{-1}	1.89	0.73
Canola Density, plants m^{-2}	102.8	19.6

Table 2.1: Mean and standard deviation of price, weed-free crop yields, and crop density for barley and canola from the literature (Ali, 2001; Atkinson, 2001; Harker, 2001; O'Donovan, 1991; O'Donovan et al., 1999; O'Donovan et al., 1988) [1, 4, 62, 108, 113, 114].

Crop	Herbicide	ED_{50} (g ai ha^{-1})	Standard Deviation
Barley	Diclofop-methyl	1.37	0.54
Barley	Fenoxaprop	0.74	0.22
Barley	Tralkoxydim	0.38	0.12
Canola	Glufosinate	140.0	13.31
Canola	Glyphosate	146.5	13.93
Canola	Imazethapyr	235.0	22.34

Table 2.2: Means and standard deviations for dose-responses of wild oat to 6 herbicides that are applied in barley and canola (Lemerle & Verbeek, 1995; Madsen et al., 1999; Olofsdotter et al., 1994) [84, 87, 116].

university researchers.

Herbicide application cost and herbicide retail price are assumed to be constant for the economic model; the 2001 retail herbicide prices are utilized in numerical examples described later in this thesis (Ali, 2001) [1].

Uncertainty for time of emergence of weed and crop is not quantified in this work.

2.4.1 Accounting for Uncertainty

In presence of uncertainty, we must determine the locally varying optimal rates that maximize expected profit or minimize expected cost:

$$\overline{pc(a;\mathbf{u})} = E\{[f(d(\mathbf{u}),c(\mathbf{u}),t(\mathbf{u}),a(\mathbf{u})) - f(d(\mathbf{u})\cdot H(a),c(\mathbf{u}),t(\mathbf{u}),a(\mathbf{u}))]\cdot Y_{wf}(\mathbf{u})\cdot np - hc\cdot a\} \tag{2.32}$$

The optimal rate, $a_{opt}(\mathbf{u})$, minimizes expected cost or maximizes expected profit at location $\mathbf{u}$, that is, $max\{\overline{pc(a;\mathbf{u})}\}$. In the context of expected profit, there are N pairs for weed density and weed-free yield, $\{f(d_v^{(i)}(\mathbf{u}),c_v^{(i)}(\mathbf{u}),t_v^{(i)}(\mathbf{u}),a_v^{(i)}(\mathbf{u}))\}$, respectively. The expected value is then approximated as:

$$\begin{aligned}\overline{pc(a;\mathbf{u})} \approx \tfrac{1}{N}\textstyle\sum_{i=1}^{N}[f(d_v^{(i)}(\mathbf{u}),c_v^{(i)}(\mathbf{u}),t_v^{(i)}(\mathbf{u}),a_v^{(i)}(\mathbf{u})\\ -f(d_v^{(i)}(\mathbf{u})\cdot H(a)_v^{(i)},c_v^{(i)}(\mathbf{u}),t_v^{(i)}(\mathbf{u}),a_v^{(i)}(\mathbf{u}))]\cdot Y_{wf}^{(i)}(\mathbf{u})\cdot np - hc\cdot a\end{aligned} \tag{2.33}$$

The consequence of uncertainty is that we have to calculate an expected profit instead of the single profit from perfectly known values. The amount of computer work for this added calculation is reasonable. The result is a map of optimal locally varying herbicide application rates for use in computer integrated, GPS-guided, herbicide application equipment.

Two features characterize the expected cost or profit decision process. First, there is a quantified way of measuring value. Risk and uncertainty are expressed as probabilities and probability distributions. Second, the expected value calculation condenses a range of possibilities into a single number. When maximizing over a number of possibilities, the maximum revenue is determined for each possibility in order to obtain a robust solution over all possibilities. Thus, decisions about an optimal herbicide treatment are made repeatedly so that the average return of individual decisions approximates the expected value.

Total expected profit, in dollars ha^{-1}, over an entire field is summed:

$$Total\ Expected\ Profit = \sum_{i=1}^{n} max\{\overline{pc(a;\mathbf{u}_i)}\} \qquad i = 1, ..., n \tag{2.34}$$

A herbicide treatment that generates the highest total expected profit for a field would be declared the optimal choice. The significance of this expected profit or revenue can be assessed by comparing means from two treatments using a Student's t test at the 1% level of probability (Steel et al., 1999) [139]. A locally varying herbicide treatment using simulation is hypothesized to provide the optimal choice since it accounts for spatial correlation and uncertainty.

2.4.2 Alternative Methods

An optimum herbicide treatment is defined as the one that minimizes expected cost of crop yield loss and herbicide. Each realization could be processed to generate a number of optimum rates, see Figure 2.10. Then a loss-function based approach could be used to establish the optimal rate, see the arrow on the histogram below the abscissa axis of Figure 2.10; however, when locally varying herbicide rates are applied, numerous decisions are made within a field and the minimum expected cost approach, see Figure 2.11, will be preferred because it offers the best total economics.

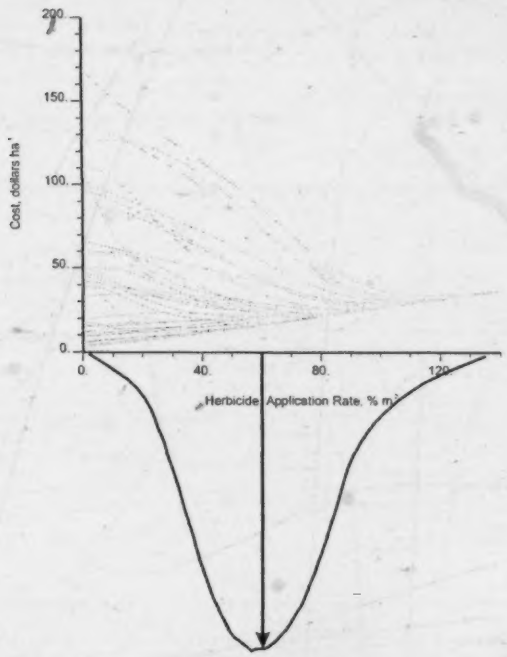

Figure 2.10: Probability distribution of optimal herbicide rates (bottom figure) from 51 realizations of weed density at a single location based on the crop-weed-herbicide model. The arrow points to the expected value that is optimal for this model from the probability distribution.

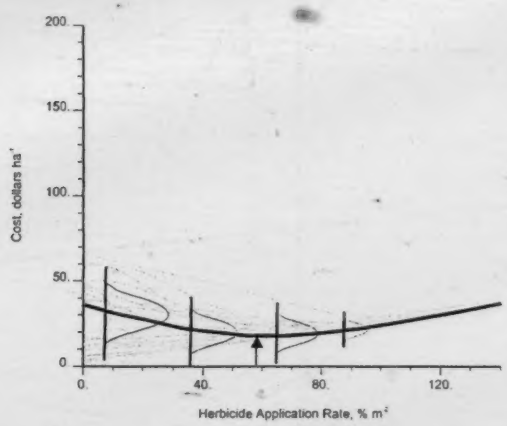

Figure 2.11: Four probability distributions of cost from 51 realizations of weed density at a single location based on the crop-weed-herbicide model. The arrow points to the minimum expected cost that is optimal for this model. The black, curved line represents expected cost that is an average of the 51 realizations.

Chapter 3

Sampling

Correct site-specific treatment decisions would require exhaustive knowledge of the weed density across the entire field. This is impractical and there is uncertainty because of incomplete sampling.

Sampling is expensive in terms of labor and related costs. The best sampling pattern is one that maximizes the accuracy of the spatial information. Accuracy is measured by total expected profit. Consequently, a methodology for establishing the overall profitability of sampling patterns must be determined. This will be discussed in Chapter 6. Several detailed factors are considered here. From weed density data, a variogram is required to allow kriging estimates to be made. These estimates can be used to evaluate sampling patterns based on a pattern's error variance from kriging.

Sample spacing for nested patterns is chosen to reflect spatial variation of weeds that has been reported in the literature (Cardina et al., 1997; Rew & Cousens, 2001) [16, 125]. Sample patterns are randomly chosen in the field so that there is no reason to expect a bias in the mean or variance. A different simulated synthetic would lead to completely different statistics.

Weed density data collected in the field are subject to error. The kriged or simulated weed density values do not account for these errors. Model variograms are assumed to represent experimental variograms. Curve fitting of a model variogram relies on expert judgement that is subject to interpretation. Finally, sampling costs were based on a survey of researchers who may not have included all fixed and variable costs in their responses.

In this chapter, I compare different sampling patterns based on their ability to infer a variogram, minimize the kriging error variance and minimize sampling costs.

3.1 Synthetic Data

Herbicide rate maps could be based on estimated values of weed density determined just prior to post-emergent herbicide application. The true weed density may be unavailable; therefore, simulated distributions of wild oat densities are proposed to replace the unknown values. These synthetic, reference distributions will be used to evaluate the efficiency and cost effectiveness of various sampling patterns.

A data set of wild oat densities from a 800 x 800 m field near Stony Plain, Alberta is utilized. Wild oat in this field was counted in $\frac{1}{4}$ m^{-2} areas at 355 locations in 2000. A map of the sampling locations is provided in Figure 3.1. A histogram of wild oat density from this field has a mean of 102 wild oat plants m^{-2}, variance of 19400, and maximum of 950

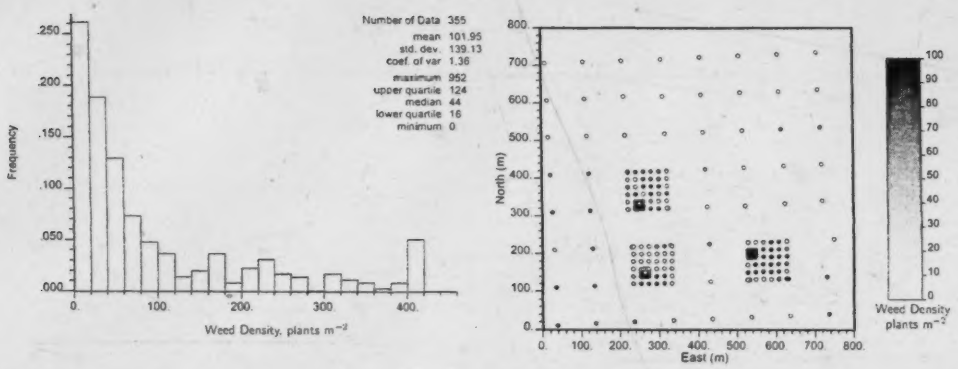

Figure 3.1: Histogram and location map of wild oat density from a field near Stony Plain, Alberta. This is used for generating unconditional simulated wild oat densities for evaluating different sampling schemes. Wild oat, in plants m^{-2}, are identified at each location. Increasing greyscale indicates increasing wild oat density so white is no wild oat while black represents over 200 wild oat m^{-2}.

plants m^{-2}, see Figure 3.1. The experimental data are modeled with a variogram having a nugget of 0.04 and two nested spherical structures with a contribution of 0.78 and range of 15 m for the first structure and contribution of 0.18 with a range of 410 m for the second structure, see Figure 3.2.

Sequential Gaussian simulation is used to generate unconditional, simulated wild oat density values using the mean and variogram of the data collected from this field. A histogram and map of the unconditional simulated wild oat density values are displayed in Figure 3.3. The synthetic distribution has a mean of 107 wild oat m^{-2}, variance of 17020 and minimum of 1 to a maximum of 952 wild oat m^{-2}. Model variogram parameters are used in SGS to create 11 synthetic references of wild oat density for this 64 ha field. These references are realizations each of which has approximately the same variogram and variance as the original data.

Nested and Square Patterns

The synthetic distributions created above are now considered for evaluating different sampling patterns. Wild oat density is sampled from the first synthetic distribution on square and nested sampling patterns. Square grids are sampled with 10 x 10, 13 x 13, 19 x 19 and 38 x 38 samples.

Nested designs had weed density data spaced on a hierarchy with 4 levels except $Nest_{10}$ that had 5 levels. For each level, sample locations are spaced 1, 5, 20, and 100 m apart except $Nest_{10}$ with sample locations spaced 2, 4.2, 6.7, 50, and 200 m. The purpose of nested sampling is to permit improved inference of the variogram at different scales. Table 3.1 summarizes the sampling patterns and levels. Number of sampling locations is less in the nested design compared to the square design due to the repetitive locations in the nested design. Maps of the square and nested sampling locations are shown in Figures 3.4 and 3.5.

A nested design includes different scales and has data at distances that are suited to variogram calculation. The smallest, 1 m grids of weed density, provide an indication of

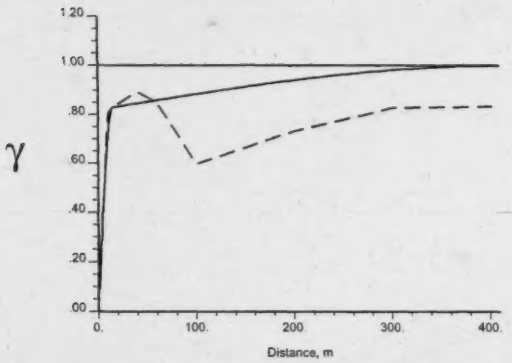

Figure 3.2: Original variogram of wild oat density in a 64 ha field near Stony Plain, Alberta (solid line is model and dashed line is experimental).

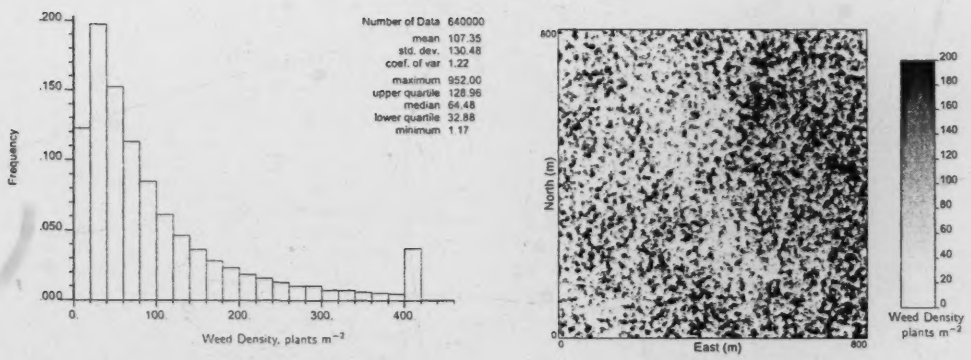

Figure 3.3: Histogram and map of synthetic reference wild oat densities from a field near Stony Plain, Alberta that is used for assessment of sampling patterns.

Sample Pattern	Pattern	Number of Sampling Locations for 800 x 800 m field
$Square_{10}$	10x10	100
$Square_{13}$	13x13	169
$Square_{19}$	19x19	361
$Square_{38}$	38x38	1444
$Nest_{10}$	4x4, 5x5, 4x4(2), 5x5, 2x2	85
$Nest_{13}$	8x8, 5x5, 4x4(2), 5x5(2)	151
$Nest_{19}$	8x8, 6x6(3), 5x5(3), 6x6(3)	319
$Nest_{38}$	8x8, 6x6(14), 5x5(14), 6x6(14)	1254

Table 3.1: Sampling pattern and number of sampling locations for square and nested. The number in parenthesis for each pattern indicates the number of times a particular pattern is repeated at different locations in the field. $Nest_{10}$ represents a nested sampling pattern with five different levels and 85 sampling locations.

Sampling Pattern	Mean Density plants m^{-2}	Variance
Synthetic	107	17020
$Square_{10}$	116	16690
$Square_{13}$	91	7780
$Square_{19}$	111	24000
$Square_{38}$	104	15030
$Nest_{10}$	106	13990
$Nest_{13}$	90	14370
$Nest_{19}$	138	35050
$Nest_{38}$	118	17990

Table 3.2: Mean and variance of wild oat m^{-2} for square and nested sampling patterns compared to the synthetic distribution.

variation at the large scale. A medium sized grid with spacing at 5-8 m complements the information at the large scale and provides a transition to smaller scale data at 50-200 m spacings. Sample spacing is designed to maximize spatial information.

The nested designs are labeled $Nest_{10}$ subscripted by the square pattern with approximately the same number of data. Square patterns are named *Square*.

Descriptive statistics for the square and nested patterns are provided in Table 3.2. Variance in the square patterns is lowest in $Square_{13}$ and highest in $Square_{19}$. Variability in the nested patterns is lowest in the $Nest_{10}$ pattern but highest in the $Nest_{19}$ pattern. The other 2 nested patterns have similar variability to the synthetic model. Mean wild oat density is lowest for the $Nest_{13}$ pattern while the $Nest_{19}$ has the highest average wild oat density.

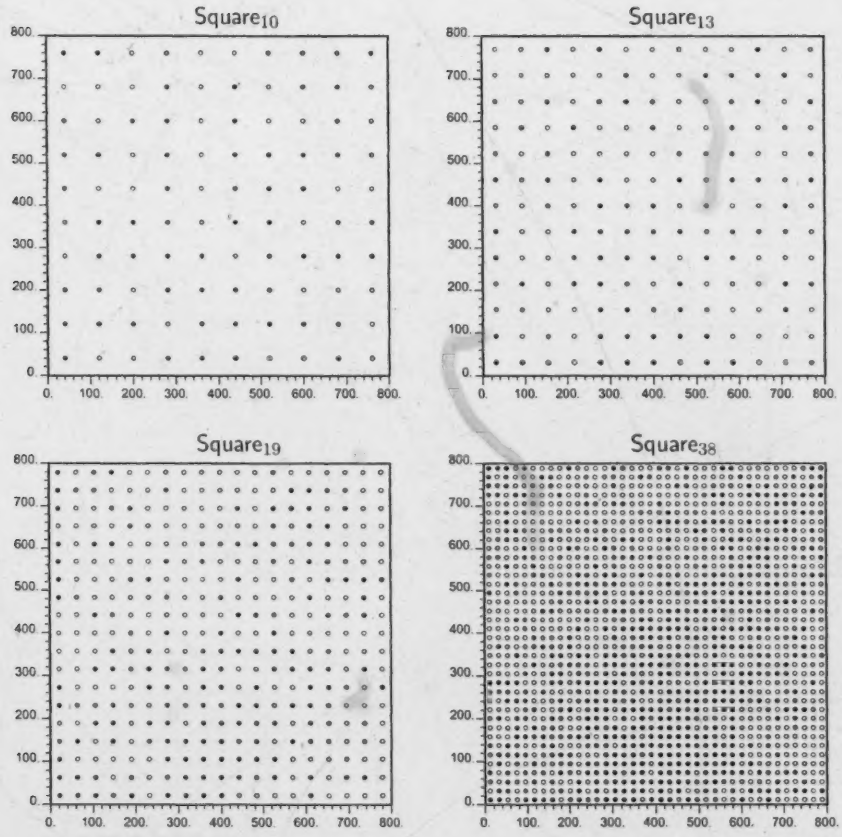

Figure 3.4: Wild oat sampling locations for 10 x 10, 13 x 13, 19 x 19, and 38 x 38 nodes for the square patterns.

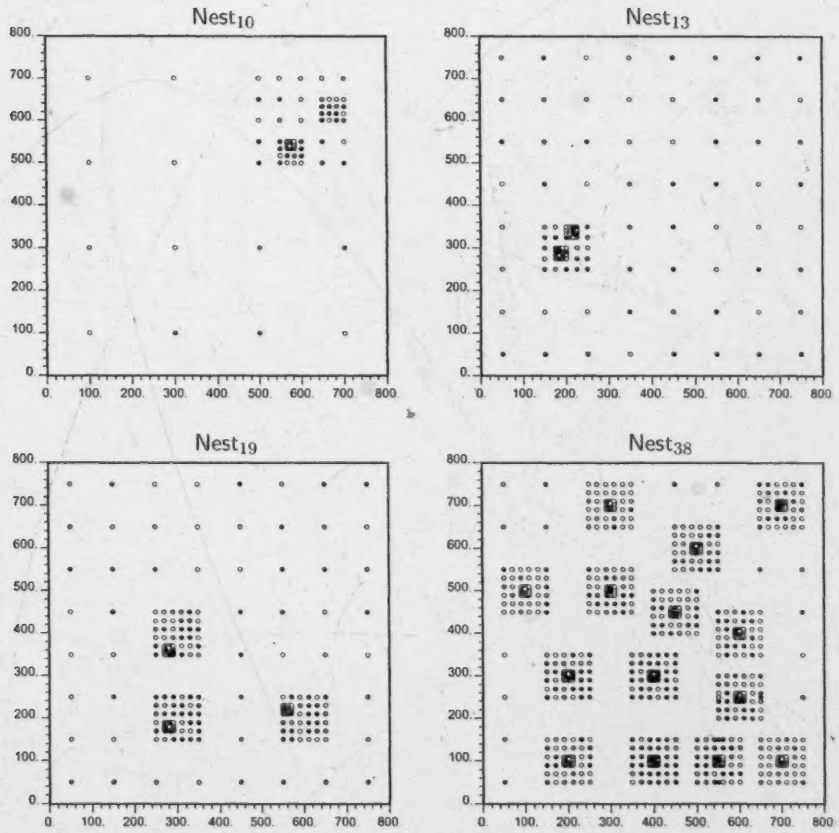

Figure 3.5: Wild oat sampling locations at 102, 171, 355 and 1422 nodes for the nested patterns, that is $Nest_{10}$, $Nest_{13}$, $Nest_{19}$, and $Nest_{38}$.

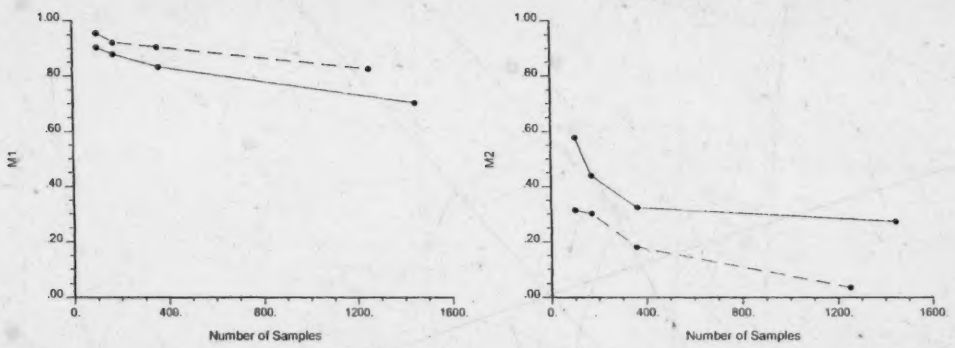

Figure 3.6: M_1 and M_2 for square and nested sampling designs at different sampling numbers. M_2 represented by the dots is an average of the variogram values from 11 synthetic references. The solid line represents the square while the dashed line is the nested pattern.

3.2 Case Study

3.2.1 Nested and Square Patterns

A numerical exercise is undertaken to compare nested and square patterns at different sample spacings. Variograms are calculated and kriging is performed for each sampling pattern. Sampling efficiency is determined as the difference between the kriging estimate and the reference value that results in M_1 (Equation 2.15). The differences are averaged over all estimated locations.

Another measure of sampling pattern efficiency is closeness of the experimental to the reference variogram. A measure of mismatch is calculated once a model variogram has been fitted to the experimental variogram (M_2). The mismatch measures the difference between the fitted model and the reference variogram.

M_1 and M_2 decrease with increasing number of samples, see Figures 3.6 and 3.7. The relation between M_2 and number of samples in Figure 3.6 is exponential with M_2 approaching 0 as sample number increases in the case of a nested sampling pattern. For the square pattern, M_2 levels off at the largest sample pattern, $Square_{38}$. As the number of samples is further increased, M_2 is expected to continue decreasing.

Kriged maps from the M_1 analysis and model variograms for M_2 analysis of square grids are presented in Figures 3.8 and 3.9. For square patterns $Square_{10}$ through $Square_{38}$, the kriged map appears to visually match the reference map. Similarly, the model variogram from $Square_{10}$ to $Square_{38}$ more closely matches the reference variogram in Figure 3.9. The coefficients of determination are 0.73, 0.75, 0.73 and 0.79 between the variogram values of $Square_{10}$, $Square_{13}$, $Square_{19}$ and $Square_{38}$ and the reference variogram. Additionally, the variograms are shown on logarithm scale for the square sampling patterns in case there is a closer match between the reference and model variograms, see Figure 3.10. The visual match between the logarithm of a variogram from any of the square patterns and the logarithm of a reference variogram is poor. The coefficients of determination are 0.56, 0.53, 0.46 and 0.57 between the logarithm variogram values of $Square_{10}$, $Square_{13}$, $Square_{19}$ and $Square_{38}$ and the reference variogram.

For nested sampling patterns, kriged maps and variograms are displayed in Figures 3.11

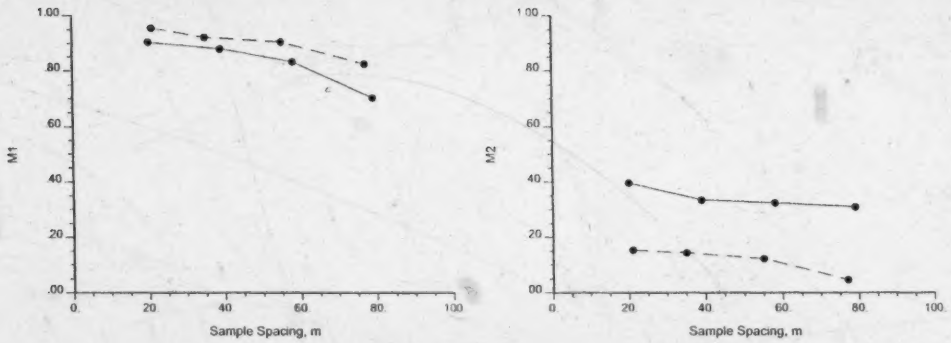

Figure 3.7: M_1 and M_2 for square and nested sampling designs at different sample spacing. M_2 represented by the large dots is an average of the variogram values from 11 synthetic references. The solid line represents the square while the dashed line is the nested pattern.

and 3.12. $Nest_{38}$ in Figure 3.11 is very similar visually to the reference kriged map in Figure 3.3. Coefficients of determination are 0.64, 0.74, 0.81 and 0.92 between the variogram values of $Nest_{10}$, $Nest_{13}$, $Nest_{19}$ and $Nest_{38}$ and the reference variogram. The parameters for each model variogram of a nested sampling pattern are listed in Table 3.3. The nugget is very high for all square patterns since the range of the first structure in the variogram is 70 to 300 m while the reference variogram has 78% of each its variance at 14 m.

Model variograms on logarithm scaling for each nested sampling patterns are compared to the reference variogram in Figure 3.13. $Nest_{38}$ has the closest match to the reference variogram of the nested patterns since it has 66% of its variance at 4 m. The match is better than any of the square sampling patterns. Coefficients of determination are 0.47, 0.85, 0.81 and 0.98 between the logarithm variogram values of $Nest_{10}$, $Nest_{13}$, $Nest_{19}$ and $Nest_{38}$ and the reference variogram.

Reference and estimated wild oat densities are cross plotted in Figures 3.14 and 3.15 for 640000 values. The correlation coefficient that measures linear relationships increases from 0.36 for $Square_{10}$ to 0.53 for $Square_{38}$, see Figure 3.14. Similarly, the correlation coefficient improved from 0.23 for $Nest_{10}$ to 0.42 for $Nest_{38}$, see Figure 3.15. The stove pipe effect observed in each figure is a result of unequal variances; less variability is coming from the estimate due the smoothing effect of kriging. These correlation coefficients are reasonable given the variability of the reference distribution. Sample spacing and the range of the variogram at large scale affected the relationship between the predicted and reference values for square and nested designs. Of course, more sample locations improves the closeness of the match between the estimated and reference values especially for the square grid patterns.

3.2.2 Costs

Costs of sampling consist of a fixed cost, C_{fix}, and a variable cost, $C_{variable}$ that depends on the number of samples, $N_{samples}$:

$$C_{sampling} = C_{fix} + C_{variable} \cdot N_{samples} \tag{3.1}$$

Office overhead, vehicle depreciation, and equipment are included in fixed costs. Variable costs include wages for technical help, fuel, flags, and equipment maintenance. A survey of

Sample Pattern	Nugget	Cont. 1	Range (m) 1	Cont. 2	Range (m) 2	Cont. 3	Range (m) 3
Reference	0.07	0.78	14.0	0.15	450		
$Square_{10}$	0.85	0.15	90.0				
$Square_{13}$	0.80	0.20	70.0				
$Square_{19}$	0.90	0.10	160.0				
$Square_{38}$	0.83	0.17	300.0				
$Nest_{10}$	0.12	0.88	10.0				
$Nest_{13}$	0.08	0.67	5.0	0.25	12		
$Nest_{19}$	0.01	0.48	3.5	0.46	70	0.05	450
$Nest_{38}$	0.01	0.66	4.0	0.33	330		

Table 3.3: Spatial parameters for isotropic variograms of various sampling patterns compared to the reference wild oat distribution for one realization. "Cont." refers to the variance contribution of each nested structure. The variograms are modeled with 1, 2, or 3 nested spherical structures.

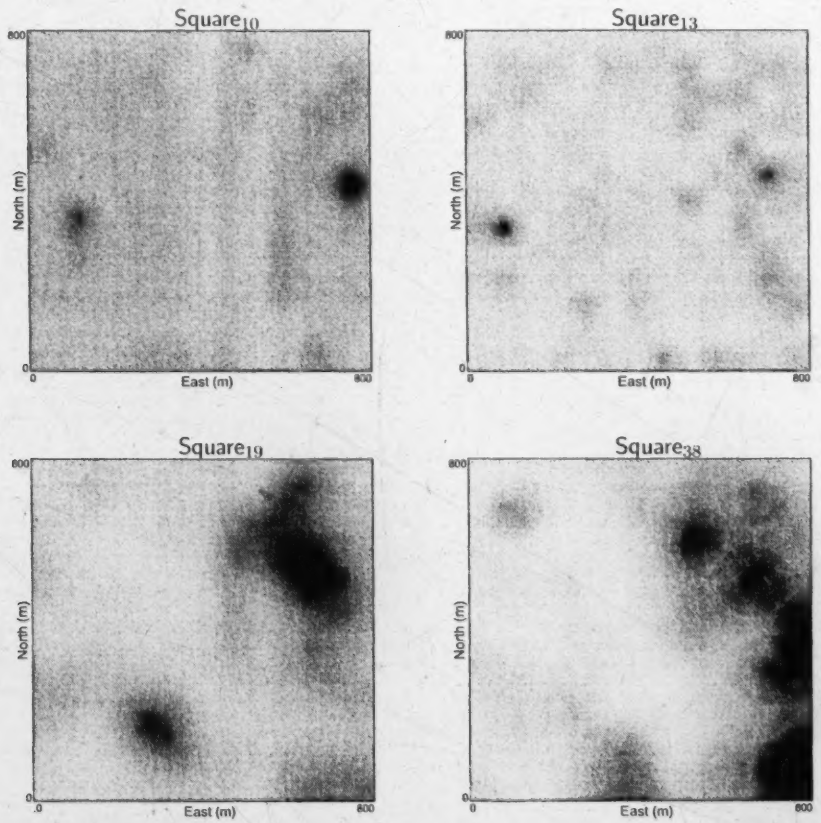

Figure 3.8: Kriged wild oat distributions using the 4 different square sampling patterns. These kriged maps are generated for M_1 calculation.

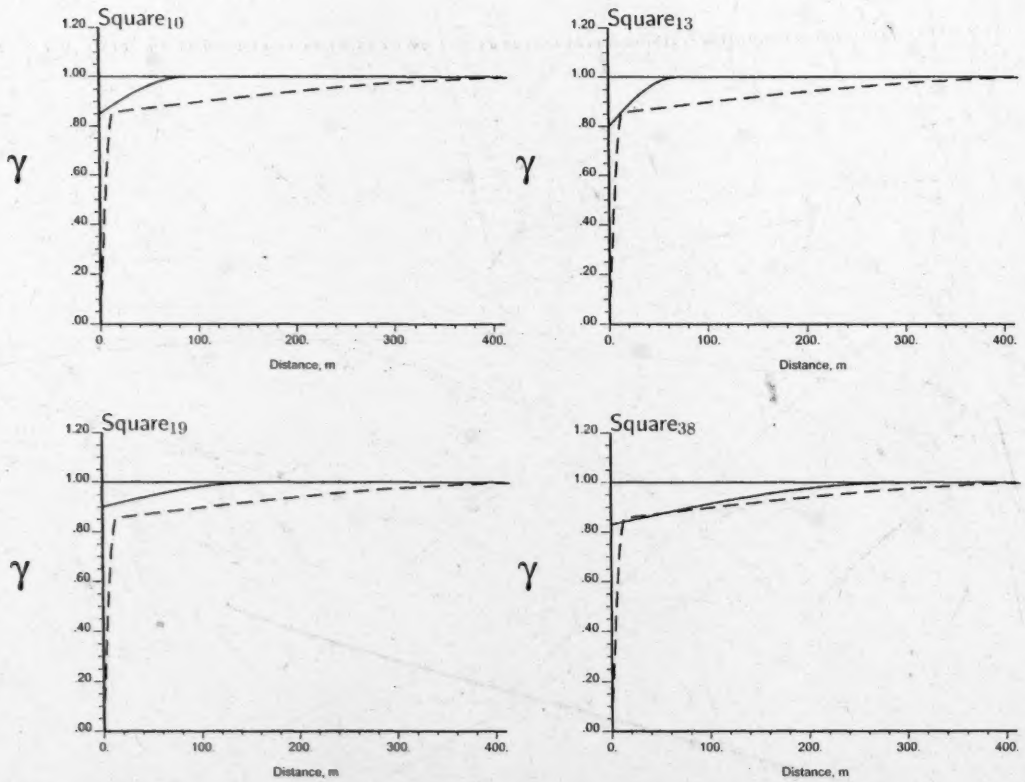

Figure 3.9: Model variograms fitted from the experimental variogram using the 4 different square sampling patterns. The dashed line is the reference variogram while the solid line is the model. These variograms are generated for M_2 calculation.

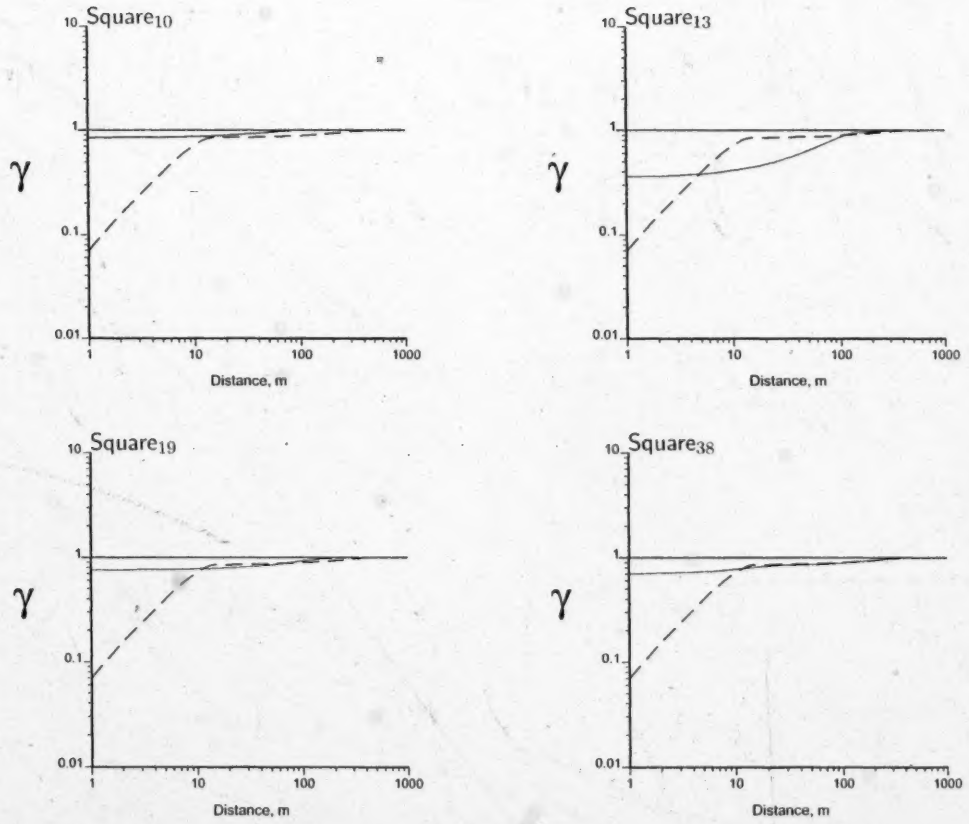

Figure 3.10: Model and experimental variograms are shown on logarithm scale using the square patterns. The dashed line is the reference variogram while the solid line is the model. These variograms are generated for M_2 calculation.

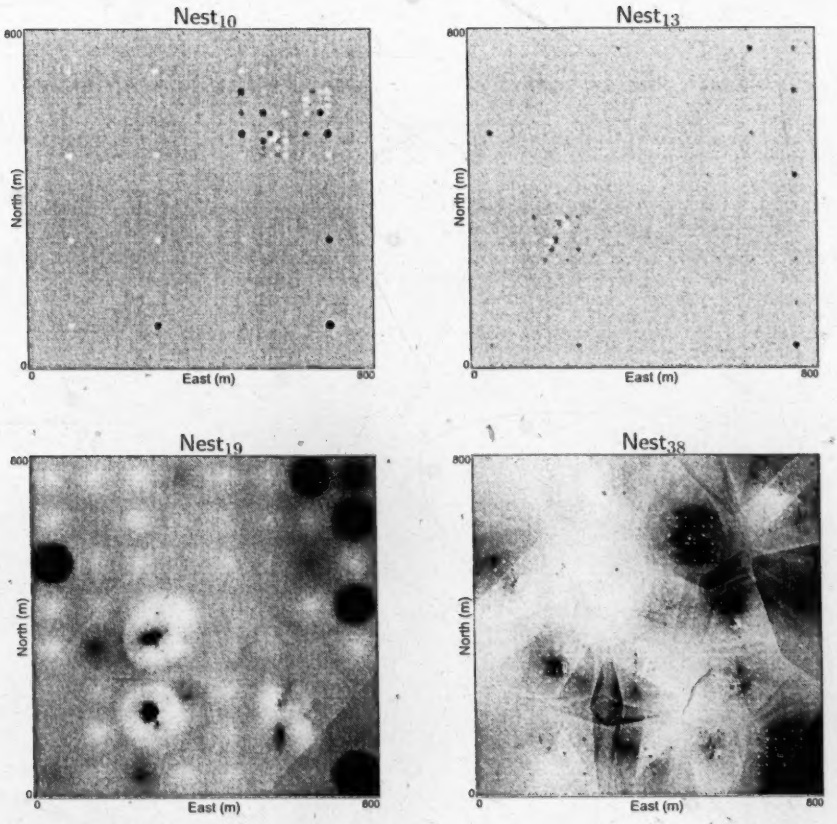

Figure 3.11: Kriged wild oat distributions using the 4 different nested sampling patterns. These kriged maps are generated for M_1 calculation.

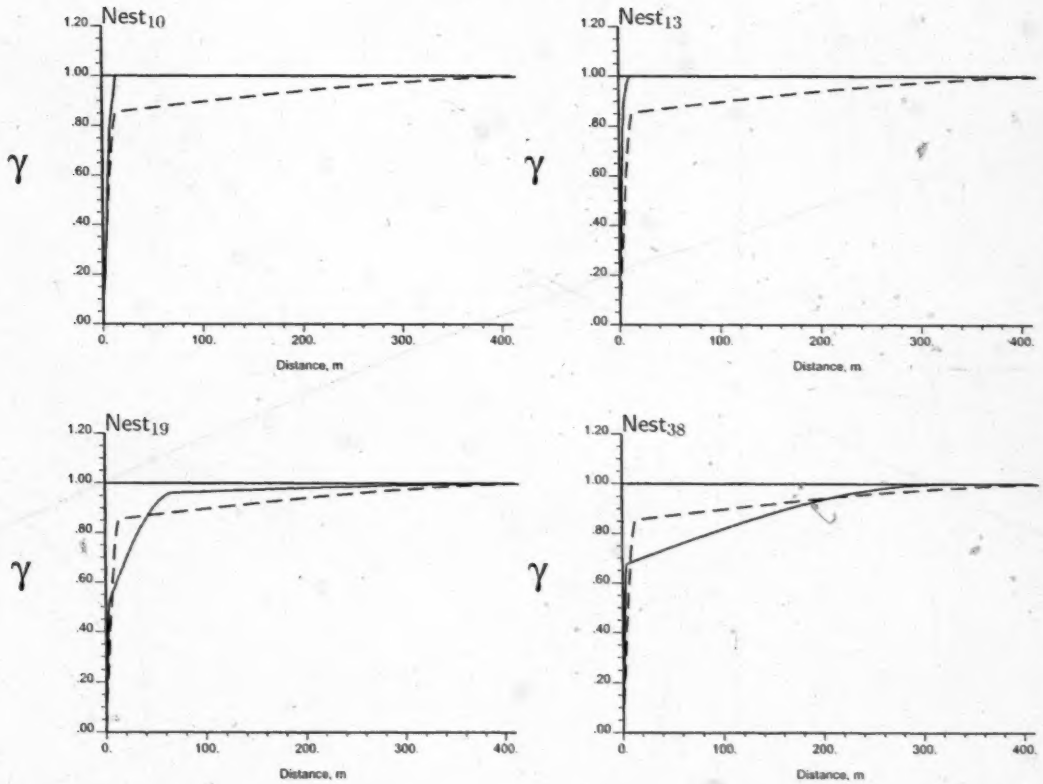

Figure 3.12: Model variograms fitted from the experimental variogram using the 4 nested patterns. The dashed line is the reference variogram while the solid line is the model.

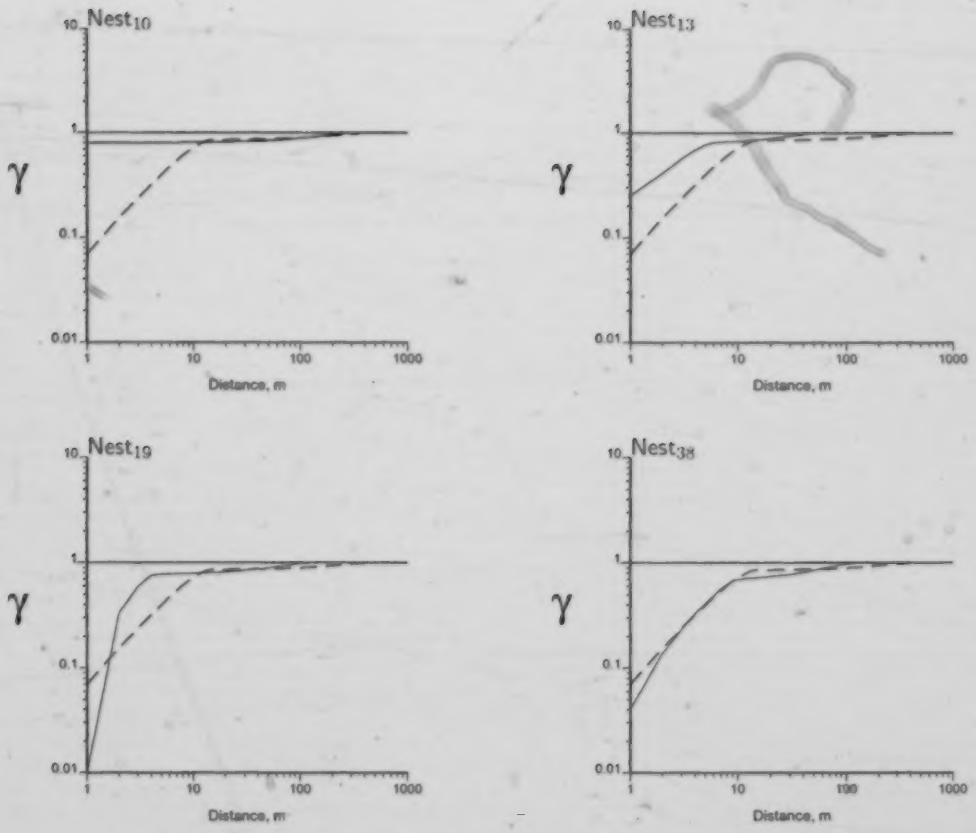

Figure 3.13: Model and experimental variograms are shown on logarithm scale using the nested patterns. The dashed line is the reference variogram while the solid line is the model.

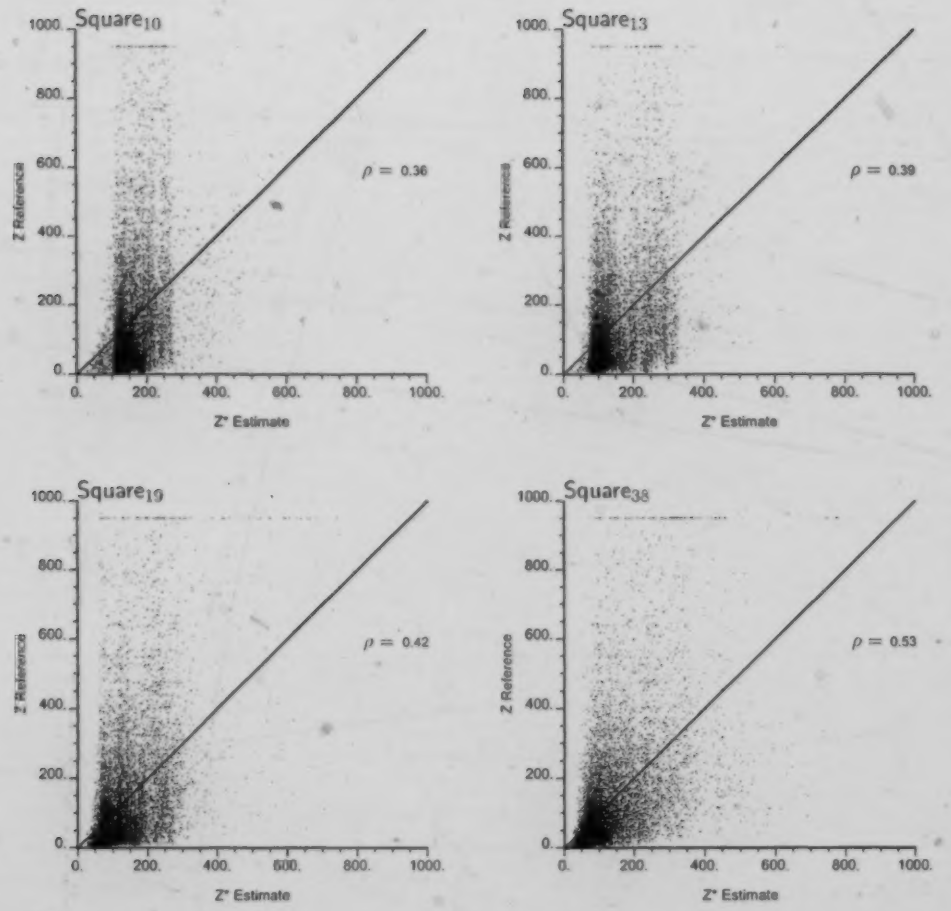

Figure 3.14: Scatterplots of reference and estimated values for square patterns.

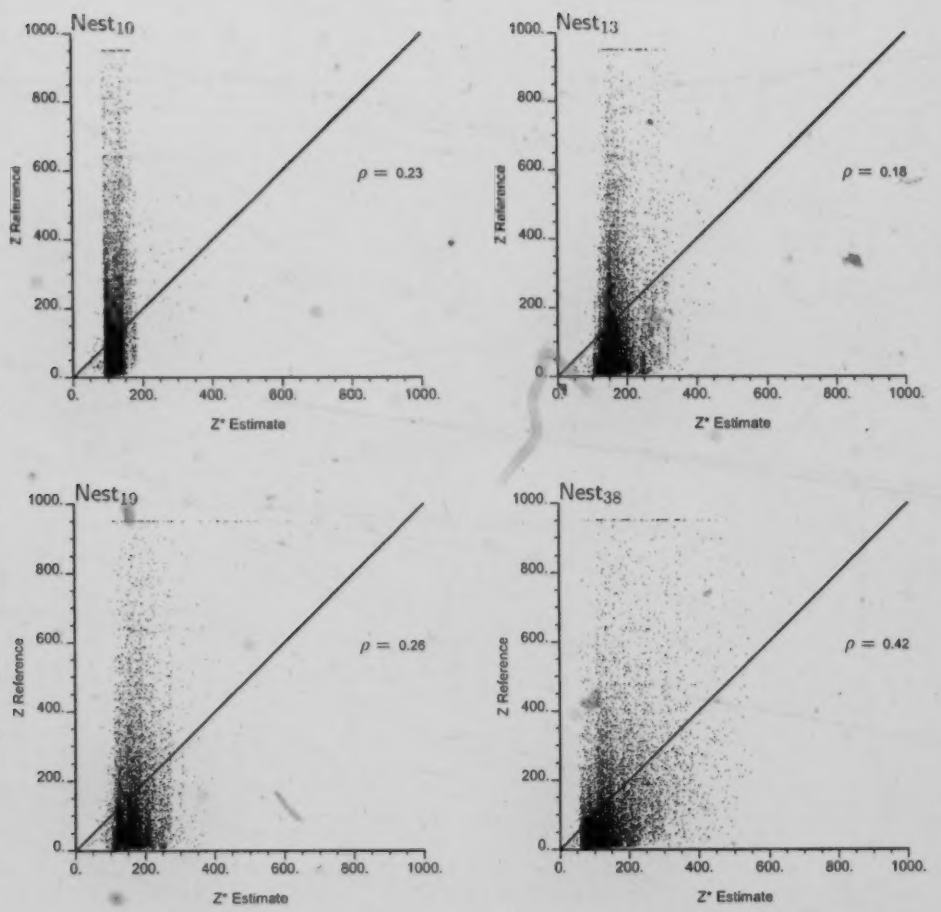

Figure 3.15: Scatterplots of reference and estimated values for nested patterns.

Sampling Pattern	SIE_{M_1}	SIE_{M_2}
$Square_{10}$	4.98	1.98
$Square_{13}$	4.13	1.40
$Square_{19}$	3.46	1.15
$Square_{38}$	2.74	0.97
$Nest_{10}$	5.33	0.82
$Nest_{13}$	4.32	0.63
$Nest_{19}$	3.37	0.45
$Nest_{38}$	2.47	0.15

Table 3.4: Sampling inefficiency, in dollars sample^{-1}, for 4 different square and nested sampling patterns using SIE_{M_1} and SIE_{M_2}.

weed researchers in western Canada revealed that fixed costs would approximate $200 per field in 2001. Variable costs are based on a charge of $3.00 per sample. For the sample pattern, $Square_{10}$, sample cost per field is $200 + (3 \times 100) = $500.

Sampling inefficiency, SIE, could be determined with sampling cost and M_1 or M_2 standardized per sample:

$$SIE_{M_1} = \frac{C_{sampling} \cdot M_1}{N_{samples}} \tag{3.2}$$

$$SIE_{M_2} = \frac{C_{sampling} \cdot M_2}{N_{samples}} \tag{3.3}$$

where SIE is dollars sample^{-1}. Results from Table 3.4 for SIE_{M_1} indicate that the $Square_{10}$ and $Square_{13}$ patterns are more cost efficient than their equivalent nested patterns. However, $Nest_{19}$ and $Nest_{38}$ are more efficient than square patterns with the same number of samples. For SIE_{M_2}, the most efficient pattern is $Nest_{38}$ at $0.15 sample^{-1} while the least efficient is the $Square_{10}$ pattern at $1.98. All nested patterns are more efficient than the equivalent square patterns for SIE_{M_2}. Lower M_2 values compared to M_1 result in lower costs of SIE_{M_2} compared to SIE_{M_1}.

Spatial information is critical and a nested design is an appropriate pattern for collecting this information in an initial investigation. This will ensure a reliable and robust variogram is generated. The nugget, range and sample spacing are essential for variogram estimation and prediction. Choice of sample spacings for a nested pattern can result in inaccurate prediction since the model variogram is interpolated over the range of correlation. Such a variogram can be used to complement the variogram from square patterns to provide the best overall coverage.

Location of the nested patterns in a field can result in a biased sample that is not representative of the weed population. This is overcome by random sampling that allows each nested pattern an equal chance of being drawn.

3.3 Discussion

Many studies discuss the theoretical and practical advantages of sampling patterns (Burgess et al., 1981, Corsten & Stein, 1994; Olea, 1984; Pettitt & McBratney, 1984; Yfantis et al., 1987) [15, 26, 93, 115, 122, 167]. Estimation variance or M_1 and variogram values or M_2 are used to evaluate the effectiveness of different sampling patterns. Sampling inefficiency

incorporates the costs of sampling and sampling efficiency, as measured by the mean squared error, for each sampling pattern.

Economics of data collection and the acceptable level of uncertainty will influence any decision on sampling strategy. For initial characterization of a weed distribution in a field, nested sampling is appropriate to provide information on the spatial structure. Next, square sampling can be used for decision-making. Choice of the particular grid size can be determined according to total profitability. This topic will be examined in Chapter 6. The M_1 values for these sampling patterns are plateauing since density of sample points in these patterns is becoming adequate to capture most of the spatial variation and minimize the estimation variance. Determining an optimal combination of nested and square pattern will prevent over-sampling.

A quick, cost-effective method to determine the range of correlation is the key to optimal sampling. The best sampling plan for weed density could be constructed if the range of the variogram is known a priori. The plan can be designed by ensuring sample spacing is smaller than the range for satisfactory prediction. For most fields, the range of spatial correlation is unknown before sampling. Sampling at different scales and spacings with a nested pattern is a good first step.

Sample spacing that optimizes time and labor costs compared to gains in accuracy can be inferred from the reference data. This will be investigated in Chapter 6. Local calibration of these ideal sample spacings must be validated in several fields.

Reliability of the estimates for M_1 and M_2 depend on the model variogram being an accurate representation of the experimental variogram. The model is determined by fitting a curve to the estimated values of the experimental variogram. The shape of the model variogram at distances smaller than the sampling interval is unknown, consequently the nugget variance is subject to error. Secondly, fitting a model to the experimental variogram requires expert judgement in determining the angles, distances and type of structure for each model.

Chapter 4

Examples of Weed Density Mapping

Weed management strategies have historically considered fields to be homogenous units. Researchers have controlled the spatial variability of weeds in small plots by uniform planting that does not represent what occurs at smaller scales (Cardina et al., 1997; Radosevich et al., 1997) [16, 123]. Geostatistics provides tools for considering locally varying weed management strategies.

Geostatistics assumes stationarity in the data values. This denotes that a mean exists, is constant and independent of location. Additionally, the covariance exists and is dependent on the distance between any two values, and not on their location. Random variables of a random function (RF) are normally distributed and uncorrelated while their covariance is independent. Kriging assumes the error variance is independent of the data values and relies only on the data configuration. Simulation assumes the random variable components follow a Gaussian distribution while the random residual is independent.

Weed sampling can result in errors due to protocol, inappropriate quadrat size, operator fatigue, misidentification, or incorrect transfer of data onto record sheets. Weed data for this study are assumed to be error free. Weeds are categorized as either broad-leaved or grass based on herbicide choice. This assumes that there are no differences among species within these categories to local environmental conditions.

Affordable GPS units have driven interest in precision application of weed control for the agricultural industry. The overall goal of this chapter is to increase our understanding of the spatial and temporal variability of weeds. Data description, variography, and weed density mapping techniques will be described in detail. This information will be used to quantify uncertainty in weed density.

4.1 Data Description

Weed density data are taken from a 34 ha field near Saskatoon, Saskatchewan that was seeded to spring wheat in 1995, canola in 1996 and barley in 1997. All weed species are identified and counted at the 3-4 leaf stage in all years on a 50 m by 50 m grid. In 1996, two 100 point sampling grids with a 10 m by 10 m spacing are established in areas of high weed density. Weeds are counted by species in four (1995) and nine (1996 and 1997) 50 by 50 cm quadrats at each sampling point in the field prior to post emergent herbicide application.

Weed density data are also recorded in two 64 ha fields near Viking, Alberta and Stony

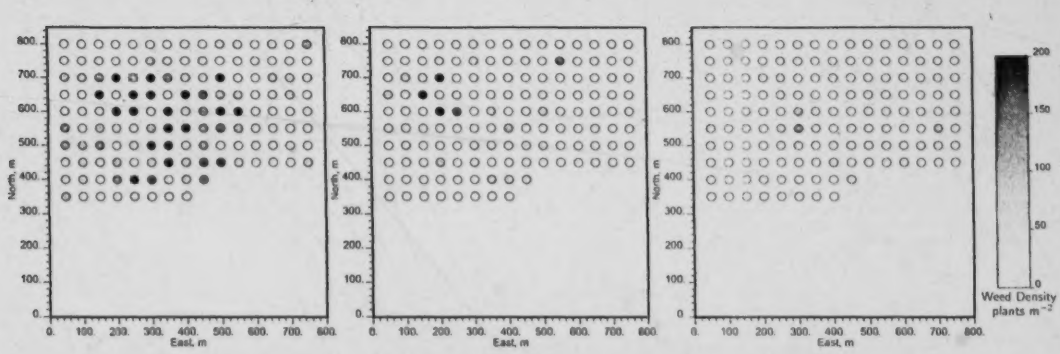

Figure 4.1: A map of weed density sampling locations for 1995, 1996 and 1997 from left to right near Saskatoon. Weed species and counts, in plants m^{-2}, are identified at each location. Increasing greyscale indicates increasing weed density so white is no weeds while black represents over 200 broad-leaved weeds m^{-2}.

Plain, Alberta in 2000. These fields are planted to barley at both sites. Wild oat are identified and counted at the 3-4 leaf stage prior to post-emergent herbicide application in a nested grid sampling pattern. The Saskatoon, Viking and Stony Plain fields are located in the black or thin black soil zone of western Canada. These soil zones are noted for higher rainfall and soil fertility compared to the brown and dark brown soil zones (Penney, 1995) [118].

4.2 Saskatoon Data

Weed species are identified and counted on a 50 x 50 m grid for 1995. A 10 x 10 m grid is used in 1996 and 1997. For the purposes of comparison between years, the 1996 and 1997 data sets are truncated to conform to the 1995 data set as shown in Figure 4.1, that is the larger area sampled in 1996 and 1997 is not considered. This larger area for the 1996 and 1997 data included the 800 x 800 m area in Figure 4.1.

Two small grids of 10 m spacing are sampled in 1996 over a 100 x 100 m area, see Figure 4.2. Because the data are truncated to conform to the 1995 data set, only the small grid in the northeast corner of the field is used in this analysis.

There are 14 different recorded weed species in 1995, 13 in 1996, and 12 in 1997. Of the recorded species, one is classed as a grass weed in 1995, 3 in 1996, and 1 in 1997. All remaining species are categorized as broad-leaved weeds. Grass weeds are present at 54% of the sites in 1995, 35% in 1996 and 41% in 1997. Broad-leaved weeds are present at 100% of the sites in 1995, 93% in 1996 and 97% in 1997. For the three most abundant weeds, the frequency of occurrence is 51% to 99% for *P. convolvulus*; 54% to 91% for *A. fatua*; and 99% to 100% for *T. arvense*, see Table 4.2. Other weed species identified at this site with a frequency of occurrence less than 25% included *C. arvense* (Canada thistle) and *T. officinale* (dandelion).

For the purposes of this study, all weed species are grouped into broad-leaved or grass. This grouping is based on the herbicide for these two categories. Grass weeds are denoted GR subscripted by the year (where applicable). For example, GR_{95} indicates grass weeds in 1995. Broad-leaved weeds are BL.

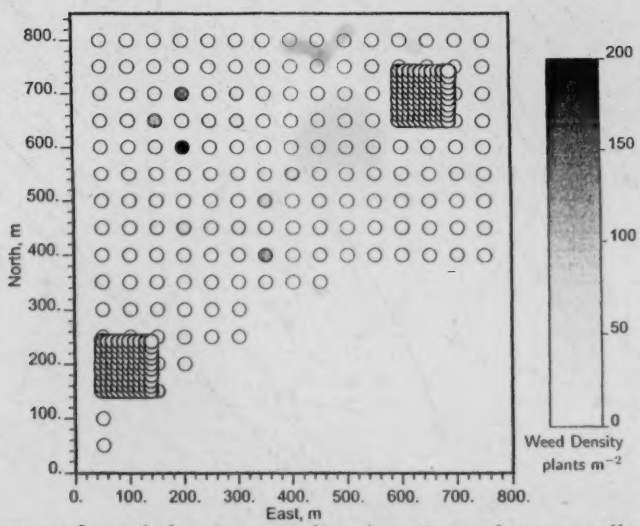

Figure 4.2: A map of weed density sampling locations of two small grids taken in 1996 near Saskatoon. The grid in the north-east corner of the field is used for variography. The small dots represent sampling locations of weed density in 1996 and 1997. Weed species and counts, in plants m^{-2}, are identified at each location.

Bayer Code Name	Latin Name	Common Name
AVEFA	*Avena fatua* L.	Wild oat
BRAXX	*Brassica spp.*	Canola
CHEAL	*Chenopodium album* L.	Common lamb's-quarters
CIRAR	*Cirsium arvense* (L.)Scop.	Canada thistle
CVPTE	*Crepis tectorum* L.	Narrow leaf hawksbeard
DRBNE	*Draba nemorosa* L.	Wood whitlowgrass
GALAP	*Galium aparine* L.	Cleavers
LENCU	*Lens culunaris* L.	Volunteer lentil
MEDSA	*Medicago sativa* L.	Alfalfa
POLCO	*Polygonum convolvulus* (L.)	Wild buckwheat
ROSXX	*Rosa spp.*	Wild rose species
SINAR	*Brassica kaber* (DC.)L.C. Wheeler	Wild mustard
SONAR	*Sonchus arvensis* Bieb.	Perennial sow thistle
TAROF	*Taraxacum officinale* Weber in Wiggers	dandelion
THLAR	*Thlapsi arvense* L.	field pennycress
TRZAS	*Triticum aestivum* L.	wheat
VAAPY	*Saponaria vaccaria* L.	Cow cockle
VICSA	*Vicia sativa* L.	Common vetch

Table 4.1: The Bayer code name, Latin name, and common name of weed species measured in 1995, 1996 and 1997 for a field near Saskatoon, Saskatchewan. Weed species found in this field are referred to by the Bayer code in Table 4.2.

Weed	1995			1996			1996 Small			1997		
	% Occur	Mean	St. Dev.	% Occur	Mean	St. Dev.	% Occur	Mean	St. Dev.	% Occur	Mean	St. Dev.
AVEFA	54	3	5	76	8	18	89	11	19	40	3	8
BRAXX	26	0.5	1							53	6	10
CHEAL	0.7	0.007	09							2.1	0.03	0.2
CIRAR	10	0.2	0.7	25	0	1	8	0.1	0.5	17	0.4	1.3
CVPTE	2	0	0.3	4	0.06	0.34	8	0.1	0.5			
DRBNE				12	0.6	2						
GALAP										1	0.007	0.09
LENCU				3	0.03	0.2						
MEDSA	2	0.02	0.1				2	0.02	0.1	1	0.02	0.3
POLCO	63	1	2	83	1	1	51	1	2	48	1	2
ROSXX	3	0.1	0.6									
SINAR	0.7	0.007	0.09	0.7	0.007	0.09	1	0.01	0.1	4	0.1	0.3
SONAR	6	0.3	1	3	0.05	0.4	7	0.2	0.9	2	0.06	0.4
TAROF	21	0	1	4	0.04	0.2	5	0.08	0.4			
THLAR	99	68	81	99	87	91	100	112	141	77	12	20
TRZAS				36	2	4	15	1	5			
VAAPY	1	0.01	0.09	2	0.01	0.1				0.7	0.04	0.5
VICSA	4	0.1	0.6	2	0.03	0.2	3	0.05	0.3	0.7	0.01	0.2

Table 4.2: A summary table of the mean and standard deviation, in plants m^{-2}, for all the weeds near Saskatoon. Occurrence represents the percentage of the total sampling locations for which a weed species appears. The 1996 small is the 100 point sampling grid.

Year	Weed Type	Mean	St. Dev.	Maximum
1995	Grass	3.1	5.4	42
	Broad-leaved	70.8	80.3	408
1996	Grass	2.4	6.4	42
	Broad-leaved	23.2	34.9	198
1997	Grass	4.6	9.3	52
	Broad-leaved	18.9	20.7	118

Table 4.3: A summary table of the mean, standard deviation, and maximum count, in plants m^{-2}, for each weed category in each year near Saskatoon.

4.2.1 Statistics

Declustering revealed no appreciable difference between the declustered mean and the naive, equal weighted mean since the data are evenly spaced. Declustering is a weighting technique that adjusts data to be representative of the entire area of interest.

There is a decline in the population mean and variance of broad-leaved weeds over three years, whereas the grass population shows no decline, see Figure 4.3. The grass and broad-leaved weed distributions are positively skewed for all years. Table 4.3 shows the mean, standard deviation, and maximum weed count for each year and weed type. Broad-leaved weeds are more numerous in 1995. Grass weeds had a significantly lower average weed density compared to broad-leaved weeds for all 3 years.

Histograms for the grass and broad-leaved data are shown in Figure 4.4. The overall mean for grass weeds is low at 3.4 plants m^{-2} compared to broad-leaved weeds at 37.6 plants m^{-2}, see Figure 4.4. There is more variation in the broad-leaved weed distribution. Both distributions have a positively skewed shape.

Scatter plots in Figure 4.5 indicate that there is no correlation between grass and broad-leaved data for each year. The correlation coefficients are very low at 0.02, 0.06 and 0.04 for 1995, 1996 and 1997 data. The lack of correlation between grass and broad-leaved weeds implies they can be modeled independently.

There are broad-leaved weeds at virtually all locations in all years. The fraction of locations with grass weeds is 0.54, 0.35 and 0.53 for 1995 to 1997. The conditional probability of grass weeds given the previous year are 0.41 and 0.54 for 1996 given 1995 and 1997 given 1996. These are only slightly higher than the marginal probabilities; therefore, there is very little temporal persistence in the weed locations.

4.2.2 Variography

Omnidirectional variograms are shown in Figures 4.6 and 4.7 for the 1995, 1996, 1997 and small grid broad-leaved and grass weed density data. The experimental variograms are calculated from normal score transformed data. Variograms for broad-leaved and grass weed density at the 50 m spacing do not permit reliable inference of the nugget effect. The small grid variogram shows a nugget effect of 40% for the broad-leaved weeds and 55% for the grass weeds.

Directional variograms are shown in Figure 4.8 for the 1995, 1996, 1997 and small grid grass weed density. The dashed lines show the experimental variogram calculated from normal score transformed data for the direction of minimal continuity (N-S). The solid lines

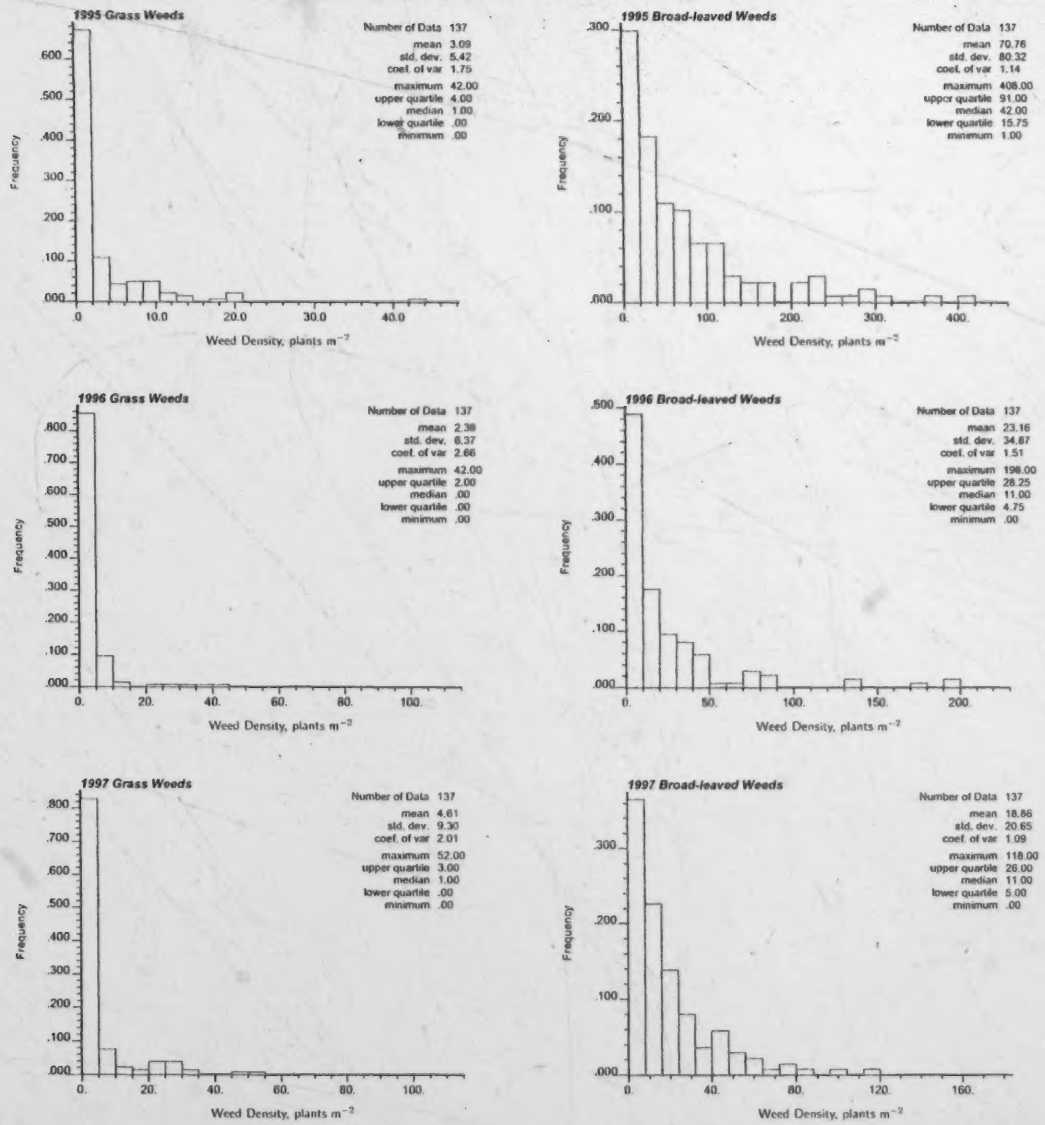

Figure 4.3: Histograms of the weed data near Saskatoon for each year. The histograms on the left are for grass weeds and the histograms on the right are for broad-leaved weeds. The top two histograms are 1995 data, the middle two histograms 1996 data, and the bottom two histograms 1997 data.

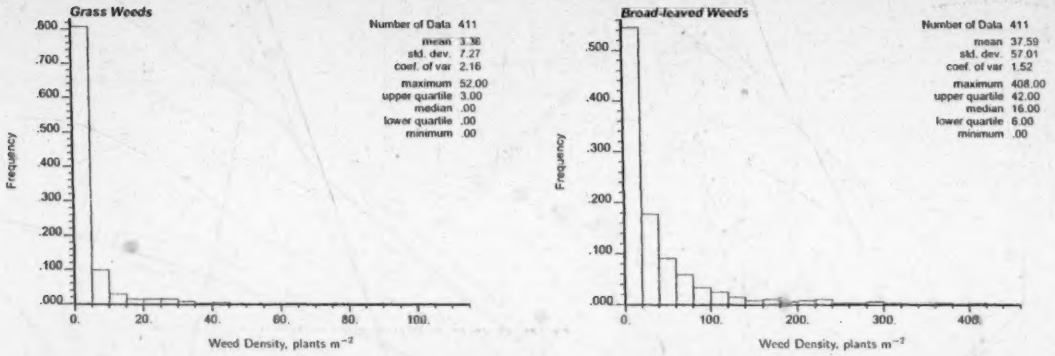

Figure 4.4: Histograms of grass and broad-leaved weed data for all years, 1995 to 1997, near Saskatoon. The histogram on the left is for grass weeds and the histogram on the right is for broad-leaved weeds.

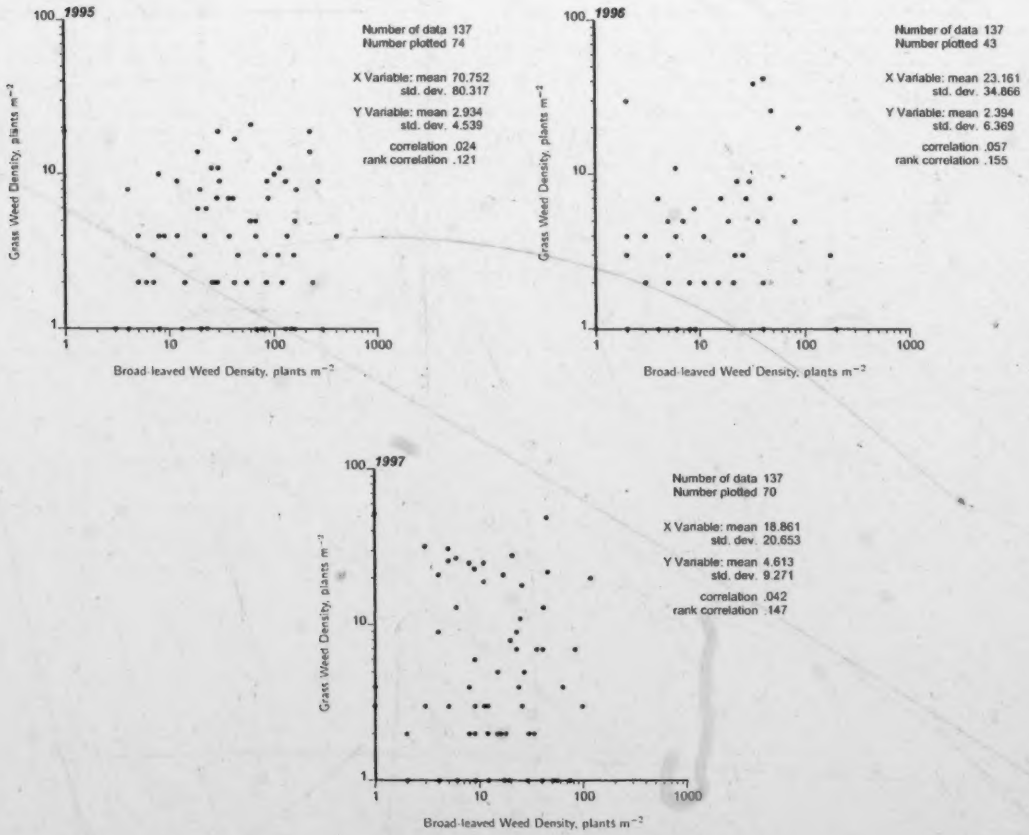

Figure 4.5: Scatter plots of grass weed density compared to broad-leaved weed density for 1995, 1996, and 1997 near Saskatoon indicating that there is no correlation between grass and broad-leaved weed data.

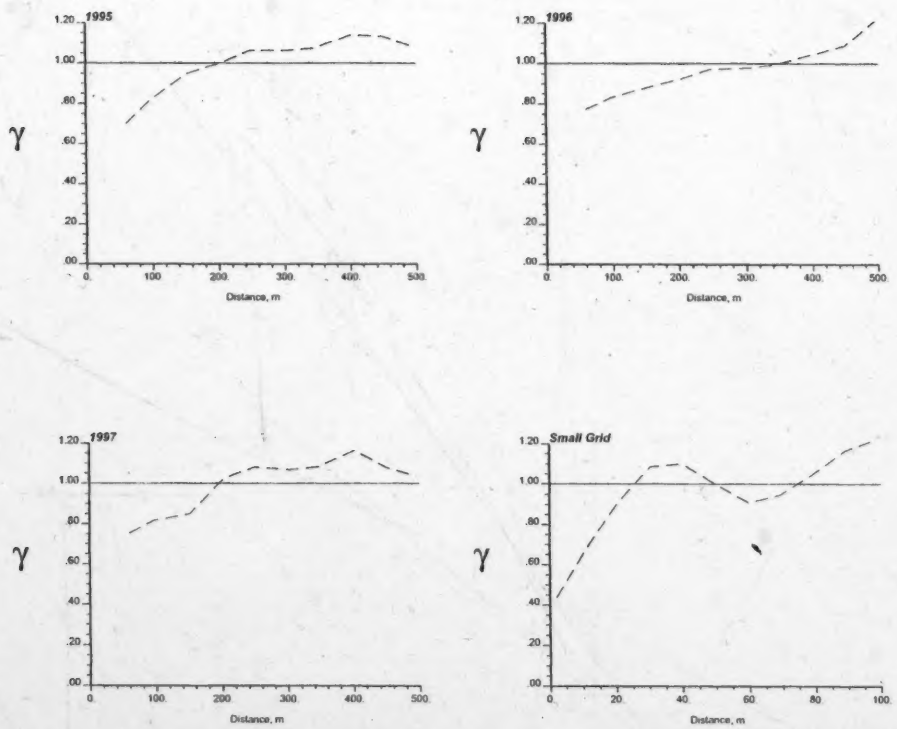

Figure 4.6: Omnidirectional, experimental variograms of the continuous broad-leaved data near Saskatoon. The variogram on the top left is from 1995, top right is from 1996, bottom left is from 1997, and the bottom right is from the small grid in 1996.

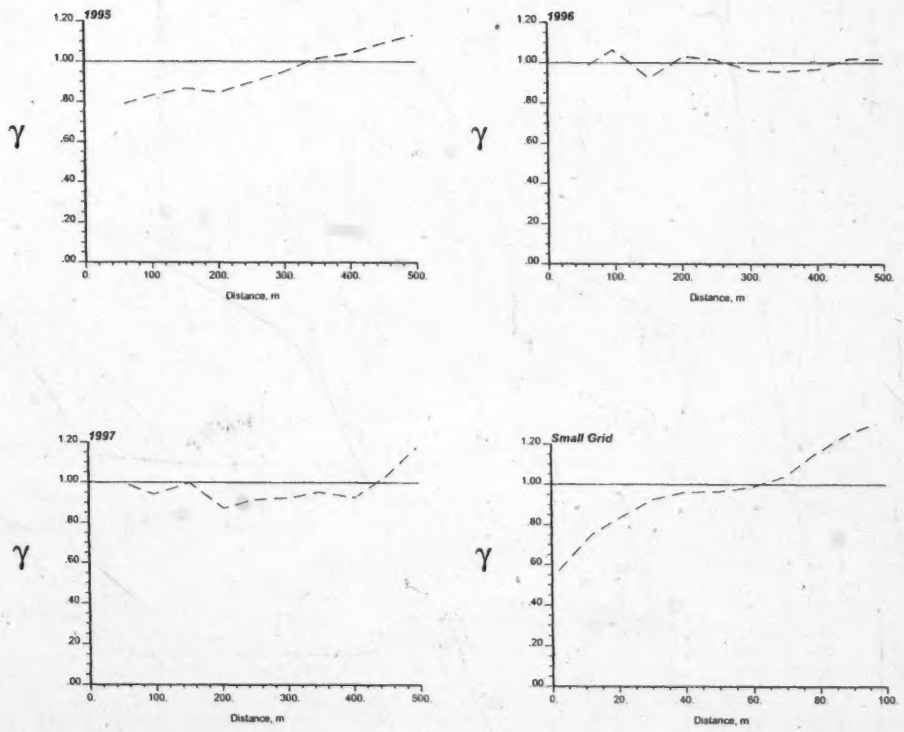

Figure 4.7: Omnidirectional, experimental variograms of the continuous grass data near Saskatoon. The variogram on the top left is from 1995, top right is from 1996, bottom left is from 1997, and the bottom right is from the small grid in 1996.

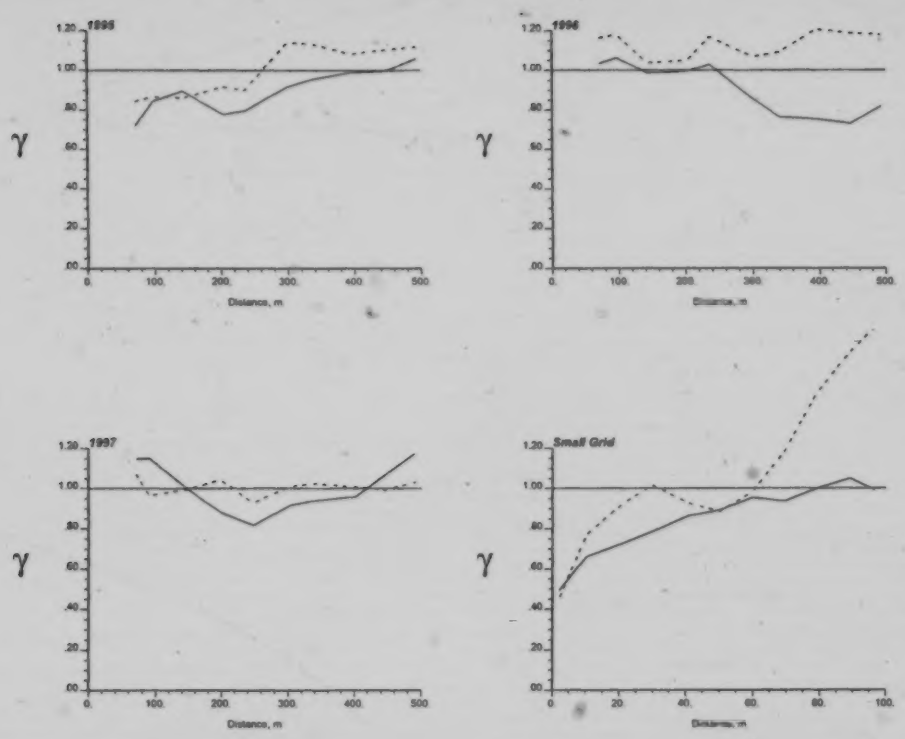

Figure 4.8: Directional, experimental variograms of the continuous grass data near Saskatoon. The variogram on the top left is from 1995, top right is from 1996, bottom left is from 1997, and the bottom right is from the small grid in 1996. The dark, solid line is the experimental variogram in the direction of maximal continuity ($N90^oE$), and the fine, dashed line represents the experimental variogram for the direction of least continuity ($N0^oE$).

are experimental variograms for the direction of maximum continuity (E-W).

Directional variograms for the grass weed density data have a high nugget effect for all years, see Figure 4.8. Directional variograms for broad-leaved weeds have a similar nugget effect, see Figure 4.9. Data from the 1996 small grid are used to infer the nugget effect. This assumes the large scale character of the weed density does not change over time.

Modeling Grass Weeds

Indicator formalism involves coding all data in a common probability. The indicator values are defined as follows for the grass weed density data as present or absent at a location:

$$i(\mathbf{u}; GR_k) = Prob\{\text{grass weeds } k \text{ present}\} = \begin{cases} 1 & \text{if grass weeds } k \text{ present at location } \mathbf{u} \\ 0 & \text{otherwise} \end{cases}$$

For the grass weed density data, an indicator approach is chosen for modeling the location of where grass could be present; then, the continuous grass density data are assigned where grass is present.

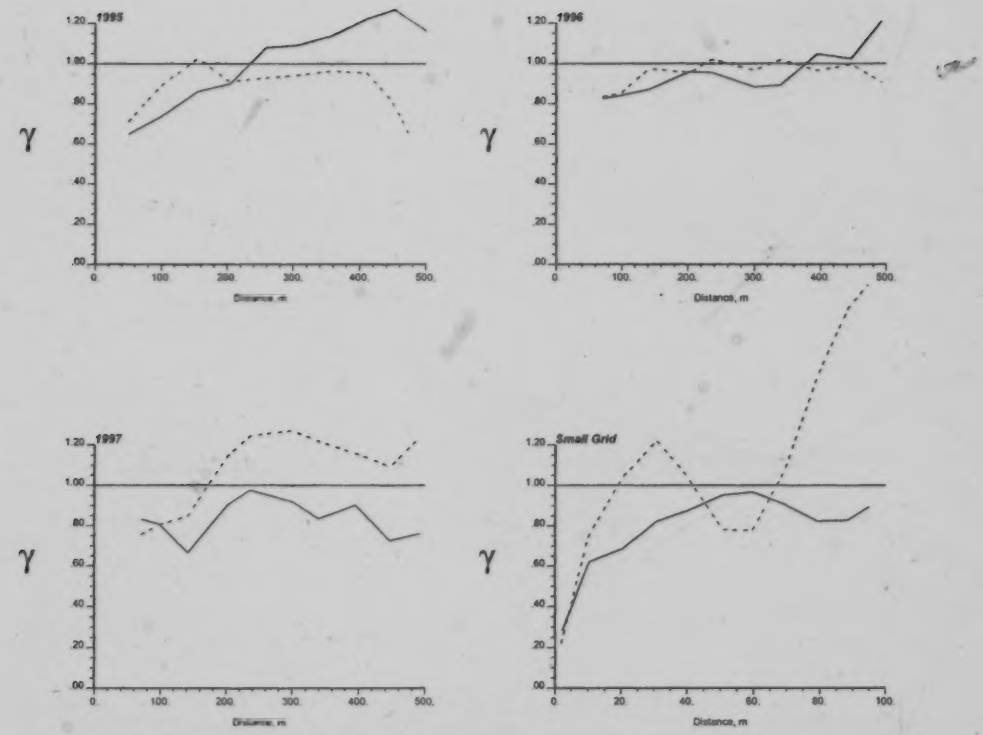

Figure 4.9: Directional, experimental variograms of the continuous broad-leaved data near Saskatoon. The variogram on the top left is from 1995, top right is from 1996, bottom left is from 1997, and the bottom right is from the small grid in 1996. The dark, solid line is the experimental variogram in the direction of maximal continuity ($N90^oE$), and the fine, dashed line represents the experimental variogram for the direction of least continuity ($N0^oE$).

Year	Nugget	Cont. 1	Range (m) 1	Cont. 2	Range (m) 2
1995(max)	0.12	0.10	20	0.03	∞
1995(min)	0.12	0.10	30	0.03	250
1996(max)	0.12	0.10	20	0.03	∞
1996(min)	0.12	0.10	15	0.03	150
1997(max)	0.12	0.09	20	0.04	400
1997(min)	0.12	0.09	15	0.04	300

Table 4.4: Directional parameters for indicator grass weed density variograms models for 1995, 1996 and 1997 near Saskatoon. "Cont." refers to the variance contribution of each nested structure. The direction of maximal continuity is the E-W direction and variograms are modeled with 2 nested spherical, structures.

Directional indicator variogram parameters given in Table 4.4 indicate that 2 nested structures are modeled with spherical structures for each year. The sill is standardized to a unit variance using $p(1-p)$ where p is probability of the grass data being present or 0.5. The direction of maximal continuity for all years is E-W while the direction of minimal continuity is N-S. The corresponding variograms are shown in Figures 4.10, 4.11, and 4.12. The gray dashed and solid lines show the experimental variogram calculated from normal score transformed data for the direction of maximal continuity. The gray and dark solid lines are model variograms while the gray and dark dashed lines represent experimental variograms. The large scale 1996 variogram points are used for all years.

Sequential indicator simulation is applied to the grass weed density data. Locations that have grass weeds present are simulated as categorical variables using the spatial parameters from the model indicator variograms. The global cdf values for the 1995, 1996 and 1997 data are 0.54 and 0.46, 0.35 and 0.65, and 0.52 and 0.48. Indicator simulation is calculated at a 1 m size since sampling for weed density data in the small grid is at this scale. Eleven realizations are created with sequential indicator simulation using GSLIB software (Deutsch & Journel, 1998) [36]. The number of realizations is small since substantial computer time is required to process them. Two realizations from the Saskatoon site for each year are illustrated in Figure 4.13. The realizations in Figure 4.13 are different in size from Figure 4.1 due to truncation of the data sets. These realizations can be used for decision-making and quantifying uncertainty by the numerical differences between them at a given location.

Model variogram parameters used for simulating grass weed counts are given in Table 4.5. The nugget effect is 40% and 2 nested structures are used. Direction of maximal continuity is E-W and N-S is the direction of minimal continuity. The model and experimental variograms for each year are displayed in Figures 4.14, 4.15, and 4.16. The gray dashed and solid lines represent variograms in the direction of maximal continuity, and the dark dashed and solid lines are variograms in the direction of least continuity. The gray and dark solid lines are model variograms while the gray and dark dashed lines represent experimental variograms.

Modeling Broad-leaved Weeds

Broad-leaved weeds are modeled as a continuous variable throughout the domain of study, see Figure 4.17. The direction of maximal continuity is E-W and the direction of minimal

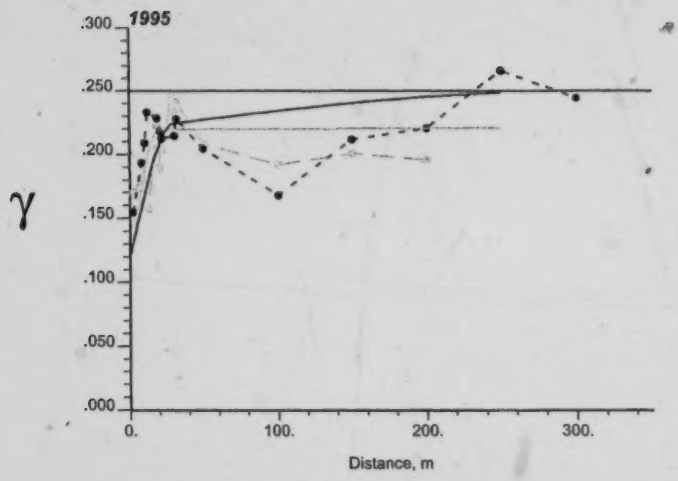

Figure 4.10: The 1995 directional, indicator, variograms of continuous grass data near Saskatoon. The gray dashed and solid lines represent variograms in the direction of maximal continuity, and the dark dashed and solid lines are variograms in the direction of least continuity. The gray and dark solid lines are model variograms while the gray and dark dashed lines represent experimental variograms.

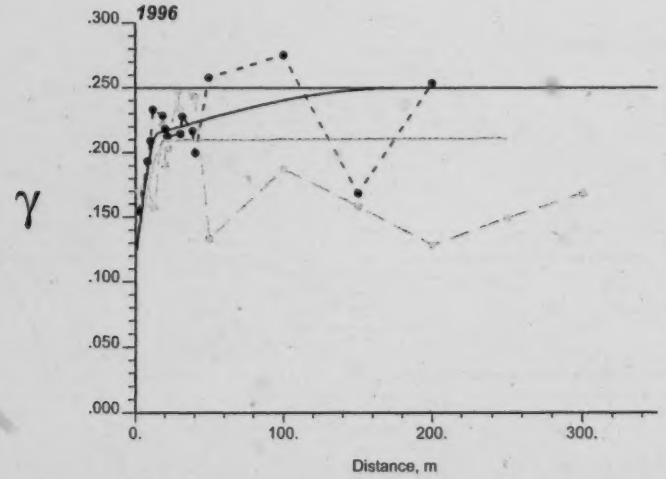

Figure 4.11: The 1996 directional, indicator, variograms of continuous grass data near Saskatoon. The gray dashed and solid lines represent variograms in the direction of maximal continuity, and the dark dashed and solid lines are variograms in the direction of least continuity. The gray and dark solid lines are model variograms while the gray and dark dashed lines represent experimental variograms.

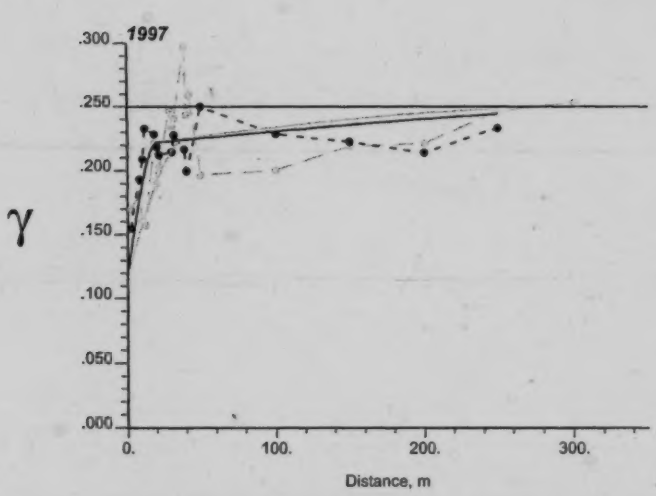

Figure 4.12: The 1997 directional, indicator, variograms of continuous grass data near Saskatoon. The gray dashed and solid lines represent variograms in the direction of maximal continuity, and the dark dashed and solid lines are variograms in the direction of least continuity. The gray and dark solid lines are model variograms while the gray and dark dashed lines represent experimental variograms

Year	Nugget	Cont. 1	Range (m) 1	Cont. 2	Range (m) 2	Cont. 3	Range (m) 3
1995(max)	0.40	0.35	20	0.25	500	-	-
1995(min)	0.40	0.35	40	0.10	340	-	-
1996(max)	0.40	0.30	40	0.20	75	0.10	120
1996(min)	0.40	0.30	20	0.20	50	0.10	75
1997(max)	0.40	0.30	40	0.10	75	0.10	120
1997(min)	0.40	0.30	20	0.10	50	0.10	75

Table 4.5: Directional parameters for continuous grass weed density variograms models for 1995, 1996 and 1997 near Saskatoon. "Cont." refers to the variance contribution of each nested structure. Two or 3 nested spherical, structures are used to model each variogram.

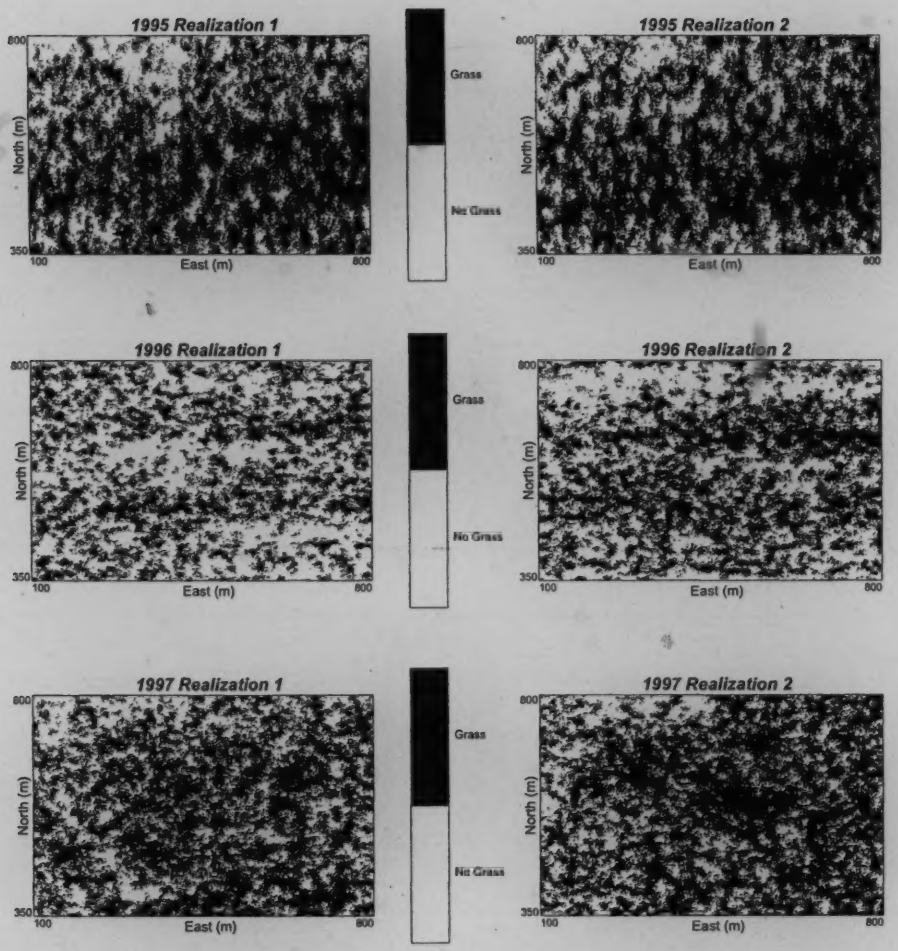

Figure 4.13: Two realizations from sequential indicator simulation of weed density for grass data for 1995, 1996 and 1997 near Saskatoon. The top figures are 1995, the middle are 1996, and the bottom are 1997 where black represents presence of grass weeds.

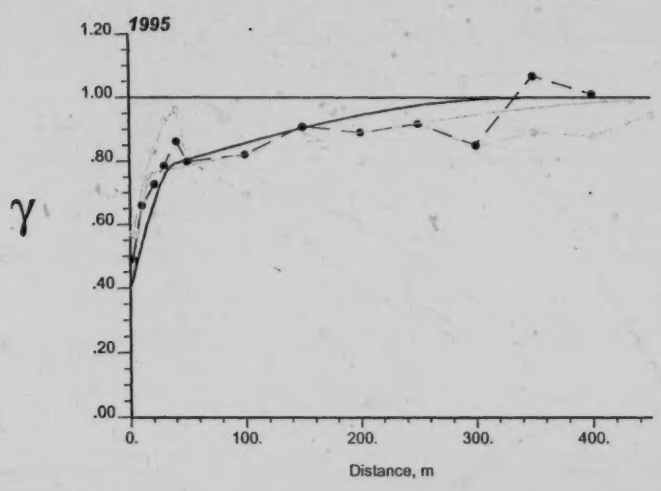

Figure 4.14: The 1995 directional variograms of continuous grass data near Saskatoon. The gray dashed and solid lines represent variograms in the direction of maximal continuity, and the dark dashed and solid lines are variograms in the direction of least continuity. The gray and dark solid lines are model variograms while the gray and dark dashed lines represent experimental variograms.

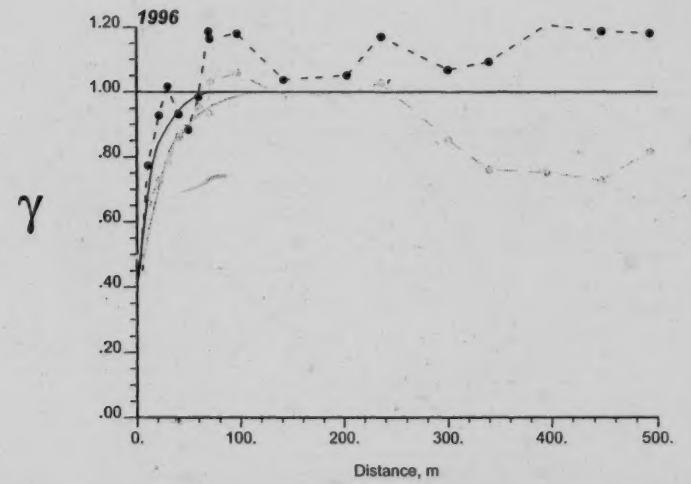

Figure 4.15: The 1996 directional variograms of continuous grass data near Saskatoon. The gray dashed and solid lines represent variograms in the direction of maximal continuity, and the dark dashed and solid lines are variograms in the direction of least continuity. The gray and dark solid lines are model variograms while the gray and dark dashed lines represent experimental variograms.

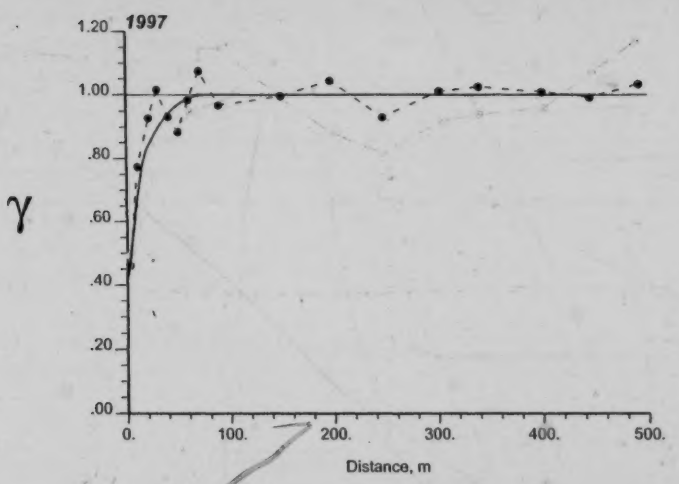

Figure 4.16: The 1997 directional variograms of continuous grass data near Saskatoon. The gray dashed and solid lines represent variograms in the direction of maximal continuity, and the dark dashed and solid lines are variograms in the direction of least continuity. The gray and dark solid lines are model variograms while the gray and dark dashed lines represent experimental variograms.

continuity is N-S direction for the 1995 and 1996 variograms while in 1997 the direction of maximal continuity is $N60^oE$ and the direction of minimal continuity is perpendicular to this direction. Two nested structures modeled the spatial variability for each variogram in 1995, 1996 and 1997. Table 4.6 provides the directional, model variogram parameters used for broad-leaved weed densities in each year.

A waterway crosses the south east corner of the field. This may have influenced the anisotropy of the broad-leaved and grass weed distributions.

To determine if the original variogram used to model spatial correlation is correct, variograms can be calculated from each realization. Only the broad-leaved variograms are calculated from each realization and compared to the original variogram model; however, the grass indicator variograms could be compared to their original variogram model. The variograms from each of the 11 realizations and the original variogram model are displayed in Figures 4.18, 4.19, and 4.20. The solid line represent the variogram model while the dashed lines are the variogram models for each of the 11 realizations. The realization variograms closely match the original models in each year implying that the simulation program is working correctly.

Sequential Gaussian simulation is performed with the broad-leaved weed density data at the 1 m scale. Eleven realizations are created with sequential Gaussian simulation using GSLIB software (Deutsch & Journel, 1998) [36]. The number of realizations is small since considerable computer time is required to process them. A realization and histogram of that realization for each year are illustrated in Figures 4.21 and 4.22. The mean and standard deviation of each realization for each year closely match the mean and standard deviation of the original broad-leaved weed distribution for that year, see Table 4.3.

Year	Nugget	Cont. 1	Range (m) 1	Cont. 2	Range (m) 2
1995(max)	0.05	0.68	30	0.27	210
1995(min)	0.05	0.68	23	0.27	23
1996(max)	0.06	0.69	30	0.10	150
1996(min)	0.06	0.69	27	0.10	27
1997(max)	0.05	0.75	30	0.20	150
1997(min)	0.05	0.75	25	0.20	25

Table 4.6: Directional parameters for continuous broad-leaved weed density variogram models for 1995, 1996 and 1997 near Saskatoon. "Cont." refers to the variance contribution of each nested structure. Two nested spherical, structures are used to model each variogram.

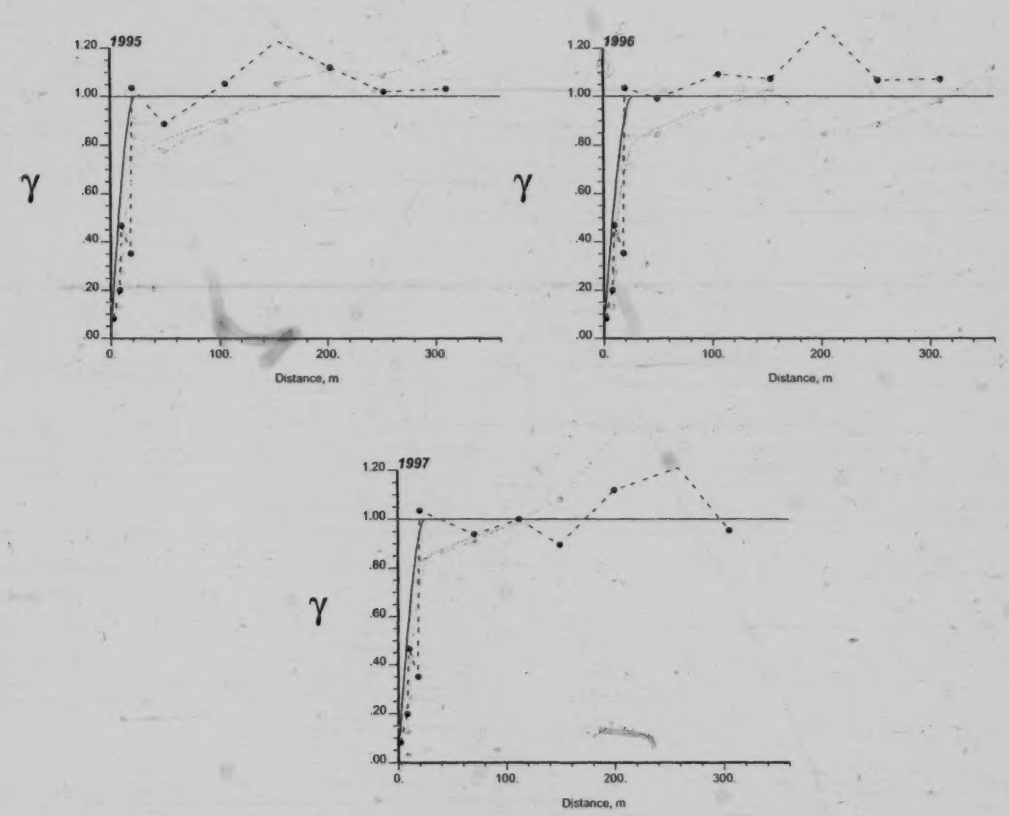

Figure 4.17: The 1995, 1996 and 1997 directional variograms of continuous broad-leaved data near Saskatoon. The gray dashed and solid lines represent variograms in the direction of maximal continuity, and the dark dashed and solid lines are variogram in the direction of least continuity. The gray and dark solid lines are model variograms while the gray and dark dashed lines represent experimental variograms.

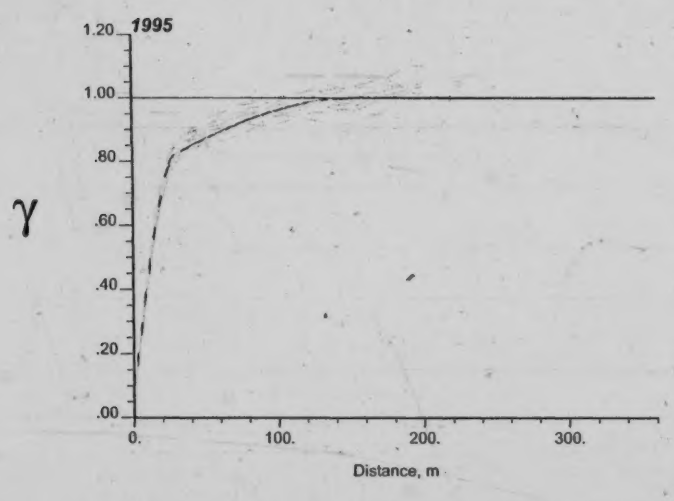

Figure 4.18: The 1995 simulated, variograms of continuous broad-leaved data near Saskatoon. The solid line represent the variogram model while the dashed lines are the variogram models for each of the 11 realizations for the E-W direction.

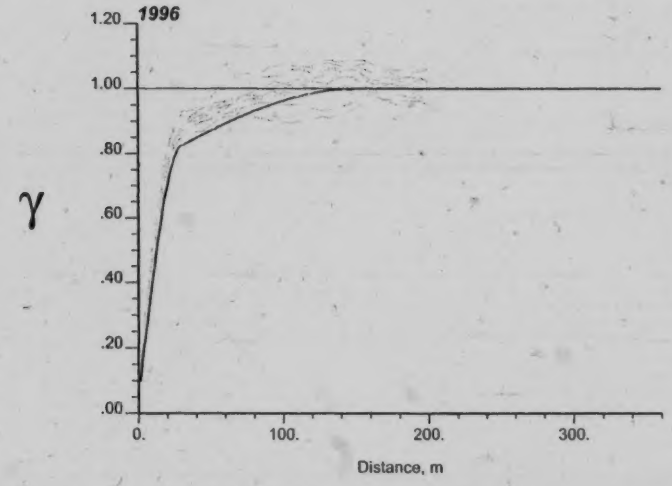

Figure 4.19: The 1996 simulated, variograms of continuous broad-leaved data near Saskatoon. The solid line represent the variogram model while the dashed lines are the variogram models for each of the 11 realizations for the E-W direction.

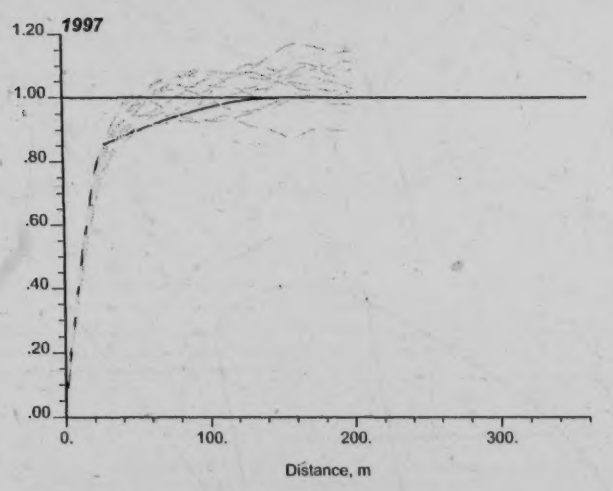

Figure 4.20: The 1997 simulated, variograms of continuous broad-leaved data near Saskatoon. The solid line represent the variogram model while the dashed lines are the variogram models for each of the 11 realizations for the E-W direction.

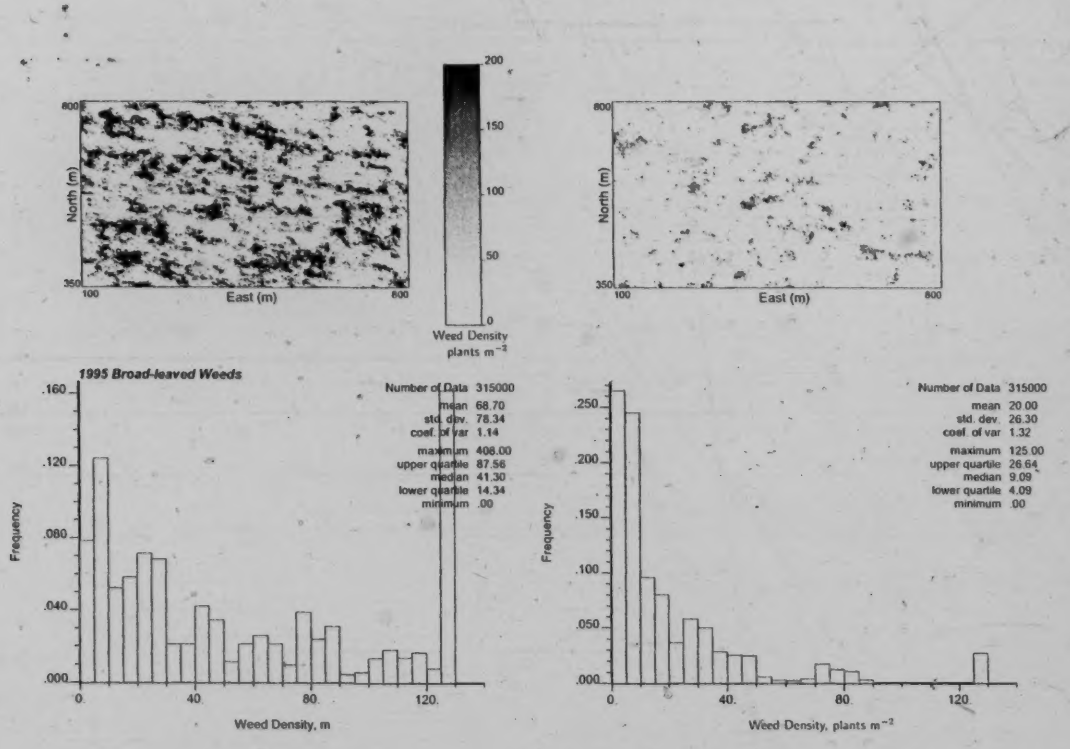

Figure 4.21: Simulation of broad-leaved weed density data illustrating a realization and histogram of the 1995 (left) and 1996 (right) weed distributions for the Saskatoon site. The last interval of weed density for the 1995 histogram represents number of weeds greater than 125 plants m^{-2}.

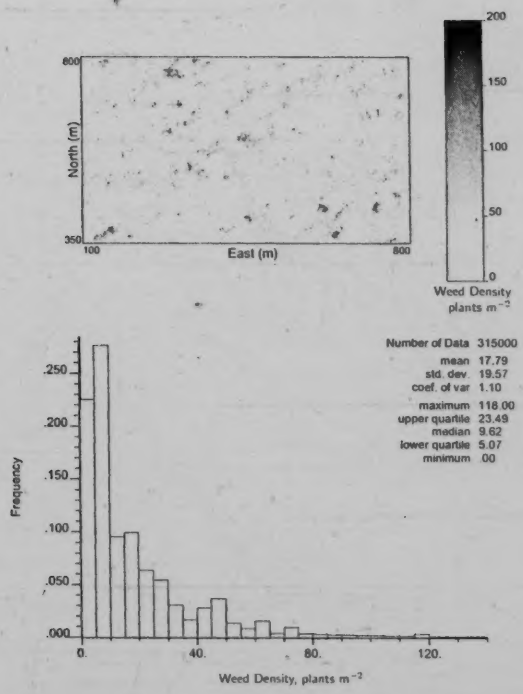

Figure 4.22: Simulation of 1997 broad-leaved weed density data illustrating a realization with a histogram of the weed distribution for that realization for the Saskatoon site.

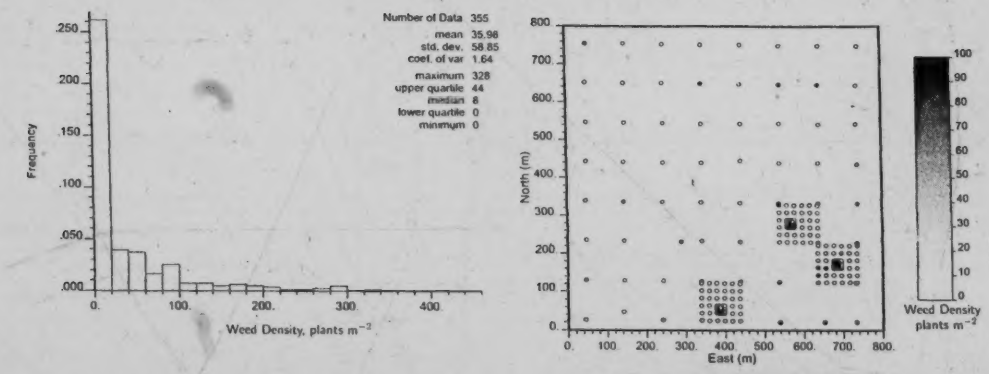

Figure 4.23: A histogram and map of wild oat density sampling locations from a field near Viking, Alberta in 2000 that is used for generating a synthetic, reference wild oat distribution. Wild oat, in plants m^{-2}, is identified at each location. Increasing greyscale indicates increasing wild oat density so white is no wild oat present while black represents over 200 wild oat m^{-2}.

4.3 Viking and Stony Plain Data

Wild oat density data are recorded in two 64 ha fields near Viking and Stony Plain, Alberta in 2000. Wild oat is identified and counted at the 3-4 leaf stage prior to post-emergent herbicide application in a nested grid sampling pattern, see Figure 4.23. The Stony Plain site is described in Figure 3.1 at the beginning of Chapter 3.

4.3.1 Statistics

Lower wild oat numbers are recorded at the Viking field compared to the Stony Plain site. The mean, standard deviation and maximum wild oat m^{-2} are 102, 139 and 952 for the Stony Plain site and 36, 59 and 328 for the Viking site, respectively. A positively skewed distribution is noted for both sites as 18% and 54% of the sampling locations at the Stony Plain and Viking fields, respectively, had fewer than 10 wild oat m^{-2} in 2000. There are 29% and 40% of all the locations that had no wild oat in 2000 and 2001 for the Viking field. Wild oat density measured at different spatial scales in these fields for 2000 and 2001 indicated that the mean plant density and number of quadrats occupied varied considerably, see Table 4.7.

4.3.2 Variography

Variograms are calculated for wild oat density data from the nested pattern of sampling locations that are displayed in Figure 4.23. A similar pattern of sampling locations for the Stony Plain site is displayed in Figure 3.1, Chapter 3. The omnidirectional variogram models for the Stony Plain and Viking sites are presented in Figure 4.24 and Table 4.8. Two nested structures are used to model the experimental wild oat density data with a nugget of 0.02 and 0.04 for the Viking and Stony Plain fields, respectively. The range of correlation for the large scale variation is $4\frac{1}{2}$ m at the Viking site while it is 15 m at the Stony Plain site. Variation in wild oat density over the smaller scale also differs between

Sampling Scale	Mean plants m^{-2} in 2000	% Quadrates Occupied in 2000	Mean plants m^{-2} in 2001	% Quadrates Occupied in 2001
Large	34	75.0	60	65.6
Medium	14	55.6	19	47.2
Fine	34	76.0	28	58.7
Super fine	61	80.6	56	70.4

Large	49	67.2	50	70.3
Medium	111	97.2	32	65.7
Fine	103	97.3	99	70.7
Super fine	124	100.0	94	67.6

Table 4.7: A comparison of the mean wild oat density and occupied 1 m^{-2} quadrats from 2 fields, the top table being for Viking, Alberta and the bottom table from Stony Plain, Alberta over 2 years. Sample scale refers to distance between sampling locations of 100, 20, 5, and 1 m for large, medium, fine and super fine grids.

Field	Nugget	Cont.	Range (m)	Cont.	Range (m)
		1	1	2	2
Viking	0.02	0.64	4.5	0.34	150.0
Stony Plain	0.04	0.78	15.0	0.18	410.0

Table 4.8: Omnidirectional variogram model parameters using the nested pattern of sampling for the Viking and Stony Plain sites. "Cont." refers to the variance contribution of each nested structure. Two nested spherical, structures are used to model each variogram.

the 2 sites with the Viking site having a shorter variation than the Stony Plain site.

The omnidirectional variogram parameters from Table 4.8 are used to create a kriged map of wild oat density for each 64 ha field. Similarly, the same variogram parameters are used to create realizations using stochastic simulation for each field. When directional variograms are calculated for the Viking field, the direction of maximal continuity is in the N-S direction compared to the E-W direction for the Stony Plain field, see Figure 4.25. The gray, solid lines are the experimental variogram in the direction of least continuity; the dark, solid lines represent experimental variograms for the direction of maximal continuity.

Kriged and simulated wild oat density maps are shown in Figures 4.26 and 4.27. Mean wild oat densities are higher at the Stony Plain site compared to the Viking field. These differences are reflected in the histogram shape for each field. The average wild oat density for the Stony Plain field is 80 and 114 plants m^{-2} for kriging and simulation while the standard deviation is 41 and 136 plants m^{-2} for kriging and simulation. There is three times the variation in the simulated wild oat density map compared to the kriged wild oat density map for each field.

4.3.3 Reference Map

Assessing the validity of a crop-weed-herbicide model can be undertaken by using a reference map of weed density. Different models are applied to the reference map and total revenue in dollars $field^{-1}$ for each model is used for comparison purposes.

To begin, reference maps of wild oat density, in numbers m^{-2}, are taken to be realizations

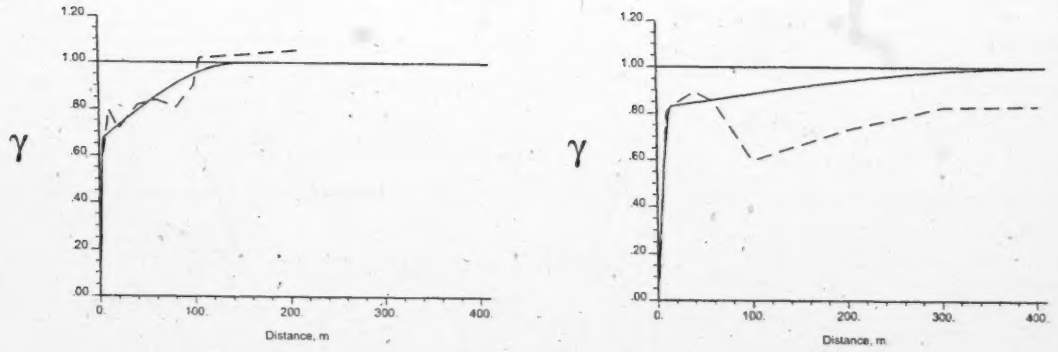

Figure 4.24: Omnidirectional variogram models from the nested sampling pattern of wild oat density for each 64 ha field near Stony Plain, Alberta (left) and Viking, Alberta (right). The solid lines are model variograms while the dashed lines represent experimental variograms.

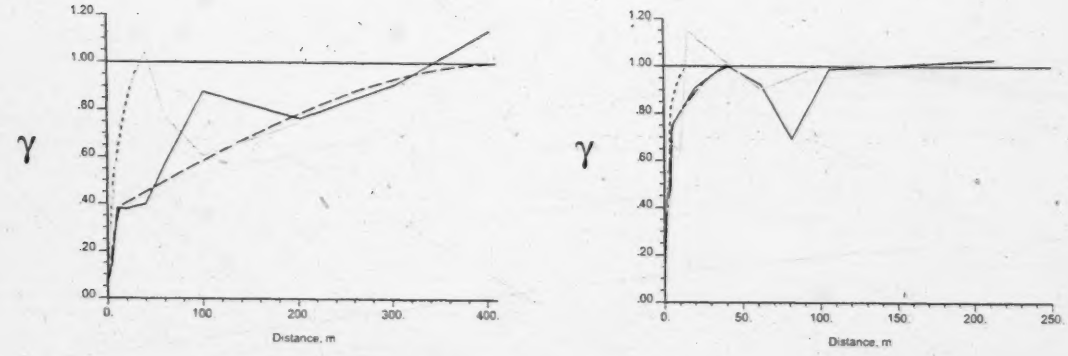

Figure 4.25: Directional variograms of continuous wild oat data from a nested sampling pattern for each 64 ha field near Stony Plain, Alberta (left) and Viking, Alberta (right). The dashed lines are model variograms while the solid lines represent experimental variograms. The gray solid and short dashed lines represent variograms in the direction of least continuity, and the dark dashed and solid lines are variograms in the direction of maximal continuity.

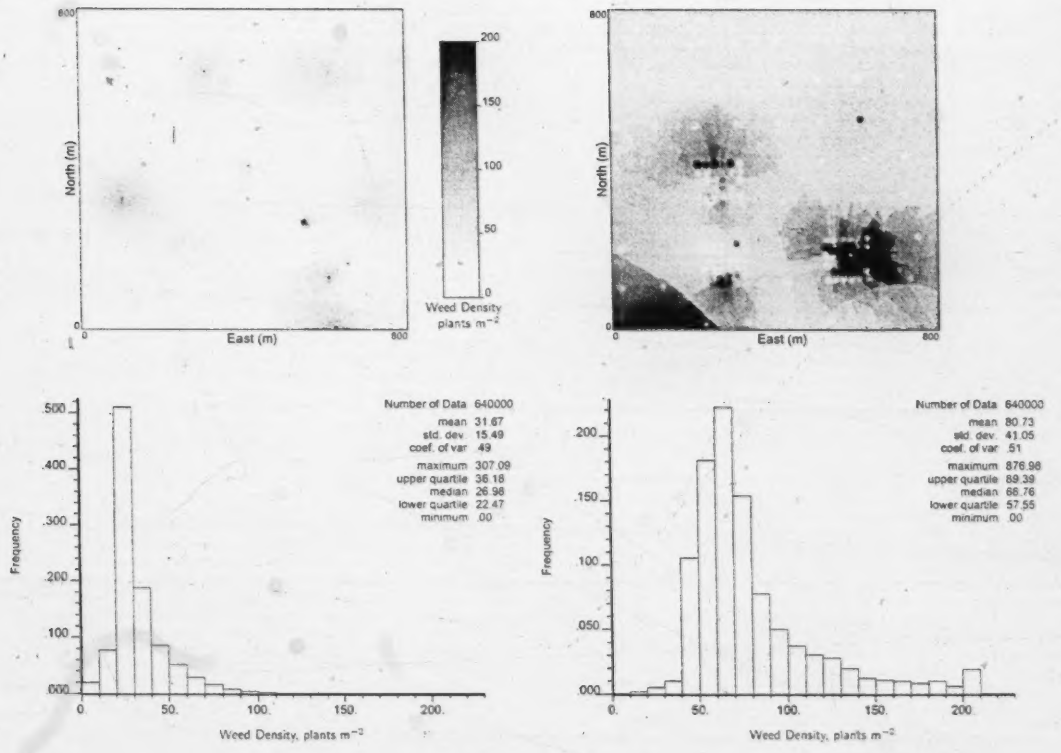

Figure 4.26: Kriged maps and histograms of wild oat density from fields near Viking, Alberta (left) and Stony Plain, Alberta (right).

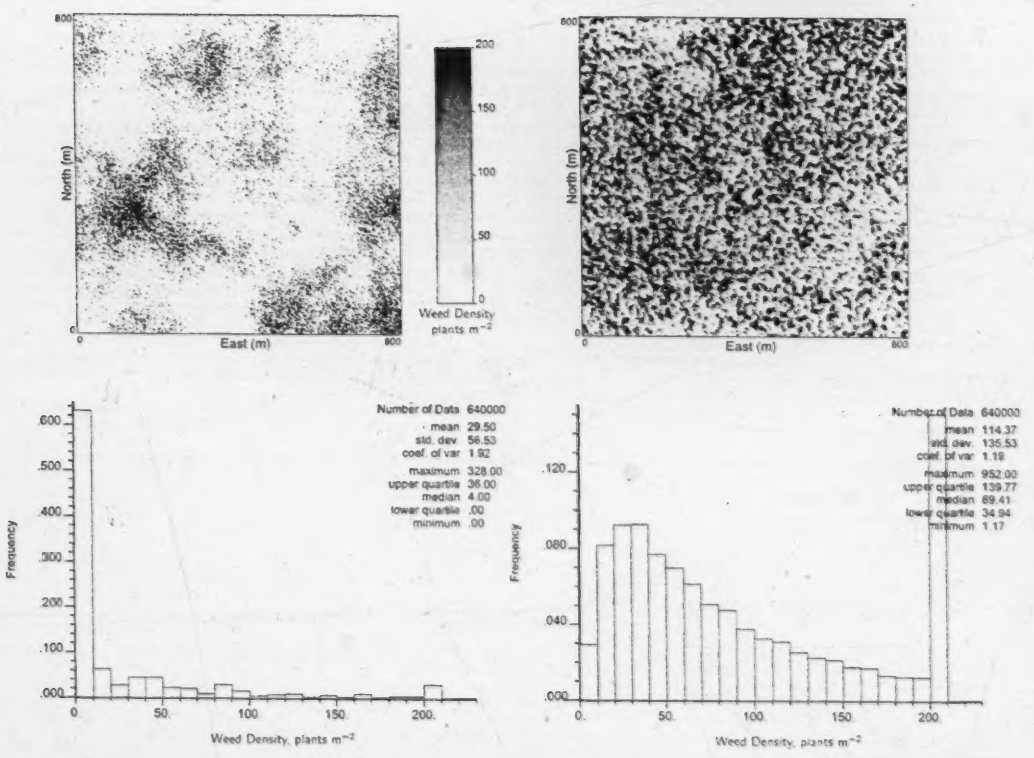

Figure 4.27: Simulated maps and histograms of wild oat density from fields near Viking, Alberta (left) and Stony Plain, Alberta (right). Each simulated map is one realization. The last interval of wild oat density for the Stony Plain histogram represents number of weeds greater than 200 plants m^{-2}.

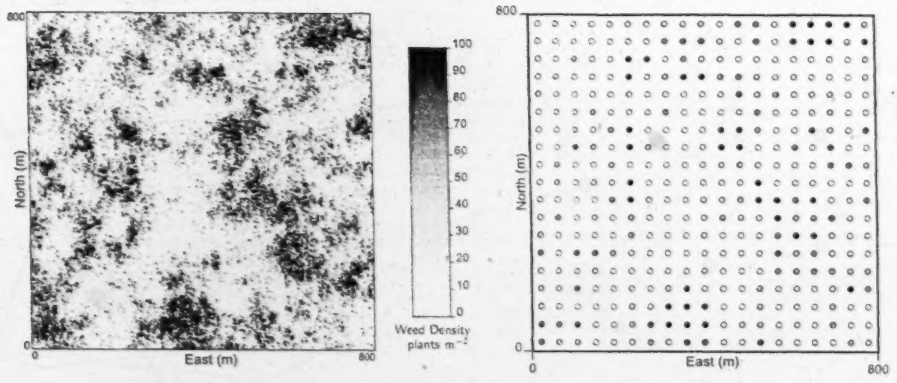

Figure 4.28: Reference map (left) of wild oat density for a 64 ha field near Viking, Alberta and location map (right) of wild oat density for grid map from this same field.

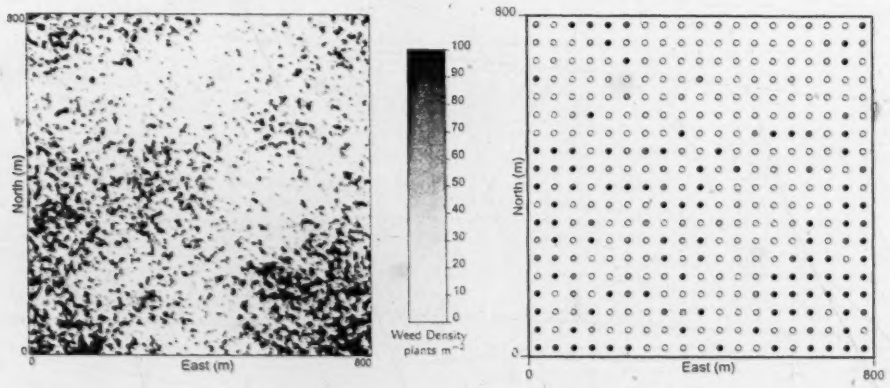

Figure 4.29: Reference map (left) of wild oat density for a 64 ha field near Stony Plain, Alberta and location map (right) of wild oat density for grid map from this same field.

of a 64 ha field near Viking and Stony Plain, Alberta. The reference maps of wild oat density values are sampled at 42 m intervals for a total of 361 sampling locations, see Figures 4.28 and 4.29.

An omnidirectional variogram is calculated for wild oat density from the grid map of each reference map. Variogram model parameters for each grid map are presented in Table 4.10 and Figure 4.30. There are differences in nugget effect and small and large scale variation between the fields. These parameters are used to create kriged and simulated maps of wild oat density for each field. A kriged and simulated wild oat density map is shown in Figures 4.31 and 4.32. Dark areas of the map indicate heavy infestations of wild oat that require herbicide treatment. Light gray areas indicate no wild oat or low infestations. Correlation coefficients between the reference maps in Figures 4.28 and 4.29 and the kriged or simulated maps in Figures 4.31 and 4.32 for the 2 sites indicate about half the linear relationship is associated, see Table 4.9. This means that about 25% of the wild oat density variance from the reference map can be predicted by the variance of the kriged or simulated

Field	Wild Oat Density	Kriging	Simulation
Viking	Single	0.41	0.42
	Double	0.41	0.42
	Triple	0.41	0.43
Stony Plain	Single	0.51	0.50
	Double	0.51	0.50
	Triple	0.51	0.50

Table 4.9: Correlation coefficients between the reference wild oat density map and the kriged or simulated wild oat density map for fields near Viking and Stony Plain, Alberta.

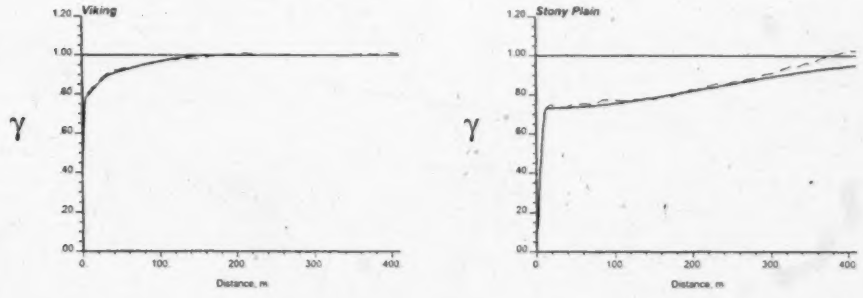

Figure 4.30: Omnidirectional variogram models for the grid maps of wild oat density for a 64 ha field near Viking, Alberta (left) and Stony Plain, Alberta (right). The solid lines are model variograms while the dashed lines represent experimental variograms.

map.

The mean, variance and minimum and maximum wild oat density are described for the reference, grid, kriged and simulated maps in Table 4.11. The lowest amount of variance occurs for the kriged map in both fields. Mean wild oat density is similar for all maps.

Different herbicide treatments are compared using reference maps in Chapters 5 and 6. The crop-weed-herbicide model is applied to kriged and simulated wild oat density maps at a 1 m^{-2} scale from a field that results in herbicide rate maps. If these herbicide rate maps are scaled up to a SSA for spraying, variability will be reduced and expected revenue will be lower. Revenue from these herbicide rate maps is compared to revenue from the reference map of that field. The map with revenue closest to the reference is the optimal treatment.

Field	Nugget	Cont.	Range (m)	Cont.	Range (m)	Cont.	Range (m)
		1	1	2	2	3	3
Viking	0.45	0.31	4.0	0.10	39.0	0.14	170.0
Stony Plain	0.04	0.69	13.0	0.27	545.0		

Table 4.10: Omnidirectional variogram model parameters using the grid map derived from the Viking and Stony Plain reference maps of each field. "Cont." refers to the variance contribution of each nested structure. A spherical model is used for the 3 nested structures for the Viking grid map while a spherical model is used for the first structure and a Gaussian model for the second nested structure in the Stony Plain grid map.

Field	Map	Mean	Variance	Minimum - Maximum Density, plants m^{-2}
Viking	Reference	34.9	1014	1 - 546
	Grid	36.4	1196	3 - 308
	Kriged	36.5	142	15 - 86
	Simulated	34.9	1024	0 - 309

Field	Map	Mean	Variance	Minimum - Maximum Density, plants m^{-2}
Stony Plain	Reference	65.4	11064	0 - 950
	Grid	64.8	12740	0 - 906
	Kriged	63.8	2839	10 - 331
	Simulated	59.1	12134	0 - 907

Table 4.11: Wild oat density parameters for the reference, grid, kriged and simulated map. The grid map is sampled every 42 m for a total of 361 sampling locations in each 64 ha field near Viking and Stony Plain, Alberta.

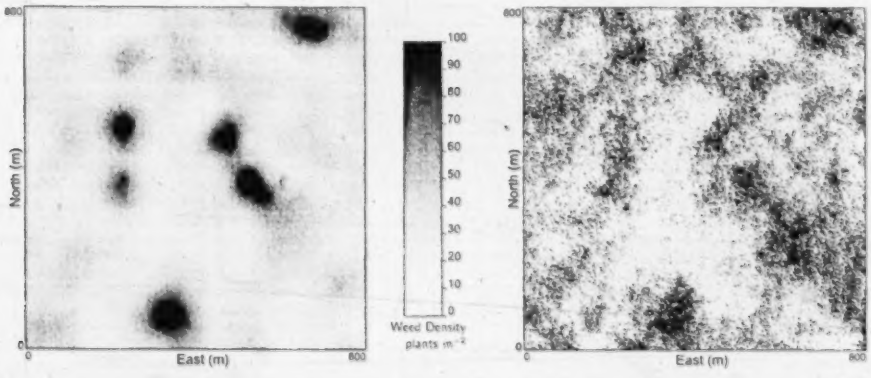

Figure 4.31: A kriged and simulated weed density map, in wild oat plants m^{-2}, from a 64 ha field near Viking, Alberta. The simulated wild oat density map represents one realization.

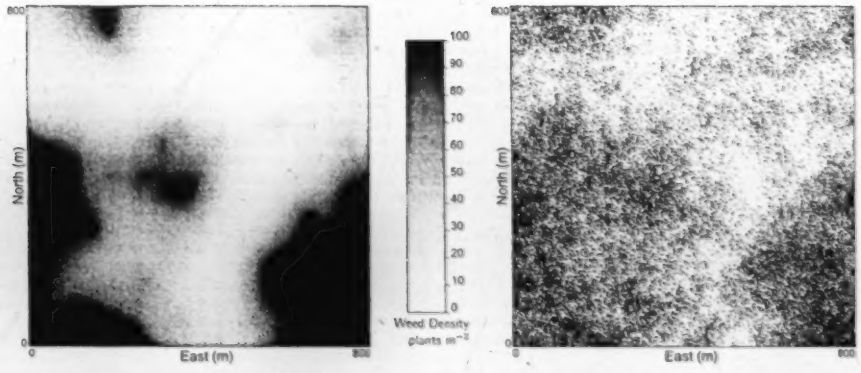

Figure 4.32: A kriged and simulated weed density map, in wild oat plants m^{-2}, from a 64 ha field near Stony Plain, Alberta. The simulated wild oat density map represents one realization.

Chapter 5

Application

A model to quantify the uncertainty of various parameters for determining optimal herbicide rate is derived. The model relies on building distributions of uncertainty for factors that influence the crop, weed and herbicide. Sample values of weed density are utilized to describe the effect of the herbicide on weed distribution. Weed density is simulated based on the available samples. The model accounts for the effect of weeds on crop yield and herbicide treatment is optimized. The final outcome is a herbicide rate map in % m^{-2}. This result may be multiplied by the label rate, in g ai m^{-2}, to give an actual herbicide treatment rate. In this chapter, a crop-weed-herbicide model for wild oat infestations is applied in canola and barley crops.

Components of the crop-weed-herbicide model including herbicide dose response curves and crop yield loss equations have parameter values that are assumed to represent field conditions. Herbicide application costs for the crop-weed-herbicide model are assumed to be \$12 ha^{-1} while a technology use agreement fee is \$37 ha^{-1} and retail herbicide prices in Canadian dollars from 2001 are used. Selling price of crops in 1992 Canadian dollars may not reflect future prices. Wild oat-free crop yields are taken from published studies and represent many environmental and management conditions. Local calibration with wild oat-free crop yields will increase the model's predictive ability.

Herbicide application rate is proportional to weed density such that a crop's competitive position relative to the weeds is enhanced. A larger crop loss is anticipated with a higher weed density while a higher herbicide application rate implies a higher dose per plant.

Herbicide rates that vary from the label rate in Canada are illegal and imply a liability for the end user. It is assumed that locally varying herbicide rates can be implemented by farm managers in Canada.

Model Parameters

Dose response curves are described for three different herbicides applied to reduce wild oat biomass in crops such as barley and canola, see Figure 5.1. The parameter values for these models are taken from the literature and described in Chapter 2 (Lemerle & Verbeek, 1995; Madsen et al., 1999; Madsen et al., 1999; Seefeldt et al., 1995) [84, 87, 88, 134].

Sampling a 64 ha field near Stony Plain, Alberta provided wild oat density data at a square meter scale with a minimum plant density of 0 to a maximum of 950 plants. Wild oat-free yield is 4.7 t ha^{-1} for barley and 1.9 t ha^{-1} for canola, see Table 5.1. These yields are obtained from different studies in western Canada (O'Donovan, 1994; O'Donovan et al., 1999) [109, 113].

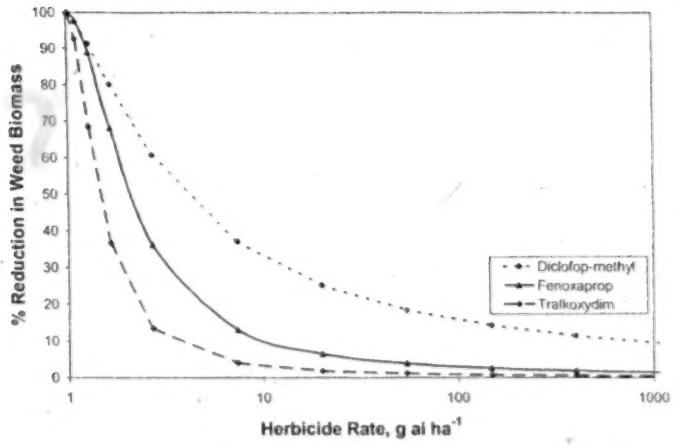

Figure 5.1: Comparison of dose-response curves for diclofop-methyl, fenoxaprop, and tralkoxydim where different herbicide rates result in different levels of wild oat injury as measured by a per cent decrease in weed biomass.

Crop	Herbicide	Label Rate (g ai ha^{-1})	Weed Free Yield (t ha^{-1})	Crop Price (dollars t^{-1})	Herbicide Cost (dollars l^{-1} of product)
Barley	Diclofop-methyl	771.9	4.7	74	14
Barley	Tralkoxydim	197.7	4.7	74	162
Barley	Fenoxaprop	92.1	4.7	74	39
Canola	Glyphosate	439.8	1.9	214	46
Canola	Glufosinate	500.4	1.9	214	21
Canola	Imazethapyr	50.4	1.9	214	1470

Table 5.1: Economic parameters for barley and canola yield loss due to wild oat with different herbicides.

Seeding rates that result in a barley density of 75 to 260 plants m^{-2} in western Canada are 85 to 144 kg ha^{-1} (O'Donovan et al., 1999) [113]. For canola, seeding rates range from 4 to 8 kg ha^{-1} for a density of 40 to 220 plants m^{-2} (O'Donovan, 1994) [109]. The average barley and canola density for this study are 147 and 102 plants m^{-2}, respectively (O'Donovan, 1994; O'Donovan et al., 1999) [109, 113].

Economic parameters for determining crop yield loss for wild oat in barley and canola are provided in Table 5.1. Herbicide application costs of \$12 ha^{-1} are included in the calculation of herbicide costs. Label rates and estimated retail herbicide prices for wild oat control in barley and canola are derived from published rates and prices (Ali, 2001) [1]. A technology use agreement fee of \$37 ha^{-1} is included in the glyphosate cost. Imazethapyr plus imazamox is applied for wild oat control in canola; however, only imazethapyr was used in the crop-weed-herbicide model since ED_{50} values were unavailable for imazamox. When glufosinate is applied to canola for wild oat control, clethodim at 15.4 g ai ha^{-1} (\$14 ha^{-1}) is recommended and therefore included in the glufosinate herbicide cost, see Table 5.1.

5.1 Model Application

A simulated realization is taken as a reference map of wild oat density, in numbers m^{-2}, over a 64 ha field near Stony Plain, Alberta. The wild oat density is sampled at 42 m intervals for a total of 361 sampling locations. An omnidirectional variogram model is calculated and used in SGS to create 51 simulated realizations of wild oat density for this 64 ha field. The number of realizations is chosen to avoid introducing error with too few realizations and balance computer time required for processing the realizations.

The first location of this field is used to illustrate the crop-weed-herbicide model. The first location has an average wild oat density of 45.6 plants m^{-2} over the 51 realizations with a minimum of 3 to a maximum of 232 plants. The effect of different herbicides at an average rate between 52 to 64% of the label is shown in Table 5.2. The standard deviations are larger in Table 5.2 compared to those in Table 5.3 due to variation from the realizations. Mean herbicide rates in Table 5.3 are a result of averaging 51 realizations at a location. There is a strong correlation between herbicide rate and simulated weed density.

A histogram of wild oat density values for the simulated location and the corresponding kriged value are shown in Figure 5.2. The histogram is not expected to be Gaussian in shape since simulated wild oat density values are generated in Gaussian space when SGS is implemented and back-transformed to original units after simulation. The optimal rate of tralkoxydim is 77% m^{-2} for kriging while the simulated value is 81% m^{-2}. The lower, left figure in Figure 5.2 provides a comparison of the expected revenue loss for kriging and simulation of \$62 and \$51, respectively, for these rates of herbicide.

Two additional herbicides, diclofop-methyl and fenoxaprop, that are applied in barley for wild oat control, are illustrated in Figure 5.3. Herbicide rates based on kriging and simulation are 94% and 95% for fenoxaprop and 101% and 97% for diclofop-methyl, respectively. The expected revenue loss for fenoxaprop is \$87 for kriging and \$67 for simulation while for diclofop-methyl, the loss is \$86 and \$67 for kriging and simulation. The mean revenue loss curves for the 2 herbicides illustrates a different shape that reflects each herbicide's efficacy, price and application rate for wild oat control in barley.

Canola herbicides applied at one location for wild oat control are presented in Figures 5.4 and 5.5. Imazethapyr rates are highest at 80% and 81% for kriging and simulation, respectively. Next is glufosinate at 67% for both kriging and simulation while glyphosate rates are 46% and 42% for kriging and simulation, respectively. Expected revenue loss for imazethapyr is \$119 and \$98 for kriging and simulation while expected revenue loss is \$114 and \$94 for glufosinate that is kriged and simulated. The difference between kriging and simulation is small for glyphosate at \$44 and \$45 for kriging and simulation.

To investigate if the findings at a single location and 361 locations apply on a smaller scale 64 ha field with 640000 locations, a 42 x 42 m spacing is simulated 51 times from a 19 x 19 grid of sample data. The 640000 locations indicates that there is a herbicide rate every square meter that can be averaged up to a SSA for the spraying equipment. The average wild oat density for the 19 x 19 grid with 361 locations is 94.5 plants m^{-2}, see Table 5.3, compared to 65.4 plants m^{-2} for the 64 ha field, see Table 5.4. Mean herbicide rate varied from 53 to 105% of the label for the 361 locations in Table 5.3 compared to 44 to 74%, see Table 5.4. This is consistent with the previous results at one location (Table 5.2) and 361 locations (Table 5.3) given the average wild oat densities. Average herbicide rate from herbicide treatment in Table 5.4 is significantly lower compared to the label rate. The correlation between herbicide rate and wild oat density ranged from 79 to 95% indicating

Crop	Herbicide	Mean Herbicide Rate % m^{-2}	Std. Dev. % m^{-2}	Correlation Coefficient
Barley	Diclofop-methyl	58.4	42.8	0.55
Barley	Tralkoxydim	52.3	35.9	0.66
Barley	Fenoxaprop	61.7	41.8	0.64
Canola	Glyphosate	42.2	19.0	0.75
Canola	Glufosinate	51.7	39.7	0.73
Canola	Imazethapyr	60.5	40.9	0.70

Table 5.2: Six herbicides applied to different crops using the crop-weed-herbicide model at one location with 51 simulated wild oat density values. The correlation is between herbicide rate and simulated wild oat density. Average wild oat density is 45.6 plants m^{-2} with a minimum of 3 to a maximum of 232.

Crop	Herbicide	Mean Herbicide Rate % m^{-2}	Std. Dev. % m^{-2}	Correlation Coefficient
Barley	Diclofop-methyl	105.1	15.7	0.55
Barley	Tralkoxydim	85.0	8.3	0.75
Barley	Fenoxaprop	99.5	9.3	0.65
Canola	Glyphosate	52.7	5.2	0.77
Canola	Glufosinate	71.8	16.5	0.77
Canola	Imazethapyr	87.1	13.4	0.79

Table 5.3: Six herbicides applied to different crops using the crop-weed-herbicide model at 361 locations with 51 simulated wild oat density values. The correlation is between herbicide rate and simulated wild oat density. Average wild oat density is 94.5 plants m^{-2} with a minimum of 0 to a maximum of 885.

Crop	Herbicide	Mean Herbicide Rate % m^{-2}	Std. Dev. % m^{-2}	Correlation Coefficient
Barley	Diclofop-methyl	70.6	38.3	0.79
Barley	Tralkoxydim	60.3	27.6	0.83
Barley	Fenoxaprop	67.8	34.8	0.79
Canola	Glyphosate	44.2	11.3	0.95
Canola	Glufosinate	72.9	25.0	0.90
Canola	Imazethapyr	74.0	22.8	0.91

Table 5.4: Six herbicides applied to different crops using the crop-weed-herbicide model on a 64 ha field (640000 locations) with 51 simulated wild oat density values. The correlation is between herbicide rate and simulated wild oat density. Average wild oat density is 65.4 plants m^{-2} with a minimum of 0 to a maximum of 950.

Crop	Herbicide	Revenue $ ha^{-1}	Wild Oat Numbers after Herbicide Application	Revenue from Constant Rate
Barley	Diclofop-methyl	261	41.5	249
Barley	Tralkoxydim	292	15.4	281
Barley	Fenoxaprop	273	28.6	263
Canola	Glyphosate	359	1.8	335
Canola	Glufosinate	295	11.8	278
Canola	Imazethapyr	290	13.4	275

Table 5.5: Average revenue, in dollars ha^{-1}, and wild oat density, plants m^{-2}, after herbicides have been applied to different crops using the crop-weed-herbicide model on a 64 ha field. Revenue from a constant rate represents herbicide applied at a constant 100% of label rate.

a strong relationship, see Table 5.4.

Revenue for tralkoxydim is \$293 ha^{-1} for wild oat control in barley, see Table 5.5. Total revenue for wild oat-free crop yield is \$349 ha^{-1} for barley and \$403 for canola. Revenue when no herbicide is applied is \$283 ha^{-1} and \$282 ha^{-1} for barley and canola. Weed infestations result in a revenue reduction of 19% and 30% in barley and canola. Herbicide treatment resulted in a significant increase in revenue compared to a label rate. Diclofop-methyl and fenoxaprop treatments generated less revenue compared to no herbicide due to herbicide costs and poor wild oat control.

All herbicide treatments are \$10 to \$24 ha^{-1} higher in revenue compared to a constant, label rate, see Table 5.5. These differences between the mean of each herbicide treatment and the mean label rate are significant at the 1% level of probability. This represents an additional \$640 to \$1540 per 64 ha field for implementing locally varying herbicide rates compared to a constant rate. Glyphosate application averaged \$359 ha^{-1} while average wild oat remaining after herbicide application is 1.8 plants m^{-2}.

Herbicide rate maps for tralkoxydim, fenoxaprop, and glyphosate for the 64 ha field are shown in Figure 5.6. Wild oat left after application of these herbicides is shown in Figure 5.7. The wild oat density map is also shown. There are 35% and 34% of the field area where tralkoxydim and fenoxaprop application rates are less than 25% m^{-2} compared to glyphosate at 14%. This may be a result of the competitive nature of barley with respect

to wild oat, the higher threshold of barley in wild oat infestations and the herbicide's effect on wild oat. Less wild oat is left after treatment with glyphosate compared to the other herbicides and consequently, there is less risk for carryover of wild oat seed in the soil.

The crop-weed-herbicide model is tested for wild oat density, see Figure 5.8. The expected revenue loss increases as wild oat density increases for barley and canola. The slope of the curve is shallower for barley compared to canola signifying less revenue loss for barley. When no herbicide is applied revenue is \$283 ha^{-1} and \$282 ha^{-1} for barley and canola at wild oat density of 65 plants m^{-2}.

Crop density impacts weeds since all plants must compete for limited resources. As crop density increases, the expected revenue increases until an upper limit is reached, see Figure 5.9. Seed costs of \$2.90 kg^{-1} and \$4.80 kg^{-1} for barley and canola are considered in determining expected revenue at different crop densities. The increase in revenue is initially steep for barley and canola but peaks at 150 barley plants m^{-2} and 100 canola plants m^{-2}. The barley density chosen for this study is 147 plants m^{-2} while the canola density is 102 plants m^{-2}. Seed densities beyond these rates are impractical to consider since seed cost is prohibitive. The decline in revenue is faster for canola compared to barley due to higher seed costs of herbicide tolerant canola.

Relative time of wild oat emergence compared to the crop is displayed in Figure 5.10. Revenue increases \$50 ha^{-1} as barley emerges from 0 to 14 days ahead of the wild oat. If wild oat emerges 5 days before the barley, there is a \$7 ha^{-1} loss of revenue. For canola, the increase in revenue is \$51 from 0 to 14 days. If wild oat emerges 10 days prior to the canola, the loss in revenue is \$23 compared to \$10 for barley. The slope of the curve is shallower for barley compared to canola indicating less revenue loss with barley due to its competitive nature.

Herbicides vary in their efficacy on wild oat that influences crop yield and expected revenue loss. Expected revenue loss is shown for 6 herbicides applied to control wild oat in barley and canola, see Figure 5.11. The herbicide cost, $hc(\mathbf{u})$, for each herbicide is added to the crop loss from weeds $r(\mathbf{u})$ to obtain $pc(\mathbf{u})$. The optimal herbicide rate, $a_{opt}(\mathbf{u})$, is the value that minimizes cost or maximizes profit.

The optimal herbicide rate, in % m^{-2}, occurs at 25% and 50% for glufosinate and imazethapyr, while the 50% rate is optimal for glyphosate, see Figure 5.11. For diclofop-methyl, fenoxaprop, and tralkoxydim, the optimal rates are 0%, 0% and 50%. The optimal rate is 0% for diclofop-methyl and fenoxaprop since no herbicide provides the most expected revenue and there is a moderate response to the herbicide ($H(a)$ rises slowly). Increased crop yield from wild oat control does not exceed the cost of herbicide and the correct decision is not to spray, see Figure 5.11. Few weeds and an expensive herbicide will also result in a zero herbicide rate or a no spray decision.

Optimal herbicide rate and revenue are affected by several factors. For each of the herbicides, the revenue curve $r(a;\mathbf{u})$ flattens as a increases since weed control, $H(a)$, and yield loss flatten off, see Figure 5.11. The cost of glufosinate, $hc(\mathbf{u})$, decreases linearly from \$0 to -\$246 ha^{-1} for the 0 to 300% rate of herbicide since a constant per-liter cost is used. The cost of the other wild oat herbicides decrease linearly although at a different slope since retail herbicide cost $hc(\mathbf{u})$ is different for each herbicide.

Wild oat density after herbicide treatment in Figure 5.12 illustrates that different rates of herbicide result in different amounts of killed wild oat. Tralkoxydim rates result in a high barley yield, 4.3 t ha^{-1}, compared to the weed-free yield at a low rate of herbicide, 50%. Expected revenue loss for tralkoxydim is \$293 ha^{-1} compared to \$281 and \$349 for

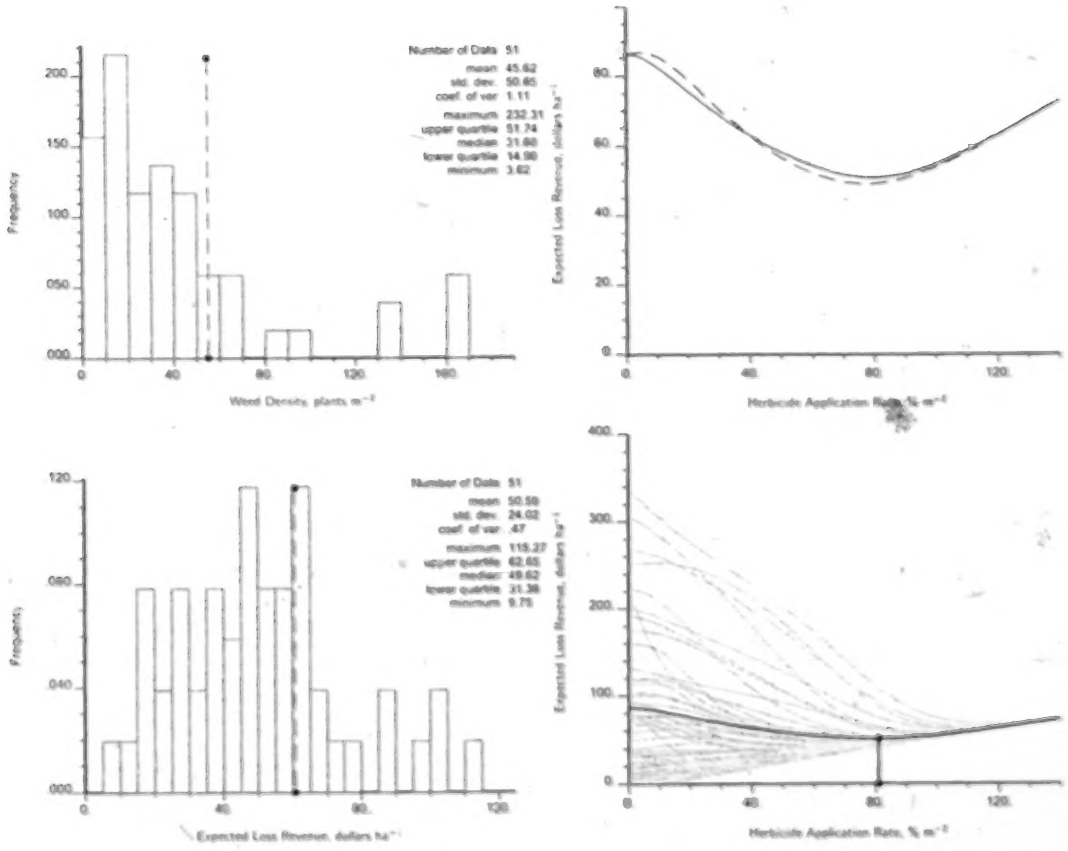

Figure 5.2: A histogram of wild oat density, in plants m^{-2}, for simulation at one location and the kriged weed density value for that location indicated by the dashed line (top, left figure). A comparison of the kriged, tralkoxydim cost curve (solid curve) and the average of 51 realizations from simulation (dashed curve) at the same location (top, right figure). A histogram of expected loss revenue, in dollars ha^{-1}, for simulation at one location and the kriged revenue value for that location indicated by the dashed line (bottom, left figure). The average of 51 realizations (black curve) and the 51 realizations (gray curves) from simulation at the same location (bottom, right) with the solid line indicating optimal herbicide rate.

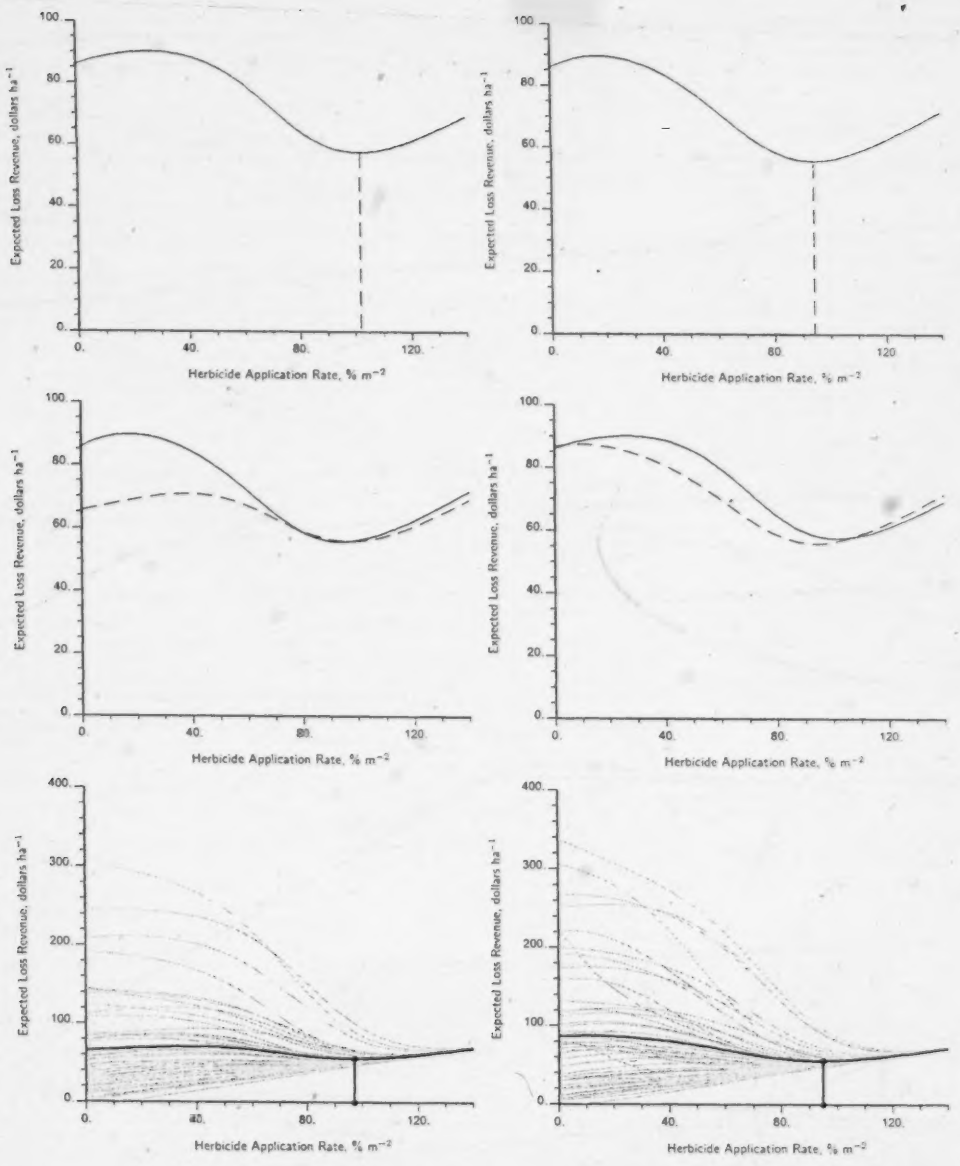

Figure 5.3: Optimal diclofop-methyl (left) and fenoxaprop (right) cost curves in barley, in % m^{-2}, at one location from kriging (top figures). A comparison of the kriged, diclofop-methyl (left) and fenoxaprop (right) cost curves (solid curve) and the average of 51 realizations from simulation (dashed curve) at the same location (middle figures). The average of 51 realizations (black curve) and the 51 realizations (gray curves) from simulation at the same location for diclofop-methyl (left) and fenoxaprop (right), respectively (bottom figures) with the solid line indicating optimal herbicide rate.

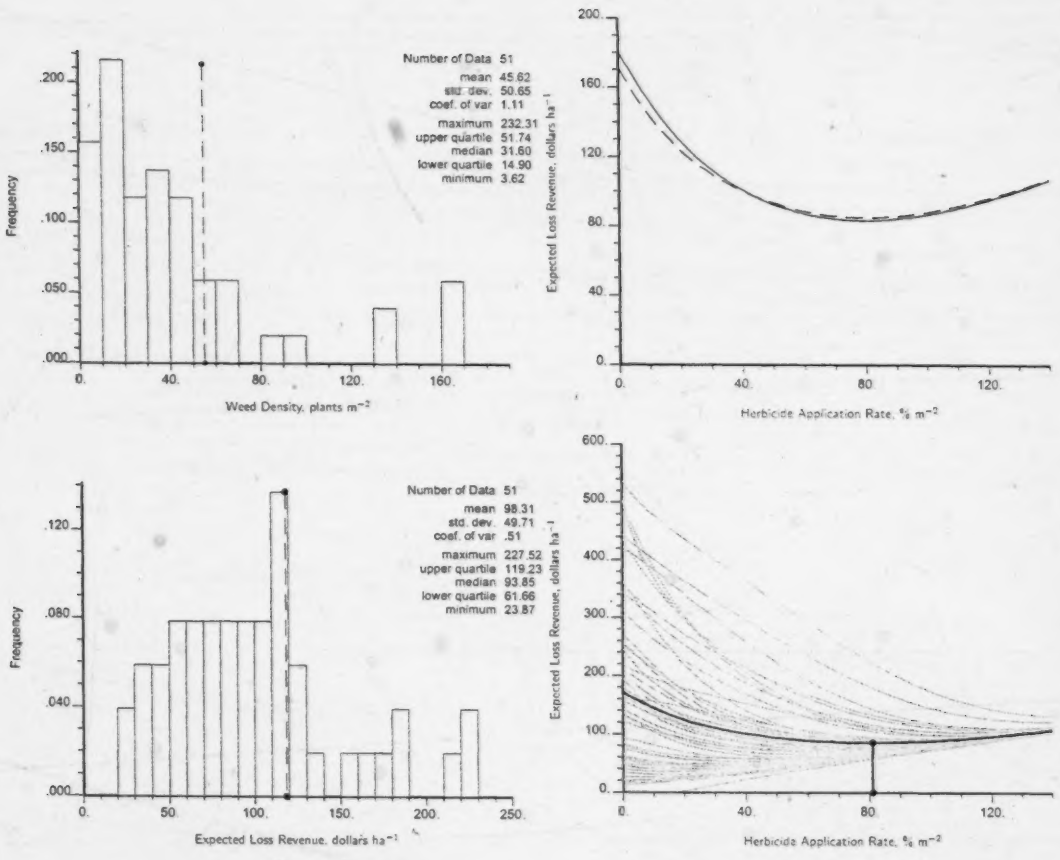

Figure 5.4: A histogram of wild oat density, in plants m^{-2}, for simulation at one location and the kriged weed density value for that location indicated by dashed line (top, left figure). A comparison of the kriged, imazethapyr cost curve (solid curve) and the average of 51 realizations from simulation (dashed curve) at the same location (top, right figure). A histogram of expected loss revenue, in dollars ha^{-1}, for simulation at one location and the kriged revenue value for that location indicated by the dashed line (bottom, left figure). The average of 51 realizations (black curve) and the 51 realizations (gray curves) from simulation at the same location (bottom, right) for imazethapyr with the solid line indicating optimal herbicide rate.

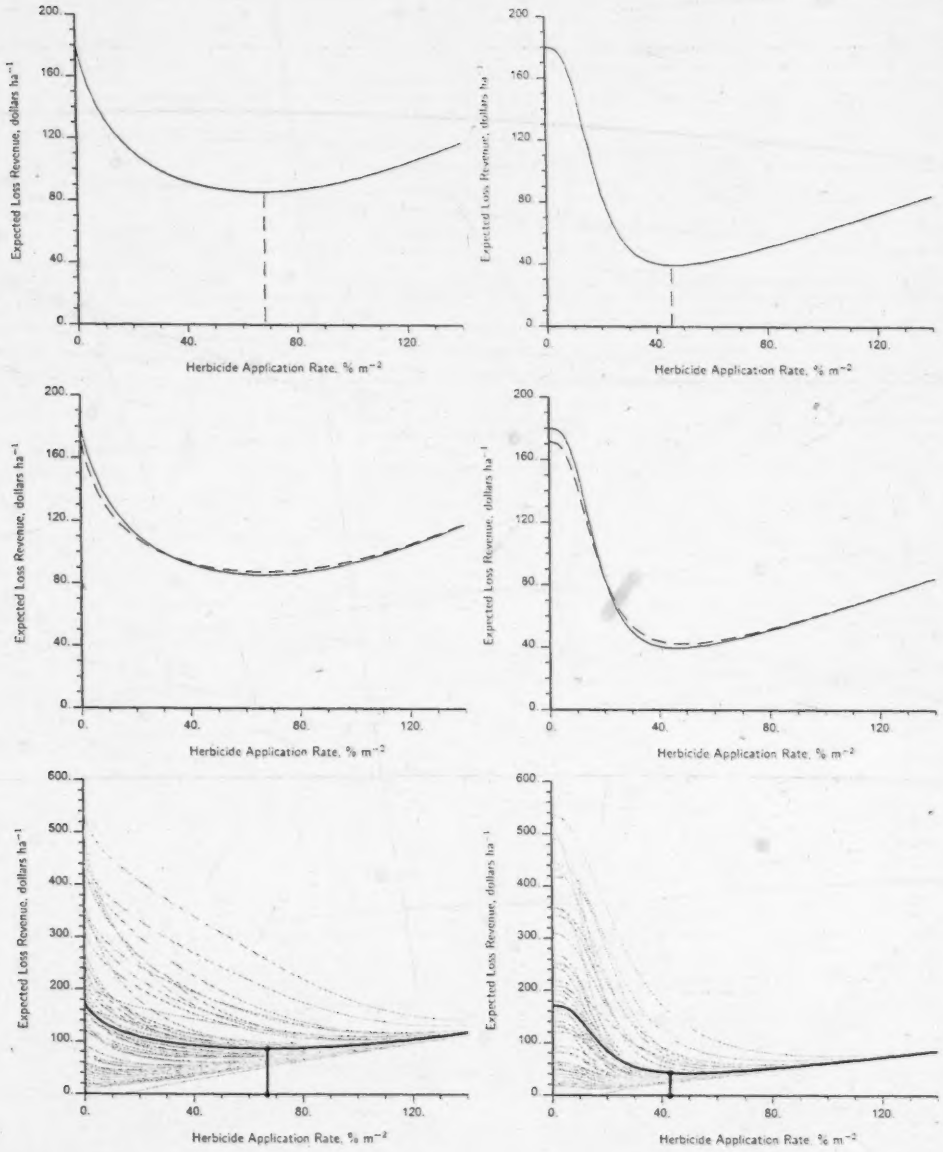

Figure 5.5: Optimal glufosinate (left) and glyphosate (right) cost curves in canola, in % m^{-2}, at one location from kriging (top figures). A comparison of the kriged, glufosinate (left) and glyphosate (right) cost curves (solid curve) and the average of 51 realizations from simulation (dashed curve) at the same location (middle figures). The average of 51 realizations (black curve) and the 51 realizations (gray curves) from simulation at the same location for glufosinate (left) and glyphosate (right), respectively (bottom figures) with the solid line indicating optimal herbicide rate.

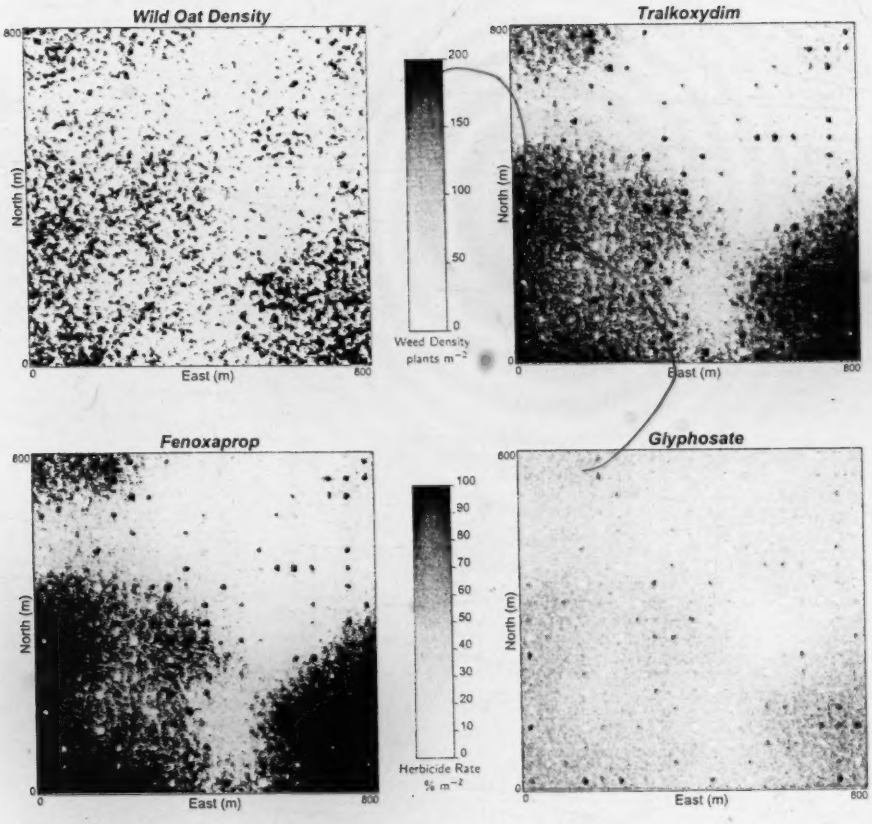

Figure 5.6: Wild oat density, in plants m^{-2}, for a 64 ha field near Stony Plain, Alberta prior to herbicide treatment (top left). The other maps are optimal herbicide rates, in % m^{-2}, for tralkoxydim (top right), fenoxaprop (bottom left), and glyphosate (bottom right).

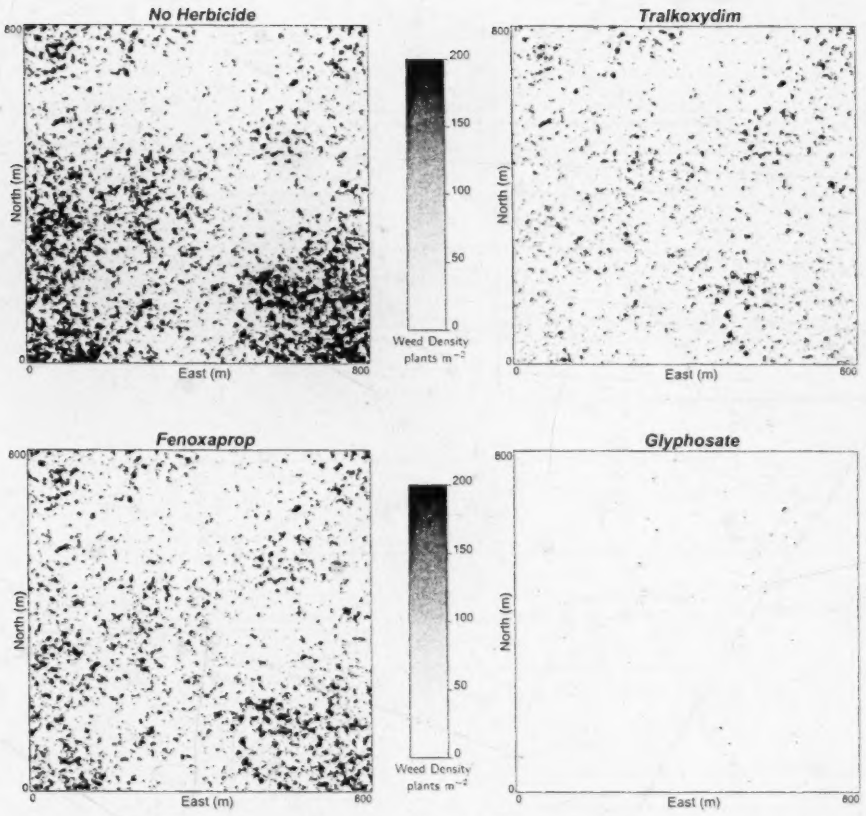

Figure 5.7: Wild oat density, in plants m^{-2}, after treatment with tralkoxydim (top right), fenoxaprop (bottom left), and glyphosate (bottom right) compared to the same 64 ha field near Stony Plain with no herbicide treatment (top left).

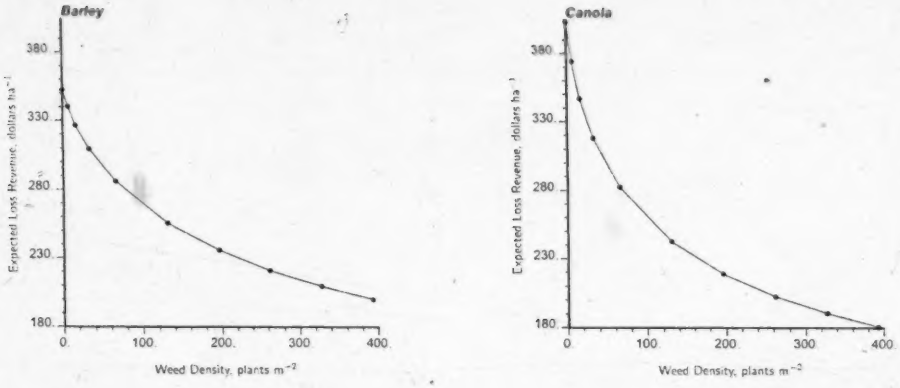

Figure 5.8: Average expected revenue loss, in dollars ha^{-1}, for a barley and canola crop after herbicide has been applied to wild oat using the crop-weed-herbicide model in a 64 ha field near Stony Plain, Alberta as wild oat density, in plants m^{-2}, varies. Each average expected revenue value represents wild oat density values from 640000 locations.

the label and weed-free yield. Glyphosate application results in a canola yield, 1.84 t ha^{-1}, at a herbicide rate of 50%; the average wild oat density after treatment is 1.8 wild oat m^{-2}; and expected revenue loss is \$359 ha^{-1}. This represents 88% of the revenue compared to weed-free yield and the same average wild oat density after treatment compared to the label rate of glyphosate.

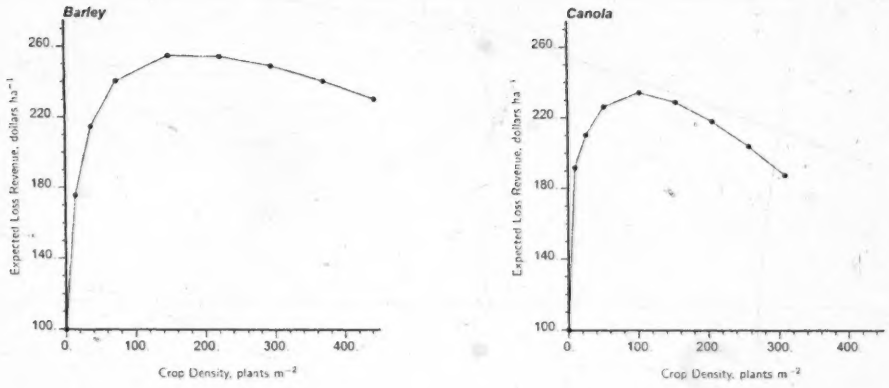

Figure 5.9: Average expected revenue, in dollars ha^{-1}, for a barley and canola crop after herbicide has been applied to wild oat using the crop-weed-herbicide model in a 64 ha field near Stony Plain, Alberta as crop density, in plants m^{-2}, varies. Each average expected revenue value represents crop density values from 640000 locations.

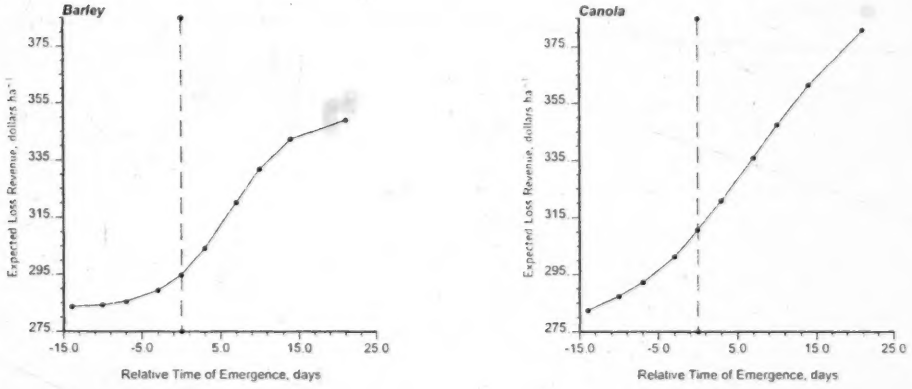

Figure 5.10: Average expected revenue, in dollars ha^{-1}, for a barley and canola crop after herbicide has been applied to wild oat using the crop-weed-herbicide model in a 64 ha field near Stony Plain, Alberta as time of weed emergence, in days, varies. The dashed line represents when crop and wild oat emerge at the same time. Each average expected revenue value represents time of wild oat emergence values from 640000 locations.

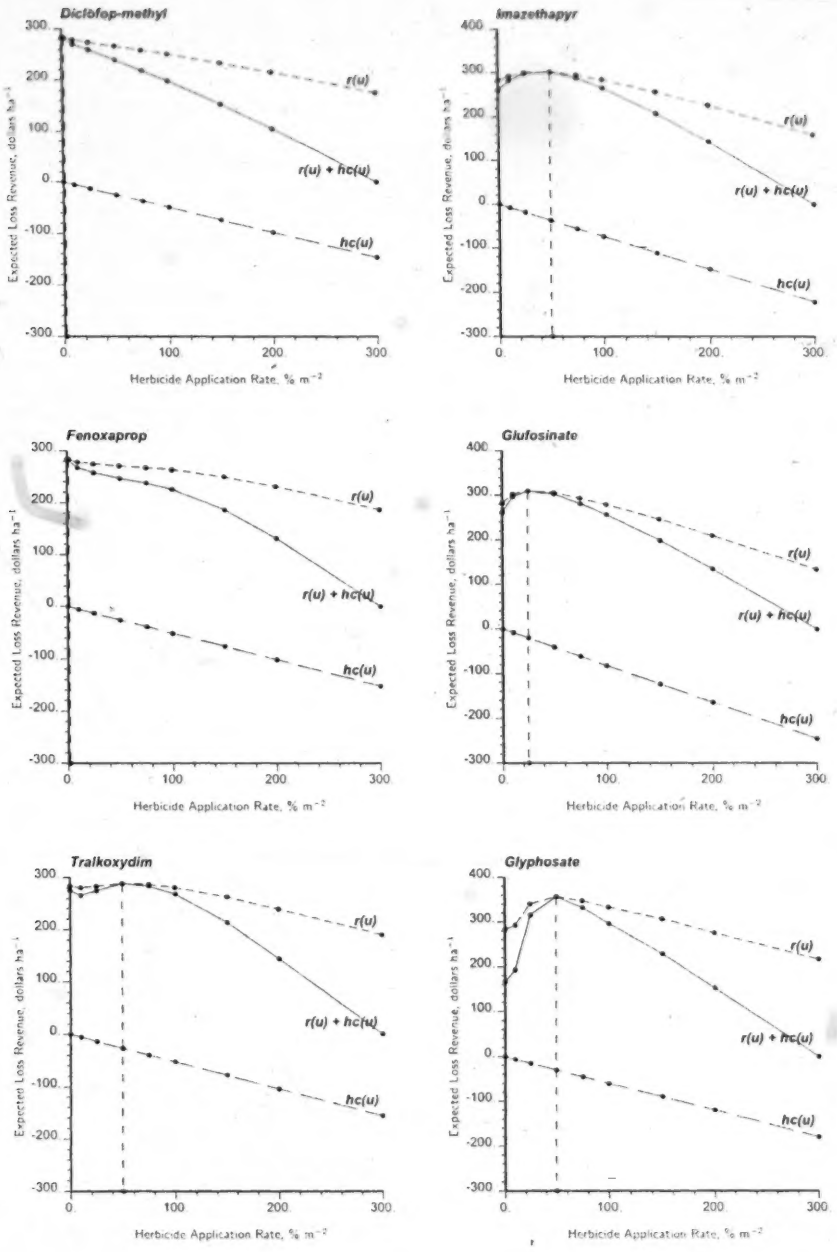

Figure 5.11: Increasing herbicide application rate, in % m^{-2}, of diclofop-methyl, fenoxaprop and tralkoxydim on the left and imazethapyr, glufosinate and glyphosate on the right for treatment of wild oat in barley and canola in a 64 ha field near Stony Plain, Alberta. The herbicide cost $hc(\mathbf{u})$(long dash) and cost due to crop loss from wild oat $r(\mathbf{u})$(short dash) are summed to obtain herbicide cost + crop loss cost $pc(\mathbf{u})$(solid). The optimal herbicide rate, $a_{opt}(\mathbf{u})$, is indicated by the medium dashed vertical line. Each average expected revenue value, in dollars ha^{-1}, represents 640000 locations.

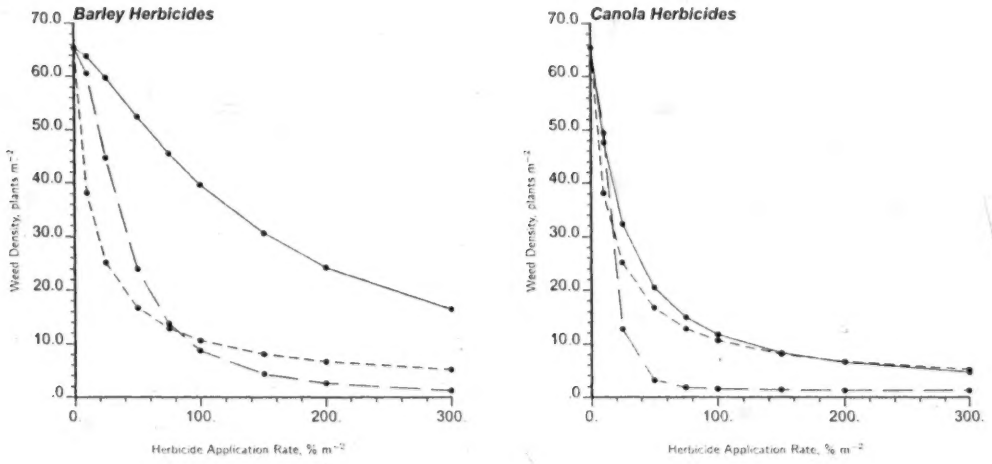

Figure 5.12: Average wild oat density, in plants m^{-2}, after herbicide treatment using the crop-weed-herbicide model in a 64 ha field near Stony Plain, Alberta as herbicide rate, in % m^{-2}, varies. Each average wild oat density represents 640000 locations. Rates of tralkoxydim (long dash), fenoxaprop (short dash), and diclofop-methyl (solid) in a barley field (right figure) and rates of glyphosate (long dash), glufosinate (short dash), and imazethapyr (solid) in a canola field (left figure). Average wild oat density is 65.4 plants m^{-2} with no herbicide.

Chapter 6

A Comparative Example

Uncertainty is quantified by multiple, simulated realizations that honor the wild oat density data, histogram and variogram model. This chapter describes how numerical models of herbicide rates are generated. They are compared to a conventional approach for herbicide treatment.

Parameters for the crop-weed-herbicide model can vary from field to field. For example, noxious weeds can affect the grain quality. Consequently, other variables may need to be included in the model when it is applied in different areas. Maximum revenue for a wild oat-free barley crop is assumed to be \$22340. If sampling costs are less than \$700 field^{-1}, locally varying herbicide rates with kriging or simulation can be more cost effective than a label rate of herbicide. Significance is determined with a paired t test that assumes the data are normally distributed and independent with unequal variances.

Wild oat remaining after locally varying herbicide application are added to the seedbank. It was assumed these wild oat will not impact future crop yield losses given recent research (Beckie & Kirkland, 2002) [7]. Crop rotation, chaff collection and tillage are management practices that limit weed invasion. Their effects are not evaluated with the crop-weed-herbicide model. This assumes that more complexity needs to be incorporated into the model for improved decision-making. A sensitivity analysis will quantify what components need to be included.

Different sampling designs for mapping wild oat density data are evaluated for profitability. In this chapter, I discuss the assessment of profitability for these sampling designs based on their pattern and number of locations.

6.1 Approach

Conventional herbicide treatment involves applying a constant rate of herbicide over a field. Since weeds vary in density throughout the field, herbicide treatment rates are often too high or too low from location to location. The other option farm managers implement is to apply a low rate or no herbicide treatment where weeds are in low numbers or absent. These 2 approaches are widely practiced by farm managers (Dieleman & Mortensen, 1998; Holm et al., 2000) [40, 69].

Determination of local herbicide rate requires estimates of wild oat density. Interpolation techniques tend to smooth out the spatial variation for wild oat density. Hence, an estimated map over-estimates low wild oat densities and under-estimates high wild oat densities.

An alternative to interpolation from sparse wild oat density data sets is stochastic

Design	Sampling Locations	Design	Sampling Locations	Design	Sampling Locations
$Grid_{10}$	100	$Grid_{13}$	169	$Grid_{19}$	361
$Gridnest_{10}$	100	$Gridnest_{13}$	169	$Gridnest_{19}$	361
$Square_7$	98	$Square_9$	162	$Square_{13}$	338

Table 6.1: Sampling designs with a varying number of sample locations applied to two 64 ha fields near Stony Plain and Viking, Alberta.

simulation. Simulation reproduces data at their location, the histogram of simulated wild oat density values, and the variogram model. Moreover, multiple realizations measure uncertainty in wild oat density. Realizations of wild oat density can be used for optimizing herbicide rates based on maximum profitability.

Four mapping approaches are considered in optimizing herbicide rates for decision-making: (1) no herbicide, (2) herbicide applied at a constant 100% of label rate, (3) locally varying based on kriging, and (4) locally varying based on simulation.

6.2 Comparative Example

We simulate a grid of wild oat densities to serve as a reference map. The purpose of this reference map is to understand the different approaches to herbicide treatment with different levels of sampling. Care is taken to avoid circular reasoning and over-interpretation of the results.

A realization representing a 64 ha field near Viking, Alberta is one reference map. A second reference map is taken as a realization of a 64 ha field near Stony Plain, Alberta. The wild oat density values for each field are sampled at 42 m intervals (19 x 19 m square) for a total of 361 sampling locations. This grid sample pattern is the same for each field and is used to evaluate the profitability of each prescription mapping technique.

Total profitability of a sample design is revenue from a prescription map of a field minus the expense of sampling. The sample designs include a grid, square and modified grid with a varying number of sampling locations, see Table 6.1. The modified grid utilizes the variogram from a nested design with a similar number of locations and the grid sample design. For example, kriging with a $Gridnest_{10}$ design has 100 sampling locations (10 x 10) and a variogram from the $Nest_{10}$ sampling design.

An omnidirectional variogram model is used to estimate a kriged map of wild oat density values for each 64 ha field. The same variogram model is used to simulate 101 realizations. The number of realizations is chosen to avoid introducing error with too few realizations. Kriged and simulated wild oat density maps are shown in Figures 6.1 and 6.2. A higher wild oat density that is more patchy is visually observed by the occurrence and extent of the dark areas in the Stony Plain maps compared to the Viking maps.

The wild oat densities are multiplied by 2 and 3 to generate double and triple density reference maps. The square 19 x 19 sampled grid is used to generate kriged and simulated maps of wild oat density values. The mean, variance and minimum and maximum plant density for the reference, sample, kriged and simulated maps are provided in Tables 6.2 and 6.3. The Stony Plain field has a higher density, variance and wider range of wild oat compared to the Viking field. Wild oat density variability is similar to the reference map

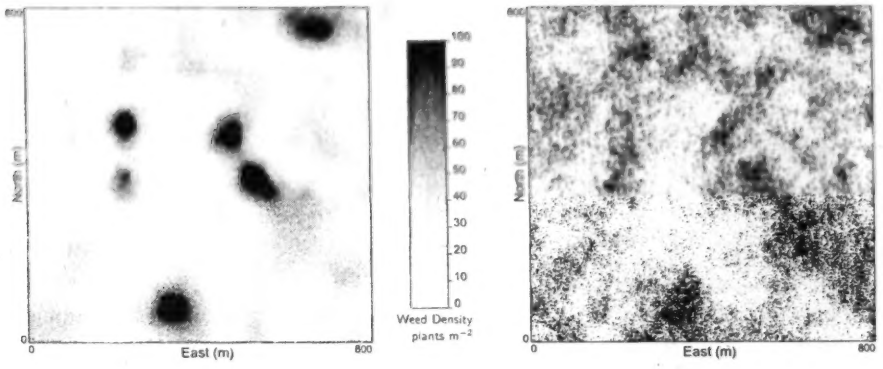

Figure 6.1: Wild oat density, in number m^{-2}, from kriging (left) and simulation (right) from a 64 ha field near Viking, Alberta. The simulation represents one realization.

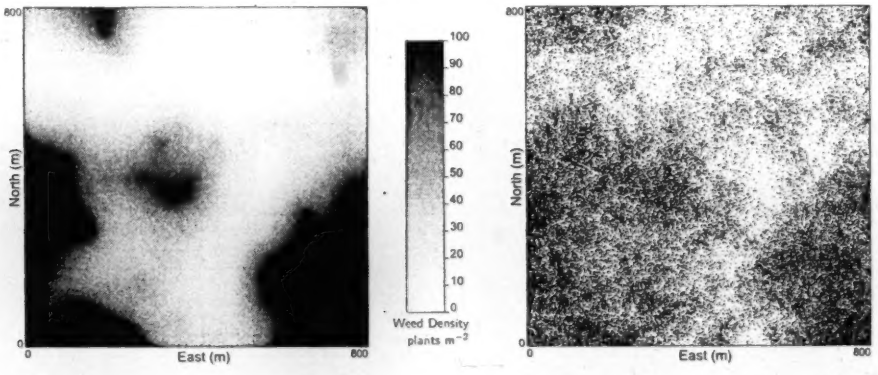

Figure 6.2: Wild oat density, in number m^{-2}, from kriging (left) and simulation (right) from a 64 ha field near Stony Plain, Alberta. The simulation represents one realization.

for the samples and simulation; however, kriging led to a lower variance for all wild oat density maps.

Results

Recall the four weed treatments, (1) no herbicide, (2) 100% herbicide, (3) kriging and (4) simulation. Average herbicide rates for kriging are higher for the single wild oat density, see Table 6.4. The minimum-maximum of herbicide rates is wider for simulation compared to kriging. These rates exceed the label rate up to 31.2% of the field area in the Stony Plain field. The area above label rates for the Viking field is only 0.001%, 0.01% and 1.7% for the simulated single, double and triple wild oat density. Of course, these areas would increase in presence of more weeds that is indicated by the Stony Plain field compared to the Viking field, see Table 6.4. The Stony Plain field has a single, wild oat density of 65 plants m^{-2} compared to 35 plants m^{-2} for the Viking field.

The revenues for the four different prescription techniques are listed in Tables 6.5 and 6.6

Map	Mean	Variance	Minimum - Maximum Density, plants m^{-2}
Reference Single	34.9	1014	1 - 546
Sample	36.4	1196	3 - 308
Krige Single	36.5	142	15 - 86
Simulate Single	34.9	1024	0 - 309

Map	Mean	Variance	Minimum - Maximum Density, plants m^{-2}
Reference Double	69.7	4058	2 - 1093
Sample	72.9	4784	5 - 617
Krige Double	72.8	568	31 - 172
Simulate Double	70.0	4710	0 - 617

Map	Mean	Variance	Minimum - Maximum Density, plants m^{-2}
Reference Triple	104.6	9131	3 - 1640
Sample	109.3	10765	8 - 925
Krige Triple	109.4	1279	46 - 258
Simulate Triple	104.7	9071	0 - 925

Table 6.2: Wild oat density parameters for the reference, sample, kriged and simulated prescription maps for a field near Viking, Alberta. The grid is sampled every 42 m on a square pattern for a total of 361 sampling locations in a 64 ha field. Single, double and triple refer to single, double, and triple wild oat density.

Map	Mean	Variance	Minimum - Maximum Density, plants m^{-2}
Reference Single	65.4	11064	0 - 950
Sample	64.8	12740	0 - 906
Krige Single	63.8	2839	10 - 331
Simulate Single	59.1	12134	0 - 907

Map	Mean	Variance	Minimum - Maximum Density, plants m^{-2}
Reference Double	130.8	44257	0 - 1900
Sample	129.6	50962	0 - 1814
Krige Double	127.5	11357	20 - 662
Simulate Double	118.4	48209	0 - 1814

Map	Mean	Variance	Minimum - Maximum Density, plants m^{-2}
Reference Triple	196.3	99576	0 - 2850
Sample	194.4	114664	0 - 2720
Krige Triple	191.3	25550	31 - 993
Simulate Triple	175.3	108154	0 - 2720

Table 6.3: Wild oat density parameters for the reference, sample, kriged and simulated prescription maps for a field near Stony Plain, Alberta. The grid is sampled every 42 m on a square pattern for a total of 361 sampling locations in a 64 ha field. Single, double and triple refer to single, double, and triple wild oat density.

Field	Wild Oat Density	Prescription Technique	Ave. Herbicide Rate, % m^{-2}	Minimum - Maximum Herbicide Rate, % m^{-2}	% of Area Above Label
Viking	Single	Kriging	63.0	30 - 86	0
		Simulation	61.2	5 - 110	0.001
	Double	Kriging	81.8	61 - 97	0
		Simulation	81.9	11 - 119	0.01
	Triple	Kriging	89.3	74 - 103	1.9
		Simulation	89.9	16 - 124	1.7
Stony Plain	Single	Kriging	68.9	20 - 107	3.3
		Simulation	60.0	0 - 120	3.4
	Double	Kriging	86.2	42 - 116	14.2
		Simulation	78.7	0 - 130	17.4
	Triple	Kriging	93.7	61 - 121	30.8
		Simulation	87.7	0 - 125	31.2

Table 6.4: Average (Ave.) herbicide rates, in % m^2, for wild oat distributions in fields near Viking and Stony Plain, Alberta. Area, in %, that herbicide rates exceed label rate for different wild oat distributions.

Single Weed Density	Herbicide Prescription Technique			
	No Herbicide	Label	Krige	Simulation
Revenue, dollars ha^{-1}	288.6	287.2	298.6	298.8
Yield, t ha^{-1}	3.9	4.6	4.5	4.5
Weed Density, m^{-2}	34.9	4.8	9.0	9.5
Herbicide Cost, dollars	0.00	52.0	32.7	31.8

Double Weed Density	Herbicide Prescription Technique			
	No Herbicide	Label	Krige	Simulation
Revenue, dollars ha^{-1}	246.2	278.2	283.0	282.9
Yield, t ha^{-1}	3.3	4.4	4.4	4.4
Weed Density, m^{-2}	69.7	9.3	12.5	12.5
Herbicide Cost, dollars	0.00	52.0	42.4	42.6

Triple Weed Density	Herbicide Prescription Technique			
	No Herbicide	Label	Krige	Simulation
Revenue, dollars ha^{-1}	214.7	269.7	272.7	272.7
Yield, t ha^{-1}	2.9	4.4	4.3	4.3
Weed Density, m^{-2}	104.6	14.0	16.4	16.2
Herbicide Cost, dollars	0.00	52.0	46.4	46.8

Table 6.5: Total revenue, in dollars ha^{-1}, for a 64 ha field near Viking, Alberta for different mapping options. Weed density, in plants m^{-2}, represents the number of wild oat after herbicide treatment. Maximum total revenue with no wild oat interference is \$349 ha^{-1}.

Single Weed Density	Herbicide Prescription Technique			
	No Herbicide	Label	Krige	Simulation
Revenue, dollars ha^{-1}	250.8	279.3	290.3	291.7
Yield, t ha^{-1}	3.4	4.5	4.4	4.4
Final Weed Density, m^{-2}	65.4	8.8	13.2	15.5
Herbicide Cost, dollars	0.00	52.0	35.8	31.2

Double Weed Density	Herbicide Prescription Technique			
	No Herbicide	Label	Krige	Simulation
Revenue, dollars ha^{-1}	195.8	263.6	272.9	274.1
Yield, t ha^{-1}	2.7	4.3	4.3	4.3
Final Weed Density, m^{-2}	130.8	17.5	21.6	20.0
Herbicide Cost, dollars	0.0	52.0	44.8	40.9

Triple Weed Density	Herbicide Prescription Technique			
	No Herbicide	Label	Krige	Simulation
Revenue, dollars ha^{-1}	160.6	249.4	261.5	262.4
Yield, t ha^{-1}	2.2	4.1	4.2	4.2
Final Weed Density, m^{-2}	196.3	26.3	26.1	27.4
Herbicide Cost, dollars	0.0	52.0	48.7	46.0

Table 6.6: Total revenue, in dollars ha^{-1}, for a 64 field near Stony Plain, Alberta for different mapping options. Final weed density, in plants m^{-2}, represents the number of wild oat after herbicide treatment. Maximum total revenue with no wild oat interference is \$349 ha^{-1}.

Single Weed Density	Herbicide Prescription Technique			
	No Herbicide	Label	Krige	Simulation
Dollars field^{-1}	18470	18380	19110	19120
% Difference	100.0	99.5	103.5	103.5

Double Weed Density	Herbicide Prescription Technique			
	No Herbicide	Label	Krige	Simulation
Dollars field^{-1}	15760	17810	18110	18100
% Difference	100.0	113.0	114.9	114.9

Triple Weed Density	Herbicide Prescription Technique			
	No Herbicide	Label	Krige	Simulation
Dollars field^{-1}	13740	17260	17460	17450
% Difference	100.0	125.6	127.0	127.0

Table 6.7: Total revenue, in dollars ha^{-1}, for a 64 ha field near Viking, Alberta using different mapping options. Herbicide and application costs are included in the total revenue while maximum total revenue with no wild oat interference is \$22340 field^{-1}.

for each field. Revenue, in Canadian dollars m^{-2}, is calculated for each weed prescription assuming a weed-free yield of 4.7 t ha^{-1}, crop price of \$73.69 t^{-1}, crop density of 148 plants m^{-2}, ED_{50} of 0.38 for tralkoxydim, relative emergence time of -14 days, and herbicide cost of \$0.003 g ai m^{-2}. While the -14 days is unrealistic for crop-weed interference, it is chosen to present the case where weeds have a clear, competitive advantage. The total revenue for each herbicide prescription technique is averaged and expressed as dollars ha^{-1} or added and expressed in dollars field^{-1}. Maximum revenue per field is \$22340 or \$349 ha^{-1} based on a wild oat-free barley yield of 4.7 t ha^{-1} at a crop price of \$73 t^{-1}. Herbicide costs include herbicide product and a \$12 ha^{-1} cost of application.

Revenue from different herbicide treatments varies between \$161 and \$299 ha^{-1} for the two fields, see Tables 6.5 and 6.6. The 100% rate of herbicide, kriging and simulation generate more revenue than no herbicide except at the single wild oat density for the Viking field. The economic threshold for wild oat is very close to a weed density of 16 plants m^{-2} for the Viking field based on the total revenues. Barley yield drops as wild oat density is increased and the decrease is greater than 50% compared to the wild oat-free yield with no herbicide at the triple density. This barley yield loss at the Stony Plain field results in \$2400 less revenue compared to the Viking field. If herbicide is applied, the yield decrease is only about 15% at the highest wild oat density.

Wild oat density is higher in the Stony Plain field, 65 to 196 plants m^{-2}, compared to the Viking field at 35 to 105 plants m^{-2}. Herbicide treatment reduces this weed density by 73% to 87% compared to the no herbicide treatment. More herbicide is applied at the Stony Plain field compared to the Viking field since wild oat densities are higher.

Total revenue for each field is calculated and presented in Tables 6.7 and 6.8. Revenues of each prescription treatment from the Stony Plain site are significantly different at the 1% level of probability from each other. This is true for the Viking site except the revenue of the locally varying rates from kriging and simulation at the double and triple weed density. Revenue maps for the 4 prescription techniques are presented in Figures 6.3 and 6.4 and the darkest maps reflecting the most revenue at either site are the simulated maps.

Single Weed Density	Herbicide Prescription Technique			
	No Herbicide	Label	Krige	Simulation
Dollars field^{-1}	16050	17880	18580	18670
% Difference	100.0	111.4	115.7	116.3

Double Weed Density	Herbicide Prescription Technique			
	No Herbicide	Label	Krige	Simulation
Dollars field^{-1}	12530	16870	17470	17540
% Difference	100.0	134.6	139.4	140.0

Triple Weed Density	Herbicide Prescription Technique			
	No Herbicide	Label	Krige	Simulation
Dollars field^{-1}	10280	15960	16740	16790
% Difference	100.0	155.2	162.8	163.4

Table 6.8: Total revenue, in dollars ha^{-1}, for a 64 ha field near Stony Plain, Alberta using different mapping options. Herbicide and application costs are included in the total revenue while maximum total revenue with no wild oat interference is \$22340 field^{-1}.

The 100% herbicide map is a consistent dull gray indicating a constant label rate. The locally varying maps for kriging and simulation are darker than the 100% of label signifying higher revenues. Additionally, the average and total revenue for each field is summarized in Table 6.9. Simulation of locally varying herbicide rates are significantly the lowest compared to those from kriging and the label rate. This prescription technique generates the most revenue at \$3480 per field followed by kriging and the 100% rate of herbicide. Locally varying herbicide rate application with kriging or simulation significantly increases revenue by an average of \$570 compared to a 100% label rate.

A comparison of total revenue between fields, see Tables 6.7 and 6.8, illustrates the effect of higher wild oat density on the barley crop. At the single and double wild oat density, the Viking field generates significantly more revenue (\$2400 and \$3200) than the Stony Plain field. Revenue decreases to \$10280 for the Stony Plain field that is \$3460 less than at the Viking field for the triple wild oat density. This is a result of barley yields of 2.9 t ha^{-1} for the Viking field compared to 2.2 t ha^{-1} for the Stony Plain field, see Tables 6.5 and 6.6. These economic outcomes are a direct consequence of the wild oat density and its affect on the crop.

Locally varying herbicide rates are compared to a conventional approach of 100% over all wild oat densities for each field. Herbicide cost is lower by \$670 and \$770 for the locally varying herbicide rates at the Stony Plain and Viking fields compared to a conventional approach since 80% and 77% of the herbicide rate is applied. However, lower barley yields of 4.3 and 4.4 t ha^{-1} for the Stony Plain and Viking fields result in less revenue. Wild oat density is reduced 78% with locally varying herbicide compared to 86% with the conventional approach. Net revenue after considering lower yields and herbicide costs for the Stony Plain and Viking fields is \$730 and \$410 for implementing locally varying herbicide rates over a conventional approach. Wild oat density after herbicide treatment is higher by 6 plants m^{-2} for the locally varying maps compared to the 100% label. Field research will need to confirm if these additional wild oat plants will increase the wild oat population.

Maps of herbicide rates vary as the wild oat density varies for the kriged and simulated

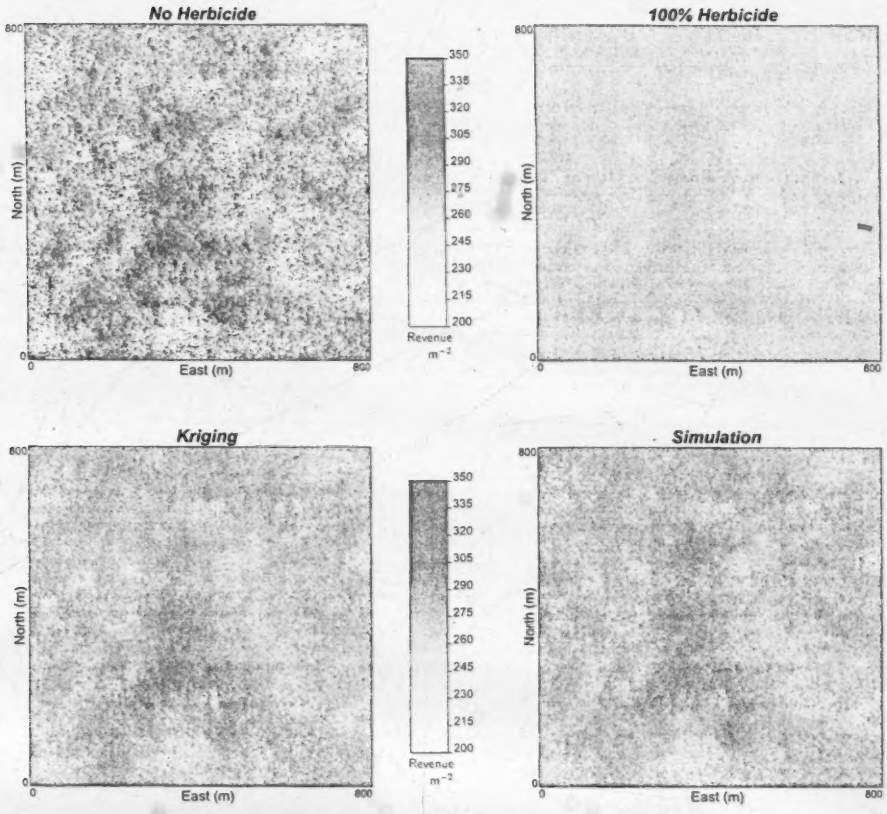

Figure 6.3: Total revenue, in dollars m^{-2}, for no herbicide, a 100% herbicide rate, a kriged map and simulated map of herbicide rates for a single wild oat density at Viking, Alberta.

Dollars Field^{-1}	Herbicide Prescription Technique			
	No Herbicide	Label	Krige	Simulation
Viking	0.00	1830	2240	2240
Stony Plain	0.00	3950	4640	4710
Average	0.00	2890	3440	3480

Table 6.9: Total revenue, in dollars ha^{-1}, for two 64 ha fields near Viking and Stony Plain, Alberta using different mapping options. This revenue represents the difference between no herbicide and a herbicide prescription.

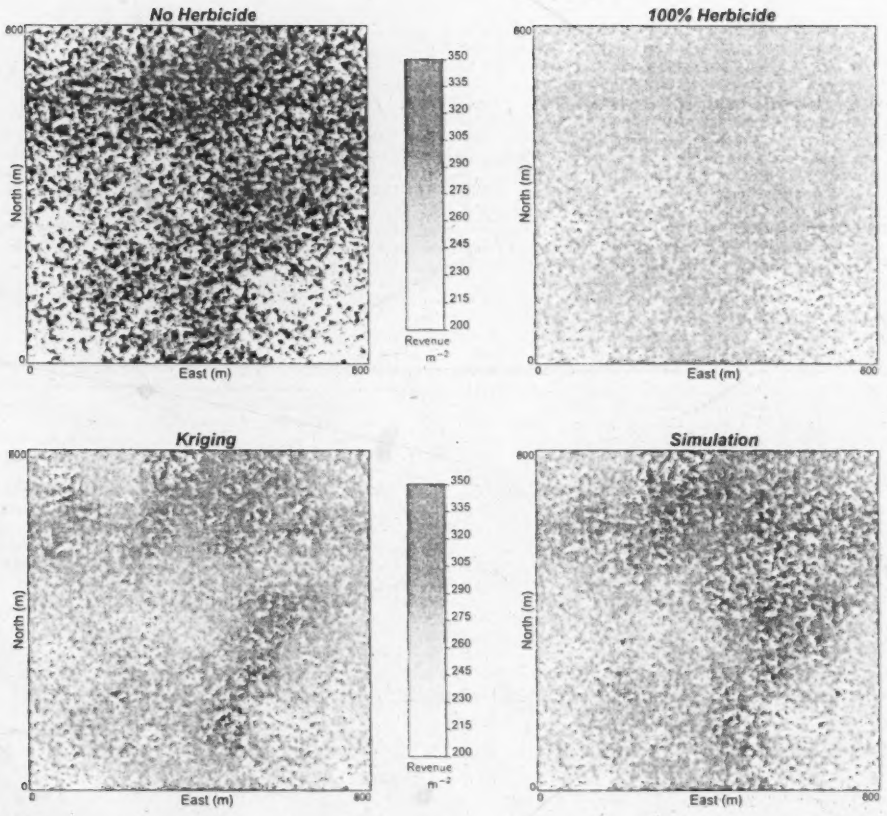

Figure 6.4: Total revenue, in dollars m^{-2}, for no herbicide, a 100% herbicide rate, a kriged map and simulated map of herbicide rates for a single wild oat density at Stony Plain, Alberta.

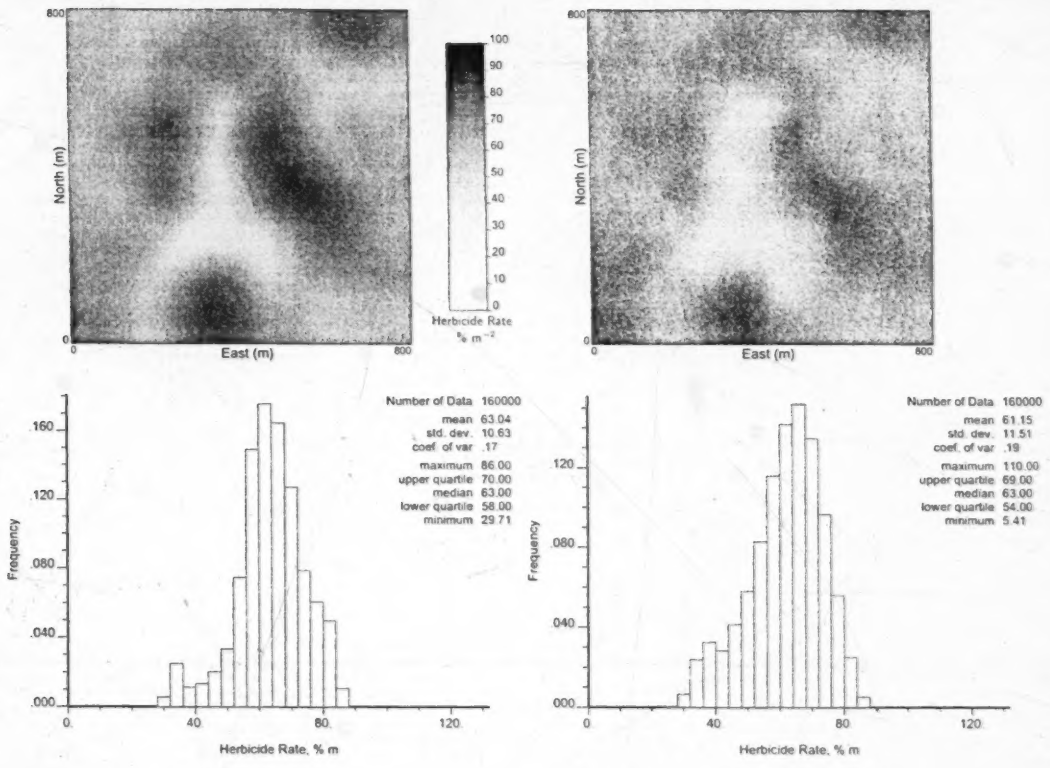

Figure 6.5: The top kriged (right) and simulated (left) maps of herbicide rates, in % m^{-2}, for a single wild oat density from a field near Viking, Alberta. The bottom histograms are the kriged (left) and simulated maps (right) of herbicide rates.

maps in the Viking field, see Figures 6.5, 6.6, and 6.7. Higher herbicide rates are observed in the center and bottom of the kriged and simulated maps. This corresponds with the weed density maps in Figure 6.1. The range of herbicide rates for the kriged single, double, and triple wild oat density maps indicate less variability as weed density increases. This is evident in the histogram shape, range and the declining standard deviation for each density. The mean, simulated herbicide rate increases from 61 to 90% while the mean, kriged rate increases from 63 to 89% for increasing wild oat density.

Herbicide rates vary as the wild oat density varies for the kriged and simulated Stony Plain maps, see Figures 6.10, 6.11, and 6.12. These maps display a different herbicide rate pattern compared to the Viking field. The bottom corners of the Stony Plain maps require high herbicide rates to control wild oat. The histogram shape of the wild oat density distributions approximate a log-normal shape for the kriged and simulated maps (see Figure 6.8) while the herbicide rate distributions are bimodal in shape except the kriged herbicide rate maps for the double and triple wild oat densities that are Gaussian. Herbicide rate variability that is indicated by the standard deviation and histogram is half in the Viking field compared to the Stony Plain field. This significant difference in variability is due to the different wild oat densities between the fields.

Application of the crop-weed-herbicide model to wild oat density data provides a diag-

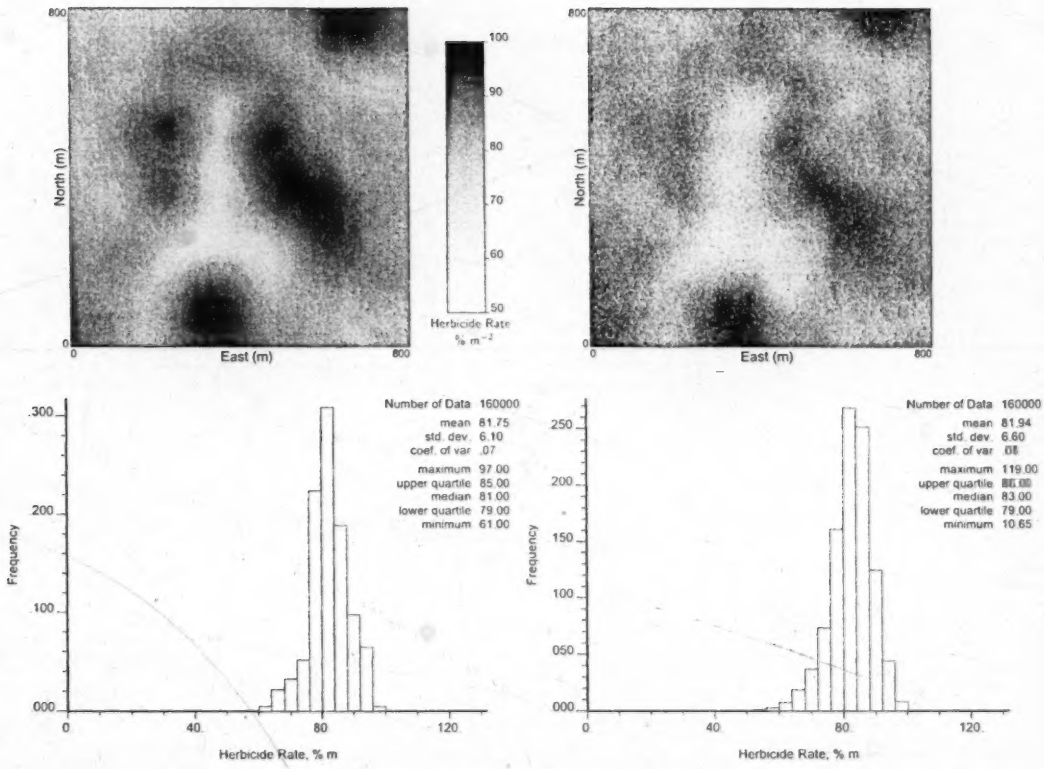

Figure 6.6: The top kriged (right) and simulated (left) maps of herbicide rates, in % m^{-2}, for a double wild oat density from a field near Viking, Alberta. The bottom histograms are the kriged (left) and simulated maps (right) of herbicide rates.

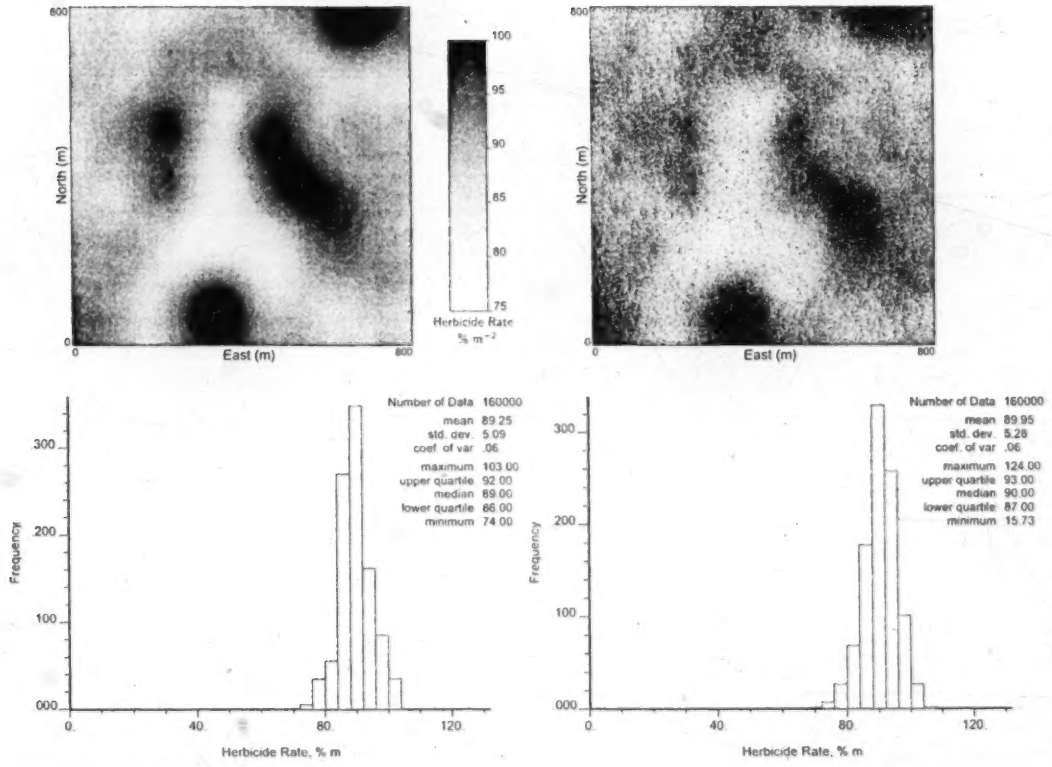

Figure 6.7: The top kriged (right) and simulated (left) maps of herbicide rates, in % m^{-2}, for a triple wild oat density from a field near Viking, Alberta. The bottom histograms are the kriged (left) and simulated maps (right) of herbicide rates.

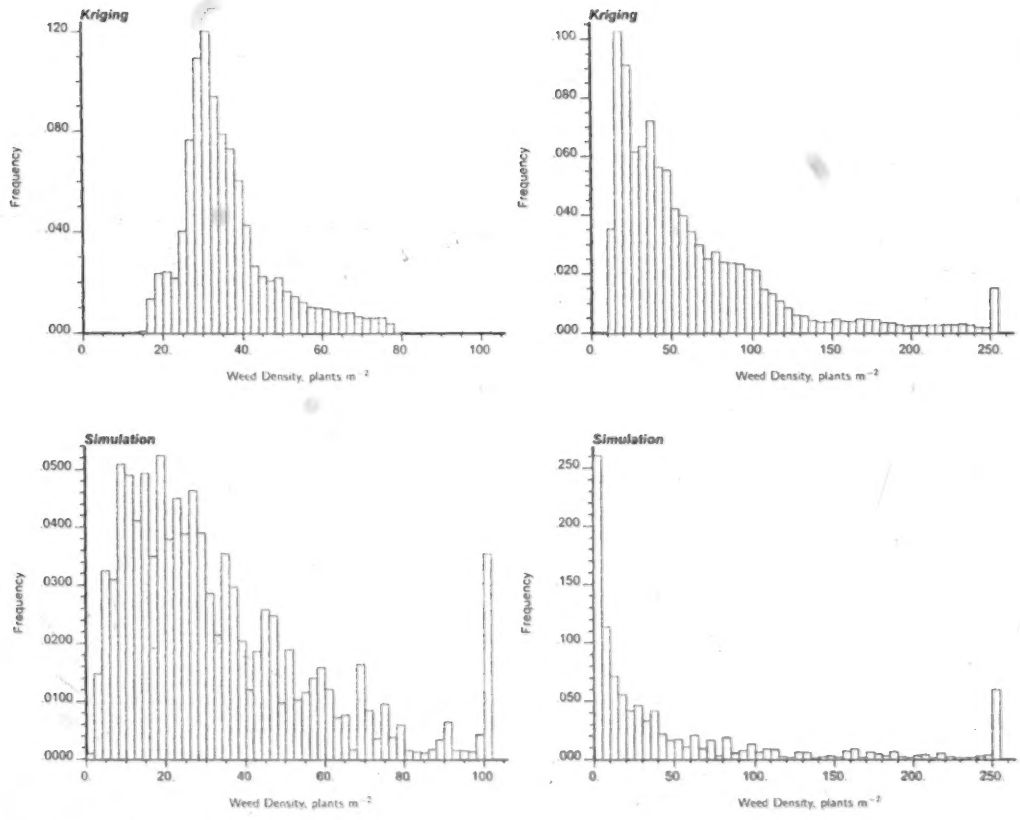

Figure 6.8: Histograms of a single wild oat density, in plants m^{-2}, for kriged (top) and simulated (bottom) maps for the Viking (left) and Stony Plain (right) fields. The last interval of weed density for each histogram represents number of weeds greater than 100 or 250 plants m^{-2}.

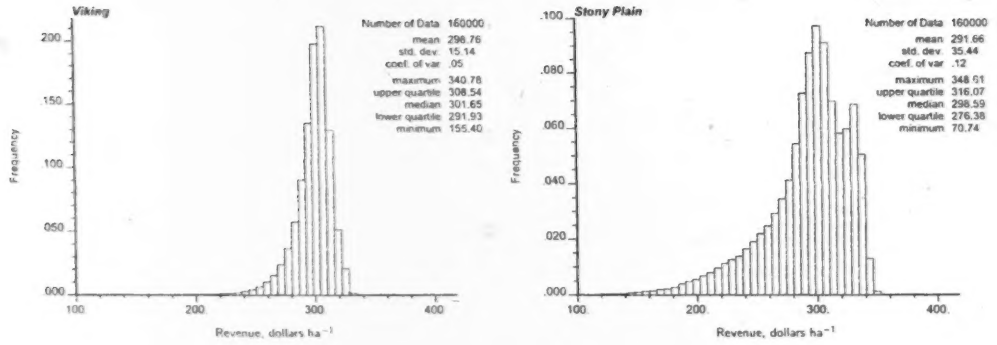

Figure 6.9: Histograms of revenue, in dollars ha^{-1}, for a single, simulated wild oat density at the Viking (left) and Stony Plain (right) sites. The histograms characterize uncertainty in revenue from the simulated maps.

nostic tool for implementing herbicide rates. The histogram of herbicide rates for a single wild oat density at the Stony Plain field is bimodal, see Figure 6.10. If a constant herbicide rate of 80% is applied at all locations above an arbitrary threshold of 40% and 25% is applied at the rest of the locations, revenue is \$18580 for the field and average herbicide rate is 61.2%. This compares favorably with total revenue from kriging. Weed distributions may occur where herbicide rates can be determined according to a histogram of locally varying rates without loss of revenue.

A visual comparison of herbicide rates between the 2 fields at the single wild oat density for kriging and simulation is displayed in Figure 6.13. Wild oat density in the reference map is significantly higher for the Stony Plain site at 65 plants m^{-2} compared to the Viking site at 35 plants m^{-2}. This is reflected in the higher herbicide rates for the Stony Plain field.

The smoothing effect of kriging is noticeable in the Viking and Stony Plain fields compared to the simulated maps for both fields. Simulation was developed to correct for the smoothing effect of kriging while also providing a measure of uncertainty for the attribute of interest. Uncertainty of revenue from simulation at the Viking and Stony Plain fields in Figure 6.9 illustrates how risk assessment can be considered. Uncertainty can also be quantified for the profitability of different sampling designs.

Kriging and simulation of locally varying herbicide rates provide economic and environmental benefits. Economic benefits from determining optimum herbicide rates are large when comparing them to a conventional approach. For all wild oat densities in this thesis, herbicide rate is 20% to 40% lower when applying locally varying rates compared to a conventional approach. Environmental loading of herbicides with a conventional application is higher resulting in lower revenues compared to locally varying rates. There is also a higher risk of selecting for herbicide resistant wild oat with the conventional approach. Locally varying rates need to be considered for weed management since they offer economic and environmental returns.

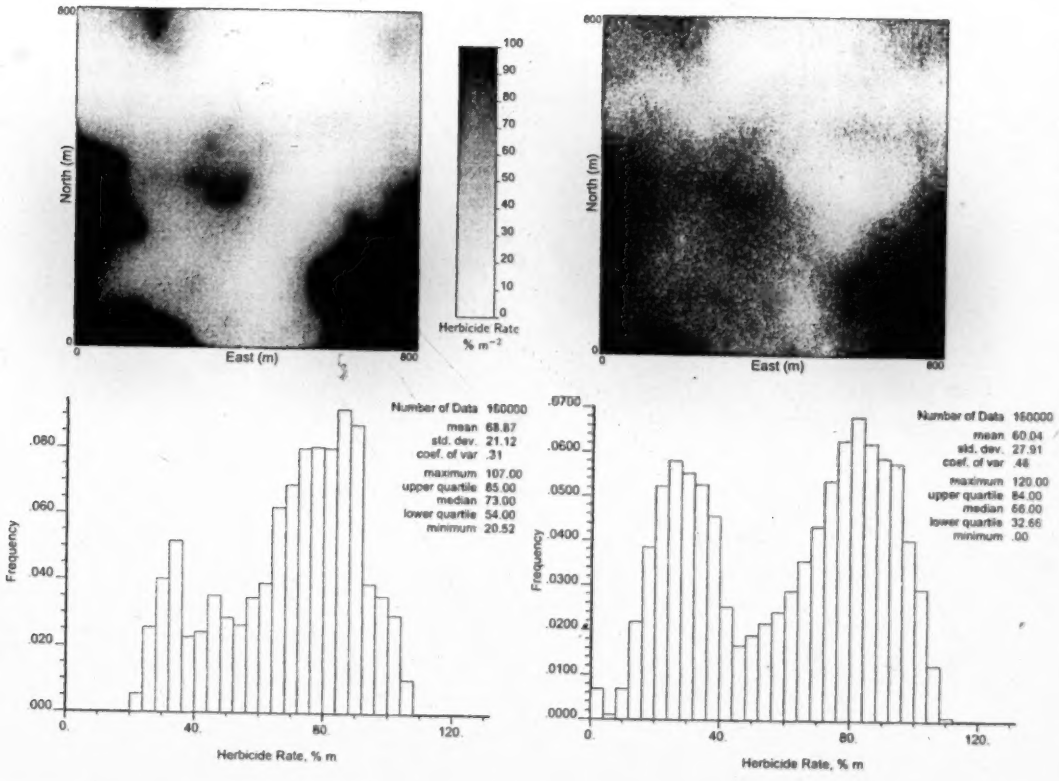

Figure 6.10: The top kriged (left) and simulated (right) maps of herbicide rates, in % m^{-2}, for a single wild oat density from a field near Stony Plain, Alberta. The bottom histograms are the kriged (left) and simulated maps (right) of herbicide rates.

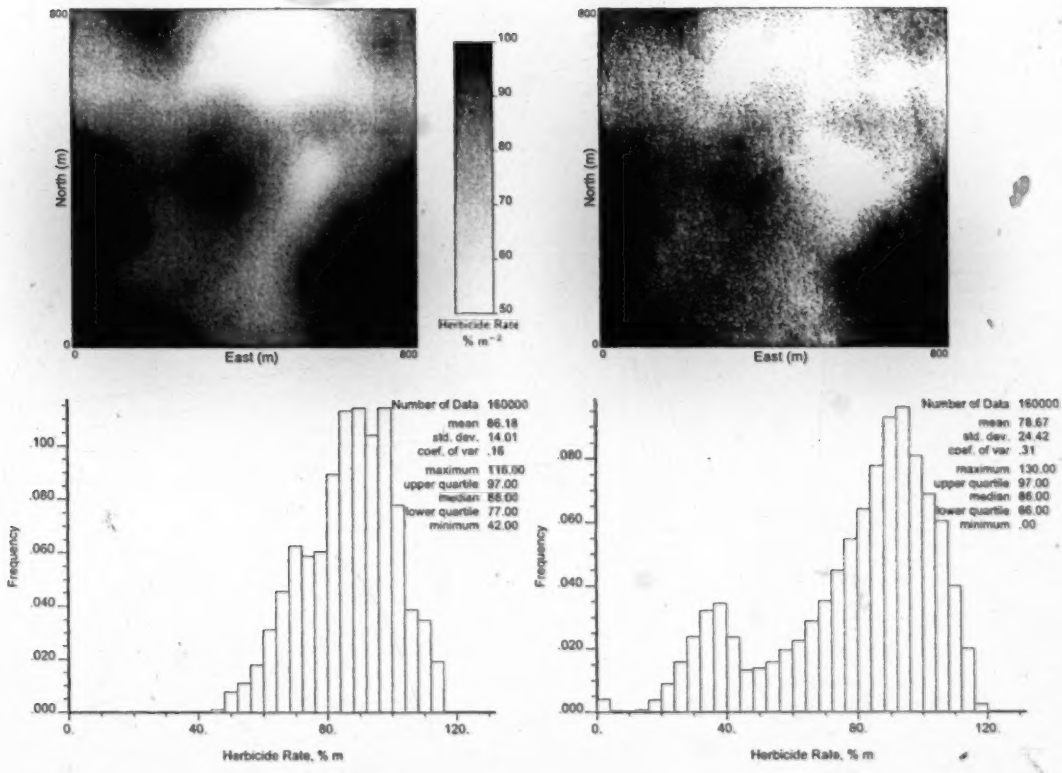

Figure 6.11: The top kriged (left) and simulated (right) maps of herbicide rates, in % m^{-2}, for a double wild oat density from a field near Stony Plain, Alberta. The bottom histograms are the kriged (left) and simulated maps (right) of herbicide rates.

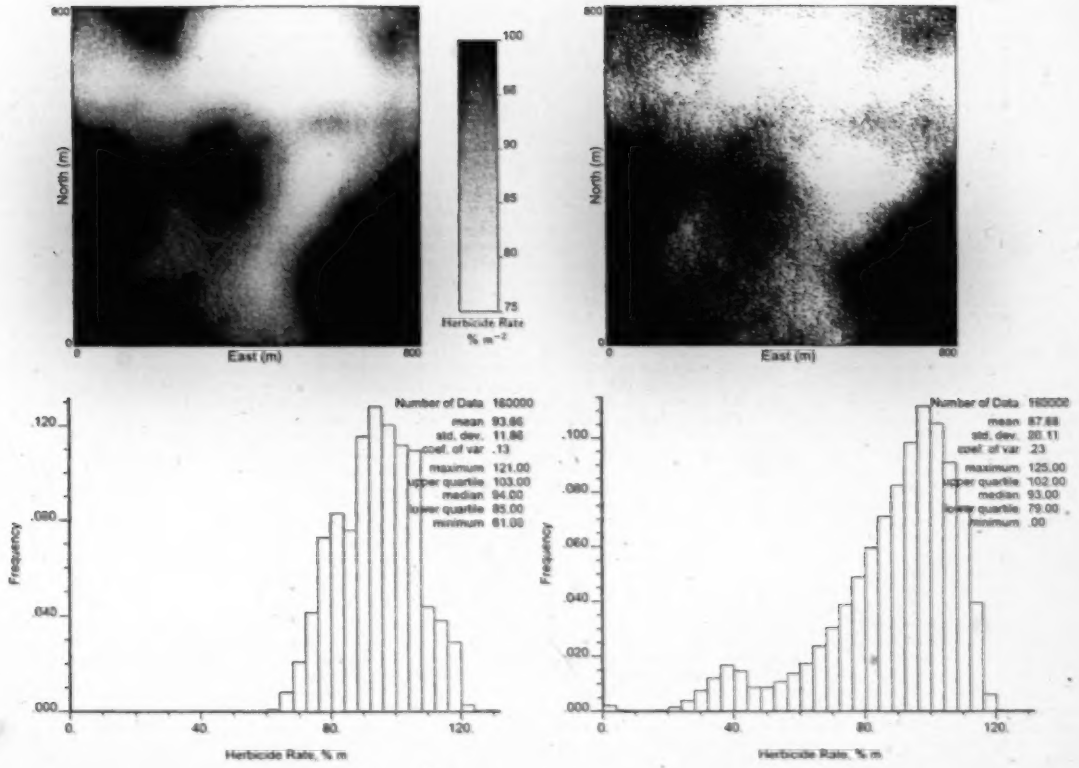

Figure 6.12: The top kriged (left) and simulated (right) maps of herbicide rates, in % m^{-2}, for a triple wild oat density from a field near Stony Plain, Alberta. The bottom histograms are the kriged (left) and simulated maps (right) of herbicide rates.

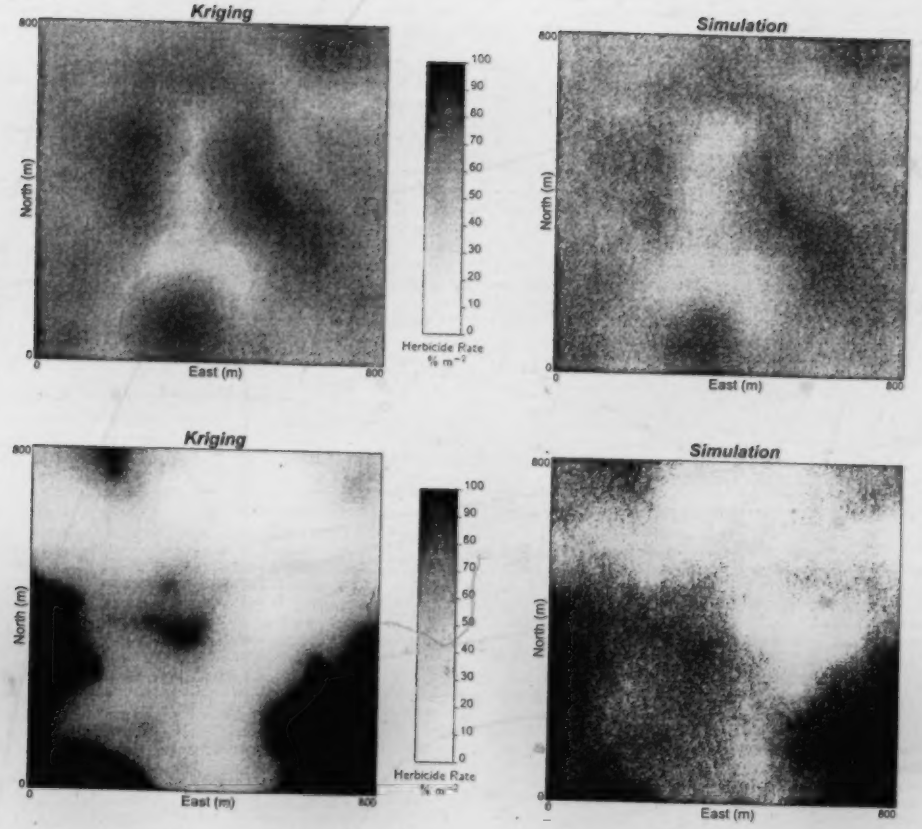

Figure 6.13: Kriged and simulated herbicide rates, in % m^{-2}, for a single wild oat density from the Viking (top) and Stony Plain (bottom) fields.

Simulation			Kriging		
Design	Revenue	Weed Density	Design	Revenue	Weed Density
$Square_7$	18600	15	$Square_7$	18520	14
$Grid_{10}$	18580	16	$Grid_{10}$	18580	14
$Gridnest_{10}$	18580	16	$Gridnest_{10}$	18590	14
$Square_9$	18600	16	$Square_9$	18560	14
$Grid_{13}$	18640	15	$Grid_{13}$	18540	13
$Gridnest_{13}$	18630	15	$Gridnest_{13}$	18530	13
$Square_{13}$	18490	13	$Square_{13}$	18420	12
$Grid_{19}$	18670	15	$Grid_{19}$	18580	13
$Gridnest_{19}$	18700	18	$Gridnest_{19}$	18660	15
Mean	18610	15	Mean	18550	13

Table 6.10: Revenue, in dollars field^{-1}, for 3 sampling designs and 3 configurations from a 64 ha field of barley near Stony Plain, Alberta. Weed density, in plants m^{-2}, represents the number of wild oat after herbicide treatment and the field average is 65 plants m^{-2}.

6.3 Optimal Sampling Design

A methodology is developed to evaluate sampling designs for cost effectiveness. Spatial information is necessary to characterize the variability of wild oat. This information is applied in a crop-weed-herbicide model for locally varying herbicide rate maps.

Revenue, in dollars m^{-2}, is calculated for each weed prescription using the parameters presented in section 6.2. Total revenue from each herbicide prescription map is averaged over the field. The expense of sampling is subtracted from total revenue for total profitability.

Maximum attainable revenue, given the reference weed distribution and corresponding herbicide rate, is \$19280 for the Stony Plain field and \$19400 for the Viking field. If no herbicide is applied to wild oat, revenue decreases to \$16050 and \$18470 for the Stony Plain and Viking fields. This significant difference in revenue at the 1% level of probability is a result of higher wild oat densities for the Stony Plain field compared to the Viking field. These densities affect the barley yield that decreases from 4.7 weed-free t ha^{-1} to 3.4 and 3.9 for the Stony Plain and Viking fields. Revenue changes to \$17880 and \$18380 for the Stony Plain and Viking fields when a 100% rate of herbicide is applied. Barley yield with a 100% rate is 4.5 t ha^{-1} and wild oat density is 9 and 5 plants m^{-2} after herbicide treatment for the Stony Plain and Viking fields.

To determine the value of simulation compared to kriging, revenue from simulation is subtracted from revenue due to kriging for the same design and configuration, see Tables 6.10 and 6.13. Simulation results in significantly more revenue (\$20 and \$60) compared to kriging for the Viking and Stony Plain fields over all designs and configurations. Simulation generates significantly more revenue compared to kriging for the Stony Plain and Viking sites except for the $Grid_{10}$ and $Gridnest_{10}$ designs at the Stony Plain site. Final wild oat density after herbicide treatment is similar for kriging and simulation.

Wild oat density variograms from each sampling design and configuration are used in mapping to determine revenue, see Tables 6.10 and 6.13. A variogram is expected to be

more robust when it is correct at different distances. For the gridnest design, the variogram from the nested design that defines the variogram at 4 different scales is applied to a grid sample pattern. Revenues averaged over configurations and mapping techniques indicate that the gridnest design is highest at \$18610, next is the grid at \$18590 while the square generates \$18530 for the Stony Plain field. The revenues for the Viking field are \$19120, \$19090 and \$19070 for the gridnest, grid and square designs.

The most revenue is generated by the simulated $Gridnest_{19}$ and $Grid_{19}$ designs using 361 locations while a kriged $Square_{13}$ design with 338 locations has the lowest revenue at the Stony Plain field, see Table 6.10. When averaging revenues over designs and mapping techniques 3 and 4, small configurations include $Grid_{10}$, $Gridnest_{10}$ and $Square_7$; medium refers to $Grid_{13}$, $Gridnest_{13}$ and $Square_9$; and large consists of $Grid_{19}$, $Gridnest_{19}$ and $Square_{13}$. Revenue from each configuration is the same at \$18580 while total profitability is \$18080, \$17900, and \$17360 for the small, medium and large configurations. Herbicide rate, barley yield and wild oat left after treatment are the same for the small, medium and large configurations at 66%, 4.4 t ha^{-1} and 14 wild oat m^{-2}. Spacing between sample locations for each configuration declines from 111 to 13 m for the small, 86 to 2 m for the medium and 42 to 1 m for the large. Choosing a design with more locations or closer spacing to increase the correctness of the variogram did not result in more profit. However, when sampling expenses are considered, fewer samples are the most profitable.

Revenue and wild oat density from different sampling designs are compared to a conventional approach for the Stony Plain field, see Table 6.11. The conventional approach, a 100% herbicide rate, has revenue of \$17880 and a final density of 9 wild oat m^{-2} after treatment. Average herbicide rates for kriging and simulation are 69% and 62% that represents \$1020 and \$1250 less for herbicide. This is offset by lower crop yields, 4.4 t ha^{-1} for kriging and simulation compared to 4.5 t ha^{-1} for the conventional approach. This is \$470 per field less for kriging and simulation compared to the conventional approach. After accounting for lower yields and less herbicide, net revenue is \$670 and \$730 for kriging and simulation compared to a conventional treatment. Average extra revenue due to the use of locally varying wild oat densities and the crop-weed-herbicide model is \$700 for kriging or simulation compared to the conventional approach. Initial sampling costs, on average, have to be less than \$700 for kriging or simulation to be more cost effective than a conventional approach in this field. The crop-weed-herbicide model is density dependent and sampling of patch centers would need to be determined annually. Since this sampling update would concentrate on patch centers, costs would be reduced. Additionally, these costs can be amortized over several years since weed patches are stable and are being contained by optimal herbicide treatment (Dieleman, 1998; Heisel et al., 1996; Mortensen & Dieleman, 1998) [39, 65, 98].

A sampling design with the least number of sampling locations would be expected to be the most profitable since sampling costs are the lowest, see Table 6.12. The most profitable sampling design in the Stony Plain field is the simulated $Square_7$ that has 98 sampling locations. The kriged and simulated $Grid_{10}$ designs with 100 sampling locations are the next most profitable with \$18080 and \$18070 per field. Sampling costs reduce the profitability of the $Square_{13}$, $Grid_{19}$ and $Gridnest_{19}$ designs and they generate \$340 to \$720 less than applying a 100% rate of herbicide. A comparison of the designs that generate the most profitability indicates a difference of \$90 when applying the $Gridnest_{19}$ design compared to \$1060 in profit when applying the $Square_7$ design. The increase in profit due to more sample locations and a variogram defined at a larger scale does not outweigh the additional

Simulation			Kriging		
Design	Revenue	Weed Density	Design	Revenue	Weed Density
$Square_7$	730	7	$Square_7$	650	5
$Grid_{10}$	700	7	$Grid_{10}$	700	5
$Gridnest_{10}$	700	7	$Gridnest_{10}$	710	5
$Square_9$	730	7	$Square_9$	680	6
$Grid_{13}$	760	6	$Grid_{13}$	660	4
$Gridnest_{13}$	760	6	$Gridnest_{13}$	650	4
$Square_{13}$	610	4	$Square_{13}$	500	3
$Grid_{19}$	790	7	$Grid_{19}$	700	4
$Gridnest_{19}$	820	9	$Gridnest_{19}$	790	7
Mean	730	7	Mean	670	5

Table 6.11: Revenue and wild oat density differences, in dollars field^{-1}, when comparing 3 sampling designs and 3 configurations to a conventional approach from a 64 ha field of barley near Stony Plain, Alberta. The conventional approach is a 100% rate of herbicide. Weed density, in plants m^{-2}, represents the number of wild oat after herbicide treatment.

expenses of sampling. All sampling patterns and configurations provide more profit than applying no herbicide.

The value of quantifying uncertainty via simulation compared to kriging with the same design and similar number of locations varied from \$0 to \$110 in the Stony Plain field, see Table 6.12. Simulation averaged \$18090 in profit at the smallest configuration. Profit from kriging with a similar number of sample locations is next at \$18060. Kriging at the largest configuration had the lowest profit at \$17320. When averaging over sample design, the most profit is provided by designs with the smallest configuration at \$18070 while designs with a medium configuration generate \$17900 and the large configuration designs net a profit of \$17360. The most profitable sampling design for this field is the gridnest at \$17840 averaged over mapping techniques and sampling locations. The grid design generated \$17770 while the square is \$17730.

Wild oat density and herbicide rate maps for the Stony Plain field are displayed for a reference, kriged $Grid_{10}$, simulated $Grid_{10}$ and simulated $Square_7$ design in Figures 6.14 and 6.15. The herbicide rate maps in Figure 6.15 closely match the wild oat density maps in Figure 6.14. There is a larger area of lower herbicide rates in the locally varying maps compared to the kriged $Grid_{10}$ map in Figure 6.15. The simulated $Square_7$ provides the highest, significant profitability in this field followed by the simulated $Grid_{10}$ and kriged $Grid_{10}$ design. The wild oat density and herbicide rate maps for the kriged $Grid_{10}$ design are smooth compared to the other 3 maps.

A field near Viking, Alberta with a lower wild oat density and different spatial pattern provides a comparison to the Stony Plain field, see Table 6.13. At the Viking field, the most profitable sampling design is the simulated $Grid_{10}$ design. The kriged $Grid_{10}$ and simulated $Gridnest_{10}$ designs are the next most profitable at \$18600 and \$18590 per field. Sampling costs reduce the profitability of the $Grid_{19}$, $Gridnest_{19}$, and $Square_{19}$ designs and they provide less profit than the conventional treatment. Applying no herbicide generates

Simulation		Kriging	
Design	Profit dollars field^{-1}	Design	Profit dollars field^{-1}
$Square_7$	18110	$Square_7$	18030
$Grid_{10}$	18080	$Grid_{10}$	18080
$Gridnest_{10}$	18070	$Gridnest_{10}$	18070
$Square_9$	17920	$Square_9$	17870
$Grid_{13}$	17930	$Grid_{13}$	17830
$Gridnest_{13}$	17980	$Gridnest_{13}$	17870
$Square_{13}$	17270	$Square_{13}$	17160
$Grid_{19}$	17380	$Grid_{19}$	17290
$Gridnest_{19}$	17540	$Gridnest_{19}$	17510
Mean	17810	Mean	17750

Table 6.12: Profitability, in dollars field^{-1}, for 3 sampling designs and 3 configurations from a 64 ha field of barley near Stony Plain, Alberta. The *Gridnest* design used the variogram from a nested design while the other designs used the variogram from their design. Maximum attainable profit for this field given the reference weed distribution and corresponding herbicide rate is \$19280.

Simulation		Kriging	
Design	Profit dollars field^{-1}	Design	Profit dollars field^{-1}
$Square_7$	18560	$Square_7$	18540
$Grid_{10}$	18610	$Grid_{10}$	18600
$Gridnest_{10}$	18590	$Gridnest_{10}$	18570
$Square_9$	18410	$Square_9$	18390
$Grid_{13}$	18410	$Grid_{13}$	18390
$Gridnest_{13}$	18460	$Gridnest_{13}$	18420
$Square_{13}$	17900	$Square_{13}$	17880
$Grid_{19}$	17860	$Grid_{19}$	17850
$Gridnest_{19}$	17960	$Gridnest_{19}$	17930
Mean	18310	Mean	18290

Table 6.13: Profitability, in dollars field^{-1}, for 3 sampling designs and 3 configurations from a 64 ha field of barley near Viking, Alberta. The *Gridnest* design used the variogram from a nested design while the other designs used the variogram from their design. Average wild oat density is 35 plants m^{-2} for this field. Maximum attainable profit for this field with the reference weed distribution and corresponding herbicide rate is \$19400.

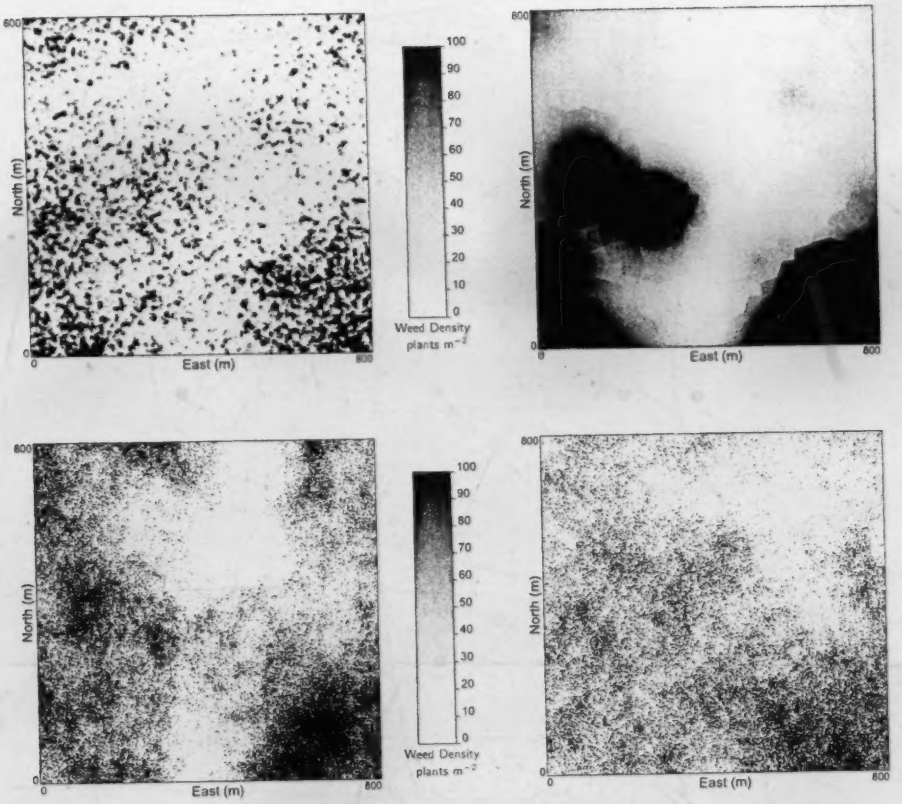

Figure 6.14: Wild oat densities, in plants m^{-2}, for reference, kriged $Grid_{10}$, simulated $Grid_{10}$ and simulated $Square_7$ designs, clockwise respectively, for a field near Stony Plain, Alberta in 2000. For the simulated $Grid_{10}$ and $Square_7$ designs, this is one realization of 101.

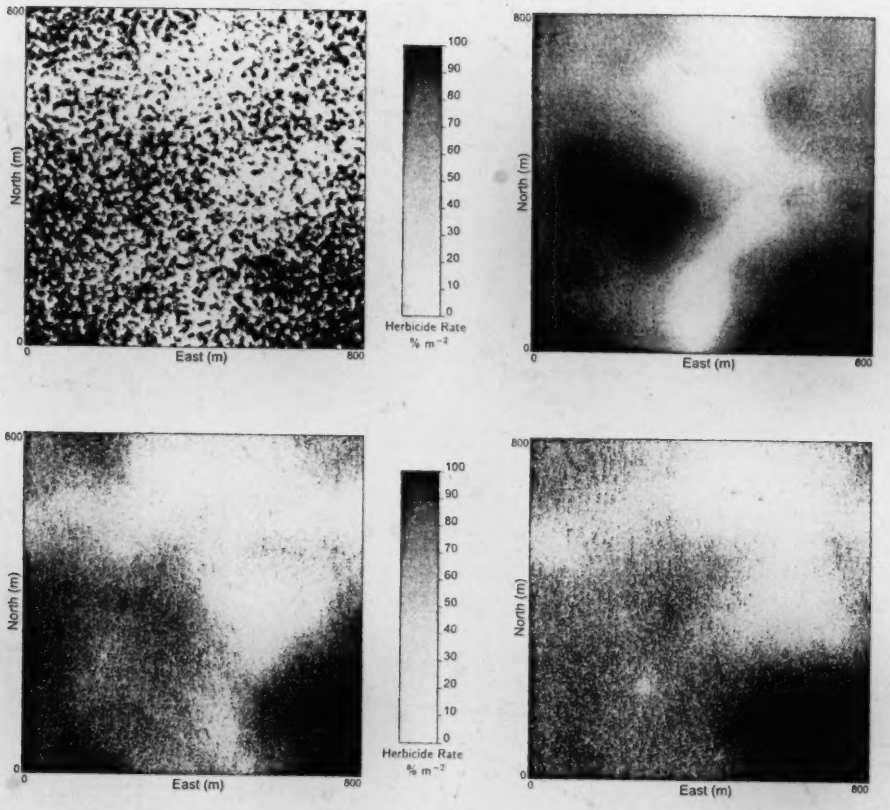

Figure 6.15: Herbicide rates, in % m^{-2}, for reference, kriged $Grid_{10}$, simulated $Grid_{10}$ and simulated $Square_7$ designs, clockwise respectively, for a wild oat infested field near Stony Plain, Alberta in 2000.

$620 less revenue compared to the average of all sampling designs and configurations. The conventional treatment with a 100% rate of herbicide generated $18380 in profit that is $120 less than the average of the small and medium configurations.

The value of simulation compared to kriging with the same sample design and size ranged from $10 to $40 from the small to large configurations in the Viking field, see Table 6.13. Simulation averaged $18580 in profit at the smallest configuration while kriging averaged $18570. Kriging at the largest configuration had the lowest profit at $17890. Averaging over sample design, the most profit is provided by designs with the smallest configuration at $18580 while designs with a medium configuration generate $18410 compared to large configurations at $17900. The most profitable sampling design for this field is the *Gridnest* design at $18320 averaged over all sampling locations. The *Grid* design generated $18290 followed by the *Square* at $18280.

Wild oat density and herbicide rate maps are displayed for a reference, kriged $Grid_{10}$, simulated $Grid_{10}$ and $Gridnest_{10}$ design in Figures 6.16 and 6.17 for the Viking field. The wild oat density and herbicide maps visually match, but the kriged wild oat density and herbicide maps are smooth. The location of black dots representing high wild oat density on the simulated $Grid_{10}$ map closely match those from the reference map and the high herbicide rates from the simulated $Grid_{10}$ map resemble those of the reference map in Figure 6.17. The simulated $Grid_{10}$ results in the highest, significant profitability compared to all designs and configurations from this field.

6.4 Summary of Results

Results from this study illustrate a methodology for evaluating sampling design and configuration that can be optimized with locally varying weed densities. The methodology evaluates the profitability of designs and configurations based on design expenses and spatial models. Of the 3 designs and 3 configurations assessed, the simulated $Square_7$ with 98 sample locations for the Stony Plain field is the most profitable while at the Viking field, a simulated $Grid_{10}$ design generates the most profit. These designs have the smallest number of sampling locations and the lowest sampling expenses. Additionally, sample spacing and the range of spatial correlation for wild oat density contribute to the profitability of these designs.

Differences in profitability between designs and configurations are significant. The crop-weed-herbicide model is parameterized for maximum impact of wild oat on the crop. If timing of wild oat emergence relative to the crop is set at 0 days rather than -14 days, profitability increases by $250 to $350 for kriging and simulation.

Although the revenue differences between configurations within designs is small, wild oat spatial variability varies from field to field and requires quantification within each field. The *Gridnest* design that utilizes a more robust variogram resulted in a higher amount of revenue compared to the *Grid* and *Square* designs. The expense of sampling at different scales to quantify wild oat spatial variability may be economically justified. Further research is necessary to confirm this finding.

Determining locally varying herbicide rate includes simulation with alternative numerical models and kriging. For the Stony Plain and Viking fields, there are 101 realizations that modeled the uncertainty of wild oat density. Applying herbicide with locally varying maps results in $3440 to $3480 more revenue compared to a no herbicide option. The locally varying herbicide maps based on simulation or kriging generate an average of $570 field^{-1}

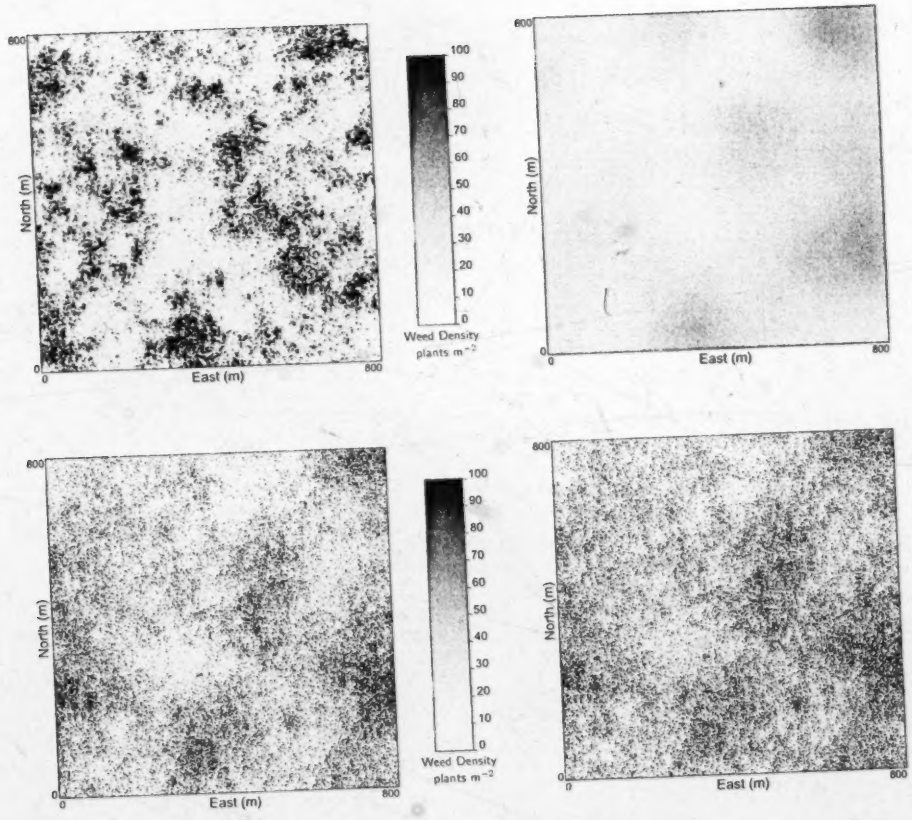

Figure 6.16: Wild oat densities, in plants m^{-2}, for reference, kriged $Grid_{10}$, simulated $Grid_{10}$ and simulated $Gridnest_{10}$ designs, clockwise respectively, for a field near Viking, Alberta in 2000. For the simulated $Nest_{10}$ and $Gridnest_{10}$ designs, this is one realization of 101.

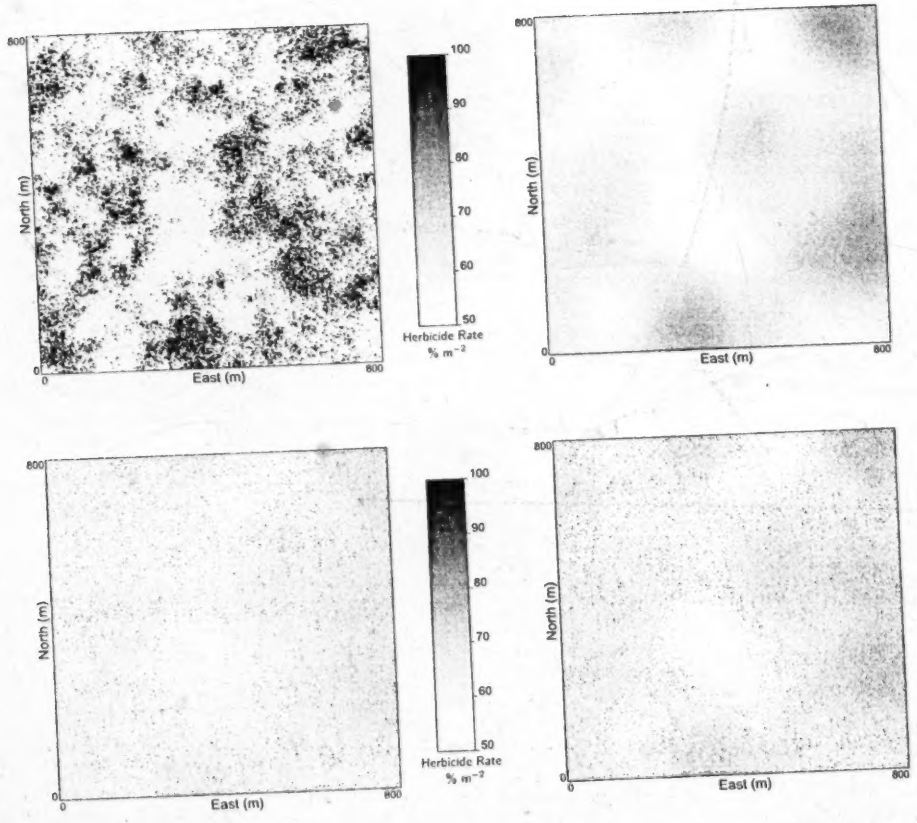

Figure 6.17: Herbicide rates, in % m^{-2}, for reference, kriged $Grid_{10}$, simulated $Grid_{10}$ and simulated $Gridnest_{10}$ designs, clockwise respectively, for a wild oat infested field near Viking, Alberta in 2000.

more revenue than the conventional approach of 100% of label. When comparing locally varying maps, average revenue over all designs is significantly higher for simulation by $20 for the Viking field and $80 for the Stony Plain field compared to kriging. Quantifying uncertainty for these 2 fields increased revenue for simulation; however, more fields will need to be assessed to confirm this finding.

Locally varying herbicide maps provide economic and environmental advantages for consideration. The profit of locally varying maps is based on weed sampling. Less expensive methods of determining weed density such as elevation data, historical records and satellite imagery will improve the profit of locally varying maps. Locally varying maps reduce environmental loading of herbicides by up to 40% compared to the conventional approach. This methodology applies geostatistical tools to wild oat data and decision making in the presence of uncertainty. Optimizing herbicide rates with locally varying maps needs to be integrated into weed control management programs.

Chapter 7

Future Work and Implementation

Locally varying herbicide application reduces environmental loading of herbicides and cost to farm managers. Such technology requires a farm manager to know the locations of weed populations. Exhaustive sampling would provide the exact locations of all weeds and allow implementation of a targeted application program; however, the cost would be prohibitively expensive. Instead, some reasonably spaced samples should be collected to identify weed locations and design an optimum treatment program. The optimum treatment program will give the most profitable total system economics, that includes revenue due to increased yield, herbicide cost, and the costs associated with sampling. The methodology to implement such a treatment program has been developed in this thesis with consideration of (1) wild oat in western Canadian crops, (2) locally varying herbicide treatments, (3) uncertainty in the predicted maps, and (4) economics in decision making.

There are limitations and future research required for the application of such a treatment program to consider for each component of the crop-weed-herbicide model.

Crop

Crop loss equations have been developed for wild oat in barley and canola; however, equations for more crop-weed combinations must be developed and evaluated. The current crop loss multiregression equations rely on empirical evidence generated from numerous data sets. The model is subject to change due to environmental, crop and weed interactions. Field trials could be set up where different weed densities are compared to weed-free crop yield to refine the crop loss equation.

Crop cultivar, rotation, timing of planting, crop density, seed spacing, tillage and fertilizer placement influence weed species and distribution. The intent of managing these factors is to provide the crop with its best opportunity to compete given the current environmental conditions. Additional research is needed to maximize a crop's competitive ability.

Crop rotation is not considered in the model in terms of uncontrolled weeds and their effect on succeeding crops. Volunteer crops and weeds in one year could result in challenges for a succeeding crop.

The effects of the spatial pattern of wild oat on crop growth is considered in this study. The spatial pattern of a crop is indirectly addressed in the crop-weed-herbicide model with changing crop densities. Additional information on the effects of row spacing and seeding pattern for crops could be included.

Weed

Wild oat is a major annual weed in western Canada and substantial herbicide expenditures are spent on controlling this weed. The crop-weed-herbicide model is developed to account for crop yield loss in barley or canola due to wild oat. Narrowleaf hawksbeard, horsetail, perennial sowthistle, dandelion and volunteer crops have become more abundant with the cropping system changes of reduced tillage (Derksen et al., 2002) [34]. Consequently, the effects of a mixed weed species infestation on crop yield must be incorporated into crop yield loss equations. Two species models have been developed and a competitive index has been established for multiple weed types in soybean (Berti & Zantin, 1994; Doyle, 1991; Wilkerson et al., 1991) [8, 45, 159]. There may be limits to the number of weeds that are incorporated into a multi-weed model for crop loss due the interactions of environment, crop and weed and increased sampling costs. Additional research is required to generalize this model for other crops and weeds.

A prime focus of weed control is to manage a weed population. Given the increasing array of herbicide choices and the fact that weed species continue to cause crop yield loss, this goal has not been consistently achieved. The agricultural industry may need to reconsider this primary focus in light of integrated weed management practices.

Recognizing that wild oat occurs at different densities in various parts of a field, a patch may be obvious at one scale but not at another. Patch models cannot be identified by location (Crawley, 1997) [32]. With the implementation of GPS and GIS in agriculture, spatial variation at larger and larger scales can be determined.

Weed counts are a common technique for measuring weed impact on crop yield. Size and density of weeds change over the course of a growing season. Another measure of plant development such as leaf area index may be more appropriate in describing the emergence of separate flushes of weeds than simple weed counts; however, there are no simple and accurate methods to estimate leaf area index for large fields.

Weed seeds exhibit dormancy in the soil. This provides a supply of future weeds for crop competition and yield reduction. It is difficult to predict future weed seedlings and their abundance wrong reference (Sagar & Mortimer, 1976) [132]. This factor may be considered in future crop-weed-herbicide models if the prediction of weed seedling improves.

Herbicide

Dose response curves have been characterized for economic thresholds and weed biomass for genetically modified canola (Madsen et al., 1999; Madsen et al., 1999; Streibig, 1989) [87, 88, 142]. Information on dose response curves is proprietary since it is researched and developed by private companies for government registration and licensing purposes. Consequently, the information is unavailable to weed scientists in public research.

Regulations for herbicide registration in Canada do not require disclosure of dose response curves for a range of environmental crop-weed-herbicide conditions. A herbicide's label rate is the dose legally required to reduce weed biomass by at least 80%. The label rate plus additional dose response curves would allow farm managers flexibility in implementing locally varying optimal herbicide rates.

The crop-weed-herbicide model relies on parameters from dose response curves that have been published in the literature. Site-specific agriculture will depend on the cooperation of herbicide manufacturers, or on extensive additional research.

The duration of herbicide exposure will influence the herbicide's effect on the weed. To

optimize herbicide rate and timing, experiments to quantify the relationship between rate and exposure need to be completed.

Weed response to herbicide is sometimes expressed as a percentage relative to the growth of the weed without herbicide. Weed growth without herbicide is subject to error and may misrepresent the herbicide's effect on the weed. A more common approach with a constant dilution factor that gives a logarithmic transformation of doses is used to determine herbicide dose response curves (Streibig & Kudsk, 1993) [144].

Biological systems are very complex and current knowledge does not allow the derivation of theoretical dose response curves (Streibig & Kudsk, 1993) [144]; however, the choice of a parametric function to fit the bioassay data is important. The relationship between a dose variable, x, and a response variable, y, is described by the model, $y = f(x, \beta) + \varepsilon$ where ε is the error term and β represents parameters of the model. Assumptions for dose response curves consider uniformity, size, number, and growth stage of weeds at the time of herbicide application. Sub-toxic doses that stimulate weed growth need to be acknowledged. Active ingredient of the standard and test herbicides need to be similar for potency testing. Comparison of estimates of herbicide potency assume that the assay is independent of weed species, experimental conditions, and response technique.

Herbicide application rate is adjusted in the crop-weed-herbicide model to account for variations in the spatial distribution of weed density. This assumes crop damage and that weed density is a satisfactory measure of weed competition. A critical consequence of this model is that the optimal application rate is proportional to weed density, that is, areas with high weed density receive more herbicide and areas with low weed density receive less herbicide for effective control.

Varying the herbicide application rate from the label rate is unsupported by manufacturers because of regulations that require a guaranteed response at the label rate. Herbicide performance testing is conducted on a range of crop varieties, weed densities and species, soil types and weather conditions. The label rate is established for a wide range of conditions. A central premise of this work is that deviations from the label rate could be optimal for local conditions. The optimal application rate strikes an economic balance between cost, control and crop yield loss.

Model Assumptions

The model relies on weed density data collected in the field. Accurate counts are sometimes difficult to obtain especially in areas of high weed density. Errors in weed species identification will affect the geostatistical models used for herbicide rate maps.

The crop-weed-herbicide model contains many parameters including herbicide dose response curves, crop-loss equations, crop price, weed-free crop yield, crop density, and herbicide efficacy. A limitation is the empirical nature of some components such as the multi-regression crop-loss formula and the dose response curves for different herbicide rates.

Environmental conditions affect the crop, weed and herbicide. A herbicide rate map that is generated from the crop-weed-herbicide model does not account for all environmental conditions at the time of spraying. Hot dry field conditions will reduce the density of weeds; however, the weeds may be difficult to control. A cold spring can reduce crop emergence allowing weeds to out compete the crop. Herbicide rates need to be adjusted to account for these changing environmental conditions. Parameters for these conditions could be eventually incorporated into the model.

The spatial distribution and uncertainty in weed density can be characterized using geostatistics and weed density data. Additional data will reduce uncertainty, but at increased cost. Optimal sample spacing balances additional sampling costs with the benefits of improved decisions. Supplementary data could come from weed surveying using an all terrain vehicle. A visual rating of weed numbers provides qualitative data for analysis (Hall & Faechner, 1999) [59]. This extensive, qualitative weed data will improve quantification of the nugget effect at short distances compared to a sparsely sampled, 10 x 10 grid. Digital elevation maps may also improve weed density mapping because weeds favor specific regions (Faechner et al., 2000) [47]. A review of sampling strategies for arable crops highlights some of the challenges facing weed scientists in site specific weed management (Rew & Cousens, 2001) [125].

Crop quality, harvesting ease, impacts on beneficial organisms, and social implications are not directly accounted for in the model. These factors are important in the development an integrated pest management program. Future development of this methodology could include these factors.

This crop yield loss model may overestimate herbicide rates since some of the weed density data used to develop this model was obtained from experiments where crop and weed are seeded at a similar time. Field validation of this crop loss model will confirm the significance of the relative time of crop and weed emergence.

7.1 Implementation

A general procedure for establishing a locally varying herbicide rate is:

1. Establish a nested sampling pattern for measuring weed density in a study area. Weed species are identified and counted in a pre-determined area at all these locations.

2. Create a variogram from this weed density data. With the nested sampling, spatial correlation at different scales will ensure the variogram is reliably informed.

3. To quantify the spatial continuity of weeds over the entire study area, set up a square sample pattern and identify and count weeds at each of these locations. Collect areally extensive soft data for additional constraints.

4. Using the weed density data from the square sample pattern and the variogram generated from the nested sampling pattern, apply SGS to generate geostatistical realizations of weed density for the study area.

5. Establish a measure of crop yield loss to be minimized for each realization and the loss measure is determined from the expected value over all realizations. The measure of loss decreases with less weeds, and increases with more weeds and less crop. The loss depends on herbicide and crop prices, crop and weed density, time of weed emergence relative to the crop, and herbicide efficacy. Realizations of weed density plus parameters such as crop density and price, time of weed emergence relative to the crop, herbicide efficacy and price are combined into numerical models that represent herbicide rate on a locally varying basis.

6. Define an optimal herbicide rate that has a minimum cost or maximum profit. The rate, weed density, herbicide price and crop revenue on a weed-free basis are used to assess total expected loss or profit, in dollars ha^{-1}, over the study area.

This procedure could be followed by weed scientists, agronomists and farm managers with extensive holdings.

7.2 Conclusion

There has been a paradigm shift in mapping of biological phenomenon. Increasing the number of samples cannot remove all uncertainty; therefore, we must predict biological variables with probability distributions. The concern is no longer a single "best" map, but how we create probability distributions at all locations. The challenge is to make optimal decisions in presence of such uncertainty. If the weed density is underestimated, then escapes will continue to propagate the species and crop yield may be reduced. Overestimating the weed density results in excessive application of herbicide, which is economically and environmentally unsound. Optimal decision making in presence of uncertainty balances these risks.

Spatial variation occurs at all scales and such patterns are not always immediately apparent. This is due to macro and microclimate variation, soil moisture, temperature, weed distribution, and crop competition. Spatial resolution may require a large number of samples; however, resources are finite and some effort must be made to collect an optimum number of samples. A crop-weed-herbicide model is constructed to include (1) herbicide efficacy, (2) competitive relationships between weeds and crops, and (3) the cost of applying herbicide. Then, optimal locally varying herbicide rates are derived and uploaded into a computer that controls the spraying equipment.

The variability of weed density is considerable. Within the same field there may be small areas of high density amid a background of low density. Conventional mapping methods, including kriging, smooth spatial variations and fail to reflect extreme high or low values. The smoothing effect of conventional mapping methods is exacerbated in areas where data are sparse. Increasingly, conventional maps are being supplemented by a probabilistic assessment of variability. Simulation may then be used to create maps with the correct spatial variability of the variable under consideration. The resulting quantification of uncertainty is used in conjunction with the costs of herbicide application to provide a farm manager with knowledge for decision making. This will improve recommendations for herbicide application and result in reduced environmental loading.

Spatial correlation in weed density reduces uncertainty for a given level of sampling. Thus, the greater the spatial correlation, the fewer samples needed to build maps with the same level of uncertainty. Another consequence of greater correlation is that there is less "value" attributed to additional samples. The value of data are assessed before collection with the crop-weed-herbicide model. A simulation methodology could be devised to assess the value of information. That is, synthetic reference maps could be generated with the correct pattern of spatial variability and different sampling protocols evaluated.

Alternatively, the less spatial correlation, the more samples needed to generate herbicide treatment maps. Costs of sampling become prohibited and the farm manager's decision is to apply a uniform treatment to the field. If the range over which there is spatial correlation is less than the length of the spraying equipment, then a uniform rate is an optimal treatment. To assess spatial correlation and manage sample costs, a nested design with different sample spacings is advised.

Expressing quantitative assessments of crop yield loss as lost revenue and acknowledging the spatial distribution of weeds will encourage farm application of the crop-weed-herbicide

model. Its practical implementation will assist farm managers in optimizing weed control decisions.

Bibliography

[1] Ali, S. (2001). *Crop Protection 2001.* Alberta Agriculture, Food and Rural Development, 7000-113 Street, Edmonton, Alberta, T6H 5T6.

[2] Anonymous (1998). *Registration Handbook.* Pest Management Regulatory Agency and Government of Canada, Ottawa.

[3] Anonymous (2001). 2000 sales survey pest - control products in canada report and discussion. `http://www.croplife.ca/english/aboutcpi/industrystatistics.html`. Etobicoke.

[4] Atkinson, G. (2001). Agriculture statistics yearbook table 78 alberta major crops unit value 1951-52 to 1999-2000. `http://www.agric.gov.ab.ca/economic/yearbook/crops.html`.

[5] Audsley, E. (1993). Operational research analysis of patch spraying. *Crop Protection*, 12:111–119.

[6] Auld, B. A., Menz, K. M., and Tisdell, C. A. (1987). *Weed Control Economics.* Academic Press Inc, London.

[7] Beckie, H. J. and Kirkland, K. J. (2002). Implication of reduced herbicide rates on resistance enrichment in wild oat (Avena fatua). In Cloutier, D., editor, *Proceedings of the 2002 National Meeting*, page 65, Saskatoon, Canada. Canadian Weed Science Society.

[8] Berti, A. and Zanin, G. (1994). Density equivalent: A method for forecasting yield loss caused by mixed weed populations. *Weed Research*, 34:327–332.

[9] Blackshaw, R. E., Molnar, L. J., and Lindwall, C. W. (1998). Merits of a weed-sensing sprayer to control weeds in conservation fallow and cropping systems. *Weed Science*, 46:120–126.

[10] Bostrom, U. and Fogelfors, H. (2002). Response of weeds and crop yield to herbicide dose decision-support guidelines. *Weed Science*, 50:186–195.

[11] Bourgault, G., Journel, A. G., Rhoades, J. D., Corwin, D. L., and Lesch, S. M. (1997). Geostatistical analysis of a soil salinity data set. *Advances in Agronomy*, 58:241–292.

[12] Brain, P. and Cousens, R. (1990). The effects of weed distribution on predictions of yield loss. *Journal Applied Ecology*, 27:735–742.

[13] Brain, P., Wilson, B. J., Wright, K. J., Seavers, G. P., and Caseley, J. C. (1999). Modelling the effect of crop and weed on herbicide efficacy in wheat. *Weed Research*, 39:21–35.

[14] Buhler, D. D., King, R. P., Swinton, S. M., Gunsolus, J. L., and Forcella, F. (1997). Field evaluation of a bioeconomic model for weed management in soybean (*Glycine max*). *Weed Science*, 45:158–165.

[15] Burgess, T. M., Webster, R., and McBratney, A. B. (1981). Optimal interpolation and isarithmic mapping of soil properties. IV sampling strategy. *Journal of Soil Science*, 32:643–659.

[16] Cardina, J., Johnson, G. A., and Sparrow, D. H. (1997). The nature and consequence of weed spatial distribution. *Weed Science*, 45:364–373.

[17] Cardina, J., Sparrow, D. H., and McCoy, E. (1996). Spatial relationships between seedbank and seedling populations of common lambquarters (*Chenopodium album*) and annual grasses. *Weed Science*, 44:298–308.

[18] Cardina, J., Sparrow, D. H., and McCoy, E. L. (1995). Analysis of spatial distribution of common lambquarters (*Chenopodium album*) in no-till soybean (*Glycine max*). *Weed Science*, 43:258–268.

[19] Christensen, S., Heisel, T., and Secher, B. J. M. (1997). Spatial variation of pesticide doses adjusted to varying canopy density in cereals. *Precision Agriculture*, 1:211–218.

[20] Christensen, S., Heisel, T., and Walter, A. M. (1996). Patch spraying in cereals. *Second International Weed Control Congress*, pages 963–969.

[21] Christensen, S., Nordbo, E., Heisel, T., and Walter, A. M. (1998). Overview of developments in precision weed management, issues of interest and future directions being considered in Europe. In Medd, R. W. and Pratley, J. E., editors, *Weed Management in Crops and Pastures*, pages 3–13, Australia. CRC for Weed Management Systems.

[22] Christensen, S., Walter, A. M., and Heisel, T. (1999). The patch treatment of weeds in cereals. In *Brighton Crop Protection Conference-Weeds*, pages 591–600.

[23] Clay, S. A., Lems, G. J., Clay, D. E., Forcella, F., Ellsbury, M. M., and Carlson, C. G. (1999). Sampling weed spatial variability on a fieldwide scale. *Weed Science*, pages 674–681.

[24] Colbach, N., Forcella, F., and Johnson, G. A. (2000). Spatial and temporal stability of weed populations over five years. *Weed Science*, 48:366–377.

[25] Colliver, C. T., Maxwell, B. D., Tyler, D. A., Roberts, D. W., and Long, D. S. (1996). Georeferencing wild oat infestations in small grains: Accuracy and efficiency of three weed survey techniques. In Robert, P. C., editor, *Precision Agriculture*, pages 453–463. American Society of Agronomy, Madison, Wisconsin.

[26] Corsten, L. C. A. and Stein, A. (1994). Nested sampling for estimating spatial semivariograms compared to other designs. *Applied Stochastic Models and Data Analysis*, 10:103–122.

[27] Cousens, R. (1985). A simple model relating yield loss to weed density. *Annals Applied Biology*, 107:239–252.

[28] Cousens, R., Brain, P., O'Donovan, J. T., and O'Sullivan, P. A. (1987). The use of biologically realistic equations to describe the effects of weed density and relative time of emgerence on crop yield. *Weed Science*, 35:720–725.

[29] Cousens, R., Doyle, C. J., Wilson, B. J., and Cussans, G. W. (1986). Modelling the economics of controlling *Avena fatua* in winter wheat. *Pesticide Science*, 17:1–12.

[30] Cousens, R. and Mortimer, M. (1995). *Dynamics of Weed Populations*. Cambridge University Press, Cambridge, U.K.

[31] Cousens, R., Wilson, B. J., and Cussans, G. W. (1985). To spray or not to spray: The theory behind the practice. In *Brighton Crop Protection Conference-Weeds*, pages 671–678.

[32] Crawley, M. J. (1997). The structure of plant communities. In Crawley, M. J., editor, *Plant Ecology*, pages 475–531. Blackwell Science, UK.

[33] Deen, W., Weersink, A., Turvey, C., and Weaver, S. (1993). Weed control decision rules under uncertainty. *Review of Agricultural Economics*, 15:39–50.

[34] Derksen, D. A., Anderson, R. L., Blackshaw, R. E., and Maxwell, B. (2002). Weed dynamics and management strategies for cropping systems in the northern great plains. *Agronomy Journal*, 94:174–185.

[35] Deutsch, C. V. (2002). *Geostatistical Reservoir Modeling*. Oxford University Press, New York, 1st edition.

[36] Deutsch, C. V. and Journel, A. G. (1998). *GSLIB: Geostatistical Software Library and User's Guide*. Oxford University Press, New York, 2nd edition.

[37] Devine, M. D. (1989). Phloem translocation of herbicides. *Weed Science*, 4:191–213.

[38] Devine, M. D., Duke, S., and Fedtke, C. (1993). *Physiology of Herbicide Action*. Prentice Hall.

[39] Dieleman, J. A. (1998). *Spatial Biology of Weed Populations: Influence of Abiotic, Biotic, and Anthropogenic Processes*. PhD thesis, University of Nebraska.

[40] Dieleman, J. A. and Mortensen, D. A. (1998). Influence of weed biology and ecology on development of reduced dose strategies for integrated weed management systems. In Hatfield, J. L., Buhler, D. D., and Stewart, B. A., editors, *Integrated Weed and Soil Management*, pages 333–362, Michigan, USA. Sleeping Bear Press.

[41] Dieleman, J. A. and Mortensen, D. A. (1999). Characterizing the spatial pattern of (*Abutilon theophrasti*) seedling patches. *Weed Research*, 39:455–467.

[42] Dieleman, J. A., Mortensen, D. A., and Buhler, D. D. (1995). Linking field-scale variability of soil properties to weed populations:a multivariate analysis. *North Central Weed Science Society*, 50:154.

[43] Dieleman, J. A., Mortensen, D. A., and Martin, A. R. (1999). Influence of velvetleaf (*Abutilon theophrasti*) and common sunflower (*Helianthus annuus*) density variation on weed management outcomes. *Weed Science*, 47:81–89.

[44] Donald, W. W. (1994). Geostatistics for mapping weeds, with a Canada thistle (*Cirsium arvense*) patch as a case study. *Weed Science*, 42:648–657.

[45] Doyle, C. J. (1991). Mathematical models in weed management. *Crop Protection*, 10:432–444.

[46] Faechner, T. and Hall, L. (1999). Operational site specific spraying. *Proceedings of Weed Science Society of America*, 39:34–35.

[47] Faechner, T., Hall, L., and MacMillan, R. (2000). Landscape influence on wild oat (*Avena fatua*) distribution. *Proceedings of Weed Science Society of America*, 40:101–102.

[48] Faechner, T., Norrena, K., Thomas, A. G., and Deutsch, C. V. (2002). A risk-qualified approach to calculate locally varying herbicide application rates. *Weed Research*, 42:476–485.

[49] Firbank, L. G., Cousens, R., Mortimer, A. M., and Smith, R. G. R. (1990). Effects of soil type on crop yield-weed density relationships between winter wheat and *Bromus sterilis*. *Journal of Applied Ecology*, pages 308–318.

[50] Gerhards, R., Sokefeld, M., Schulze-Lohne, K., Mortensen, D. A., and Kuhbauch, W. (1997a). Site specific weed control in winter wheat. *Journal Agronomy and Crop Science*, 178:219–225.

[51] Gerhards, R., Wyse-Pester, D. Y., Mortensen, D. A., and Johnson, G. A. (1997b). Characterizing spatial stability of weed populations using interpolated maps. *Weed Science*, 45:108–119.

[52] Gold, H. J., Bay, J., and Wilkerson, G. G. (1996). Scouting for weeds, based on the negative bionomial distribution. *Weed Science*, 44:504–510.

[53] Goovaerts, P. (1997). *Geostatistics for Natural Resources Evaluation*. Oxford University Press, New York.

[54] Goovaerts, P. (1999). Geostatistics in soil science:state-of- the-art and perspectives. *Geoderma*, 89:1–45.

[55] Goudy, H. J. (2000). *Evaluation of Site-Specific Weed Management and Implications for Spatial Biology of Weeds*. Master's thesis, University of Guelph, Ontario.

[56] Goudy, H. J., Tardif, F. J., Brown, R. B., and Bennett, K. A. (1999). Evaluating site-specific weed control in a maize-soybean rotation system. In *Brighton Crop Protection Conference-Weeds*, pages 621–626.

[57] Groenendael, J. M. V. (1988). Distribution of weeds and some implications for modelling population dynamics:a short literature review. *Weed Research*, 28:437–441.

[58] Gunsolus, J. L. and Buhler, D. D. (1999). A risk management perspective on integrated weed management. In Buhler, D. D., editor, *Expanding the Context of Weed Management*, pages 167–187. Food Products Press.

[59] Hall, L. and Faechner, T. (1999). Herbicide efficacy of site specific and blanket spraying with clopyralid for Canada thistle (*Cirsium arvense*) and sow-thistle (*Sonchu sp*) control. *Proceedings of Weed Science Society of America*, 39:167–168.

[60] Hamlett, J. M., Horton, R., and Cressie, N. A. C. (1986). Resistant and exploratory techniques for use in semivariogram analysis. *Soil Science Society America Journal*, 50:868–875.

[61] Hanson, L. D., Robert, P. C., and Bauer, M. (1995). Mapping wild oats infestations using digital imagery for site-specific management. In Robert, P. C., editor, *Site-Specific Management for Agricultural Systems*, pages 495–503. American Society of Agronomy, Madison, Wisconsin.

[62] Harker, K. N. (2001). Survey of yield losses due to weeds in central alberta. *Canadian Journal of Plant Science*, 81:339–342.

[63] Harker, K. N. and Blackshaw, R. E. (1999). Predicting when low herbicide rates will kill weeds. Technical Report 960677, Alberta Agriculture Research Institute Project.

[64] Harker, K. N. and O'Sullivan, P. A. (1991). Effect of imazamethabenz on green foxtail, tartary buckwheat and wild oat at different growth stages. *Canadian Journal of Plant Science*, 71:821–829.

[65] Heisel, T., Ersboll, A., and Andreasen, C. (1996). Annual weed distribution can be mapped with kriging. *Weed Research*, pages 325–337.

[66] Heisel, T., Ersboll, A., and Andreasen, C. (1999). Weed mapping with co-kriging using soil properties. *Precision Agriculture*, 1:39–52.

[67] Hill, B. D., Harker, K. N., Hasselback, P., Moyer, J. R., Inaba, D. J., and Byers, S. (2001). Phenoxy herbicides in Alberta rainfall as affected by location, season, and weather patterns. AARI/AESA project no. 990059, Alberta Agricultural Research Institute.

[68] Hill, B. D., Harker, K. N., Hasselback, P., Moyer, J. R., Inaba, D. J., and Byers, S. (2002). Phenoxy herbicides in alberta rainfall: Potential effects on sensitive crops. *Canadian Journal of Plant Science*, 82:481–484.

[69] Holm, F. A., Kirkland, K. J., and Stevenson, F. C. (2000). Defining optimum herbicide rates and timing for wild oat (*Avena fatua*) and control in spring wheat (*Triticum aestivum*). *Weed Technology*, 14:167–175.

[70] Hume, L. (1989). Yield losses in wheat due to weed communities dominated by green foxtail (*Setaria viridis* (L.) Beauv.):a multispecies approach. *Canadian Journal of Plant Science*, 69:521–529.

[71] Isaaks, E. H. and Srivastava, R. M. (1989). *An Introduction to Applied Geostatistics*. Oxford University Press, New York.

[72] Jensen, P. K. and Kudsk, P. (1988). Prediction of herbicide activity. *Weed Research*, 28:473–478.

[73] Johnson, G. A., Cardina, J., and Mortensen, D. A. (1997). Site-specific weed management: Current and future directions. In *The Site-Specific Management for Agricultural Systems*, pages 131–147, Madison, Wisconsin. American Society of Agronomy.

[74] Johnson, G. A., Mortensen, D. A., and Gotway, C. A. (1996a). Spatial and temporal analysis of weed seedling populations using geostatistics. *Weed Science*, 44:704–710.

[75] Johnson, G. A., Mortensen, D. A., and Martin, A. (1995a). A simulation of herbicide use based on weed spatial distribution. *Weed Research*, 35:197–205.

[76] Johnson, G. A., Mortensen, D. A., Young, L. J., and Martin, A. R. (1995). The stability of weed seedling population models and parameters in eastern Nebraska corn (*Zea mays*) and soybean (*Glycine max*) fields. *Weed Science*, 43:604–611.

[77] Johnson, G. A., Mortensen, D. A., Young, L. J., and Martin, A. R. (1996b). Parametric sequential sampling based on multistage estimation of the negative binomial parameter. *Weed Science*, 44:555–559.

[78] Journel, A. G. (1989). *Fundamentals of Geostatistics in Five Lessons*, volume 8 of *Short Course in Geology*. American Geophysical Union, Washington, D. C.

[79] Journel, A. G. and Huijbregts, C. J. (1978). *Mining Geostatistics*. Academic Press New York.

[80] Kareiva, P. (1990). Population dynamics in spatially complex environments: Theory and data. *Philos. Trans. Royal Society London B*, 330:175–190.

[81] Krueger, D. W., Wilkerson, G. G., and Gold, H. J. (2000). An economic analysis of bionomial sampling for weed scouting. *Weed Science*, 48:53–60.

[82] Krusemark, M. G. (1998). *Using Geographic Information Systems (GIS) to Analyze Weed Populations on Agricultural Landscapes: A Literature Review, Methodology and Evaluation Study*. Master's thesis, St. Mary's University, Minnesota.

[83] Lamb, D. L., Weedon, M. M., and Rew, L. J. (1999). Evaluating the accuracy of mapping weeds in seedling crops using airborne digital imaging: *Avena* Spp. in a seedling triticale crop. *Weed Research*, 39:481–492.

[84] Lemerle, D. and Verbeek, B. (1995). Influence of soil water deficit on performance of foliar-applied herbicides for wild oat and annual ryegrass in wheat. *Plant Protection Quarterly*, 10:143–147.

[85] Lindquist, J. L., Dieleman, J., Mortensen, D., Johnson, G., and Wyse-Pester, D. (1998). Economic importance of managing spatially heterogeneous weed populations. *Weed Technology*, 12:7–13.

[86] Lutman, P. J. W. and Perry, N. H. (1999). Methods of weed patch detection in cereal crops. In *Brighton Crop Protection Conference-Weeds*, pages 627–634.

[87] Madsen, K. H., Blacklow, W. M., Jensen, J. E., and Streibig, J. C. (1999a). Simulation of herbicide use in a crop rotation with transgenic herbicide-tolerant oilseed rape. *Weed Research*, 39:95–106.

[88] Madsen, K. H., Poulsen, E. R., and Streibig, J. C. (1999b). Modelling of herbicide use in genetically modified herbicide resistant crops - 2. Environmental project no. 450, Danish Environmental Protection Agency.

[89] Matern, B. (1960). *Spatial Variation*. Springer-Verlag.

[90] Maxwell, B. D. (1992). Weed thresholds: The space component and considerations for herbicide resistance. *Weed Technology*, 6:205–212.

[91] Maxwell, B. D. and Colliver, C. T. (1995). Expanding economic thresholds by including spatial and temporal weed dynamics. In *Brighton Crop Protection Conference-Weeds*, pages 1069–1076.

[92] McBratney, A. B. and Webster, R. (1981). The design of optimal sampling schemes for local estimation and mapping of regionalized variables - II. *Computers and Geosciences*, 7:335–365.

[93] McBratney, A. B. and Webster, R. (1983). How many observations are needed for regional estimation of soil properties. *Journal of Soil Science*, 135:177–183.

[94] McDonald, A. J. and Riha, S. J. (1999). Model of crop:weed competition applied to maize: *Abutilon theophrasti* interactions. II. assessing the impact of climate: Implications for economic thresholds. *Weed Research*, 39:371–381.

[95] Miller, P. C. H., Stafford, J., Paice, M., and Rew, L. J. (1995). The patch spraying of herbicides in arble crops. In *Brighton Crop Protection Conference-Weeds*, pages 1077–1086, Brighton, U.K.

[96] Mortensen, D. A., Dieleman, J., Johnson, G., and Young, L. J. (1993). Weed distribution in agricultural fields. In Robert, P., Rust, R. H., and Larson, W. E., editors, *Soil Specific Crop Management*, pages 113–124, Madison, WI. American Society of Agronomy.

[97] Mortensen, D. A. and Dieleman, J. A. (1997). The biology underlying weed management treatment maps in maize. In *Brighton Crop Protection Conference-Weeds*, pages 645–648.

[98] Mortensen, D. A. and Dieleman, J. A. (1998). Why weed patches persist:dynamics of edges and density. In Medd, R. and J.E.Pratley, editors, *Integrated Weed and Soil Mangement*, pages 14–19. CRC for Weed Management Systems, Australia.

[99] Mortensen, D. A., Dieleman, J. A., and Johnson, G. A. (1998). Weed spatial variation and weed management. In Hatfield, J. L., Buhler, D., and Stewart, B. A., editors, *Integrated Weed and Soil Mangement*, pages 1–17. Ann Arbour Press.

[100] Mortensen, D. A., Dieleman, J. A., and Williams II, M. M. (2001). Using remote sensing in integrated weed management: What do we need to see? *Agronomy Journal of America (in press)*.

[101] Mortensen, D. A., Johnson, G. A., Wyse, D. Y., and Martin, A. R. (1995). Managing spatially variable weed populations. In *Site-Specific Management for Agricultural Systems*, pages 397–415, Madison, Wisconsin. American Society of Agronomy.

[102] Mulla, D. J. (1997). Geostatistics, remote sensing and precision farming. In Stein, A. and Bouma, J., editors, *Precision Agriculture: Spatial and Temporal Variability of Environmental Quality- Ciba Foundation Symposium No. 210*, pages 100–119. John Wiley and Sons, Somerset, NJ.

[103] Navas, M. L. (1991). Using plant population biology in weed research: A strategy to improve weed management. *Weed Research*, 31:171–179.

[104] Navas, P. C., Roouse, D. I., and Yandell, B. S. (1984). Comparison of statistical methods for studying spatial pattern of soilborne plant pathogens in the field. *American Phytopathological Society*, pages 1399–1402.

[105] Nordbo, E., Christensen, S., Kristensen, K., and Walter, M. (1994). Patch spraying of weed in cereal crops. *Aspects of Applied Biology*, 40:325–334.

[106] Nordho, E. and Christensen, S. (1995a). Spatial variability of weeds. In *SP-Report No. 26: Proceedings of the Seminar on Site Specific Farming*, pages 67–89. Foulum, Denmark: Statens Planteavlsforsoeg.

[107] Nordho, E. and Christensen, S. (1995b). Weed patchiness and localised control. In *Report from the EC-Project 'Patchwork' on Ecological and Agronomical Aspects of Patch Management of Weeds*, pages 1–98. Danish Institute of Plant and Soil Science, Flakkebjerg, Slagelse, Denmark.

[108] O'Donovan, J. T. (1991). Seed yields of canola and volunteer barley as influenced by their relative times of emergence. *Canadian Journal of Plant Science*, 72:263–267.

[109] O'Donovan, J. T. (1994). Canola (*Brassica rapa*) plant density influences tartary buckwheat (*Fagopyrum tataricum*) interference, biomass and seed yield. *Weed Science*, 42:385–389.

[110] O'Donovan, J. T. (1996). Weed economic thresholds:useful agronomic tool or pipe dream? *Phytoprotection*, 77:13–28.

[111] O'Donovan, J. T., de St. Remy, E. A., O'Sullivan, P. A., Dew, D. A., and Sharma, A. K. (1985). Influence of the relative time of emergence of wild oat (*Avena fatua*) on yield loss of barley (*Hordeum vulgare*) and wheat (*Triticum aestivum*). *Weed Science*, 33:498–503.

[112] O'Donovan, J. T., Harker, K. N., Clayton, G. W., Blackshaw, R. E., Robinson, D., and Maurice, D. (2001). Evaluation of a yield loss model based on wild oat and barley density and relative time of emergence. In *Brighton Crop Protection Conference-Weeds*, pages 639–644.

[113] O'Donovan, J. T., Newman, J. C., Harker, K. N., Blackshaw, R. E., and McAndrews, D. W. (1999). Effect of barley plant density on wild oat interference, shoot biomass and seed yield under zero tillage. *Canadian Journal of Plant Science*, 79:655–662.

[114] O'Donovan, J. T., Sharma, A. K., Kirkland, K. J., and de St. Remy, E. A. (1988). Volunteer barley (*Hordeum vulgare*) interference in canola (*Brassica campestris* and *B napus*). *Weed Science*, 36:734–739.

[115] Olea, R. A. (1984). Sampling design optimization for spatial functions. *Mathematical Geology*, 16:369–392.

[116] Olofsdotter, M., Olesen, A., Andersen, S. B., and Streibig, J. C. (1994). A comparison of herbicide bioassays in cell cultures and whole plants. *Weed Research*, 34:387–394.

[117] Paice, M. E. R., Day, W., Rew, L. J., and Howard, A. (1998). A stochastic simulation model for evaluating the concept of patch spraying. *Weed Research*, 38:373–388.

[118] Penney, D. (1995). Soils, cropping practices, and fertilizer use. `http://www.agric.gov.ab.ca/agdex/500/4100001a.html-cropping`.

[119] Perry, N. and Lutman, P. J. W. (2001). Saptial and population dynamics of patches of wild-oats. In *Workshop on Specific Weed Management November, 2000, Odense, Denmark*. EWRS Working Group Site Specific Weed Management.

[120] Peters, N. C. B. (1984). Time of onset of competition and effects of various fractions of an *Avena fatua* l. population on spring barley. *Weed Research*, 24:305–315.

[121] Peterson, D. E. and Nalewaja, J. D. (1992). Green foxtail (*Setaria viridis*) competition with wheat (*Triticum aestivum*). *Weed Technology*, 6:291–296.

[122] Pettitt, A. N. and McBratney, A. B. (1984). Sampling designs for extimating spatial variance components. *Applied Statistics*, 42:185–209.

[123] Radosevich, S., Holt, J., and Ghersa, C. (1997). *Weed Ecology - Implications for Management*. John Wiley and Sons Inc, New York, NY, 2th edition.

[124] Rew, L. J. and Cousens, R. D. (1998). What do we know about the spatial distribution of arable weeds? In Medd, R. W. and Pratley, J. E., editors, *Weed Management in Crops and Pastures*, pages 20–26, Australia. CRC for Weed Management Systems.

[125] Rew, L. J. and Cousens, R. D. (2001). Spatial distribution of weeds in arable crops: Are current sampling and analytical methods appropriate? *Weed Research*, 41:1–18.

[126] Rew, L. J. and Cussans, G. W. (1995). Patch ecology and dynamics-how much do we know? In *Brighton Crop Protection Conference-Weeds*, pages 1059–1068.

[127] Rew, L. J., Cussans, G. W., Mugglestone, M. A., and Miller, P. C. H. (1996). A technique for mapping the spatial distribution of *Elymus repens*, with estimates of the potential reduction in herbicide usage from patch spraying. *Weed Research*, 1996:283–292.

[128] Rew, L. J., Miller, P., and Paice, M. (1997). The importance of patch mapping resolution for sprayer control. *Aspects of Applied Biology*, 48:49–55.

[129] Rew, L. J., Whelan, B., and McBratney, A. B. (2001). Does kriging predict weed distributions accurately enough for site-specific weed control? *Weed Research*, 41:245–263.

[130] Rossel, R. A. V., Goovaerts, P., and McBratney, A. B. (2001). Assessment of the production and economic risks of site-specific liming using geostatistical uncertainty modelling. *Environmetrics*, 12:699–711.

[131] Russo, D. (1984). Design of an optimal sampling network for estimating the variogram. *Soil Science Society of America Journal*, 48:708–716.

[132] Sagar, G. R. and Mortimer, A. M. (1976). An approach to the study of the population dynamics of plants with special reference to weeds. In Coaker, T. H., editor, *Applied Biology*, pages 1–47. Volume 1, Academic Press, London.

[133] Schabenberger, O., Tharp, B. E., Kells, J. J., and Penner, D. (1999). Statistical tests for hormesis and effective dosages in herbicide dose response. *Agronomy Journal*, 91:713–721.

[134] Seefeldt, S. S., Jensen, J. E., and Fuerst, E. P. (1995). Log-logistic analysis of herbicide dose-response relationships. *Weed Technology*, pages 218–227.

[135] Shirtliffe, S. J. (1999). *The Effect of Chaff Collection on the Combine Harvester Dispersal of Wild Oat (Avena fatua L.)*. PhD thesis, University of Manitoba.

[136] Simard, Y., Legendre, P., Lavoie, G., and Marcotte, D. (1992). Mapping, estimating biomass, and optimizing sampling programs for spatially autocorrelated data: case study of the northern shrimp (*Pandalus borealis*). *Canadian Journal of Fishery and Aquatic Science*, 49:32–45.

[137] Smith, M. C., Shaw, D. R., Lamastus, F. L., and Henry, B. (2000). How species and population densities influence spectral reflectance and detection capabilities. *Proceedings of Weed Science Society of America*, 40:103–104.

[138] Spandl, E., Durgan, B. R., and Miller, D. W. (1997). Wild oat (*Avena fatua*) control in spring wheat (*Triticum aestivum*) and barley (*Hordeum vulgare*) with reduced rates of postemergence herbicides. *Weed Technology*, 11:591–597.

[139] Steel, R. G. D., Torrie, J. H., and Dickey, D. A. (1999). *Principles and Procedures of Statistics: A Biometrical Approach*. McGraw Hill, Boston, Massachuetts, third edition.

[140] Stougaard, R. N., Maxwell, B. D., and Harris, J. D. (1997). Influence of application timing on the efficacy of reduced rate postemergence herbicides for wild oat (*Avena fatua*) control in spring barley (*Hordeum vulgare*). *Weed Technology*, 11:283–289.

[141] Streibig, J. C. (1988). Herbicide bioassay. *Weed Research*, 28:479–484.

[142] Streibig, J. C. (1989). The herbicide dose-response curve and the economics of weed control. In *Brighton Crop Protection Conference-Weeds*, pages 927–935.

[143] Streibig, J. C., Jensen, J. E., Olofsdotter, M., Haas, H., Andreasen, C., and Lawaetz, E. (1993). Testing hypotheses with dose-response curves. In *8th EWRS Symposium Quantitative Approaches in Weed and Herbicide Research and their Practical Problems*, pages 423 – 431.

[144] Streibig, J. C. and Kudsk, P. (1993). *Herbicide Bioassays*. CRC Press, Inc., Boca Raton, Flordia.

[145] Swanton, C. J., Weaver, S., Cowan, P., Acker, R. V., Deen, W., and Shreshta, A. (1999). Weed thresholds: Theory and applicability. In Buhler, D. D., editor, *Expanding the Context of Weed Management*, pages 9–29. Food Products Press.

[146] Taylor, C. R. and Burt, O. R. (1984). Near-optimal management strategies for controlling wild oats in spring wheat. *American Agricultural Economics*, 66:50–60.

[147] Thomas, G. A., Frick, B. L., and Hall, L. M. (1998). *Alberta Weed Survey of Cereal and Oilseed Crops in 1997*, volume 98-2. Agriculture and Agri-Food Canada, Saskatoon, Saskatchawen.

[148] Thomas, P. (2001). *Canola Growers Manual*. Canola Council of Canada, Winnipeg, Manitoba.

[149] Thompson, J. F., Stafford, J. V., and Miller, P. C. H. (1991). Potential for automatic weed detection and selective herbicide application. *Crop Protection*, 10:254–259.

[150] Thorton, P. K., Fawcett, R. H., Dent, J. B., and Perkins, T. J. (1990). Spatial weed distribution and economic thresholds for weed control. *Crop Proctection*, pages 337–342.

[151] Trangmar, B. B., Yost, R. S., and Uehara, G. (1985). Application of geostatistics to spatial studies of soil properties. *Advances in Agronomy*, 38:45–94.

[152] Upchurch, D. R. and Edmonds, W. J. (1991). Statistical procedures for specific objectives. In Mausbach, M. J. and Wilding, L. P., editors, *Spatial Variabilities of Soils and Landforms*, pages 49–71. Soil Science Society of America, Madison, Wisconsin.

[153] Wallinga, J., Groeneveld, R. M. W., and Lotz, L. A. P. (1998). Measures that describe weed spatial patterns at different levels of resolution and their applications for patch spraying of weeds. *Weed Research*, 38:351–359.

[154] Walter, A. M., Heisel, T., and Christensen, S. (1997). Shortcuts in weed mapping. In *Precision Agriculture*, pages 777–784. Bios Scientific Publishers Ltd.

[155] Webster, R. (1985). Quantitative spatial analysis of soil in the field. *Advances in Soil Science*, 3:1–70.

[156] Weisz, R. J., Fleischer, S., and Smilowitz, Z. (1995). Site-specific integrated pest management for high value crops: Sample units for map generation using the colorado potato beetle (Coleopters:Chrysomeliade) as a model system. *Journal Economic Entomology*, 88:1069–1080.

[157] Wiles, L. J., Gold, H. J., and Wilkerson, G. G. (1993). Modelling the uncertainty of weed density estimates to improve post-emergence herbicide control decisions. *Weed Research*, 33:241–252.

[158] Wiles, L. J., Oliver, G. W., York, A. C., Gold, H. J., and Wilkerson, G. (1992). Spatial distribution of broadleaf weeds in North Carolina soybean (*Glycine max*) fields. *Weed Science*, 40:554–557.

[159] Wilkerson, G. G., Modena, S. A., and Coble, H. D. (1991). HERB: Decision model for post-emergence weed control in soybean. *Agronomy Journal*, 83:413–417.

[160] Wille, M. J., Thill, D. C., and Price, W. J. (1998). Wild oat (*Avena fatua*) seed production in spring barley (*Hordeum vulgare*) is affected by the interaction of wild oat density and herbicide rate. *Weed Science*, 46:336–343.

[161] Williams II, M. M., Gerhards, R., Reichart, S., Mortensen, D. A., and Martin, A. R. (1998). Weed seedling population responses to a method of site-specific weed management. In *Proceedings of the Fourth International Conference on Precision Agriculture*, pages 123–132.

[162] Williams II, M. M. and Mortensen, D. A. (2000). Crop weed outcomes from site-specific and uniform soil-applied herbicide applications. *Precision Agriculture*, 2:377–388.

[163] Wilson, B. J. and Brain, P. (1991). Long-term stability of distribution of *Alopecurus myosuroides* huds. within cereal fields. *Weed Research*, 31:367–373.

[164] Wollenhaupt, N. C., Mulla, D. J., and Crawford, C. A. G. (1997). Soil sampling and interpolation techniques for mapping spatial variability of soil properties. In *The Site-Specific Management For Agricultural Systems*, pages 19–53. American Society of Agronomy.

[165] Wyse-Pester, D., Westra, P., and Wiles, L. J. (1999). Spatial sampling and analysis of crop pests in a centre pivot corn field. In *Proceedings Second European Conference on Precision Agriculture*, pages 485–494. Odense, Denmark, SCI.

[166] Yeakel, J. D., Deutsch, C. V., and Schwans, P. (1992). The design of an optimal outcrop sampling scheme. *SPE*, 1:1–7.

[167] Yfantis, E. A., Flatman, G. T., and Behar, J. V. (1987). Efficiency of kriging estimation for square, triangular, and hexangonal grids. *Mathematical Geology*, 19:183–205.

[168] Zhang, J. and Hamill, A. (1998). Temporal and spatial distributions of velvetleaf seedlings after 1 year's seeding. *Weed Science*, 46:414–418.

[169] Zhang, J., Weaver, S. E., and Hamill, A. S. (2000). Risk and reliability of using herbicides at below-labeled rates. *Weed Technology*, 14:106–115.

Appendix

Definition of symbols

$a(\mathbf{u})$ = herbicide application rate at location $\mathbf{u}$, g ai ha^{-1}

$a_{opt}(\mathbf{u})$ = optimal local herbicide application rate at location $\mathbf{u}$, g ai ha^{-1}

$c_v(\mathbf{u})$ = crop density, plants m^{-2}

$c(a)$ = cost of application for a herbicide rate, dollars ha^{-1}

$di(\mathbf{u})$ = number of weeds or weed density at location $\mathbf{u}$, plants m^{-2}, with no herbicide

$d(\mathbf{u})$ = number of weeds or weed density at location $\mathbf{u}$, plants m^{-2}, surviving herbicide treatment

$d_v(\mathbf{u})$ = number of weeds or weed density at location $\mathbf{u}$, plants m^{-2}

ED_{50} = effective dose of a herbicide giving a 50% injury response, g ai ha^{-1}

$f(\mathbf{u})$ = fractional crop yield loss as a function of the weed density, crop density, relative time of weed emergence, and herbicide application rate, %

$H(a)$ = fractional weed control as a function of the herbicide application rate,

$hc(a;\mathbf{u})$ = cost of the herbicide, dollars ha^{-1}

hd = cost of the herbicide, dollars litre^{-1}

np = net price of grain yield, dollars tonne^{-1}

$pc(a;\mathbf{u})$ = total profit, dollars ha^{-1}

$\overline{pc(a;\mathbf{u})}$ = expected profit, dollars ha^{-1}

$r(a;\mathbf{u})$ = revenue, dollars ha^{-1}, for a herbicide application rate a at location $\mathbf{u}$

SSA = selective spraying area denoted as v, m^{-3}

$t_v(\mathbf{u})$ = relative time of weed emergence, days

$Y(\mathbf{u})$ = crop yield, tonnes ha^{-1} at location $\mathbf{u}$

$Y_{wf}(\mathbf{u})$ = maximum attainable weed-free crop yield, tonnes ha^{-1} at location $\mathbf{u}$